VASCULAR PERMEABILITY, ANGIOGENESIS AND THE ROLE OF DELTA-LIKE LIGAND 4

Rachel Boardman

A thesis submitted for the degree of Doctor of Philosophy (PhD)

Division of Cancer and Stem Cells
The school of Medicine
The University of Nottingham

Oct 2017

Abstract

Cardiovascular disease, of which ischaemic diseases such as stroke and peripheral arterial disease make up a large proportion, are the leading cause of death worldwide. The endogenous response to ischaemia is to upregulate growth factors to stimulate the growth of new vessels and in some cases, form a collateral network. The concept of therapeutic stimulation has therefore become a priority area of cardiovascular research. The collateral network formed must consist of intact, stable, non-leaky vessels that can respond appropriately to stimuli. While the potent angiogenic driver, vascular endothelial growth factor (VEGF) appeared to be a promising target, trials in peripheral ischaemia patients have been disappointing.

Upregulated by VEGF during angiogenesis, the Notch ligand Dll4 is a key regulator of vessel maturation and function. Widely known to regulate tip and stalk cell selection during sprouting angiogenesis, its role in the recruitment and growth of mural cells, regulation of permeability, compliance and signalling is poorly understood. Inhibition of Dll4 results in non-functional, poorly perfused vessels with reduced pericyte coverage suggesting a greater role for Dll4 in the formation of mature, intact, operative vessels. I therefore tested the hypothesis that the physiological characteristics of the neovasculature are regulated by Dll4 during physiological neovascularisation.

A recombinant human sDll4 protein was used to induce Notch signalling in an endothelial cell monolayer and resulted in increased expression of VE-Cadherin and cell-cell contacts. Using the Landis-Michel microvascular permeability technique, Dll4 signalling was shown to decrease the permeability of rat mesenteric vessels and then subsequent experiments showed that this could be prevented by the proteins kinase A (PKA) inhibitor H89 dihydrochloride. In the rat mesenteric angiogenesis model, inducing Notch with an adenovirus (Ad.) encoding sDll4 (Ad.sDll4) resulted in a less angiogenic vasculature and when added into arteriolargenesis stimulating adenovirus combinations it led to a more endogenous-like vasculature and a switch from sprouting to branching. In a mouse hindlimb ischaemia model, Ad.sDll4 hindered blood flow recovery to the hind paw but led to increase capillary and arteriolar density.

These results show that Dll4 plays a key role in regulating vascular permeability and that this is through a cAMP/PKA dependent pathway and involves VE-Cadherin expression. They also demonstrate a role for Dll4 in arteriolargenesis in both physiological and pathological settings and the possibility of using Dll4 as part of an ischaemic therapeutic strategy cannot yet be ruled out.

List of Conferences

This work has been presented at the following conferences

- The British Microcirculation Society Annual Meeting
    - Manchester, 2015
    - Poster presentation
- Physiology 2016
    - Dublin
    - Poster presentation

Acknowledgments

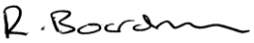
Firstly, I would like to thank my supervisors, Professor David Bates and Dr Maria Machado for giving me this opportunity and all their help and support throughout the process as well as the Medical Research Council for funding the research.

I have been fortunate enough to have had the pleasure of working with many amazing people within the TVBL and I would like to thank them all for being part of my PhD journey. I would particularly like to thank Dr Andrew Benest for giving your time and guidance however trivial the question. I will always be grateful for the support and advice you have given me and consider myself lucky to have has you as a mentor and a friend. To Zoe Blackley, Dr Kiren Yacub-Usman, Dr James Daubney and Hannah Bolland, thank you all for your endless help in the lab but most of all your emotional support and re-introducing me to a life outside of science. Finally, I would like to thank Sam Bestall. No-one knows the journey we have been on as much as we do and I want to thank you for always making me feel better about the situation (even if it is just because you're stressing more than me!), for never judging during one of our many rants and for the continuous stream of messages and photos.

Most importantly, I would like to thank my family for their unwavering support and encouragement. Thank you for being the voice of reason, my rock and my torch during the dark times – without you, I could not have done this.

Declaration

I declare that the work presented in this thesis is my own and was carried out in accordance with the regulations of the University of Nottingham. Where information has been derived from other sources, I confirm that this has been indicated in the thesis and no part of the thesis has been submitted for any other degree.

Signed: ……  ……

Date: ……08/10/2017……..

Table of Contents

Abstract i

List of Conferences iii

Acknowledgments iv

Declaration v

Table of Figures and Equations xii

List of Abbreviations xvi

Chapter 1: Introduction 1

1.1 Cardiovascular Disease 1

1.2 Microvascular Structure 3

1.2.1 Intercellular Junctions 4

1.2.2 Basement Membrane 7

1.2.3 The Glycocalyx 7

1.2.4 Support Cells 8

1.3 Angiogenesis 9

1.3.1 Sprouting Angiogenesis 10

1.3.2 Arteriolargenesis 24

1.4 Microvascular Permeability 26

1.4.1 The Formation of the Starling Hypothesis 26

1.4.2 Osmotic Refection Coefficient 28

1.4.3 Pore Theory 29

1.4.4 Accounting for the Glycocalyx 31
1.4.5 Putting the Starling Equation into Practice 33
1.4.6 Microvascular Permeability in Disease 35
1.5 Hypothesis and Aims 37
Chapter 2: Methods and Materials 39
2.1 List of Materials Used 39
2.2 Cell Culture 42
2.2.1 Cell Lines 42
2.2.2 Sub-culture 43
2.2.3 Cell Counting 43
2.2.4 Cryopreservation of Cells 44
2.2.5 Reviving Cryopreserved Cells 44
2.3 Adenovirus Expansion 45
2.3.1 Adenovirus Purification 45
2.3.2 Titration by End-Point Dilution 46
2.3.3 In Vitro Validation of Ad.sDll4 47
2.3.4 Validation of Adenoviruses In Vivo 48
2.4 RNA Extraction 48
2.4.1 In Vitro 48
2.4.2 In Vivo 49
2.4.3 Both In Vivo and In Vitro 49
2.5 cDNA Synthesis 50

2.5.1 DNase Treatment 50
2.5.2 cDNA Generation 50
2.6 Quantitative RT-PCR 51
2.6.1 Primers 51
2.6.2 qPCR 51
2.6.3 Analysis 52
2.7 Digital Droplet PCR 52
2.8 In Vitro Angiogenesis Assay 54
2.8.1 Conditioned Media 54
2.8.2 The Assay 55
2.8.3 Imaging and Analysis 56
2.9 In Vitro Immunofluorescence 56
2.9.1 Cell Culture 56
2.9.2 Treatment and Staining 57
2.9.3 Imaging and Analysis 58
2.10 In Vitro Protein Extraction 59
2.11 Protein Quantification 60
2.12 Western Blot 60
2.12.1 Sodium Dodecyl Sulphate-Polyacrylamide Gel Electrophoresis 60
2.12.2 Immunodetection and Visualization 61
2.13 Animals 62

2.14 Hydraulic Conductivity 63
2.14.1 General Solutions 63
2.14.2 Apparatus for Cannulation 63
2.14.3 Experimental Protocol 65
2.14.4 Imaging and Recording Experiments 67
2.14.5 Analysis 68
2.14.6 Animal Surgery Procedure 70
2.14.7 Image Analysis 73
2.15 Hind limb Ischaemia 73
2.15.1 Surgery and Imaging 74
2.15.2 Tissue Staining and Imaging 76
2.15.3 Imaging and Analysis 77
Chapter 3: Dll4 Regulates Endothelial Junctions Through Notch1 78
3.1 Introduction 78
3.2 Methods 81
3.2.1 Recombinant Protein and Adenovirus Sequences 81
3.2.2 Experimental Protocols 82
3.3 Results 84
3.3.1 Effect of sDll4 on the Amount and Location of Notch Intracellular Domain (NICD) 84
3.3.2 Effect of Recombinant Dll4 and sDll4 on Notch Signalling 85

3.3.3 The Effect of Ad.sDll4 on Endothelial Cell Tube Formation 91

The Effect of sDll4 on Endothelial Cell Barrier Function 97

3.4 Discussion 99

3.4.1 sDll4 Increases NICD Levels In Vitro 99

3.4.2 sDll4 Increases Hes1 and Hey1 Expression Through Induction of Notch Signalling 100

3.4.3 Ad.sDll4 Induces Hes1 Expression but Not Hey1. 103

3.4.4 Ad.sDll4 Induces Tube Formation 105

3.4.5 sDll4 Increases Adherens but Not Tight Junctions 106

3.5 Concluding Remarks 109

Chapter 4: Dll4/Notch Signalling Regulates Vascular Permeability Through cAMP/PKA Dependent Pathway 110

4.1 Introduction 110

4.2 Methods 115

4.3 Results 117

4.3.1 Part 1: Developing a Working Lp Rig and Rat Tray 117

4.3.2 Part 2: How Does Dll4/NOTCH Signaling Effect Microvascular Permeability? 123

4.4 Discussion 134

4.4.1 Dll4/Notch Signaling Regulates Microvascular Permeability 134

4.4.2 Dll4 Regulates Permeability in a PKA Dependent Manner 139

4.5 Concluding Remarks 143

Chapter 5: Dll4 and Arteriolargenesis 144

5.1 Introduction 144

5.2 Methods 148

5.3 Results 149

5.3.1 Overexpression of sDll4 Leads to a More Quiescent Vasculature. 149

5.3.2 Ad.sDll4 in Combination with Ad.Ang1 + Ad.eNOS ± Ad.VEGF Leads to a More Organised, Quiescent Vasculature .. 154

5.4 Discussion 160

5.4.1 Induction of Notch Signalling by Ad.sDll4 Dampens the Angiogenic Response 160

5.4.2 Addition of Ad.sDll4 Leads to a More Endogenous-like Vasculature 163

5.5 Concluding Remarks 169

Chapter 6: Dll4 and Peripheral Ischaemia 170

6.1 Introduction 170

6.2 Methods 173

6.2.1 Adenoviruses 173

6.2.2 Experimental Protocol 173

6.3 Results 175

6.3.1 Ad.sDll4 is Deleterious to the Recovery of Blood Flow .. 175

6.3.2 Capillary Density 184

6.4 Discussion 188

6.4.1 Ad.sDll4 Does Not Enhance Blood Flow Recovery Following Ischaemic Injury 188

6.4.2 Ad.sDll4 Increases Capillary and Arteriolar Density in the Ischaemic Adductor Muscle 193

6.5 Concluding Remarks 195

Chapter 7: Discussion 196

7.1 Summary of Findings and Future Work 196

7.1.1 Dll4 Induces VE-Cadherin Expression 196

7.1.2 Dll4/Notch Signalling Regulates Vascular Permeability . 197

7.1.3 Addition of Ad.sDll4 During Arteriolargenesis Leads to a More Endogenous-like Vasculature 199

7.1.4 Following Ischaemic Injury Dll4/Notch Signalling Enables Collateral Vessel Growth but Hinders Blood Flow Recovery 202

7.2 Implications 204

7.3 Concluding Remarks 205

References 207

Table of Figures and Equations

Figure 1.1 Schematic of the microvascular structure. 5

Figure 1.2 Schematic of the VEGF family. 10

Figure 1.3 Structure of Dll4 and Notch. Dll4 13

Figure 1.4 The Dll4/Notch Signalling Pathway 15

Figure 1.5 Tip and stalk cell selection in Sprouting angiogenesis. 17

Equation 1 28

Equation 2 29

Equation 3 29

Equation 4 32

Equation 2.1 46

Equation 2.2 47

Figure 2.1 Section of a typical image captured using a confocal microscope 57

Figure 2.2, Areas of typical confocal z-stack images captured of endothelial cells illustrating how each were analysed. 59

Figure 2.3 Pipette grinding rig 64

Figure 2.4 Pipette grinding rig set up. 64

Figure 2.5 schematic of the Lp pipette refilling system 67

Figure 2.6 Analysing Lp recordings 69

Figure 2.7 Schematic of a section of the rat mesentery 71

Figure 2.8 section of a confocal z-stack image of the rat mesentery ... 74

Figure 3.1 sDll4 increases NICD in HDBECs 87

Figure 3.2 Dll4 and sDll4 induce Notch signalling. 88

Figure 3.3 The induction of Notch signalling by sDll4 can be prevented with addition of DAPT. 89
Figure 3.4 Ad.sDll4 induces Hes1 but not Hey1. 91
Figure 3.5 Ad.sDll4 induced tubes with less branches but more sprouts than Ad.VEGF. 93
Figure 3.6 sDll4 has no effect on ZO-1 tight junctions 95
Figure 3.7 sDll4 increased VE-Cadherin thick junctions and fluorescence intensity 96
Figure 4.1 Fully operational Lp Rig. 118
Figure 4.2 The working parts of the Lp rig 119
Figure 4.3 Development of the rat tray. 120
Figure 4.4 fluid flux per unit area was measured at different pressures within the same vessel 122
Figure 4.5 Reperfusion with BSA does not alter vascular 124
Figure 4.6 Perfusion with full length Dll4 has no effect on permeability 127
Figure 4.7 Perfusion with sDll4 results in a decrease in permeability in rat mesenteric microvessels. 129
Figure 4.8 The PKA inhibitor H89 dihydrochoride (H89) prevents the induction of Notch target genes Hes1 and Hey1 by sDLL4 and VEGF 130
Figure 4.9 sDll4 reduces microvessel permeability through a PKA dependent pathway. 133
Figure 4.10 Two individual experiments (A and B) from pilot data indicating the lasting effect of sDll4 perfusion 138

Figure 5.1 Representative images of mesentery panels taken for staining on day 7. 150
Figure 5.2 Induction of Notch signalling through Ad.sDll4 results in a less angiogenic vasculature 152
Figure 5.3 Addition of Ad.sDll4 leads to a more organised quiescent vasculature. 155
Figure 5.4 Ad.sDll4 results in a less active vasculature 156
Figure 5.5 Ang1 + eNOS + VEGF + sDll4 results in vessels that are similar to but more branched than Ad.eGFP 158
Figure 6.1 Representative blood flow images from each group taken before and after surgery and on days 3, 7, 14 and 21 176
Figure 6.2 Ad.sDll4 is deleterious to blood flow recovery. 179
Figure 6.3 Representative Speckle images taken before and after surgery and at days 3, 7, 14 and 21 181
Figure 6.4 Ad.VEGF and Ad.sDll4 have an additive negative effect on blood flow recovery after ischemic injury 183
Figure 6.5 Representative images of ischemic adductor muscle tissue sections stained for capillaries and arterioles 184
Figure 6.6 Addition of Ad.sDll4 increases both capillary and arteriolar density 187
Figure 7.1 Summary Diagram of how the work done in this thesis adds to our knowledge 201

List of Abbreviations

Ad.	Adenovirus
Ad.Ang1	Adenovirus encoding Ang1
Ad.eGFP	Adenovirus encoding GFP
Ad.eNOS	Adenovirus encoding eNOS
Ad.sDll4	Adenovirus encoding sDll4
Ad.VEGF	Adenovirus encoding VEGF
Ang1	Angiopoietin 1
ANOVA	Analysis of variance
BBB	Blood brain barrier
BRB	Blood retinal barrier
BSA	Bovine serum albumin
CADASIL	Cerebral autosomal dominant arteriopathy with subcortical infarcts and leukoencephalopathy
CHO	Chinese hamster ovarian
CT	Cycle threshold
Dll4	Delta like ligand 4
DMEM	Dulbecco’s modified eagle’s medium
DSL	Delta-Serrate-Ligand
ECM	Extracellular matrix

EGF	Epidermal growth factor
eNOS	Endothelial nitric oxide synthase
FC	Fragment crystallisation
FCS	Foetal calf serum
FGF	Fibroblast growth factor
GFP	Green fluorescent protein
HDBEC	Human dermal blood endothelial cells
HGF	Hepatocyte growth factor
HUVEC	Human umbilical vein endothelial cells
LT	Lethal toxin
MOI	Multiplicity of infection
NHDF	Normal human dermal fibroblast
NICD	Notch Intracellular Domain
PAD	Peripheral arterial disease
PAF	Platelet-activating factor
PBS	Phosphate buffered saline
RBC	Red blood cells
sDll4	Soluble delta like ligand 4
SEM	Standard error of the mean
TEER	Trans endothelial electrical resistance

VEGF	Vascular endothelial growth factor
VEGFA	Vascular endothelial growth factor-A
VSMC	Vascular smooth muscle cells

Chapter 1: Introduction

1.1 Cardiovascular Disease

Cardiovascular disease (CVD) is the leading cause of death worldwide (Wong, 2014; Bhatnagar *et al.*, 2015; Naghavi *et al.*, 2015; WHO, 2015). It mainly results from ischaemic diseases such as coronary heart disease, cerebral ischaemia and peripheral arterial occlusion due to the build-up of an atherosclerotic plaque resulting in a reduced blood supply and tissue hypoxia. Coronary heart disease results from blockade of the coronary arteries of the heart and symptoms include angina and heart attack. Cerebral ischemia occurs following a reduction in blood supply to either a specific area or the entire brain and can result in a stroke and peripheral arterial disease most commonly affects the arteries of the legs.

The endogenous response to ischaemia is to upregulate growth factors and induce the growth of new vessels. In progressive ischaemic diseases where the build-up of a plaque occurs slowly over time a collateral circulation can form. Therefore, the development of treatments that promote regeneration of the vasculature in these under-perfused vessels without the need for invasive procedures such as surgery has become a priority in CVD research.

The creation of a collateral vasculature in ischaemic tissues requires the growth of a functional vascular network including capillaries,

arterioles, venules, arteries and veins. This collateral network must form intact, stable vessels that can regulate fluid and solute transport across their walls and respond to physiological stimuli. While vascular endothelial growth factor A (VEGFA, also known as VEGF) is the driver behind vessel growth (Senger *et al.*, 1983; Ferrara and Henzel, 1989) and its use in therapeutic angiogenesis emerged as a possible alternative treatment to surgery (Satoshi Takeshita *et al.*, 1994), trials in peripheral ischaemic disease saw no differences between placebo, and experimental groups (Rasmussen, Rasmussen and Macko, 2002; Saaristo, Suominen and Yla-Herttuala, 2005). Other angiogenic growth factors such as fibroblast growth factor (FGF), hypoxia inducible factor 1α (HIF-1α) and hepatocyte growth factor (HGF) have also been investigated. Clinical trials systemically administering recombinant human basic FGF had to be halted due to patients developing proteinuria (Belch *et al.*, 2011) although later studies using intra-arterial administration of FGF-2 showed improvement in patients' peak walking time (Lederman *et al.*, 2002). Similar to VEGF trials, a small pilot study suggested that HIF-1α would be tolerated well however in a larger randomised trial there was no difference between active and placebo groups (Lederman *et al.*, 2002). Interestingly, clinical trials involving HGF, which stimulates endothelial cell motility and growth, resulted in patients with improved ankle-brachial index and pain relief after two month which was still evident up to two years later (Morishita *et al.*, 2011; Makino *et al.*, 2012). The unexpected results of the clinical trials suggest that the formation of a vascular network is much more complex

than first thought and therefore a greater understanding of blood vessel physiology and the mechanisms involved in growth and remodelling is needed to create treatment regimens that will result in the development of functional collateral vessels.

1.2 Microvascular Structure

In the mature functional microvasculature, the microvascular wall forms a semi-permeable barrier which regulates the exchange of fluid and solutes between the blood and the tissues. The disruption of this barrier can lead to complications such as proteinuria, oedema and a drop in blood volume that can result in a dangerous fall in blood pressure. Therefore, an understanding of the structure and corresponding signalling mechanisms involved in the control of the barrier is key to both repairing a dysfunctional vascular barrier and ensuring that a competent barrier is formed and maintained during the neovascularisation and angiogenesis.

There are three types of microvascular beds; continuous, fenestrated and sinusoidal. Most microvessels take on the continuous phenotype and are found throughout the body including in the skin, muscle, brain and connective tissues. Fenestrated endothelia on the other hand, are found in tissues such as the kidneys where there are tissues that are associated with secretory and absorptive epithelia and have small openings called fenestrae of about 80-100nm in diameter (Levick and Michel, 2010). Sinusoidal, or discontinuous capillaries have large lumens, many fenestrations and a discontinuous or absent basal lamina

(Braet and Wisse, 2002). These capillaries are often found in the liver, spleen, lymph nodes and bone marrow. This thesis however, will focus on continuous endothelia.

1.2.1 Intercellular Junctions

The flattened, elongated endothelial cells that line the vascular wall overlap each other forming intercellular clefts. The clefts resemble a narrow channel with ~22nm between cells and take up ~0.2% of the cell surface allowing for strict control over paracellular transport (Michel and Curry, 1999; Adamson *et al.*, 2004). Within the clefts, the endothelial cells are held close together by junctional adhesion molecules which form tight and adherens junctions (Adamson and Michel, 1993; Adamson, Lenz and Curry, 1994; Fu *et al.*, 1994; Adamson *et al.*, 1998). Adherens junctions consist of calcium-dependent adhesion molecules known as cadherins. Endothelial cells express vascular endothelial (VE)-Cadherin and N-Cadherin although VE-Cadherin is seen to play a larger role than its counterpart. VE-Cadherin clusters at cell-cell contacts within the cleft and associates with the intracellular catenins β-catenin, p120 or plakoglobin thereby increasing cell adhesion (Dejana and Vestweber, 2013). In addition to promoting adhesion, VE-Cadherin can transfer intracellular signals maintaining vascular stability, for example by interacting with vascular endothelial growth factor receptor 2 (VEGFR2), the downstream proliferation signal of VEGFR2 through extracellular-regulated kinases 1 and 2 (ERK1 and ERK2) is inhibited and anti-apoptotic signals are maintained through

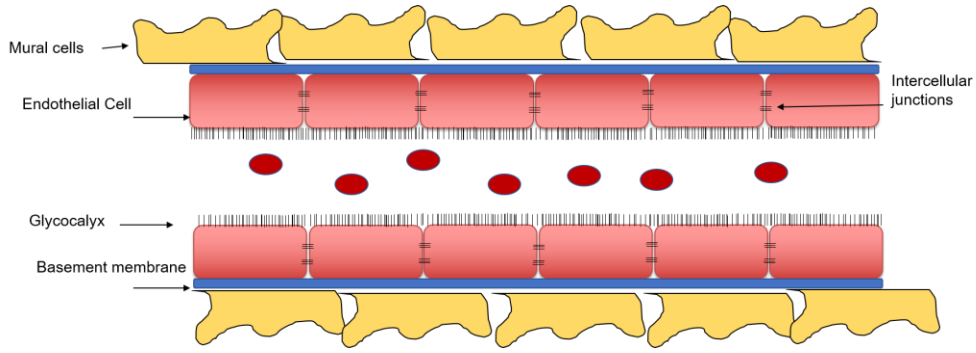


Figure 1.1 Schematic of the microvascular structure. *A cross-sectional view of the microvessel showing endothelial cells linked by adhesion and tight junctions. The endothelial cells are coated by a glycocalyx layer on the luminal surface and surrounded by mural cells on the abluminal side.*

protein kinase B (PKB) signalling (Lampugnani *et al.*, 2002, 2006). VE-Cadherin also regulates

adherens junction stability and the activation of Rho GTPase through its interaction with p120-catenin (Giannotta, Trani and Dejana, 2013) as well as contributing to cell polarity, formation of a lumen (Strilić *et al.*, 2009; Lampugnani *et al.*, 2010), the rearrangement of the cytoskeleton (Komarova and Malik, 2010) and gene transcription (Taddei *et al.*, 2008).

The Claudin family make up much of the tight junction transmembrane components. Their extracellular domains form the strands of tight junctions and exhibit homophylic and heterophilic adhesive actions (Wallez and Huber, 2008). Occludin, another component of the tight junction strands, is not strictly necessary for tight junction strand formation but is associated with increased tight junction barrier function (Hirase *et al.*, 1997). For instance, it has been to shown to be specifically expressed in the blood brain barrier (BBB) and the blood retinal barrier (BRB) and downregulation of occludin has been observed

in disease states such as stroke and diabetes which are associated with BBB or BRB disruption (Antonetti *et al.*, 1998; Erickson, Sundstrom and Antonetti, 2007). Decreased occludin was also seen in VEGF treated retinal endothelial cells and was accompanied by an increase in paracellular permeability (Antonetti *et al.*, 1998; Wachtel *et al.*, 1999).

Claudins and occludin link to intracellular partners such as zona-occludin (ZO) 1, 2 and 3, AF-6/afasdin, and PAR3 to form a molecular complex on the submembrane side of tight junctions. This complex, also known as the cytoplasmic plaque, links tight junctions to the cytoskeleton and enables signalling to aid junction assembly and control cell behaviour (Balda and Matter, 2016).

The junctional adhesion molecules (JAM)-A, -B, and -C are a family of adhesion proteins with immunoglobulin like domains that have also been associated with tight junctions although they are not directly involved in strand formation. They have been implicated in the regulation of angiogenesis, paracellular permeability, the recruitment of monocytes to injured vessel walls and the establishment of apical-basal polarity (Wallez and Huber, 2008; Balda and Matter, 2016).

A third type of intracellular junctions are the gap junctions. They are made up of connexin proteins which physically connect adjacent cell membranes. These physical connections allow the exchange of metabolites and the propagation of electrical signals via the transfer of second messengers (Nielsen *et al.*, 2012).

1.2.2 Basement Membrane

The microvessel basement membrane is made up of a complex matrix of proteins and fibres which includes; collagen type IV, perlecan, laminin, entactin and integrin (Yurchenco, 2011). It covers the abluminal surface of all microvessels, anchoring endothelial cells within the tissue. It can also act as an added barrier to leukocytes during immune surveillance and inflammation and some of the components of the matrix act as a go-between, shuttling signals between endothelial cells and support cells for maintenance, remodelling or growth of the vessel. For instance Notch3 signalling through integrins was shown to mediate smooth muscle cell adhesion to the basement membrane and so promote vessel maturation (Scheppke *et al.*, 2012).

1.2.3 The Glycocalyx

The glycocalyx is a carbohydrate-rich layer that is produced by endothelial cells and lines the luminal side of the endothelium. Its components include glycoproteins and proteoglycans which are bound to the endothelium, and soluble constituents which are linked to each other either directly or via soluble proteoglycan and/or glycosaminoglycans (Weinbaum, Tarbell and Damiano, 2007). Overall, the glycocalyx elicits a negative charge affecting its interaction with the components of the blood plasma. This can be seen by the red blood cell exclusion zone that runs parallel to the endothelium which thins when the glycocalyx is broken down (Reitsma *et al.*, 2007). The glycocalyx has been shown to be involved in the regulation of vessel permeability (Becker, Chappell and Jacob, 2010; Levick and Michel, 2010; Jacob

and Chappell, 2013; Alphonsus and Rodseth, 2014), attenuating the interaction of platelets and leucocytes (Henry and Duling, 2000; Vink, Constantinescu and Spaan, 2000; Mulivor and Lipowsky, 2009), endothelium shear stress protection (Florian *et al.*, 2003; Gouverneur *et al.*, 2006) and facilitating cellular signalling and enzyme modification through the binding of ligands and enzymes (Zhang *et al.*, 2009; Alphonsus and Rodseth, 2014).

1.2.4 Support Cells

Pericytes and vascular smooth muscle cells (VSMC) form the major support cells of the microvasculature. While pericytes are mainly found surrounding capillaries and post-capillary venules (von Tell, Armulik and Betsholtz, 2006), VSMC are found in the arterioles. Pericytes are known to stabilise new vessels upon their recruitment and are thought to be able to confer some contractile ability to their vessels (Yemisci *et al.*, 2009). They are also able to bind endothelial cells directly via gap junctions enabling cell-cell communication on top of secretory signals (Fujimoto, 1995; Ribatti, Nico and Crivellato, 2011). VSMC on the other hand surround the endothelium and regulate the vessel's tone and blood flow through the smooth muscle layer contraction and relaxation (Wang *et al.*, 2015).

All the structures described in this section play a role in the growth, maintenance and regulation of the microvasculature bed especially in terms of bestowing a resistance to water and solute flux across the vessel wall thereby contributing to permeability regulation.

1.3 Angiogenesis

The formation of new blood vessels from pre-existing ones, or angiogenesis, is a complex process involving several different molecules and signalling pathways (Carmeliet and Jain, 2011; Yoo and Kwon, 2013; Ribatti, 2014). It is a process that not only occurs in development but also in the adult in response to both physiological stimuli such as exercise and menstruation and during pathological situations such as cancer, diabetes and CVD. Thus, an understanding of the angiogenic process could be vital in the development of therapeutic strategies or stimulating the growth of a collateral network in pathologies such a CVD and 'normalising' the vasculature in other pathologies such as cancer.

There are two main pathways to form new vessels that have been identified, sprouting angiogenesis and non-sprouting or intussusceptive angiogenesis. The latter involves the formation of an endothelial pillar in the middle of the vessel which then extends either to split the pre-existing vessel in two, modify the branching angle or to prune a redundant, inefficient vessel (De Spiegelaere *et al.*, 2012; Mentzer and Konerding, 2014). Sprouting angiogenesis on the other hand, involves the formation of tip cells and stalk cells which 'sprout' from the existing vessel and grow towards the angiogenic stimulus eventually creating a new vessel (Eilken and Adams, 2010; Lee and Bautch, 2011; Ribatti and Crivellato, 2012).

1.3.1 Sprouting Angiogenesis

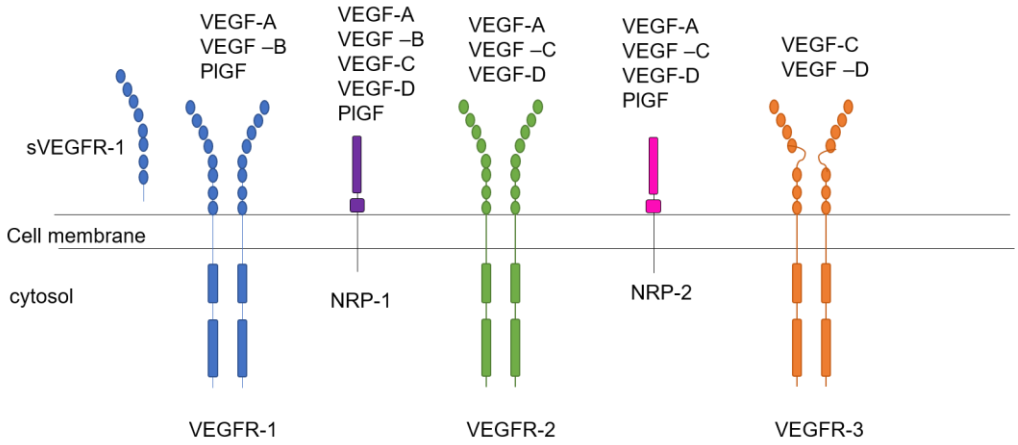


Figure 1.2 Schematic of the VEGF family. *The schematic shows the VEGF isoforms, VEGFA, VEGFB, VEGFC, VEGFD and PlGF and their binding to the receptors VEGFR1, VEGFR2, VEGFR3, NRP1 and NRP2. sVEGFR1 can act as a decoy receptor for VEGFA, VEGFB and PlGF reducing their biological actions.*

Vascular endothelial growth factor-A (VEGFA, also known as VEGF) has been established as the master regulator of angiogenesis as it has been linked to several aspects of this process. First identified as vascular permeability factor, VEGF is a well-known potent inducer of increased permeability (Senger *et al.*, 1983; Keck *et al.*, 1989; Bates and Curry, 1996) and can stimulate vasodilation due to its interactions with endothelial nitric oxide synthase (eNOS, Hood *et al.*, 1998; Kroll and Waltenberger, 1998). VEGF also has been shown to induce proliferation and differentiation in endothelial cells as well as being a marker for cell survival and deletion of just one allele leads to embryonic lethality signifying how vital it is (Carmeliet *et al.*, 1996; Shibuya, 2013).

VEGF is part of a family of growth factors that includes placental growth factor (PlGF), VEGFB, VEGFC, VEGFD and the viral VEGFE. A family

of tyrosine kinase receptors mediates the biological actions of the VEGFs. VEGFA binds to VEGFR2 and VEGFR1 whereas VEGFC and VEGFD bind VEGFR2 and VEGFR3. PlGF and VEGFB on the other hand only bind VEGFR1 and VEGFE only binds to VEGFR2 (Holmes and Zachary, 2005). The upregulation of VEGF during angiogenesis allows it to exert its potent permeability-increasing effects on the growing vessel as well as initiating several key angiogenic processes.

When an angiogenic stimulus occurs such as hypoxia, VEGF is upregulated, binds to VEGFR2 on the surface of endothelial cells inducing an angiogenic response. VEGF increases the permeability of the vessel which is mediated by the formation of fenestrations (Roberts and Palade, 1995), vesiculo-vacuolar organelles (Feng *et al.*, 1996; Hofman *et al.*, 2000) in addition to the redistribution of Vascular endothelial cadherin (VE-cadherin) which involves Src kinases (Esser *et al.*, 1998; Wallez *et al.*, 2007).

VEGF has also been shown to increase the expression of endothelial nitric oxide synthase (eNOS Bouloumié, 1999; Murohara *et al.*, 1998; Shen *et al.*, 1999), a calcium dependent enzyme which catalyses the production of nitric oxide (NO) from l-arginine (Zhao, Vanhoutte and Leung, 2015). The subsequent NO that is produced diffuses into the smooth muscle cells where it activates soluble guanylate cyclase. This then converts GTP to cGMP resulting in vasodilation seen during angiogenesis. It has also been shown to prevent platelet-derived growth factors from being released thereby inhibiting smooth muscle cell proliferation and the production of matrix molecules needed to keep the

vessel stable and therefore is considered as pro-angiogenic (Alheid, Frölich and Förstermann, 1987; Busse, Lackhoff and Bassenge, 1987; Radomski, Palmer and Moncada, 1987; von Tell, Armulik and Betsholtz, 2006).

This increase in permeability and diameter enables the extravasation of plasma proteins which create a provisional extracellular matrix (ECM) scaffold for migrating cells. The endothelial cells loosen their junctions allowing the vessel to dilate further and in response to integrin signalling endothelial cells migrate onto the ECM scaffold (Carmeliet and Jain, 2011). Angiogenic molecules which have been stored in the ECM such as VEGF, basic fibroblast growth factor (bFGF) and insulin-like growth factor-1 (IGF-1) are then liberated by proteases such as plasminogen activator, matrix metalloproteases (MMP, Carmeliet and Jain, 2011), chymases (Norrby, 2002) or heparanases (Carmeliet, 2003) and then remodel the ECM into an angio-competent environment. To prevent endothelial cells from migrating towards the stimulus en masse a leading endothelial cell is selected and takes on a tip cell phenotype (Carmeliet *et al.*, 2009; Siekmann *et al.*, 2013).

1.3.1.1 Dll4/Notch signalling in tip and stalk cell selection

Tip and stalk cell phenotypes were first described by Gerhardt *et al* (2003) despite filopodia studded cells at the angiogenic front having already been described by Kurz *et al* (1996) and Ruhrberg *et al* (2002) earlier. Tip cells are known to extend filopodia and migrate towards the angiogenic stimulus and have been shown to be characterised by increased expression of Dll4, VEGFR2, VEGFR3, Platelet derived

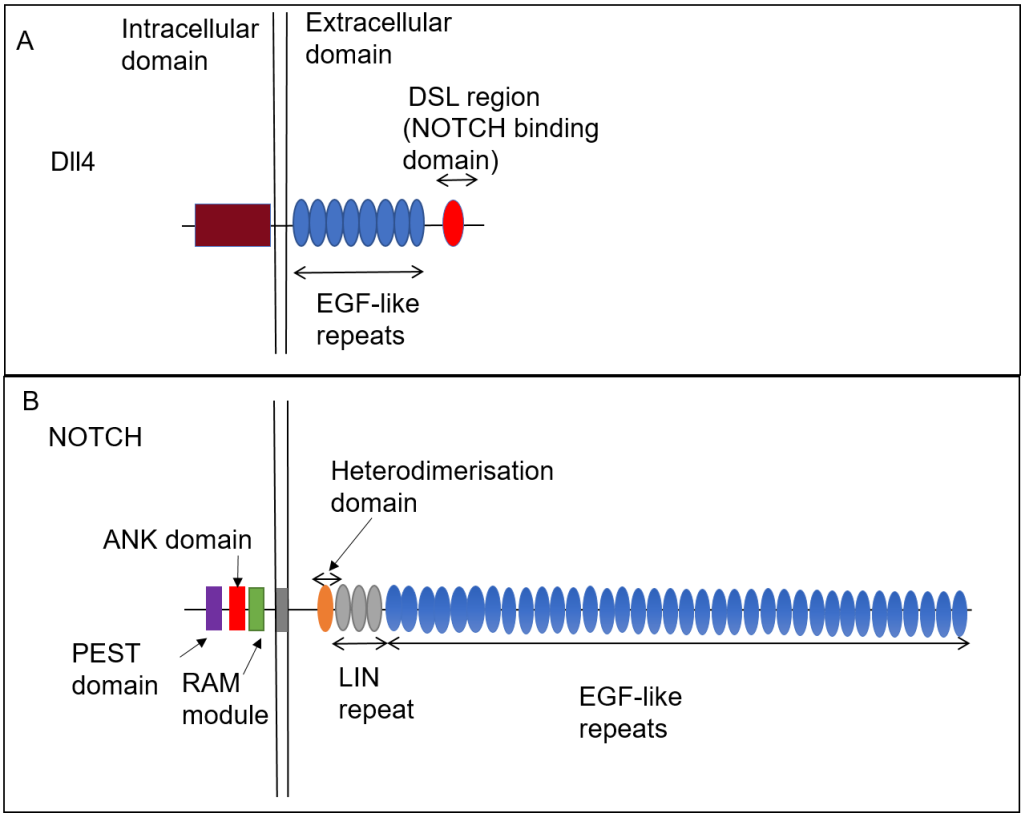


Figure 1.3 Structure of Dll4 and Notch. Dll4 *(A) is transmembrane protein consisting of an intracellular domain and an extracellular domain made up of 8 EGF-like repeats and a delta/serrate/Lag-1 (DSL) region which is critical for Notch binding. Notch (B) is also a transmembrane protein with an intracellular domain which includes a RAM (RBP-jκ associated module) module, an ANK (Ankyrin repeat) domain and a PEST (proline/glutamic acid/serine/threonine-rich motif) domain. The extracellular domain is made up of a heterodimerisation domain and 3 LIN repeats and 36 EGF-like repeats.*

growth factor-β (PDGF-β) and low levels of Notch and proliferation (Claxton and Fruttiger, 2004; Gerhardt *et al.*, 2003; Lu *et al.*, 2004; Siekmann and Lawson, 2007; Suchting *et al.*, 2007, see *Figure 1.5*). Stalk cells on the other hand, have increased proliferation, and expression of Notch, Jagged1 and VEGFR1 (Thurston and Kitajewski, 2008; Benedito *et al.*, 2009; Chappell *et al.*, 2009; Ribatti and Crivellato, 2012). However, both phenotypes are transient and using computer modelling Jakobsson *et al* (2010) demonstrated that endothelial cells

compete to become the tip cell and so the leading endothelial cell in the sprout constantly changes.

The major regulators of tip/stalk cell selection and sprouting is the ligand delta-like ligand 4 (Dll4) and its receptor Notch1. The Notch pathway is a highly conserved pathway from invertebrates (Kopan and Ilagan, 2009) to mammals and is based on ligand-activated receptor signalling between two adjacent cells. Mammals express the five canonical ligands delta-like ligand (Dll) 1, 3, 4 and jagged 1 and 2 and the four homologous receptors Notch 1-4. Four of the ligands, Dll1, 4 and jagged1 and 2, are expressed in vascular endothelial cells (Beckers *et al.*, 1999; Villa *et al.*, 2001; Sörensen, Adams and Gossler, 2009) whereas Dll3 is more pronounced in the foetus playing a role in somitogenesis (Turnpenny *et al.*, 2003; Ladi *et al.*, 2005). While Notch1 is expressed in many tissues including the heart and vascular endothelial cells (Baldi *et al.*, 2004), Notch4 is only found in vascular endothelial cells (Krebs *et al.*, 2000; Wu *et al.*, 2005) and Notch 2 and 3 are predominantly expressed in smooth muscle cells, where together they are involved in the maturation of smooth muscle (Wang *et al.*, 2012). In this thesis however, I will focus on the effects of Dll4 signalling through its receptor Notch1 (herein referred to as Notch).

Dll4 is a type 1 transmembrane protein with an extracellular domain which contains 8 epidermal growth factor (EGF)-like repeats and a delta/serrate/lag-2 (DSL) region that is vital for receptor binding (D'Souza *et al.*, 2010, see Figure 1.3A). It is a marker of arterial cell fate in endothelial cells during development and deletion of one allele results

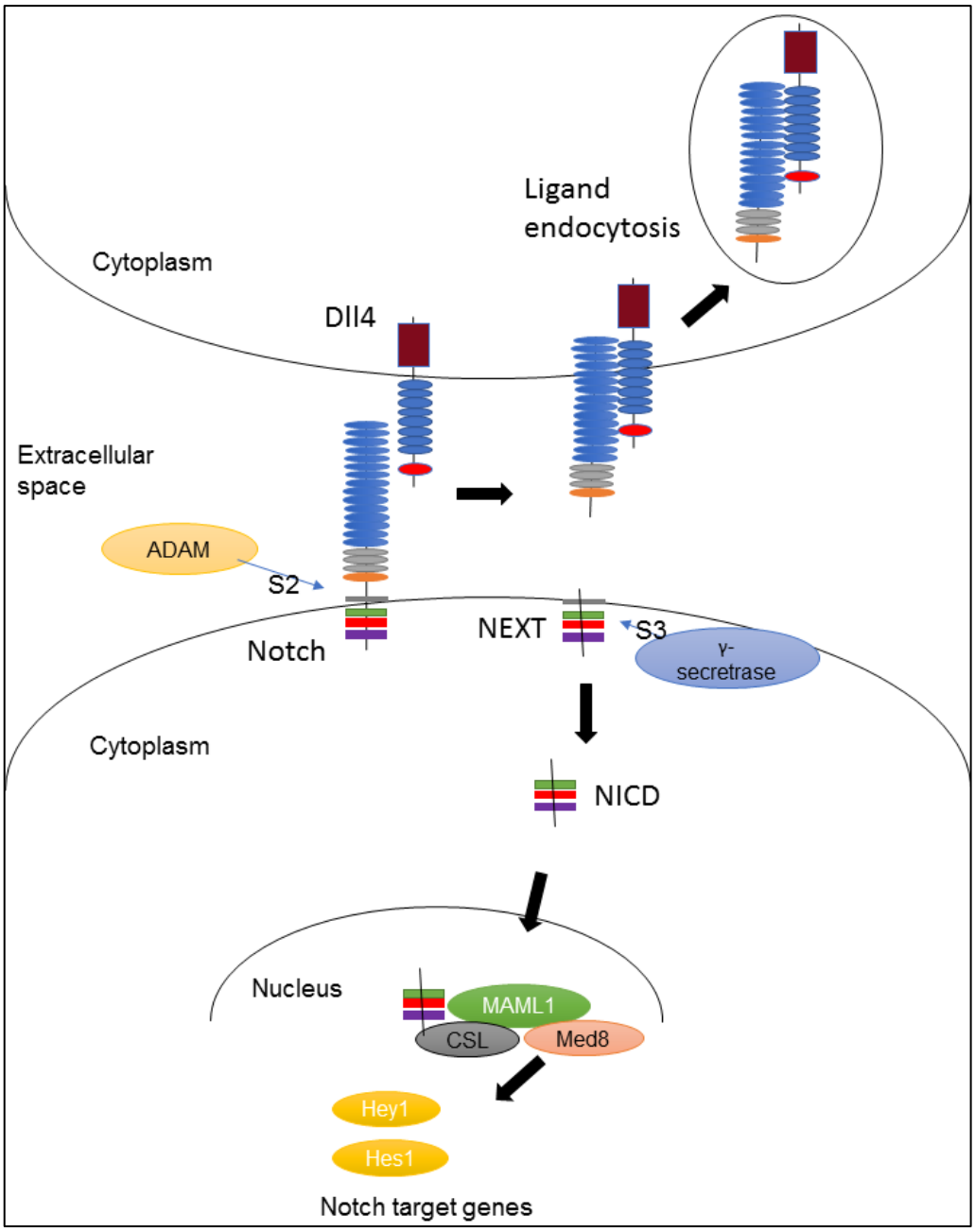


Figure 1.4 The Dll4/Notch Signalling Pathway. *Dll4 binds to Notch on an adjacent endothelial cell allowing ADAM to cleave Notch at S2. This releases the Notch extracellular domain which is subsequently endocytosed with Dll4. The remaining Notch extracellular truncation (NEXT) is then cleaved by γ- secretase releasing the NICD. The NICD then translocates to the nucleus where it associates with CSL and MAMl1 inducing targets genes such as Hes1 and Hey1.*

in embryo lethality due to vascular defects (Shutter *et al.*, 2000; Lawson *et al.*, 2001; Gale *et al.*, 2004). Its receptor, Notch, is a large single pass type 1 transmembrane protein. As part of the extracellular domain Notch contains 36 EGF-like repeats, which are followed by a negative regulatory region composing of 3 cysteine-rich Lin12-Notch repeats plus a heterodimerisation domain. There is also a transmembrane domain and an intracellular domain which comprises the recombining binding protein repressor of hairless (RBP-$_{j}\kappa$) associated module (RAM), nuclear localisation sequences, an Ankyrin repeats domain (ANK) and a transactivation domain that consists of a conserved proline/glutamic acid/serine/threonine-rich motif (PEST) (Kopan *et al.*, 2009, see Figure 1.3B).

The varying roles of the different Notch regions are beginning to be better understood; for example it is now known that the Notch EGF-like repeats 11-12 play a critical role in productive interactions (Rebay *et al.*, 1991) with ligands such as Dll4, which are presented by adjacent cells forming *trans* interactions, whereas EGF-like repeats 24-29 are involved in *cis*-inhibition whereby ligands expressed in the same cell limit the zone of Notch activity (Celis and Bray, 2000). However, more recent studies indicate that EGF-like repeats 11-12 are also needed for *cis*-inhibition suggesting a competitive mechanism for Notch-ligand interactions that result in either *trans*-activation or *cis*-inhibition (Cordle, Johnson, *et al.*, 2008; Becam *et al.*, 2010; Fiuza *et al.*, 2010). In addition, many of the EGF-like repeats can bind calcium ions and are important in shaping the structure as well as the affinity and efficiency of

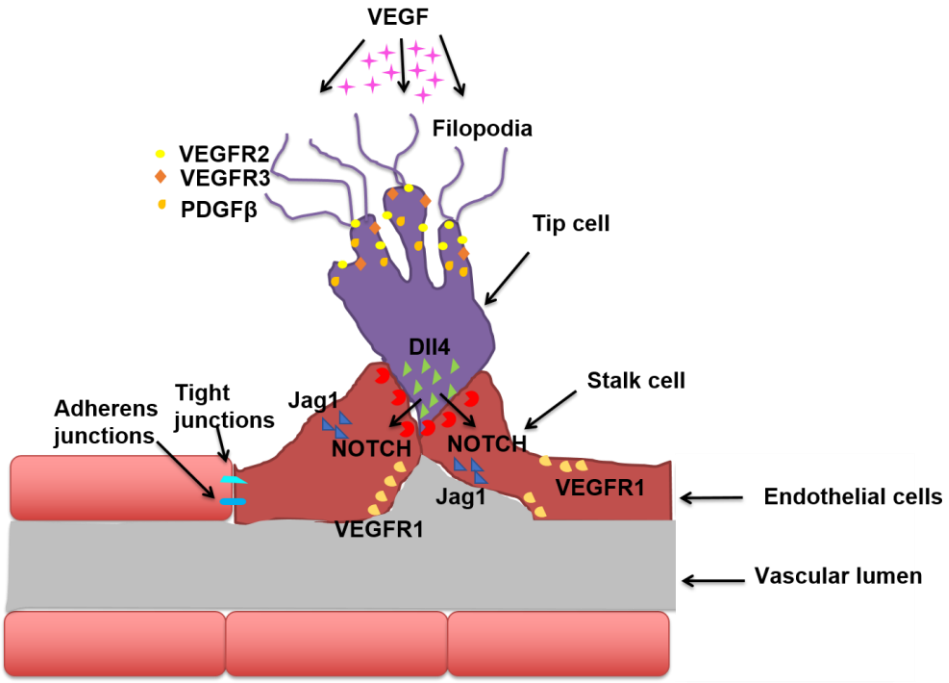


Figure 1.5 Tip and stalk cell selection in Sprouting angiogenesis. *VEGF binds to VEGFR2 on the endothelial cell surface membrane subsequently upregulating Dll4. Dll4 binds its receptor Notch1 on an adjacent endothelial cell thereby rescuing Dll4 expression and inducing a stalk cell phenotype while the Dll4 highly expressing cell takes on the tip cell phenotype. Tip cells also express high levels of VEGFR2, VEGFR3 and PDGFβ in addition to extending filopodia and migrating towards the angiogenic stimulus. Stalk cells on the other hand, express the Dll4 antagonist, Jag1 as well as VEGFR1 and are involved in endothelial cell proliferation and lumen formation.*

ligand and receptor binding (Raya *et al.*, 2004; Cordle, Redfield, *et al.*, 2008). Moreover, it has been found that the negative regulatory region is involved in preventing receptor activation in the absence of a ligand by concealing the 2nd cleavage site (S2, Sanchez-Irizarry *et al.*, 2004).

Tip cells are selected for by the signalling of VEGF through VEGFR2. This subsequently upregulates Dll4 inducing a tip cell phenotype in that cell and then Dll4 interacts with Notch on a neighbouring endothelial cell inducing a stalk cell phenotype. Upon ligand binding, a series of proteolytic cleavage events is induced, the first of which is catalysed by ADAM-family metalloproteases at site 2 (S2, S1 involves the proteolytic

cleavage by furin-like convertases which results in the production of the mature Notch polypeptide which subsequently translocates to the cell surface membrane, see *Figure 1.4*). This is located approximately 12 amino acids before the transmembrane domain and stretches deep within the negative regulatory region and is considered a regulatory step in Notch activation. This leaves the membrane bound Notch extracellular truncation (NEXT) which can then be cleaved by the enzyme complex γ-secretase. Cleavage occurs near the inner leaflet of the membrane (S3) and releases the Notch intracellular domain (NICD). Once released, the NICD translocates to the nucleus where it interacts with the DNA-binding protein CSL [CBF1/RBP-jκ/SU(H)/Lag-1] through the RAM domain. Following this the ANK domain is then able to associate with CSL to recruit the co-activator Mastermind/Lag-3 which in turn recruits the MED8 mediator transcription complex (Kopan and Ilagan, 2009; Andersson, Sandberg and Lendahl, 2011). Subsequently, the upregulation of downstream targets such as Hes (hairy enhancer of split) and Hey (hairy enhancer of split related with YRPW motif protein 1) are induced.

This signalling pathway is critical for the regulation of angiogenesis and disruption of this pathway such as the heterozygous deletion of Dll4 in mice or the inhibition of Notch by a γ-secretase inhibitor by Suchting *et al* (2007) led to increased tip cell and filopodia formation. Other studies which also inhibited either Dll4 or Notch from signalling also saw increased sprouting, proliferation and poor tissue perfusion (Hellstrom *et al.*, 2007; Scehnet *et al.*, 2007). On the other hand, blockade of

Dll4/Notch signalling appeared to prevent tumour growth which is enabled by tumour angiogenesis. Using a neutralising antibody Ridgway *et al* (2006) reported that tumour growth was inhibited and Noguera-Troise *et al* (2006) demonstrated that this was due to non-productive angiogenesis and the poor perfusion of new vessels seen when Dll4/Notch signalling is inhibited.

The signalling of Dll4/Notch in selecting tip and stalk cells during angiogenesis also affects the expression of several other molecules which help to characterise the two phenotypes. For example, VEGFR1 is upregulated by the induction of Notch signalling in stalk cells (Funahashi *et al.*, 2010; Krueger *et al.*, 2011) and reduces the ability of VEGF to signal with the cell in addition to releasing soluble VEGFR1 (sVEGFR1/sFlt1) which then binds to extracellular VEGF further reducing its availability to the sprout (Chappell *et al.*, 2009).

1.3.1.2 Lumen formation

Following sprouting and the formation of an endothelial cord, new vessels must create a lumen to allow for blood perfusion. This is a complex molecular mechanism that involves endothelial cell repulsion at the cell-cell contacts in the endothelial cell cord, intercellular junctional rearrangement and cell shape change (Iruela-Arispe and Davis, 2009). There have been two different mechanisms of lumen formation put forward; cord hollowing which involves endothelial cells adjusting their shape and junctions to open up a lumen, and pinocytic or cell hollowing where a lumen is formed by the coalescence of intracellular vacuoles which then interconnect with neighbouring

vacuoles, the latter of which is a swift way to create endothelial luminal spaces (Potente, Gerhardt and Carmeliet, 2011; Ribatti and Crivellato, 2012).

Following lumen formation by either or both mechanisms and in response to hemodynamic stimuli caused by shear stress the diameter of the lumen increases.

1.3.1.3 Remodelling and Pruning

In the wake of lumen formation, the subsequent homogenous web of endothelial cell tubes which make up the endothelial plexus usually number more than the vascular density needed. Therefore any unnecessary vessels are removed through a process of remodelling and pruning enabling a more differentiated vascular network to develop (Korn and Augustin, 2015). Remodelling is a complex process which results in the formation of large and small vessels, establishes the direction of flow and the association of mural cells.

The process of pruning involves removing the endothelial cells from redundant vessels and was first described in the embryonic retina by Ashton (1966). It is thought that one of the main initiators of pruning is the sensing of a drop in wall shear stress and pressure with the amount of pruning increasing as the pressure drops (Skalak and Price, 1996; Pries, Reglin and Secomb, 2005). Oxygen supply is also thought to be a key factor in blood vessel pruning especially in the retina (Stone *et al.*, 1995; Benjamin, Hemo and Keshet, 1998).

1.3.1.4 Pericyte Recruitment

Pericytes are adventitial cells that are embedded within the basement membrane of capillaries, pre-capillary arterioles, post-capillary venules and collecting venules (Van Dijk *et al.*, 2015). They make connections with endothelial cells described as peg-and-socket structures (Sainson and Harris, 2008) whereby pericytes form cytoplasmic elongations (the pegs) which are then inserted into invaginations of the endothelial cell and basement membrane (the sockets). These contacts are highly enriched in Connexin 43 mediated gap and N-Cadherin based adherens junctions (Winkler, Bell and Zlokovic, 2011).

The density of pericytes can vary greatly between different vascular beds with the ratio of pericytes/endothelial cells ranging from 1:100 in human skeletal muscles up to 1:3 in the central nervous system and 1:1 in the retina (Van Dijk *et al.*, 2015). The density appears to be organ specific and relates to the rate of endothelial turnover and how rigorous the endothelial barrier is. For example, in the vasculature that makes up the BBB, where it is critical that vessels are functional and do not leak, it was shown that the loss of pericyte coverage was associated with BBB breakdown (Bell *et al.*, 2010). In addition, pericyte recruitment was also shown to be vital for BBB formation during embryogenesis even before astrocyte recruitment and were a determining factor of vascular permeability (Daneman *et al.*, 2010).

To recruit pericytes to a newly formed vessel, endothelial cells secrete platelet derived growth factor (PDGF)-B. The receptor, PDGFR-β is expressed by pericytes and this signalling promotes pericyte precursor

cell proliferation and migration. The new vessel becomes stabilised and gains pericyte coverage by differentiated cells derived from the surrounding mesenchymal precursors or cells migrated from nearby vessels (Van Dijk *et al.*, 2015).

The recruitment of pericytes is essential for the stabilisation and maturation of newly formed vessels and the interactions between endothelial cells and pericytes are controlled by the Ang1-Tie2 system. The angiopoietins are a family of secreted glycoproteins which are mainly involved in angiogenesis and the subsequent maturation and stabilisation of the new vessels. There have been four angiopoietins that have been described; Ang1 and Ang2 which are expressed in the vasculature and Ang4 which is only expressed in the human lungs. Ang3 on the other hand, is only expressed in mouse tissues (Davis *et al.*, 1996; Maisonpierre *et al.*, 1997; Kim *et al.*, 1999; Valenzuela *et al.*, 1999; Lee *et al.*, 2004). The angiopoietins all signal through the receptor Tie2. The Tie1 receptor is still considered an orphan receptor although it has been shown to heterodimerise with Tie2 to regulate its activity (Fagiani and Christofori, 2013).

Ang1 and Ang2 are the most studied of the Angiopoietins. Ang1 has been shown to be predominantly antiangiogenic and is involved in mural cell (pericyte and vascular smooth muscle cell) recruitment and endothelial barrier integrity (Iivanainen *et al.*, 2003; Fagiani and Christofori, 2013). Found mainly in pericytes and VSMC, Ang1 phosphorylates Tie2 resulting in the upregulation of heparin-binding epidermal growth factor and the subsequent mural cell migration

(Iivanainen *et al.*, 2003). This Ang1-Tie2 signalling is vital for stabilisation and maturation of the vessel as deficiency of either Ang1 or Tie2 in mice during embryonic development resulted in death due to vascular defects. These included endothelial cells not associating with pericytes properly and defects in migratory responses leading to a lack of sprouting and remodelling (Suri *et al.*, 1996).

Conversely, the Ang1 antagonist, Ang2 is highly abundant in tip cells (Sundberg C *et al.*, 2002) and aids the destabilisation of vessels during the initial stages of angiogenesis (Maisonpierre *et al.*, 1997). Its binding to Tie2 in competition with Ang1 does not induce Tie2 downstream signalling and therefore leads to dissociation of pericytes and vessel destabilisation (Li, Zhang and Kirsner, 2003; Zhang *et al.*, 2003; Cao *et al.*, 2007).

Notch signalling is also involved in pericyte recruitment, however unlike the sprouting process which is under the control of Notch1, pericytes express Notch3. The importance of Notch3 in pericyte recruitment is apparent in patients suffering from CADASIL (cerebral autosomal dominant arteriopathy with subcortical infarcts and leukoencephalopathy) syndrome which is associated with Notch3 mutations and lack of pericytes (Louvi, Arboleda-Velasquez and Artavanis-Tsakonas, 2006). Studies using small interfering RNA (siRNA) to knockdown Notch3 reported that this signalling is important for mural cell differentiation and contributes to the pro-angiogenic ability of mural cells co-cultured with endothelial cells (Liu, Kennard and Lilly, 2009). More recently, Schulz *et al* (2015) demonstrated that Dll4

signalling through Notch3 enhanced pericyte adhesion to endothelial cells and limited the migratory and invasive behaviour of mural cells suggesting a further role for Dll4 in vessel stabilisation and maturation.

1.3.2 Arteriolargenesis

Arteriolargenesis, or capillary arterialisation, is the formation of muscular arterioles from capillaries (Benest *et al.*, 2008). It mainly involves the recruitment of smooth muscle cells and the enlargement of the vessel and usually occurs in parallel or following pericyte recruitment in a continuation of vascular stabilisation and remodelling to develop a functional network. Arterioles link the capillaries to the arteries and have been suggested to be important in the collateral growth of the vasculature in ischaemia (Ziegler *et al.*, 2010; Silvestre, Smadja and Levy, 2013).

Although this process has not been studied as intensely as angiogenesis, it is beginning to be better understood. The enlargement of the vessel is thought to be triggered through an increase in shear stress (usually due to increased blood flow) leading to upregulation of eNOS and subsequent relaxation of the vessel by NO (Dimmeler *et al.*, 1999; Davis *et al.*, 2001; Sandoo *et al.*, 2010). As in pericyte recruitment in the latter stages of angiogenesis, Ang1-Tie2, TGFβ and PDGF-B signalling are all also important for the recruitment and differentiation of VSMC which then form muscular layers around the vessel (Nishishita and Lin, 2004; Wang *et al.*, 2015; Gerthoffer, 2016; Baeten and Lilly, 2017). The smooth muscle layer then allows the vessel to regulate its tone and thus the flow of blood through it.

Using the rat mesentery angiogenesis assay to study arteriolargenesis by overexpressing eNOS, Ang1 and VEGF, Benest *et al* (2008) reported that this overexpression resulted in an increase in vessels, although only when they were combined did they see vessels with smooth muscle cells in addition to a further increase in functional vessels. Stone *et al* (2016) then went on to investigate how Ang1 and VEGF contribute to eNOS mediated flow induced growth. They found that inhibition of Ang1 or VEGF inhibited eNOS mediated growth and VSMC recruitment. They also reported that exogenous Ang1 could induce VSMC recruitment in the presence of increased flow whereas endogenous and not exogenous VEGF was required in NO-Tie mediated vessel growth.

The Notch ligand Dll4 is known to be a marker for endothelial cell arterial differentiation during development (Shutter *et al.*, 2000; Cristofaro *et al.*, 2013) and has been reported to be abundant in mature arterioles (Lobov *et al.*, 2007; Bernier-Latmani *et al.*, 2015). While Dll4 has not been directly implicated in arteriolargenesis when the Notch Ankyrin repeat protein, which negatively regulates Notch, was deleted there was a reduction in blood flow and an increase in vessel regression as well as a downregulation of the vasoconstrictor angiotensin (Lobov *et al.*, 2007) indicating it plays a role in remodelling and maturation. In addition, Notch1 has been reported to be able to induce smooth muscle actin expression and activate smooth muscle cells (Noseda *et al.*, 2006) and Dll4 has been implicated in the regulation of bone marrow-derived pericyte/VSMC formation (Stewart *et*

al., 2012) providing an insight into a possible role for Dll4 in VSMC recruitment. While the above studies shed some light on arteriolargenesis this complex process may require a fine balance of different signals, and that that balance has not yet been defined and so therefore I set out to investigate this.

1.4 Microvascular Permeability

One of the major roles of the vascular wall is to regulate the exchange of fluid and solutes between the blood and tissues, or its permeability. All mature, functional vessels have this ability even during growth and remodelling, however it often becomes dysregulated in disease states such as cancer or cardiovascular disease. The accurate measurement of a vessel's true permeability to both water and solutes to aid the understanding of the mechanisms involved in permeability regulation has proven a complex process to unravel and began over 100 years ago.

1.4.1 The Formation of the Starling Hypothesis

In 1896 Ernest Henry Starling injected isotonic saline into the interstitial compartment of a dog hindlimb. The fluid was then absorbed and appeared in the venous blood where it became haemodiluted. However, when he injected serum instead of saline, the serum was not absorbed. This led him to conclude that microvessel walls are semipermeable membranes which allow the movement of water and small solutes but impede the movement of macromolecules such as proteins (Starling, 1896). He then went on to propose that the fluid movement across the

microvessel walls is dependent upon a net imbalance between the oncotic pressure of the plasma proteins and the hydrostatic pressure of the blood (reviewed in Levick and Michel, 2010) and thus identified the major forces involved in fluid and solute exchange between the tissues and blood in the capillary endothelium. The forces are; capillary (P_c) and tissue (P_t) hydrostatic pressures and the blood plasma (Π_p) and tissue (Π_t) oncotic pressures.

Starling's hypothesis was then originally tested through studies conducted by Landis (1927) and Pappenheimer and Soto-Rivera (1948). Landis developed a method for measuring the hydrostatic pressure in single capillaries of the frog mesentery using a glass micropipette connected to a manometer. When he occluded the cannulated vessel, he noticed that the red blood cells moved either towards or away from the point of occlusion such that their velocity was directly proportional to the rate of filtration or absorption of the fluid. From these experiments, Landis concluded that there was a linear relation between capillary filtration rate (J_v) per unit endothelial area (A) and capillary hydrostatic pressure (P_c).

Pappenheimer and Soto-Rivera (1948) went on to provide further evidence. They perfused the isolated hind limbs of cats and dogs to investigate the movement of fluid between the blood and tissues. Through the continuous recording of the hindlimb weights they could estimate the filtration of fluid from the blood into the interstitium and demonstrated that this was proportional to the hydrostatic pressure but inversely proportional to the colloid osmotic pressure of the blood. It

seemed that Starlings hypothesis had been confirmed and could be summarised in an equation of the linear relationship between the filtration rate and capillary hydrostatic pressure:

Equation 1

$$\frac{J_v}{A} = L_p[(P_c - P_i) - (\Pi_c - \Pi_i)]$$

Where J_v/A is the filtration rate per unit area of capillary wall; L_p is the hydraulic conductivity or permeability of the capillary wall; P_c and P_i are the capillary and interstitial fluid (ISF) hydrostatic pressures; and Π_c and Π_i are the capillary plasma and ISF colloid osmotic pressures.

1.4.2 Osmotic Refection Coefficient

Staverman's osmotic reflection coefficient (σ) is a measure of how easily the solute and the solvent of a solution can pass through a membrane. If the membrane is a true semipermeable membrane in that it is completely impermeable to the solute but is permeable to the solvent, σ of the membrane to the solution is 1.0 whereas, if the concentration of the solution leaving the downstream surface of the membrane is the same as that entering upstream σ = 0. Often used as a correction factor to correct for the ineffectiveness of the oncotic pressure gradient due to capillary permeability to some but not all plasma proteins, σ can be incorporated into Equation 1 to form Equation 2;

Equation 2

$$\frac{J_v}{A} = L_p[(P_c - P_i) - \sigma(\Pi_c - \Pi_i)]$$

However, plasma and the ISF both contain many solutes thus the equation should be written as:

Equation 3

$$\frac{J_v}{A} = L_p\{\Delta P - \Sigma\sigma_n \Delta\Pi_n\}$$

Where $\Sigma\sigma_n\Delta\Pi_n$ represents the sum of the differences in osmotic pressure exerted across the vessel walls by all the solutes in plasma and ISF (species 'n'); ΔP and ΔΠ is the difference between hydrostatic and oncotic pressures across the membrane. In the majority of microvessels only the macromolecular solutes are found in largely different concentrations whereas the small solutes generally have a σ value of 0.1 or less. Under these conditions the filtration rate per unit area of capillary can be described using Equation 2 (Levick and Michel, 2010).

1.4.3 Pore Theory

The concept of fluid and solute exchange across the capillary wall via pores was first introduced in the 1950's by Pappenheimer *et al* (1951). Upon observing that the solute concentration of capillary ultrafiltrate is lower than blood plasma, as well as the ultrafiltrate's similarity to when filtered through an inert artificial porous membrane they predicted that small hydrophilic solutes diffuse across the capillary walls through

water-filled channels or pores with a radius ~40nm. They proposed that these pores were represented by the clefts between endothelial cells (at least in continuous endothelia) and that they would hinder the movement of solutes more than fluid.

Grotte (1956) and Mayerson *et al* (1960) then went on to present evidence for a bimodal size selectivity of the barrier partitioning blood from lymph. Following arterial injection of dextran, Grotte measured the dextran lymph concentration and found dextran molecules of a similar size to or smaller than albumin had a more rapid decrease in lymph to plasma concentration than dextran molecules which were larger than albumin. He then proposed that this meant there were two distinct porous pathways, one consisting of a small number of large pores with a radius of 15-30nm and the other consisting of a higher frequency of small pores.

Later the Aquaporin's were discovered. They are found in continuous endothelial where they form small pores that are exclusive to water and contribute ≤10% of the hydraulic conductance in most capillaries outside of the blood-brain barrier and skeletal muscles (Michel and Curry, 1999) although Watson and Wolf (1989; 1996; 2002) argued that their contribution could be as high as 45-50%. The large pore pathway on the other hand, was shown to be controlled by the reflection coefficient (σ) and solute permeability (P_s) to macromolecules (Curry, 1984).

1.4.4 Accounting for the Glycocalyx

The idea that a luminal barrier is involved in the regulation of permeability was first put forward over 60 years ago (Chambers and Zweifach, 1947), however it was not until 1966 using the dye ruthenium red to preserve mucopolysaccharides that this luminal barrier, or the glycocalyx, was first visualised by electron microscopy (Luft, 1966). After Louden *et al* (1979) and Clough and Michel (1979) reported that ferritin was omitted from the intercellular cleft entrance in addition to vessel fenestrations and cytoplasmic vesicles being found to be lined by the glycocalyx (Shirahama and Cohen, 1972), Curry and Michel (1980) developed the fibre-matrix junction-break permeability theory.

They proposed that ‘the molecular sieving properties of the capillary wall resides in a matrix of molecular fibres which covers the endothelial cells and fills the channels through or between them’ (Curry and Michel, 1980). They recognised that although the number of transcapillary channels varies from one site to another in the capillary bed that the structural organisation of the glycocalyx is similar in all capillaries and therefore the frictional resistance of the channels remains constant. This helped explain why the permeability and filtration coefficients measured on single capillaries were markedly varied but the porosity of the capillary wall which was assessed either by the ratio of permeability to filtration coefficient or as the σ to macromolecules appeared to be constant (Renkin *et al.*, 1977; Michel, 1979). A major concept of the fibre-matrix junction-break model is that it is the glycocalyx where the oncotic pressure gradient is exerted and not the entire barrier (Michel

and Phillips, 1987). Adamson *et al* (2004) and Hu *et al* (2000) then took this concept forward and tested it using the Landis-Michel technique in both frog and rat mesenteric microvessels. They found that when the interstitial tissue oncotic pressure (Π_i) was changed but the oncotic pressures in the cannulated vessel were kept the same there was very little change to the outward filtration of water which contradicted the standard Starling equation (Equation 3). The equation was subsequently revised with the new model of permeability proposing that the oncotic pressure difference driving the continuous convection of fluid was achieved through the steric exclusion of plasma proteins during the convective flow across the glycocalyx. This would result in the ultrafiltrate having a low oncotic pressure when entering the 'sub-glycocalyx space' on the intercellular junction (Π_g) whereas at the luminal side of the glycocalyx there would be a relatively high oncotic pressure (Π_c). In addition, this would also prevent proteins in the ISF from diffusing back into the intercellular cleft unless the outward flow of the ultrafiltrate slowed, stopped or reversed. In which case it would be expected that the Π_g would be increased by the proteins diffusing into the intercellular cleft and thus reducing absorption (Levick and Michel, 2010). The revised equation therefore appears as follows;

Equation 4

$$\frac{J_v}{A} = L_p\left[(P_c - P_i) - \sigma\left(\Pi_c - \Pi_g\right)\right]$$

1.4.5 Putting the Starling Equation into Practice

As described earlier, Landis first measured filtration rates in single capillaries of frog mesenteric microvessels using glass cannulation micropipettes connected to a manometer and red blood cells as flow markers. He demonstrated that the filtration rate (J_v/A) increased linearly in response to changes to capillary hydrostatic pressure (Landis, 1927). Later this technique was modified in order to measure hydraulic conductivity of the vessel (L_p) and reflection coefficient (σ). A version of the technique is now termed the Landis-Michel technique (Curry, 1974, 1984; Michel *et al.*, 1974; Mason *et al.*, 1979; Curry, Huxley and Adamson, 1983; Michel and Curry, 1999). In this modified version, through measuring the J_v/A at various hydrostatic pressures while keeping the oncotic pressure constant the L_p could be determined from the slope of the linear relationship between the hydrostatic pressure (x) and J_v/A (y). The reflection coefficient could then be calculated when J_v/A was extrapolated to zero as at this point the hydrostatic pressure within the vessel equals that created from the oncotic pressure only and the concentration of protein in the vessel can be controlled.

Being able to quantify these two permeability coefficients accurately using carefully controlled conditions has enabled a greater understanding of structures of the capillary wall and signalling mechanism involved in regulating vessel permeability. For example, using this technique Bates *et al* (1996) were able to record direct measurements of permeability coefficients after exposure to VEGF for

the first time confirming that VEGF acts both acutely and chronically in increasing permeability. Platelet-activating factor (PAF), a modulator of the inflammatory response, was also shown to increase permeability on rat mesenteric venules (Victorino, Newton and Curran, 2004) whereas sphingosine1-phosphate can inhibit the permeability effects of PAF (Minnear, Zhu and He, 2005). Other permeability increasing agents include nitric oxide synthase induced shear stress (Kim, Harris and Tarbell, 2005) as well as ATP and caffeine which act by inducing endothelial Ca^{2+} store release (Glass and Bates, 2004). Other molecules, such as cyclic adenosine monophosphate (cAMP) and Ang1 have been shown to decrease microvascular permeability (He, Zeng and Curry, 2000; Salmon *et al.*, 2009) and further studies revealed that this occurred through the prevention of the small GTPase Rac1 inhibition and TRPC1-dependent Ca^{2+} influx inhibition respectively (He and Curry, 1993; Waschke, Drenckhahn, Adamson, Barth, *et al.*, 2004; Jho *et al.*, 2005; Aslam *et al.*, 2014).

This technique has also aided our understanding of the microvasculature ultrastructure both directly such as Heupel *et al* (2009) who used a tandem peptide to strengthen VE-Cadherin signalling and reported that perfusion abolished permeability increases seen by tumour necrosis factor-α (TNF-α) and indirectly for example Adamson *et al* (1998) demonstrated that the reduction in permeability by cAMP was associated with an increase in tight junction through visualisation of the same tissue by electron microscopy. This coupling of L_p measurements with electron microscopy has also furthered our

knowledge of the glycocalyx and how molecules such as pronase and Ang1 increase and decrease its coverage (Adamson, 1990; Salmon *et al.*, 2009). However more recently a modified version of the Landis-Michel technique has been developed that enables the visualisation and measurement of the glycocalyx layer and the vessels' permeability to solutes *in vivo* hopefully enabling further understanding of glycocalyx interactions (Betteridge *et al.*, 2015).

1.4.6 Microvascular Permeability in Disease

Increased microvascular permeability can be an added complication in many diseases. For instance, in cancer the tumour vasculature is regularly leaky resulting in oedema formation around the tumour tissue and in age-related macular degeneration, the associated oedema contributes to the patient's poor vision (Erickson, Sundstrom and Antonetti, 2007; Azzi, Hebda and Gavard, 2013). Additionally, a common symptom of diabetes mellitus is proteinuria which occurs due to the degradation of the glycocalyx and thus an increase in permeability (Nieuwdorp *et al.*, 2006; Salmon and Satchell, 2012).

As the understanding of permeability regulation increased, focus switched to potential therapeutic targets. To reduce leaking and thus oedema a novel strategy involving the 'normalisation' of vessels was put forward whereby inducing the stabilisation and maturation of the problematic vessels would prevent further leakage and enable easier delivery of drugs (such as chemotherapeutics in cancer) to treat the other symptoms and causes of the pathology. As VEGF is a potent inducer of permeability therapeutic antibodies against it were developed

to reduce permeability back to pre-pathological levels (Jayson *et al.*, 2002; Avery *et al.*, 2006). While the antibodies succeeded in reducing permeability (Lichtenbeld *et al.*, 1999), clinical trials resulted in greater interpatient variability than first expected indicating complexity of permeability regulation (Jayson *et al.*, 2002). More recently, the therapeutic potential of Dll4 has been under investigation. It has been found to be more highly expressed in tumour vasculature compared to normal vessels and it was postulated that its signalling through Notch was contributing to the anti-VEGF resistance that has been seen (Brzozowa *et al.*, 2013). Dll4 blockade led to inhibition of tumour growth but the formation of non-functional vessels (Noguera-Troise *et al.*, 2006; Ridgway *et al.*, 2006). Other tumours treated with Dll4 inhibitors resulted in reduced pericyte coverage and increased vascular leakage associated with impaired vascular integrity giving support for Dll4 targeted therapies for cancer treatment (Djokovic *et al.*, 2010; Kalén *et al.*, 2011) with the possibility of future treatment crossover for other pathologies where increased permeability is associated such as age-related macular degeneration, diabetes and cardiovascular disease.

1.5 Hypothesis and Aims

It is clear that the formation of a mature, functional vasculature is not subject to VEGF regulation only but involves a multitude of signals. The recent insights into Dll4's roles outside of tip and stalk cell regulation suggest it plays a greater part in the formation, maturation, remodelling and maintenance of the vasculature. I therefore set out to investigate the hypothesis:

"The physiological characteristics of newly formed vasculature are regulated by Dll4 during physiological and pathological angiogenesis."

To address this hypothesis, I designed a series of experiments performed in three stages:

1. Initially, I investigated how the induction of Notch signalling by Dll4 effects endothelial barrier integrity. Firstly, I tested how Dll4 effects the formation of both tight and adherens junctions. I then went on to test the hypothesis that the induction of Notch signalling by Dll4 reduced permeability in rat mesenteric microvessels using the Landis-Michel technique before further investigating the mechanism by which this occurs.

2. I then investigated how Dll4/Notch signalling affects physiological angiogenesis and arteriolargenesis through the injection of an adenovirus encoding the extracellular portion of Dll4 into the fat pad of the rat mesentery. This would be testing the hypothesis that Notch induction by Dll4 would lead to a more mature vasculature.
3. Finally, I investigated Dll4/Notch signalling in a pathological angiogenic model of hindlimb ischaemia testing the hypothesis that Dll4 aids the formation of a collateral vasculature network post ischaemic injury.

Chapter 2: Methods and Materials

2.1 List of Materials Used

Material	Purchased	Material	Purchased
Cell lines		**Adenoviruses**	
Human dermal blood endothelial cells	Promocell	Ad.sDll4	Vector Biolabs
Normal human dermal fibroblasts	Promocell	All other adenoviruses	already present in the lab
Chinese hamster ovarian cells	ATTC	Virus purification kit	AdEasy
Human embryonic kidney cells	ATTC	Benzonase nuclease	EMD Millipore
Cell culture		**Recombinant protein**	
MV endothelial media + supplement pack	Promocell	recombinant sDll4	Sigma
alpha minimum essential medium	Sigma	recombinant Dll4	R&D
Dulbecco's modified eagle's medium	Sigma	recombinant $VEGF_{165}a$	R&D
Foetal calf serum	Sigma	H89 di-hydrochloride	R&D
L-Glutamine	Sigma	**Imaging**	
PBS	Sigma	Confocal Microscope	Leica Confocal SPC system
1 x Trypsin-EDTA	Sigma	ImageJ analysis software	ImageJ
DMSO	Sigma	**Animals**	
13mm + 19mm coverslips	VWR international	Male Wistar Han rats	Charles River
fibronectin	Sigma	Male Wister rats	Charles River
Vectashield	H-1000, Vector Laboratories	Male C57B6	Charles River

Antibodies		**Lp**	
polyclonal rabbit anti-VE Cadherin	ab33168, Abcam	NaCl	Fischer
Donkey anti-rabbit Alexa fluor 555 and 488	life technologies	KCl	Sigma
rabbit anti-ZO1	Abcam	NaHCO3	Fischer
rabbit anti-NICD	Abcam	MgSO47H2O	Fischer
phalloidin conjugated Alexa fluor 488	life tecnologies	CaCL22H2O	Fischer
DAPI	life tecnologies	D-glucose	Fischer
goat anti-mouse anti-Dll4	AF1389 R&D systems	HEPES acid	Sigma
Ki67 antibody	abcam	HEPES salt	Sigma
Streptavidin Alexa fluor 555	life technologies	0.2µm pore filter	sartorius Stedim Biotech
alpha smooth muscle actin-cy3	Sigma	borosilicate glass capilaries	Havard Apparatus
anti-VDAC	Abcam	microelectrode puller	PE-22, Narishige
RNA Extraction & PCR		grindstone	Narishige
TRI reagent	Sigma	syringe pump	Narishige
Nano drop	Thermofisher scienctific	All tubing	fischer
RQ1 10x Rnase-free Dnase buffer + stop reagent	promega	all connetors	Fischer
Prime script RT kit	Takara	vaccum pump	SLS
thermocycler	Applied Biosystems Veriti Thermal Cycler	waterbath	grant instruments
lightcycler 480 SYBR green 1 Master	Roche	waste bottle	Fischer
human Hes1 primers	Qiagen	dripper bottle	Fischer
Human Hey1 primers	Qiagen	Rat Tray	Custom, Medical Engineering

Human GAPDH primers	Qiagen	inverted light microscope	Leica DM IRB
lightcycle 480 instrument	Roche	micromanipulator	Scientifica
QX200 Droplet Digital PCR System	BioRad	video camera	Panasonic HC-X920
ddPCR reaction kit	BioRad	light sources	thorlabs
QuantaSoft ddPCR anaylsis software	BioRad	c-mount	leica
Western Blots		**Mesenteric Angiogenesis Assay**	
RIPA buffer	Sigma	Hamilton syringe	Sigma
protein inhibiter cocktail	Sigma	monastral blue	Sigma
Bovine serum albumin	Santa Cruz Biotechnology	PFA	Sigma
Bradford assay dye	BioRad	Triton x-100	Sigma
Acrylamide	Sigma	MgCl2	Sigma
ammonium persulphate	Sigma	CaCl2	Sigma
SDS	Sigma	MnCl2	Sigma
TEMED	Sigma	biotinylated isolectin B4	Sigma
isopropanol	Sigma	Hindlimb Ischaemia	
TRI-HCl	Sigma	hair removal cream	veet sensitive skin
SDS-Page loading buffer	Sigma	colour laser speckle imaging apparatus and software	FLIP2, Moor Instruments
precision plus dual colour protein prestained standards	BioRad		
Western Blot electrophoresis and transfer equipment	BioRad		
PVDF membrane	Thermofisher scienctific		
Transfer buffer	BioRad		
Tween 20	Sigma		

TBS	BioRad		
Donkey anti-rabbit western secondaries	licor		
donkey anti-goat western secondaries	licor		
Odyssey imaging system	licor		
image studio software	licor		

All anaesthetic, buprenorphine and surgical equipment was purchased through the Nottingham University Bio-Support unit.

2.2 Cell Culture

2.2.1 Cell Lines

Human dermal blood endothelial cells (HDBEC) are microvascular endothelial cells of arterial decent and were purchased from Promocell. They were used in *in vitro* assays to represent the endothelial cells seen in *in vivo* situations. Normal human dermal fibroblast cells (NHDF) were also purchased from Promocell. These cells were used in the *in vitro* angiogenesis assay to produce an ECM for the HDBECs to use as a scaffold to form endothelial cell cords and eventually tubes. Chinese hamster ovarian cells (CHO) and human embryonic kidney 293 cells (HEK) were purchased from ATTC. CHOs were used to produce adenovirus conditioned media and HEK cells were used for adenovirus expansion and titration as the adenovirus causes these cells to die

following virus replication allowing simple recovery of the virus following expansion.

2.2.2 Sub-culture

HDBECs were cultured in MV endothelial media (supplemented with 5% (v/v) Foetal calf serum, 0.4% (v/v) endothelial cell growth serum, 10ng/ml recombinant human epidermal growth factor and 1µg/ml hydrocortisone, Promocell) and CHO cells in alpha minimum essential medium (αMEM) supplemented with 10% (v/v) Foetal calf serum (FCS) and 2mM L-Glutamine. HEK293 and NHDF cells were cultured in Dulbecco's modified eagle's medium (DMEM) with 10% (v/v) FCS and 2mM L-Glutamine. All cells were incubated at 37℃ in a humidified 5% CO_2 atmosphere unless otherwise stated.

Prior to routine passage or experimental manipulation media was discarded and cells were first washed with PBS and then detached from the cell culture flasks or plates using 1 x Trypsin-EDTA. Cells were incubated for approximately 5 minutes at room temperature and the flask tapped to ensure all cells detached. They were then neutralized by addition of 8ml of media to every 1.5ml of trypsin used. Detached cells were then either seeded into new culture flasks in a 1:3 manner for general culture and stock expansion or taken forward for counting prior to seeding for experimental manipulation.

2.2.3 Cell Counting

To quantify the number of cells in a flask or plate ready for seeding cells were counted using a haemocytometer chamber. First detached cells

(as described above) were centrifuged (1200xg) for 5 minutes to create a pellet. The media was then discarded and cells were re-suspended in 1ml of media. 10µl of the res-suspended cell solution was then added into the haemocytometer and the average number of cells per millilitre was calculated.

2.2.4 Cryopreservation of Cells

To create a stock, cells were cooled to sub-zero temperatures in a solution containing the cryopreservant dimethyl sulphoxide (DMSO). Cells were cultured to 80% confluence and then detached from the adherent surface of the culture flasks as described above. The cell suspension was centrifuged (1200xg) for 5 minutes and the resulting cell pellet was re-suspended in freezing medium (90% FCS, 10% DMSO). The solution was then aliquoted into cryovials before being placed into a “Mr Frosty” freezing container filled to the appropriate level with isopropanol and frozen overnight a -80℃. The following day frozen vials were transferred to the -150℃ freezer.

2.2.5 Reviving Cryopreserved Cells

Cells were revived from frozen stocks when necessary. 10ml of media pre-warmed to 37℃ was first placed into a T75 flask and then the frozen cells were quickly thawed in a water bath also placed at 37℃. Once thawed cells were immediately transferred into the T75 flask before being incubated overnight at 37℃ in 5% CO_2 atmosphere. The following day the media was changed in order to eliminate the residual DMSO.

2.3 Adenovirus Expansion

All virus stocks (except for Ad.sDll4 which was custom designed and purchased from Vector Bio labs) were expanded to allow for sufficient quantities for both *in vivo* and *in vitro* experiments. HEK cells were cultured in 5 x T75 culture flasks as previously described in section 2.2.2. Once confluent 4 x T75 flasks were each split into 4 x T150 culture flasks. The media was removed from the remaining flask and cells washed with 1 x phosphate buffered saline (PBS) solution before 10ml of fresh media containing 10µl of virus stock solution was added. After ~3 days or when the flask containing the virus stock showed complete cytotoxic effect (CPE) 2.25ml of the virus conditioned media from this flask was added to 22.5ml of fresh media in each of the confluent T150 flasks. They were then incubated until 100% CPE was seen.

2.3.1 Adenovirus Purification

To purify the virus, the AdEasy Virus Purification Kit (2x100) was used. The media from the T150 culture flasks was harvested and cell debris was pelleted by centrifugation at 3,500 g for 15 minutes. The supernatant was decanted and stored at 4°Cand while the cell debris pellet was re-suspended in 10ml of supernatant before undergoing 3 freeze-thaw cycles to allow for the lysis of the cells and release of the virus. The debris was then pelleted by centrifugation at 3,500 g for 15 minutes before the supernatant was removed and the pellet discarded.

The supernatant containing the released virus was then treated with 12.5U of Benzonase nuclease (EMD Millipore) and incubated at 37℃ for 30 minutes. The supernatant was next filtered through a 0.45µm filter to remove any remaining debris before being filtered through a sartobind unit, which captured the virus particles and allowed contaminants to be washed away. Finally, the virus was eluted, aliquoted and stored at -80℃.

2.3.2 Titration by End-Point Dilution

HEK293 cells were plated at a density of 20,000 cells per well in a 96 well plate and cultured as described earlier. The following day 50µl of virus stock was added to 4950µl of media to produce a 10^{-2} dilution. Subsequent serial dilutions produced a range from 10^{-2} to 10^{-11}. Beginning with row 1 of the 96 well plate the media was removed and replaced with 100µl of the 10^{-4} dilution. In row 2 this was repeated with the 10^{-6} dilution and repeated in rows 3-7 to give a range between 10^{-7} – 10^{-11}. The plate was then incubated at 37℃ in 5% CO_2 for 16-18hour at which point the media was replaced with 200µl of fresh media. This was replaced every 2 days for 1 week. When CPE was observed in a well, it was marked and the media was no longer replaced. On day 7 the cells showing CPE were counted and the fraction of wells per row measured as a ratio. Tissue culture infective dose 50 ($TCID_{50}$) was calculated as described below in Equation 2.1.

Equation 2.1

$$\frac{\text{(\% positive above 50\%)-50\%}}{\text{(\%positive above 50\%)-(\% positive below 50\%)}} = \text{Proportionate Distance (PD)}$$

Given that the log of the dilution factor was -1 the 50% end point was then calculated as follows in Equation 2.2.

Equation 2.2

$$(\log of\ the\ dilution\ above\ 50\%) + (PD \times \log dilution\ factor) = logID_{50}$$

The reciprocal of the number gives rise to the virus titre in terms of infectious doses per unit volume e.g. A $TCID_{50}$ of $10^{6.3}$ with an inoculation volume of 0.1mlwould have a titre of 10 x $10^{6.3}$/ml or $10^{7.3}$/ml. Conversion of the $TCID_{50}$ to plaque forming units (PFU/ml) was achieved by multiplying the $TCID_{50}$ by 0.7.

2.3.3 In Vitro Validation of Ad.sDll4

To validate the expression of sDLL4 *in vitro*, CHO cells were cultured in 6 well plates at a density of 2.4 x 10^5 cells per well in minimum essential medium, alpha modification (αMEM) plus 10% FBS and 1% penicillin/streptomycin at 37°C and atmospheric conditions of 5% CO_2. The cells were left overnight to attach before they were infected with either Ad.eGFP at a multiplicity of infection (MOI) of 10, or Ad.sDll4 at a MOI of 10,100 and 1000. The cells were then incubated for 24hour at 37℃ in 5% CO_2 and then the media was replaced with fresh media and

incubated for 3 days. After 3 days, the media was removed and the cells were harvested for protein extraction.

2.3.4 Validation of Adenoviruses In Vivo

To ensure that the all the adenoviruses (Ad.eGFP, Ad.eNOS, Ad.Ang1, Ad.VEGF and Ad.sDll4) were working as expected *in vivo*, animals were anaesthetised and underwent surgery as described later in this chapter (section 0) and then re-anaesthetised 3 days post-surgery. Panels with no microvasculature but with a small number of microvessels were identified and then the animal culled before dissecting out the mesenteric panels. The panels were then transferred to Eppendorf tubes containing TRI reagent and kept on ice while they were homogenised. RNA was then extracted and cDNA synthesised as detailed below before template DNA was amplified and then detected using digital droplet PCR (ddPCR).

2.4 RNA Extraction

2.4.1 In Vitro

HDBECs were seeded (3 x 10^4) into 6 well plates and cultured in endothelial cell media until 90% confluent. The media was then discarded and replaced with fresh media containing either recombinant sDll4, recombinant FDll4 (1µg/ml) recombinant $VEGF_{165}$a (40ng/ml), or adenovirus conditioned media for Ad.eGFP, Ad.sDll4 or Ad.VEGF and incubated for 4 hours. After 4 hours, the media was discarded and the cells were washed with PBS before 1ml TRI Reagent (Sigma) was added to each well and left at room temperature for 5 minutes to lyse

before the plates were stored at -80℃ overnight. The following day the plates were defrosted on ice and the solution homogenized using a pipette before being transferred to a sterile Eppendorf tube.

2.4.2 In Vivo

Rat mesenteric panels were dissected out and washed in PBS to remove any residual blood. It was then cut into small sections and placed into 1ml TRI Reagent (Sigma) before homogenizing it. Once fully homogenized the tissue could progress onto the addition of chloroform

2.4.3 Both In Vivo and In Vitro

500µl of chloroform per 1ml of TRI reagent was next added into each Eppendorf tube and shook vigorously for 30sec before being allowed to incubate at room temperature for 10 minutes. Following this the sample were centrifuged at 12,000 g for 15 minutes at 4℃ and the aqueous phase was removed and placed into a new sterile Eppendorf tube.

The RNA was then pelleted by centrifugation (12,000g, 15 minutes, 4℃) and washed with 75% ethanol twice. A further centrifugation (7500g, 15 minutes, 4℃) pelleted the washed RNA, which was briefly air-dried at room temperature after discarding the supernatant. The RNA pellet was then dissolved in ddH_2O and its quality and quantity were measured using the Nano drop. RNA was discarded if the levels of phenol or organic solvents gave an absorbance ratio of less than 1.7.

2.5 cDNA Synthesis

2.5.1 DNase Treatment

After quantification of RNA, 2µg was added to ddH_2O to make a total volume of 16µl. 2µl of RQ1 10x RNase-free DNase Buffer was then added followed by 2µl of DNase. The solution was then incubated for 30 minutes at 37℃. Following incubation 2µl of stop reagent was immediately added and then incubated for a further 10 minutes at 65℃.

2.5.2 cDNA Generation

cDNA was generated using the Takara Prime script RT kit. 1µg of RNA for each sample was used to synthesis cDNA unless otherwise stated. A 20µl reaction volume per sample consisting of 4µl 5x Prime script buffer, 1µl Oligo dT, 4µl random hexamers, 1µg RNA and ddH_2O to make up to the 20µl. Samples were then heated for 10 minutes at 65℃ to denature the secondary structure of the RNA and prevent primer dimers before immediately holding the tubes at 4℃. While at 4℃ 1µl of Prime script RT enzyme, which contains an RNAase inhibitor to prevent RNA degradation, was added to each reaction. Using a thermocycler samples were incubated at 25℃ for 10 minutes then at 37℃ for 1 hour followed by 85℃ for 1 minute and then finally at 4℃ before storing the cDNA at -20℃.

2.6 Quantitative RT-PCR

Real time quantitative PCR (qRT-PCR or qPCR) allows the PCR products to be quantified throughout the reaction during each successive PCR cycle. Such reactions work by using a fluorescent dye such as the intercalating SYBR green 1 dye, which fluoresces upon binding to double-stranded DNA molecules. The fluorescence increases throughout the reaction as during each cycle the amount of double-stranded DNA PCR product is increased and so allows an amplification plot to be generated. SYBR green (unlike other qPCR probes such as TaqMan) is not sequence dependent minimizing experimental error however non-specific PCR products and primer dimers will also contribute to the signal so high product specificity is still needed. qPCR was used to understand how sDll4, Dll4 and H89 dihydrochloride (H89) effect Notch signalling through the relative changes in Hes1 and Hey1 signalling.

2.6.1 Primers

Pre-validated primers for human genes HES1, HEY1 and GAPDH were purchased from Qiagen.

2.6.2 qPCR

First a PCR reaction mastermix consisting of 7µl of ddH_2O, 2µl of primers and 10µl of mastermix (Lightcycler 480 SYBR Green 1 Master, Roche) per reaction was made up. 19µl of this solution was then pipetted into the appropriate wells of a 96-well qPCR plate. 1µl of cDNA template or no template control was then added into each well to make

a 20µl reaction volume. Where 1µl of cDNA was not sufficient, the volume was increased to a maximum of 5µl and the volume of ddH_2O adjusted accordingly so as not to exceed a 20µl reaction volume. Quantitative PCR amplification was performed using a Roche lightcycler 480 instrument using the following conditions, a pre-incubation step where samples were heated to 95℃ for 5 minutes followed by 45 amplification cycles. This consisted of raising the temperature to 95℃ for 10 seconds before an annealing step (60℃) for 10 seconds and an elongation step (72℃) for 10 seconds. A melt curve was also included at the end of each reaction to ensure that specific amplification had been achieved.

2.6.3 Analysis

To analyse the data generated the ΔΔCT method was used. This method compares the differences between the gene of interest and an endogenous control gene, such as GAPDH. The difference in the cycle threshold (CT) of the gene of interest and the endogenous control gene were calculated to give the ΔC_T value. The untreated ΔC_T value was then subtracted from the treated ΔC_T value to yield the $\Delta\Delta C_T$ value. To account for the logarithmic nature of PCR the fold change in expression was then calculated using $2^{\Delta\Delta CT}$.

2.7 Digital Droplet PCR

Digital droplet PCR (ddPCR) was used to detect the adenoviruses in *in vivo* samples. This type of PCR is based on water-oil emulsion droplet

technology where template DNA is separated in tens of thousands of tiny water-oil emulsion droplets. PCR then occurs within each droplet and once finished each droplet is analysed by flow cytometry to determine the fraction of PCR-positive droplets.

ddPCR was used to confirm the presence of the adenoviruses used in the mesenteric angiogenesis assay as its high sensitivity enabled it to distinguish the small volumes of adenovirus still present in the tissue at day 3 post surgery.

Using the BioRad QX200 Droplet Digital PCR System ddPCR mastermix was first prepared containing 10µl 2 x ddPCR buffer, 1µl Primer and 6µl sterile water. cDNA samples were then diluted to give a final ddPCR concentration below 2000. Next 17.85µl of mastermix was mixed with 3.15µl of cDNA and then the combined 20µl solution was transferred to the middle wells of the droplet cartridge. 70µl of droplet oil was then added to the oil wells of the cartridge before covering the cartridge and placing in the droplet machine. Once the droplets had been produced they were carefully transferred to a 96 well plate and the plate sealed with foil before placing in the thermal cycler. Samples were run for 40 cycles at 95℃ for 10 minutes followed by 94℃ for 30 seconds, 59℃ for 1 minute and then 98℃ for 10 minutes before holding at 4℃. PCR products were then detected using the droplet reader and each droplet was plotted into a graph of fluorescence intensity against droplet number. The droplets were then automatically thresholded using the QuantaSoft software (BioRad) where positive droplets found above

the threshold were assigned a value of 1 and negative droplets found below the threshold were given a value of 0.

2.8 *In Vitro* Angiogenesis Assay

The *in vitro* angiogenesis assay used here involved the co-culturing of NHDF and HDBECs. The assay was used to test the functionality of the adenovirus growth factors *in vitro* and how they affect angiogenesis. The NHDF were seeded first and cultured to confluence before seeding the HDBECs on top. The NHDF secrete a complex ECM which becomes remodelled into a 3D environment giving the HDBECs a structure to anchor to and reorganise into tubules. The assay is effective in testing for factors that promote or inhibit angiogenesis.

2.8.1 Conditioned Media

Virus conditioned media was prepared by first seeding CHO cells (1 x 10^6) onto 10cm^2 culture dishes and incubating overnight in DMEM media (supplemented with 10% FCS, 2mM L-Glutamine) in an atmosphere of 5% CO^2. The media was then discarded and replaced with endothelial cell media (MV supplemented with 25ml Foetal calf serum, 2ml endothelial cell growth serum, 5µg recombinant human epidermal growth factor and 500µg hydrocortisone, Promocell) with either Ad.eGFP, Ad.sDll4, Ad.VEGF or Ad.sDll4 + Ad.VEGF (MOI =100). 3 days later the media was harvested, centrifuged (2000 g 10 minutes) to remove any cell debris and then aliquoted into Eppendorf tubes before storing at -80℃.

2.8.2 The Assay

Sterilized 19mm coverslips were placed in the wells of a 12 well plate and normal NHDF were seeded onto the coverslips at 3 x 10^4 cells per well. The cells were then cultured in DMEM (supplemented with 10% FBS and 1% L-Glutamine) for 3 days or until ~70% confluence had been achieved. DMEM media was then discarded and replaced with fresh endothelial cell media overnight. The following day, HDBECs (Promocell) were seeded (3 x 10^4) on top of the NHDF and the cells were allowed to settle and attach overnight. The media was then replaced with either 350µl of fresh media plus 350µl of adenovirus conditioned media or 700µl of recombinant protein conditioned media and then changed every 2 days for 2 weeks. After 2 weeks, the media was removed and the cells were with PBS prior to being fixed in ice-cold ethanol at -20℃ for 30 minutes. The ethanol was then discarded and the fixed cells were washed 3 x 5 minutes in PBS before incubating with polyclonal rabbit anti-VE Cadherin (5µg/ml, ab33168, abcam) overnight at 4℃. The following day the primary antibody was removed and cells were washed 3 x 5 minutes in PBS before incubating for 1 hour with Donkey Anti-Rabbit Alexa fluor secondary antibodies (1µg/ml, life technologies). Secondary antibodies were then removed and cells were again washed 3 x 5 minutes with PBS prior to staining with DAPI (1:15,000) for 10 minutes. Cells were washed for a final time in distilled water (2 x 5 minutes) before coverslips were removed from the 12 well plate and mounted onto microscope slides with Vectashield (H-1000, Vector Laboratories) and sealed with nail varnish.

2.8.3 Imaging and Analysis

z-stack images of 5 sections containing tubes from each coverslip was acquired with a Leica Confocal Microscope (Leica Confocal SPC system, Leica) at 40x magnification. Analysis was undertaken blinded using ImageJ analysis software. The scale bar from the confocal was used to calibrate the software and from this, measurements were obtained for tube length (distance of a tube not interrupted by a branch or sprout, see Figure 2.1). The number of tubes as well as the number of sprouts and branches were also counted and the mean value from the 5 sections was used to calculate the density/mm^2.

One-way analysis of variance (ANOVA) was used for comparison between 2 or more groups with a Bonferroni post-test to compare between individual groups. $p<0.05$ was considered statistically significant and all data is presented as mean ± standard error of the mean (SEM). Three independent assays were undertaken in total.

2.9 *In Vitro* Immunofluorescence

The imaging of immunofluorescence stained HDBECs was used to gain a visual understanding of how Dll4 effects processes such as Notch signalling and cell-cell junction formation in the cells.

2.9.1 Cell Culture

Sterile 13mm^2 coverslips were washed twice with PBS before placing one coverslip into each well of a 24 well plate. The coverslips were then coated with 0.2mg/cm^2 fibronectin in 0.1M Na_2CO_3 (pH 9.4) and

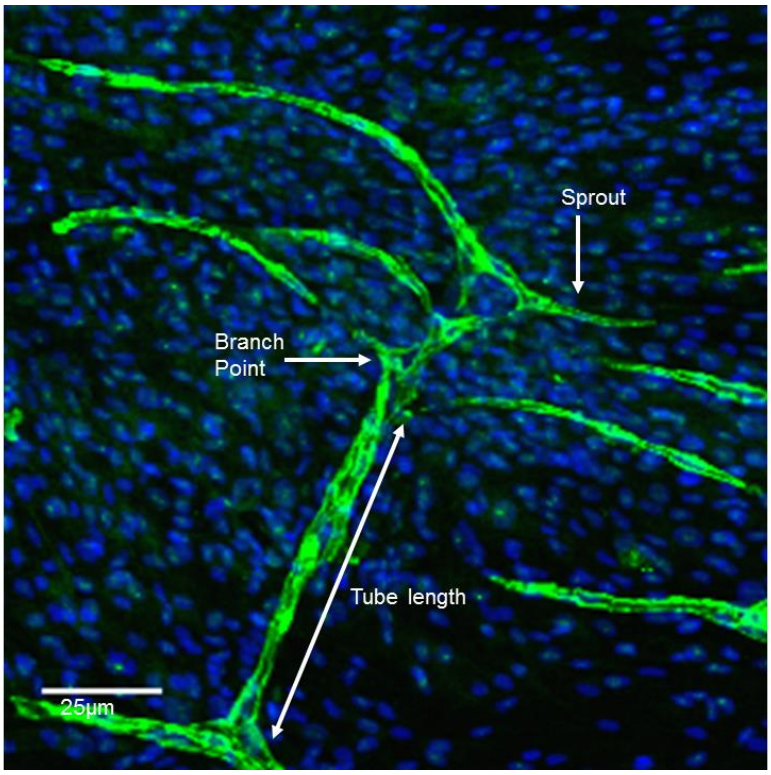


Figure 2.1 Section of a typical image captured using a confocal microscope *and the measurements recorded for each image. The tube length was defined as the distance of a tube not interrupted by a branch or a sprout. Branch points were the point where one tube split into at least two tubes and sprouts were defined as small new tubes usually found at branch points.*

incubated at 37℃ for at least 2 hours. This was then discarded and the coverslips washed twice with PBS before 3 x 10^4 HDBECs were plated onto each coverslip. The cells were incubated at 37℃ in an atmosphere of 5% CO^2 until a monolayer was formed changing the media every other day.

2.9.2 Treatment and Staining

Once confluent, the media was replaced with fresh media containing either, recombinant human sDll4 (1µg/ml), VEGF (40ng/ml) or nothing and incubated for a further 4 hours, chosen after review of the literature (Hellstrom *et al.*, 2007; Phng *et al.*, 2009; Estrach *et al.*, 2011; Hale *et*

al., 2014). The media was then discarded and the cells fixed in 75% ethanol for 30 minutes at -20℃. Cells were then washed in PBS 3 x 5 minutes before incubating with primary antibody (rabbit anti-VE Cadherin as described in section 2.8.2. Rabbit anti-ZO-1 10µg/ml, Abcam or rabbit anti-Notch intracellular domain 1:200, Abcam) overnight at 4℃ with gentle agitation. The following day, cells were again washed in PBS 3 x 5 minutes and then incubated in secondary antibody (donkey anti-rabbit Alexa Fluor 555, 1µg/ml, Life technologies, phalloidin conjugated Alexa Fluor 488, 1:500, Life technologies, DAPI 1: 10,000) for 1 hour at room temperature before a final 3 x 5minute washes in PBS. The coverslips were then removed from their wells and mounted onto microscope slides with Vectashield and sealed with nail varnish ready for imaging.

2.9.3 Imaging and Analysis

Coverslips were imaged using a Leica Confocal Microscope (Leica Confocal SPC system, Leica) at 40x magnification. 5 z-stacks per coverslip were randomly selected for imaging and subsequently taken to be analysed. All image analysis was undertaken using ImageJ image analysis software.

All antibody concentrations were decided after a period of optimisation of the protocol.

2.9.3.1 VE-Cadherin

Once imaged, each image was overlaid with a grid and 10 squares were randomly chosen to analyse from each image. For each square,

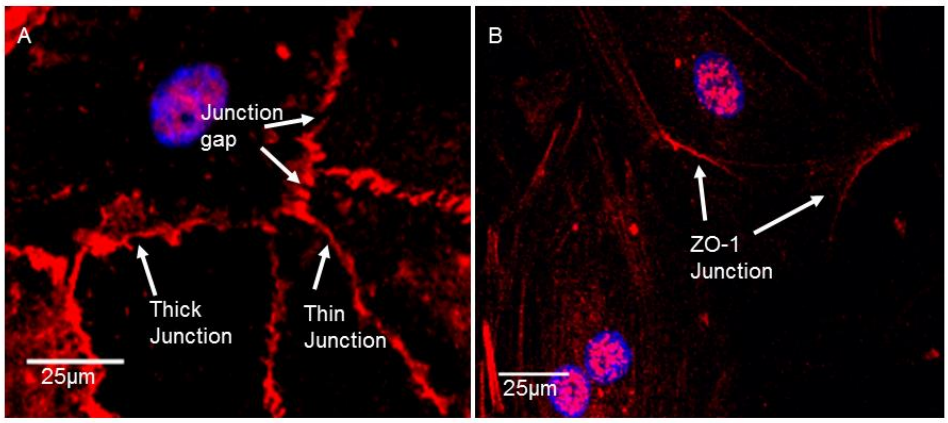


Figure 2.2, Areas of typical confocal z-stack images captured of endothelial cells illustrating how each were analysed. *A) Total VE-Cadherin junction length was measured and then the percentage of thick or thin junctions or junctional gap was calculated. B) The total number of ZO-1 junctions and their total length was measured and recorded.*

the total junctional length was measured. The percentage of the junction that was made up of thick or thin junctions or junctional gaps was then calculated (Figure 2.2A).

2.9.3.2 ZO-1

In images where cells were stained for ZO-1 total number of junctions were recorded along with mean length (*Figure 2.2*B).

2.10 *In Vitro* Protein Extraction

To extract protein from the CHO cells they were first washed twice in ice cold PBS. The PBS was then discarded and the cells were lysed using RIPA buffer (supplemented with 50µl/ml protein inhibitor cocktail, Sigma) and detached from the well using the large top end of a 200µl pipette tip. The lysate was then collected in ice cold Eppendorf tubes before the samples were centrifuged at 13,000 g for 15 minutes at 4℃

to pellet the debris. The supernatant was then transferred to a new Eppendorf tube and stored at -20℃.

2.11 Protein Quantification

To ensure that equal amounts of protein would be used for subsequent assays, the Bradford protein quantification assay was performed. Controls of known bovine serum albumin (BSA) were made up in PBS to give 1000, 500, 250, 125, 62.5, 31.25, 15.625 and 0µg/ml standards. 10µl of each standard was then added in triplicate into a 96 well plate. 10µl of each protein sample diluted at 1:50 in dH_2O was also added in triplicate to the plate. The protein assay dye reagent concentrate (BioRad) was then diluted 1:5 in PBS and 200µl of the diluted dye was added to each well and incubated at room temperature for 5 minutes. Absorbance was measured at 595nm and protein concentration calculated from the standard curve.

2.12 Western Blot

Western blots were used to detect sDll4 protein encoded by Ad.sDll4 after initial purchase.

2.12.1 Sodium Dodecyl Sulphate-Polyacrylamide Gel Electrophoresis

An 8% resolving gel consisting of 1.6ml acrylamide, 1.5ml Tri-HCl pH 8.8, 2.81ml H_2O, 0.06ml 10% ammonium persulphate (APS), 0.03ml 20% SDS and 3.6µl tetramethylethylenediamine (TEMED) was loaded into a cast and allowed to set. Isopropanol was added to the top of the

gel to ensure a level top and prevent desiccation. Once set the isopropanol was removed and a 5% stacking gel (0.5ml acrylamide, 0.75ml Tri-HCl pH 6.8, 1.705ml H_2O, 0.03ml 10% APS, 0.015ml 20% SDS and 3µl TEMED) was then overlaid, combs to form the loading wells were inserted and left to set.

Prior to loading sample into the gel, 50µg of sample protein was denatured by boiling at 95℃ with 10µl 4x SDS-PAGE loading buffer for 5 minutes. Gels were then loaded into the appropriate cassettes and submerged in running buffer (25nM Tris Base, 190nM glycine, 0.1% SDS) before the denatured samples were carefully loaded into the gel. 6µl of precision plus dual colour protein prestained standards (BioRad) protein ladder was also loaded into the gel before it was run at 70v for 15 minutes and then 90v until the dye reached the bottom of the gel. Once the electrophoresis had finished proteins were transferred to a polyvinyl difluoride (PVDF) membrane by Western blot. The PVDF was first activated in methanol and then soaked in transfer buffer (10% 10x Tris-Glycine transfer buffer, 20% methanol and 70% dH_2O) along with filter paper. Proteins were transferred using a wet-transfer blotter at 90v for 2hours.

2.12.2 Immunodetection and Visualization

Following transfer, sDll4 was detected with antibodies against the extracellular region of Dll4. Incubation steps were carried out on a rocker at room temperature unless otherwise stated. The membranes were blocked in a 3% BSA – 0.5% Tween20 – Tris-buffered saline

(TBST) solution for 20 minutes. Block solution was then discarded and replaced with a 1% BSA-TBST solution containing a goat anti-mouse anti-Dll4 antibody corresponding to amino acids 28-525 in the extracellular region of Dll4 (1:200, R&D systems AF1389) and an anti-VDAC1 (1:2000, Abcam), a porin antibody used as a mitochondrial loading control were incubated overnight at 4℃ The following day the membranes were washed 3 x 5 minutes in TBST and incubated for 1 hour with donkey anti- rabbit and donkey anti-goat secondary antibodies (1:5000, Licor). The membranes were then washed in TBST for a further 3 x 5 minutes before being visualized using the Licor Odyssey imaging system and image studio software.

2.13 Animals

All Animal experiments were performed in UK in the accordance of the UK Home Office legislation (working under PPL 30/2955 and PIL IFA54EA4D). All recovery surgical procedures performed were done so under sterile conditions and with approval of the UK Home Office and the University of Nottingham. Male Wistar Han Rats weighing ~ 300-325g were used in all Lp experiments (sourced externally from Charles River). For the Mesenteric angiogenesis assay, male Wistar rats (Charles river) weighing 300-350g were used. All rats that had been in an experimental protocol were culled by cervical dislocation without recovery from anaesthesia. For the hind limb ischemia experiments, male C57B6 mice (7-8 weeks old, Charles River) were used and were culled by cervical dislocation.

2.14 Hydraulic Conductivity

Hydraulic Conductivity (L_p) experiments were used to gain a greater understanding of the effects of Dll4 on the vascular permeability to water.

2.14.1 General Solutions

Mammalian Ringer's solution was prepared by dissolving the following compounds in distilled water: NaCl, 132mM (Fischer); KCl, 4.6mM (Sigma); $MgSO_4 7H_2O$ (Fischer), 1.27; $CaCL_2 2H_2O$ (Fischer), 2mM; $NaHCO_3$ (Fischer), 25mM; D-glucose (Fischer), 5.5mM; N-2-hydroxyethylpiperazine-N'-2-ethanesulphonic (HEPES) Acid, 3.07mM (Sigma); HEPES Sodium Salt, 1.9mM (Sigma). Once dissolved the pH of the solution was measured and adjusted to pH 7.40.

A 1% BSA-Ringer's solution for all Lp assays was prepared by adding lyophilized BSA powder (Santa Cruz Biotechnology, sc-2323A) to mammalian Ringer's solution. The pH was then readjusted back to pH7.40 and then the solution was filtered through a syringe filter of 0.2µm pore (Sartorius Stedim Biotech).

2.14.2 Apparatus for Cannulation

2.14.2.1 Cannulation pipettes

Cannulation pipettes were made from borosilicate glass capillaries with an outer diameter of 1.5mm (Harvard Apparatus). Using a microelectrode puller, (Narishige, PE-22) the capillaries were heated within a coiled filament and pulled to a fine tip. The tip was then bevelled at a 20° angle on a grindstone (Narishige), which was



Figure 2.3 Pipette grinding rig*. A) grindstone set up with dripper and pipette holder. B) microscope and C) light source used to illuminate the tip of the pipette while grinding.*

continuously soaked with water to produce sharp cannulation pipettes with bevels 15-25µm in width.

2.14.2.2 Restrainers

Restraining pipettes were made by blunting the end of an unbevelled cannulation pipette using a Bunsen burner in order for it to be able to hold down and restrict movement of the mesentery during experiments.

Occluders

These were made by increasing the temperature of the coiled filament to 41°C to produce a cannulation pipette with a longer tip. They were then bent at the shoulder of the pipette to a 45° angle so that they could

Figure 2.4 Pipette grinding rig set up.

be used to squash the cannulated vessel to block the flow of the perfusate.

2.14.2.3 Perfusion – Solution Exchange System

An adjustable water manometer attached to the back of the cannulation pipette was used to control the hydrostatic pressure of the cannulated vessel. Between the cannulation pipette and the manometer, a syringe pump was linked up with a filler tube, which fed right into the cannulation pipette, and a waste tube which was positioned at the back of the pipette. This allowed the perfusate in the pipette to be easily changed and without the need to re-cannulate the vessel (see Figure 2.5).

2.14.3 Experimental Protocol

2.14.3.1 Preparation of perfused solutions

To control for osmotic reflection coefficient all test substances were perfused in a 1% BSA Ringer's solution (see 2.1). Previously collected rat blood was then washed 3 times in Ringer's Solution to remove the plasma and any proteins before adding 100µl to 10ml of 1% BSA Ringer's solution. Appropriate volumes of sDll4, H89 di-hydrochloride (H89) or both were then added to the appropriate tubes.

2.14.3.2 Mesentery Preparation

Rats were anaesthetised using 5% isoflurane and stable anaesthesia was maintained at 2%. Upon reaching stable anaesthesia a laparotomy was performed and the gut carefully exposed. The mesentery was then draped over the quartz pillar on the rat tray and the tissue flooded with

Ringer's solution. Together, the rat and the tray were then transferred to the LP rig where a dripper line was placed onto the mesentery to allow a constant fresh supply of Ringer's solution on and around the tissue and the excess solution was syphoned away using a vacuum pump. To help keep the rat warm the Ringer solution was heated to 37°C by passing through a heat exchanger before reaching the tissue. Post-capillary venules from 25- 50μm were chosen for these experiments.

2.14.3.3 Lp Rig set up

The rat tray was positioned over the 4x objective of an inverted light microscope (Leica DM IRB). A suitable post-capillary venule was then located in the mesentery and positioned within the video-camera's field of view. A manual micromanipulator with a restraining pipette attached was next moved into position over the same area. It was then placed onto the mesentery and gently pulled up and away from the selected vessel pulling the tissue taut. A motorised micromanipulator with the cannulation pipette attached was then moved into position and the vessel was cannulated. Finally, a second manual micromanipulator with an occluding pipette was placed downstream of the point of cannulation. The microscope would then be switched to a 10x objective during the experiment.

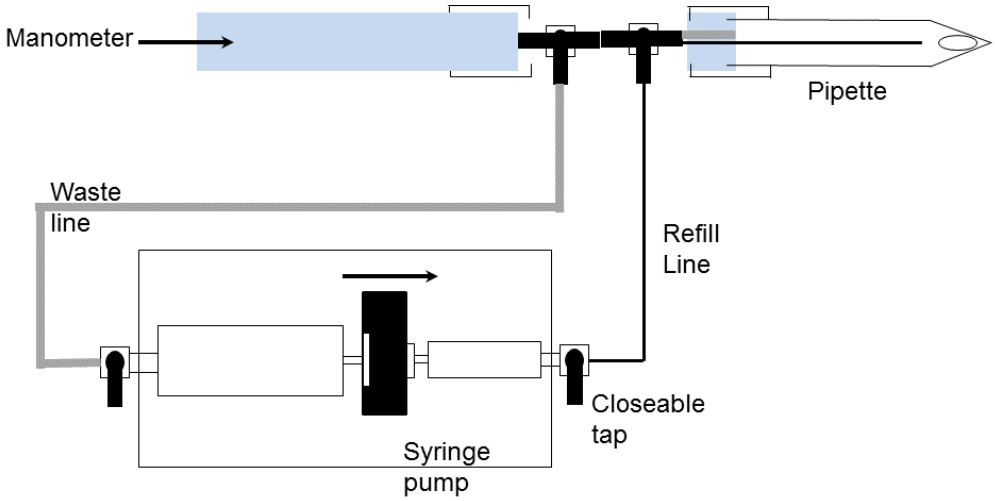


Figure 2.5 schematic of the Lp pipette refilling system. *The refill line extends from a 5ml syringe all the way to the shoulder of the pipette delivering the fresh perfusate to the tip. The waste line connects to the 50ml syringe found at the opposite end of the syringe pump and removes the previous perfusate from the pipette. This is all controlled by the action of the syringe pump and the manometer which also feeds into the back of the pipette and ensure the constant control of the hydrostatic pressure.*

2.14.4 Imaging and Recording Experiments

Once the vessel had been cannulated and the occluder was in position, the pipette was refilled to perfuse with the control perfusate 1% BSA Ringer's solution containing washed red blood cells. Occlusion of the vessel at 15-20 second intervals was then recorded using a Panasonic (HC-X920) video camera attached to the microscope. After approximately 8 minutes the pipette was then refilled again to perfuse with 1% BSA Ringer's solution containing washed red blood cells on its own or with sDll4, H89 or both before continuing with occlusions until it was necessary to refill the pipette with a third perfusate or the experiment had ended.

2.14.5 Analysis

Lp recordings were transferred off the video camera and saved in .mov format. Before any analysis could be done the video was first calibrated to establish an accurate scale bar from which to measure against. This was done using another recording of a microscope graticule taken immediately after the experiment. The recording relayed the information of how the graticule matched the eyepiece units needed to create an accurate scale. It also allowed us to measure where the edge of the field of view on the camera fell. This would be especially important in aiding in the calculation of the distance from the red blood cell to the point of occlusion, as only the red blood cell is visible on the recording. Once calibrated the distance that a red blood cell moved over 1 second in the middle of the occlusion period could be accurately determined (Figure 2.6). This was done for each occlusion in the recording and entered into a spreadsheet along with the time of the occlusion, the pressure and the point of the occlusion site which was set up to calculate the Lp. As occlusions were never at exactly the same time point for each vessel, time points were 'binned' into 30-second intervals and the corresponding L_p values for each interval were averaged. This allowed the data from all 5 vessels to be easily plotted on the same graph. As measurements of L_p in control vessels have previously been shown to not be normally distributed non-parametric statistical analysis was performed (Hargrave, Huxley and Thipakorn, 1995; Bates and Curry, 1996; Adamson *et al.*, 2013). Mann-Whitney U tests for unpaired t tests were performed using the fold change compared to baseline

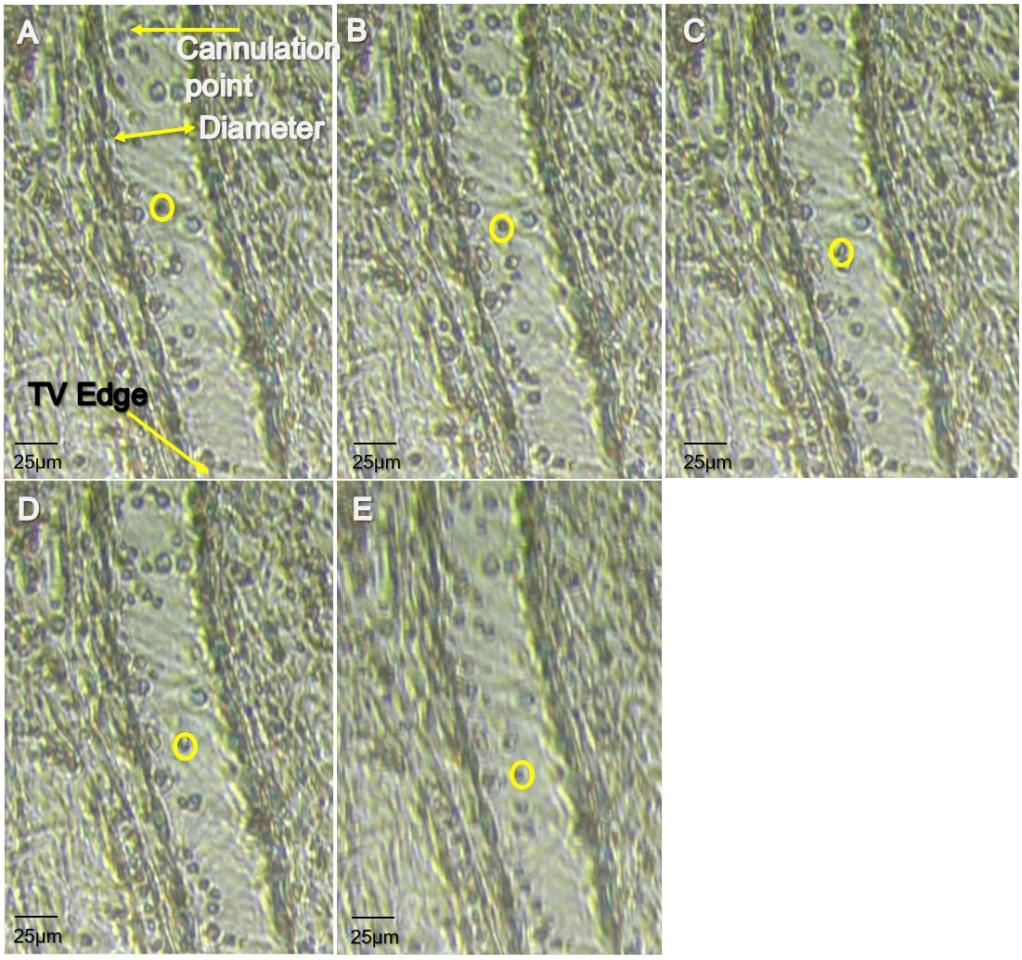


Figure 2.6 Analysing Lp recordings. *Upon occlusion of the vessel a single red blood cell (RBC) located towards the centre of the vessel was chosen for analysis (A). The RBC's distance from the TV's edge was recorded and the distance it subsequently moved each 0.25 second for 1 second was also recorded (B-E). These measurements along with the pressure readings of the manometer and the diameter of the vessel were then input into an excel spreadsheet used to calculate the Jv/A and subsequently the Lp.*

maximal responses for BSA versus Dll4 and BSA versus sDll4. Kruskal-Wallis tests (with Dunn's multiple comparison test) was performed for comparison of maximal responses for sDll4 versus H89 and H89 + sDll4. Confidence levels were set at 95% and all data is presented as mean ±SEM unless otherwise stated. The Mesenteric Angiogenesis Assay

The mesenteric angiogenesis assay is an *in vivo* assay that enables the measurement of physiological angiogenesis which has been manipulated by the introduction of adenoviruses encoding angiogenic factors such as VEGF, Ang1, eNOS and sDll4.

2.14.6 Animal Surgery Procedure

Male Wistar rats (300-350g, Charles River, UK) were anaesthetised in an induction chamber with 5% isoflurane and then stable anaesthesia was maintained at 2% throughout the surgical procedure.

A laparotomy was then performed on the animal by making a midline incision of approximately 1.5-2cm into the skin and peritoneal cavity. A small portion of the gut was then gently teased out and laid out onto the surrounding sterilised skin. The exposed tissue was kept moist by superperfusing it with warmed mammalian Ringer's solution. An appropriate mesenteric panel with a few but not an excessive number of flowing microvessels was selected and the required adenovirus was injected into the fat pad at a concentration of 5×10^8 PFU/ml using a Hamilton syringe. To enable the panel to be found easily at a later date the adjacent panels were subsequently tattooed with Monastral blue. The gut was then gently replaced and the peritoneal cavity and skin were sutured back together and the animal was provided with analgesia by intra-muscular injection of 0.3mg/kg buprenorphine. The animals were then allowed to recover in a warmed clean cage before being transferred back to the holding room. Animals were checked and weighed each day to monitor their health and reaction to the surgery.

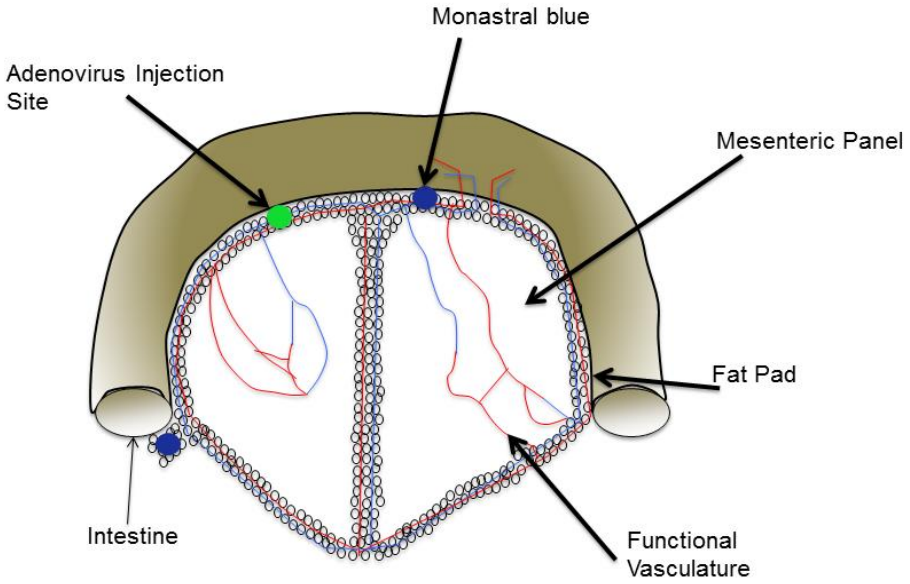


Figure 2.7 Schematic of a section of the rat mesentery *illustrating where the microvasculature is found in relation to the gut and fat pad. Adenoviruses were injected into the fat pad of mesenteric panels with some, but not excessive, microvessels and the adjacent panels were tattooed with Monastral blue to enable identification of the correct panel. Image adapted from Benest et al (2006).*

1 week later the same animal was anaesthetised as above, and the abdominal cavity was re-opened. The gut was again gently teased out and the injected panel was identified with the help of the adjacent tattooed panels. The panel was then fixed *in vivo* with 4% PFA for 3 minutes. The animal was then culled by cervical dislocation and the panel of interest was dissected out, washed in PBS and then placed into an Eppendorf tube containing 4% PFA to continue fixation for 30 minutes at room temperature. The panel was then transferred into PBS and stored at 4℃ until ready for immunofluorescence staining.Immunofluorescence of Whole Mount Mesentery

Once fixed, panels were then dissected under a dissection microscope to remove any excess fat that may have been missed. The tissue was

then washed 6 x 10 minutes in 0.5% PBLEC (1x PBS containing, 50ul 1M MgCl2, 50ul 1M CaCl2, 5ul 1M MnCl2, 5ml 10% (vol/vol) Triton X-100 in 50mls, pH6.8). All washing steps and incubation steps were carried on a rocker at room temperature unless stated. After washing panels were blocked in 1% BSA- PBX (1x PBS containing 0.5% Triton X-100) for 1 hour. The block was then discarded and replaced with biotinylated isolectin-B_4 (IB4, 1:100, Sigma) and Ki67 (1:200, abcam) in a 1:1 solution of PBS and block solution and incubated overnight at 4℃.

The following day the tissue was washed 6 x 10 minutes in 0.5% PBLEC before being incubated in a 1:1 solution of PBS and block solution containing donkey-anti-rabbit Alexa fluor 488 (1:2000, life technologies) and streptavidin Alexa fluor 555 (1:2000, life technologies) for 2 hours. After incubation with secondary antibodies the tissue was then washed another 6 x 10 minutes in 0.5% PBLEC. The mesenteric panels were then finally incubated with DAPI (1:15000) for 10 minutes in a 1:1 solution of PBS and block solution and then washed 3 x 10 minutes in PBS.

After immunostaining, the mesenteric panels were carefully laid out flat on microscope slides using forceps. Vectorshield was then used to mount the tissue and a coverslip was carefully positioned over the tissue on the slide and sealed using nail varnish. 5 random, vessel containing sections of each panel were then imaged using a Leica Confocal microscope (Leica Confocal SPC system, Leica) at 40x magnification. This magnification was chosen following comparison of images and analysis at both 40x and 10x magnification.

2.14.7 Image Analysis

Z-stack images acquired using confocal microscopy were analysed using Image J analysis software similarly to described earlier. Once the software was calibrated using the scale bar from the confocal microscope measurements for individual vessel lengths were taken. Vessel lengths were defined as the distance of a vessel not interrupted by a branch or sprout point. The numbers of vessels, sprout points and proliferating endothelial cells were also counted and the mean number per panel for each condition was used to calculate the density/mm^2 (see Figure 2.8).Samples were assumed to be from a normal distribution after passing normality testing and parametric statistical testing was performed. One-way ANOVA with a Bonferroni post-test was used to compare between 2 or more groups and then individual groups respectively. All data is presented as mean ±SEM with $p<0.05$ considered as statistically significant unless otherwise stated.

2.15 Hind limb Ischaemia

The hind limb ischaemia assay is a method used to help understand angiogenesis in pathological situations. Here, experiments were used to assess how the induction of Notch signalling effects the recovery of blood flow via the formation of a collateral network.

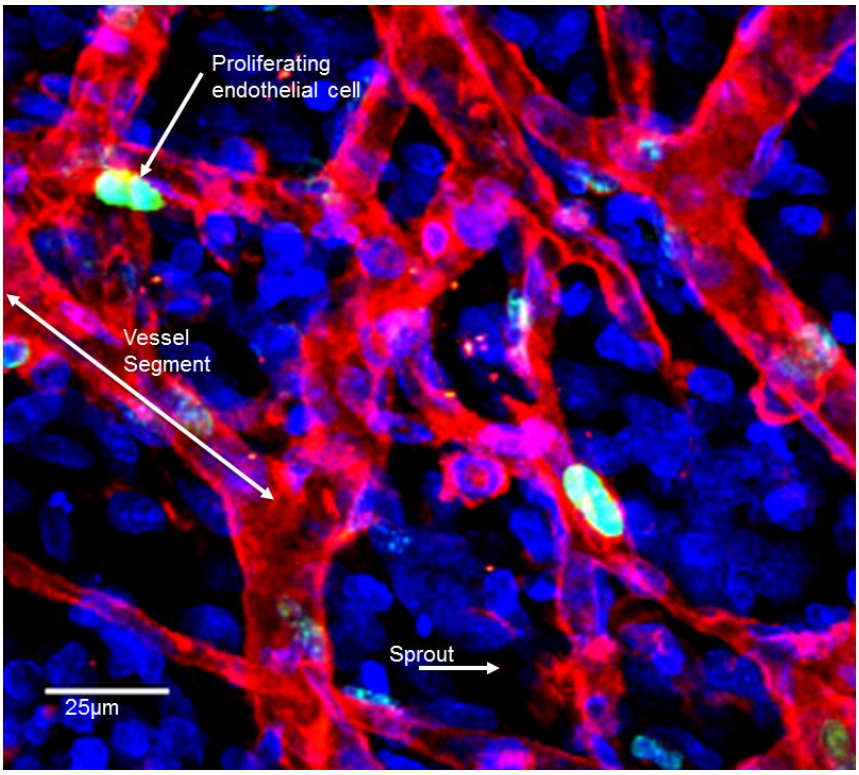


Figure 2.8 section of a confocal z-stack image of the rat mesentery *stained for microvessels (IB4), nuclei (DAPI) and proliferating cells (KI67). Images were analysed by recording the length of vessel segments and the density of vessel segments, proliferating cells and sprouts.*

2.15.1 Surgery and Imaging

Male C57Bl6 mice were anaesthetised with 5% isoflurane and then stable anaesthesia was maintained at 2% throughout the surgical procedure. Upon stable anaesthesia mice were injected with buprenorphine and where appropriate had their ears clipped to enable identification post-surgery. Hair removal cream was then used to remove hair from the area of the hind limb where surgery was to be performed. Prior to the surgical procedure taking place, the hind paws of the mice were imaged using a colour laser speckle imaging apparatus and software (FLIP2, Moor Instruments) ensuring that there was blood flow to both hind limbs.

Once imaged the mouse was transferred to the surgical area where its hindlimb was sterilised and secured in an extended position. An incision approximately 1cm in length was then made from the knee towards the abdomen. Any subcutaneous fat was then gently moved out of the way and separated to expose the femoral artery. Next the femoral nerve was carefully separated from the femoral artery and a pair of forceps placed underneath the artery. A piece of suture was then passed underneath the femoral artery and the vessel tied off above the epigastric bifurcation. A second suture was then used to tie off the vessel further towards the knee but above the previous knot. The vessel was then coagulated between the two sutures and the appropriate adenovirus or combination of adenoviruses were injected into the adductor muscle before the wound was sutured back up. Once surgery had been completed the hind limbs were imaged again to ensure the surgery was successful and ischemia had been achieved, and then the animal was allowed to recover in warmed, clean cages. The wounds and weight of each animal were monitored each day for the first week and then weekly there-after until the end of the experiment.

In addition to imaging before and after surgery the animals' hind limbs were also imaged (under anaesthesia) on day 3, 7, 14 and 21. Images were subsequently quantified and analysed using Moor Instruments FLIP2 software to show the ischaemic to contralateral hindlimb blood flow ratio for each animal at each time point. A Two-way ANOVA with a Sidak post-test was used to compare between groups. All data is

presented as mean ±SEM with $p<0.05$ considered as statistically significant unless otherwise stated.

Upon imaging at day 21 the mice were then culled and the muscle from both hind limbs were dissected out, covered in OCT solution, frozen in liquid nitrogen and stored at -80℃.

2.15.2 Tissue Staining and Imaging

Multiple 5µm thick sections of muscle were cut using a cryostat. The sections were taken at different points throughout the muscle to gain a greater insight into how the whole muscle was affected. All staining steps were undertaking using a darkened humidified staining tray. Prior to staining sections were allowed to defrost and then were then fixed in 4% PFA for 15 minutes. The slides were then washed 3 x 5 minutes in PBS and then blocked for 2 hours at 4℃ in a solution containing 10% FCS, 5% BSA in PBS. Following blocking sections were incubated in primary antibody (IB4, 20µg/ml, Sigma. α-smooth muscle actin-cy3, 1:400, sigma) in block overnight at 4℃. The following day sections were washed 3 x 5 minutes in PBS before incubating with Alexa Fluor Streptavidin (1:1000, Life Technologies) in block for 2 hours at room temperature. sections were then washed 3 x 5 minutes in PBS and incubated with DAPI (1:10,000) for 10 minutes before a final 3 x 5-minute wash with distilled water and then coverslips were mounted onto the sections with Vectorshield

2.15.3 Imaging and Analysis

5 images per tissue section were taken using a Leica Confocal Microscope (Leica Confocal SPC system, Leica) at 40x magnification. Using ImageJ image analysis software, the number or capillaries and arterioles in each image were counted and from this the capillary and arteriole densities (n/mm^2) were calculated. Due to the larger sample size and following normality testing parametric statistical analysis was performed. To compare between the groups a One-way ANOVA with a Bonferroni post-test was used. All data are presented as mean ±SEM with p,0.05 considered as statistically significant unless otherwise stated.

Chapter 3: Dll4 Regulates Endothelial Junctions Through Notch1

3.1 Introduction

A vital role of endothelial cells is to maintain vascular integrity and barrier function. Components of this barrier include the intercellular tight junctions composed of proteins such as occludins (Hirase *et al.*, 1997; Antonetti *et al.*, 1999; Murakami, Felinski and Antonetti, 2009) and claudins (Nitta *et al.*, 2003) as well as the adherens junctions made up of proteins such as VE-Cadherin (Giannotta, Trani and Dejana, 2013) and gap junctions consisting of connexin proteins (Nagasawa *et al.*, 2006; Danesh-Meyer *et al.*, 2012). The control of vascular integrity is especially important during angiogenesis when, to form new vessels, existing endothelial cells must proliferate and migrate yet still maintain barrier function.

It is generally accepted that VEGF is a key instigator of angiogenesis (Leung *et al.*, 1989). Amongst its many downstream effects, it is a potent inducer of increased permeability (Roberts and Palade, 1995) and has been shown to disrupt vascular integrity, an effect often seen during tumour angiogenesis (Weis *et al.*, 2004). Similarly, the upregulation of the Notch ligand, Dll4 (Liu *et al.*, 2003) is also a downstream consequence of VEGF signalling. The subsequent interaction of Dll4 with its ligand, Notch, in an adjacent endothelial cell has been recognized as the principal molecular mechanism giving rise

to the tip or stalk cell phenotypes in sprouting angiogenesis (Hellstrom *et al.*, 2007).

Once upregulated via VEGF signalling through VEGF receptor 2 (VEGFR2), Dll4 will bind to Notch on an adjacent endothelial cell membrane. This leads to the proteolytic cleavage of Notch and the subsequent release of the NICD. The NICD will then translocate to the nucleus where it interacts with a DNA binding protein called recombination signal binding protein for immunoglobulin kappa J region (RBPJ-κ). Upon binding, allosteric changes occur in RBPJ-κ which enable the displacement of transcriptional repressors and the subsequent transcription of Notch target genes such as Hes1 and Hey1 (Andersson, Sandberg and Lendahl, 2011; Guruharsha, Kankel and Artavanis-Tsakonas, 2012).

Interestingly, VE-Cadherin, a membrane protein that is an integral part of endothelial adherens junctions, has recently also been found to be expressed on the anterior plasma membrane and in filopodia protrusions of tip cells during sprouting angiogenesis (Almagro *et al.*, 2010). In addition to this, Bentley *et al*. (2014) suggested that the continual flux in Notch levels in individual cells results in differential VE-cadherin turnover and junctional-cortex protrusions, which powers the differential cell movement alluded to by Jakobsson et al (2010).

The above, in conjunction with the reports of Notch being a marker of endothelial quiescence (Ehling *et al.*, 2013), Dll4/Notch signalling negatively regulating VEGFR2 expression (Suchting *et al.*, 2007) as well as the recent links between Dll4/Notch signalling and endothelial

junctional control (Bentley *et al.*, 2014) suggest an as yet uncovered role for Dll4/Notch signalling in maintaining vascular integrity and barrier function. I hypothesised that induction of Notch signalling would result in tighter endothelial cell-cell junctions. To address this hypothesis, I first looked at cultured endothelial cells (HDBECs) to establish if recombinant Dll4, sDll4 and Ad.sDll4 each induced Notch signalling by measuring the change in expression of target genes such as Hes1 and Hey1 as published in the literature. Following this, I wanted to investigate how the induction of Notch signalling affects both adherens and tight junctions of cultured endothelial cells using immunofluorescence staining.

3.2 Methods

3.2.1 Recombinant Protein and Adenovirus Sequences

Human Dll4 and sDll4 proteins and an adenovirus encoding mouse sDll4 were used. The below sequences illustrate the similarities and differences between human and mouse Dll4 amino acid sequences.

Human Dll4

1 MAAASRSASG WALLLLVALW QQRAAGSGVF QLQLQEFINE RGVLASGRPC EPGCRTFFRV

61 CLKHFQAVVS PGPCTFGTVS TPVLGTNSFA VRDDSSGGGR NPLQLPFNFT WPGTFSLIIE

121 AWHAPGDDLR PEALPPDALI SKIAIQGSLA VGQNWLLDEQ TSTLTRLRYS YRVICSDNYY

181 GDNCSRLCKK RNDHFGHYVC QPDGNLSCLP GWTGEYCQQP ICLSGCHEQN GYCSKPAECL

241 CRPGWQGRLC NECIPHNGCR HGTCSTPWQC TCDEGWGGLF CDQDLNYCTH HSPCKNGATC

301 SNSGQRSYTC TCRPGYTGVD CELELSECDS NPCRNGGSCK DQEDGYHCLC PPGYYGLHCE

361 HSTLSCADSP CFNGGSCRER NQGANYACEC PPNFTGSNCE KKVDRCTSNP CANGGQCLNR

421 GPSRMCRCRP GFTGTYCELH VSDCARNPCA HGGTCHDLEN GLMCTCPAGF SGRRCEVRTS

481 IDACASSPCF NRATCYTDLS TDTFVCNCPY GFVGSRCEFP VGLPPSFPWV AVSLGVGLAV

541 LLVLLGMVAV AVRQLRLRRP DDGSREAMNN LSDFQKDNLI PAAQLKNTNQ KKELEVDCGL

601 DKSNCGKQQN HTLDYNLAPG PLGRGTMPGK FPHSDKSLGE KAPLRLHSEK PECRISAICS

661 PRDSMYQSVC LISEERNECV IATEV

Mouse Dll4

1 MTPASRSACR WALLLLAVLW PQQRAAGSGI FQLRLQEFVN QRGMLANGQS CEPGCRTFFR

61 ICLKHFQATF SEGPCTFGNV STPVLGTNSF VVRDKNSGSG RNPLQLPFNF TWPGTFSLNI

121 QAWHTPGDDL RPETSPGNSL ISQIIIQGSL AVGKIWRTDE QNDTLTRLSY SYRVICSDNY

181 YGESCSRLCK KRDDHFGHYE CQPDGSLSCL PGWTGKYCDQ PICLSGCHEQ NGYCSKPDEC

241 ICRPGWQGRL CNECIPHNGC RHGTCSIPWQ CACDEGWGGL FCDQDLNYCT HHSPCKNGST

301 CSNSGPKGYT CTCLPGYTGE HCELGLSKCA SNPCRNGGSC KDQENSYHCL CPPGYYGQHC

361 EHSTLTCADS PCFNGGSCRE RNQGSSYACE CPPNFTGSNC EKKVDRCTSN PCANGGQCLN

421 RGPSRTCRCR PGFTGTHCEL HISDCARSPC AHGGTCHDLE NGPVCTCPAG FSGRRCEVRI

481 THDACASGPC FNGATCYTGL SPNNFVCNCP YGFVGSRCEF PVGLPPSFPW VAVSLGVGLV

541 VLLVLLVMVV VAVRQLRLRR PDDESREAMN NLSDFQKDNL IPAAQLKNTN QKKELEVDCG

601 LDKSNCGKLQ NHTLDYNLAP GLLGRGSMPG KYPHSDKSLG EKVPLRLHSE KPECRISAIC

The yellow highlighted section of the human Dll4 sequence represents the recombinant Human sDll4 protein sequence whereas the full length Dll4 recombinant protein consists of the whole sequence. The green highlighted section in the mouse Dll4 sequence represents the adenovirus sDll4 sequence and the purple highlighted sections confer the transmembrane section of both the human and mouse Dll4. The red coloured amino acid letters represent those amino acids which are different to their corresponding amino acids in the other sequence and those which are underlined confer the amino acids which make up the MNNL (N-terminus) and Delta-Serrate-Ligand (DSL) regions which are integral for binding to Notch.

3.2.2 Experimental Protocols

HDBECs were cultured until confluent for use *in vitro*. Recombinant Dll4, sDll4 and $VEGF_{165}$a were used for cell culture treatment over a 4-hour period, to assess their ability to induce Notch signalling; this was consequently measured by quantitative RT-PCR (qPCR). The γ-secretase inhibitor DAPT was used to check that changes in Hes1 and Hey1 expression were due to signalling through Notch. Data was tested for statistical significance using a one-way ANOVA with a Bonferroni post-test and 95% confidence intervals.

As seen in the literature (Bates and Curry, 1996; Lobov *et al.*, 2007; Al Haj Zen *et al.*, 2010; Benedito *et al.*, 2012; Nedvetsky *et al.*, 2016), recombinant Dll4 and sDll4 were used at a concentration of 1µg/mL,

recombinant $VEGF_{165}a$ was used at a concentration of 40ng/mL (or 1nM) and DAPT was used at a concentration of 2μM in all experiments in this chapter and throughout the thesis.

Adenovirus conditioned media for Ad.eGFP, Ad.sDll4 and Ad.VEGF were also assessed by qPCR. Following this, fresh conditioned media was added in a 1:1 ratio with normal HDBEC media onto a co-culture of fibroblasts and HDBECs every other day for two weeks. Tube formation was then assessed via immunofluorescence staining and statistical significance was tested using a one-way ANOVA with a Bonferroni post-test with 95% confidence intervals.

Cultured HDBECs were also assayed for either NICD, tight junctions or adherens junctions' immunofluorescence for changes relative to Notch induction. All images presented below are representative of each condition unless otherwise stated whereas the accompanying data was collected using all images. The percentage of thick and thin junctions and junctional gaps was statistically analysed using a two-way ANOVA with a Bonferroni post-test and fluorescence intensity for both VE-Cadherin and ZO-1 staining was statistically analysed using a one-way ANOVA with a Bonferroni post-test. Both analyses used confidence intervals of 95%.

All experiments were performed in triplicate and repeated 3 times unless otherwise stated and the data are presented as mean ±SEM unless otherwise indicated. All methods are described in detail in Chapter 2.

3.3 Results

3.3.1 Effect of sDll4 on the Amount and Location of Notch Intracellular Domain (NICD)

I first wanted to investigate if the recombinant sDll4 protein could induce the cleavage of NICD in HDBECs. In addition, I wanted to examine if the hypothesised increase of NICD produced by treatment with sDll4 caused any alterations in its localisation within the cell. Confluent HDBECs were treated for 4-hours with either sDll4 (1µg/ml) or VEGF (40ng/ml) before staining and imaging by z-stack confocal microscopy (Figure 3.1).

As expected, untreated samples only led to staining in a few cells and these were often dotted around the field of view. The staining appeared speckled and was more abundant in the cytoplasm with little staining seen in the nucleus. However, on several occasions the staining appeared to be clustered around the outside of the nucleus (see arrows in Figure 3.1A).

Both VEGF and sDll4 treated samples resulted in a greater number of cells with NICD staining than in untreated conditions. The majority of the staining in VEGF treated samples again appeared in the cytoplasm, however in a few cells (as indicated by arrows in Figure 3.1B) the staining appeared more concentrated in and around the nucleus. Those cells treated with sDll4 resulted in most cells in the field of view showing NICD staining. The staining here was very granular and tended to be either spread throughout the cell (as indicated by the arrows in Figure

3.1C) or concentrated in the nucleus (as indicated by the arrowheads in Figure 3.1C).

3.3.2 Effect of Recombinant Dll4 and sDll4 on Notch Signalling

Once I had established that sDll4 induced the cleavage of NICD, I next wanted to assess whether the signalling pathway was induced in full and the Notch target genes Hes1 and Hey1 were upregulated. Again, confluent HDBECs were treated with 1µg/ml Dll4, sDll4 or VEGF (40ng/ml) for 4 hours. Expression levels of Hes1 and Hey1 were then measured by qPCR (See Chapter 2).

The CT for either Hes1 (Figure 3.2A), Hey1 (Figure 3.2B) or the housekeeping gene GAPDH for each condition (untreated, VEGF, Dll4 and sDll4) were first assessed to ensure that there were no major fluctuations in GAPDH levels indicating that the test conditions were not interfering with the housekeeping gene. As expected, GAPDH CT values for all treatments were less than Hes1 or Hey1 CT values signifying that GAPDH had higher expression levels.

Next, the CT value for Hes1 untreated samples were subtracted from the CT value for GAPDH expression for untreated samples resulting in the delta CT (ΔCT) for untreated sample (Figure 3.2C). The ΔCT for the other conditions as well as for Hey1 expression (Figure 3.2D) was calculated in the same way e.g. the CT value for Hes1 expression in VEGF treated samples was subtracted from the CT value

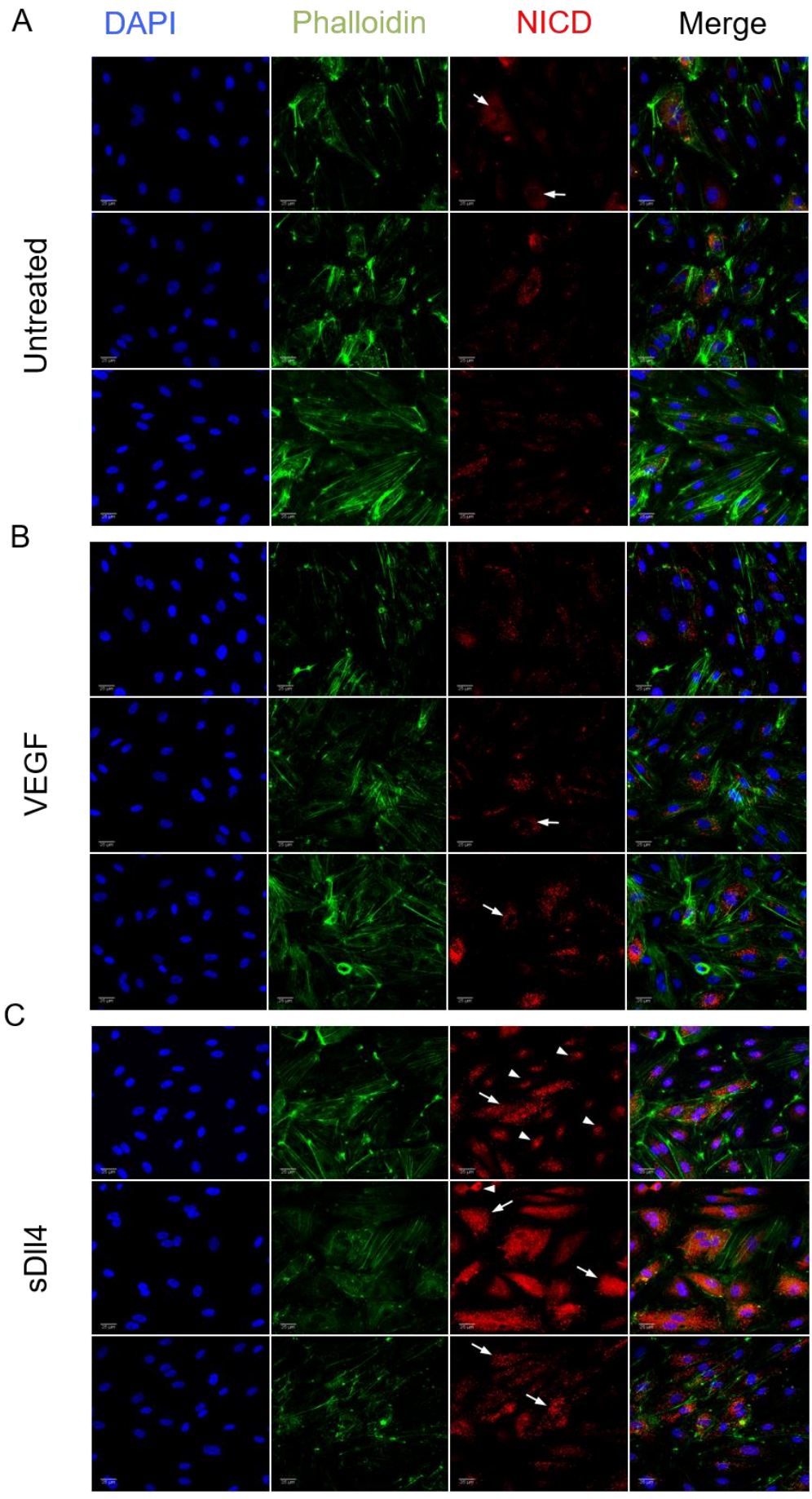

A
DAPI
Phalloidin
NICD
Merge
Untreated
B
VEGF
C
sDll4

Figure 3.1 sDll4 increases NICD in HDBECs*. Monolayers of HDBECs were treated with sDll4 (1µg/ml) or VEGF (40ng/ml) recombinant proteins for 4 hours (n=3). Cells were stained for NICD (red), the nuclear marker DAPI (blue) and the cytoskeletal marker, phalloidin (green,). Untreated cells (A) resulted in NICD staining of a few cells per field of view with the staining mainly localised to the cytoplasm (represented by arrows). VEGF treatment (B) resulted in most cells in the field of view showing granular staining which was more evenly spread through the cytoplasm. Those cells treated with sDll4 (C) resulted in very granular staining in most cells and was either spread throughout the entire cell or localised to the nucleus (arrowheads).*

for GAPDH expression in VEGF treated samples. Interestingly at this point there was little difference in Hes1 expression between any of the groups, however the ΔCT for Hey1 expression in VEGF treated cells did decrease below untreated cells more than Dll4, or sDll4.

Following the calculation of ΔCT values, the ΔCT value for Hes1 expression in untreated samples was subtracted from the ΔCT of Hes1 expression in VEGF treated samples to give the ΔΔCT value of Hes1 expression in VEGF treated samples (Figure 3.2E). Again, this was repeated for all conditions and for Hey1 expression (Figure 3.2F). At this point it starts to become clear that VEGF, Dll4 and sDll4 are all increasing Hes1 and Hey1 expression although VEGF appears to have a stronger effect.

The qPCR values are in logarithm base 2 meaning that every time that there is a doubling of DNA during the qPCR process, the CT value will decrease by 1 therefore the expression fold change is calculated by $2^{-\Delta\Delta CT}$, the results of which can be seen in Figure 3.2G and H.

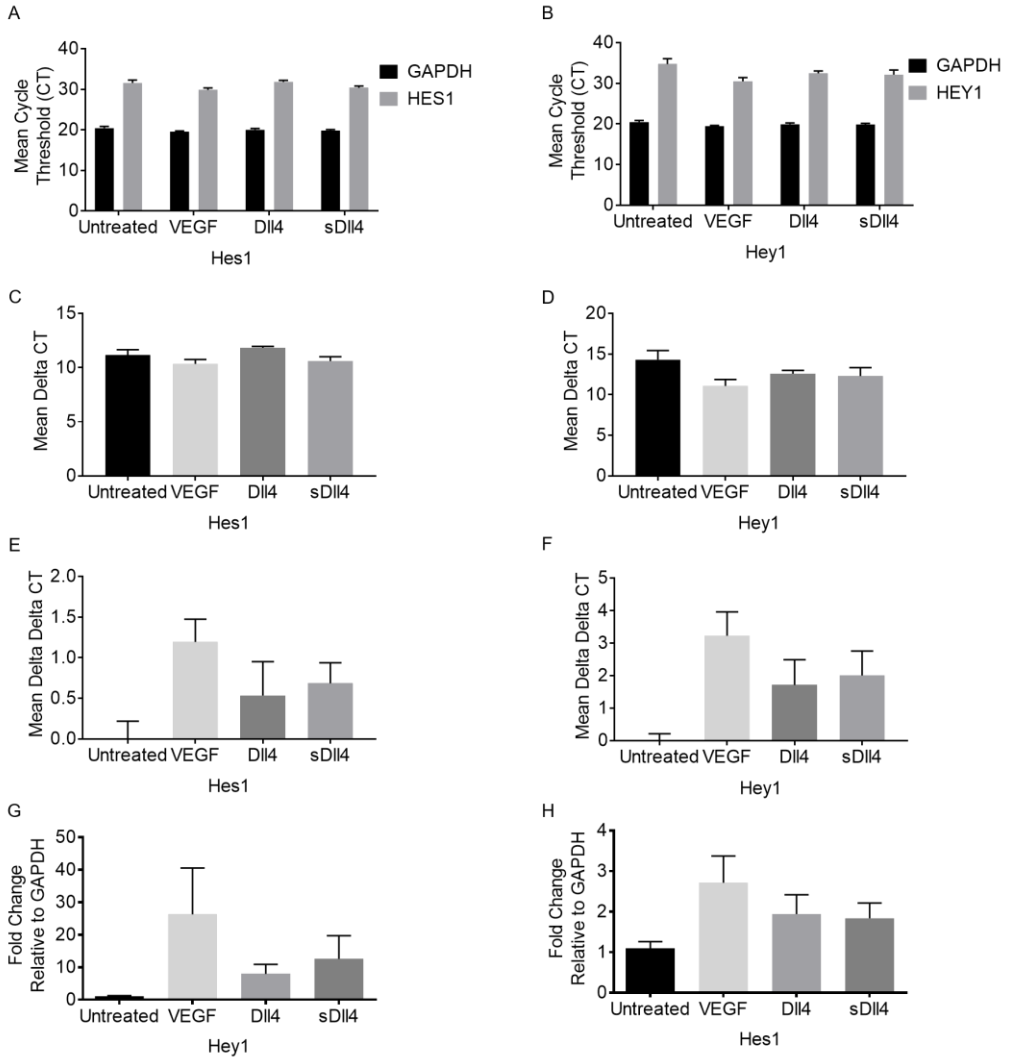


Figure 3.2 Dll4 and sDll4 induce Notch signalling. *Expression levels of Notch target genes Hes1 and Hey1 were measured by qPCR following 4 hours of incubation with sDll4, Dll4 (1µg/ml) or, VEGF (40ng/ml) recombinant proteins (n=6). CT values for Hes1 (A), Hey1 (B) and GAPDH were assessed to ensure test conditions were not affecting GAPDH expression. ΔCT values were calculated by subtracting the CT value for Hes1 or Hey1 expression from the CT value of GAPDH expression for the corresponding treatment group (C and D). Following this, ΔΔCT was calculated by subtracting the ΔCT of untreated samples from the ΔCT of either VEGF, Dll4 or sDll4 for both Hes1 (E) and Hey1 (F). Finally, the expression fold change was determined by* $2^{-\Delta\Delta CT}$ *(G and H). Dll4 and sDll4 both increased expression of Hes1 by approximately 2-fold and Hey1 to approximately 10-fold compared to untreated cells although this was not significant (One-Way ANOVA, Bonferroni post-hoc, p>0.05).*

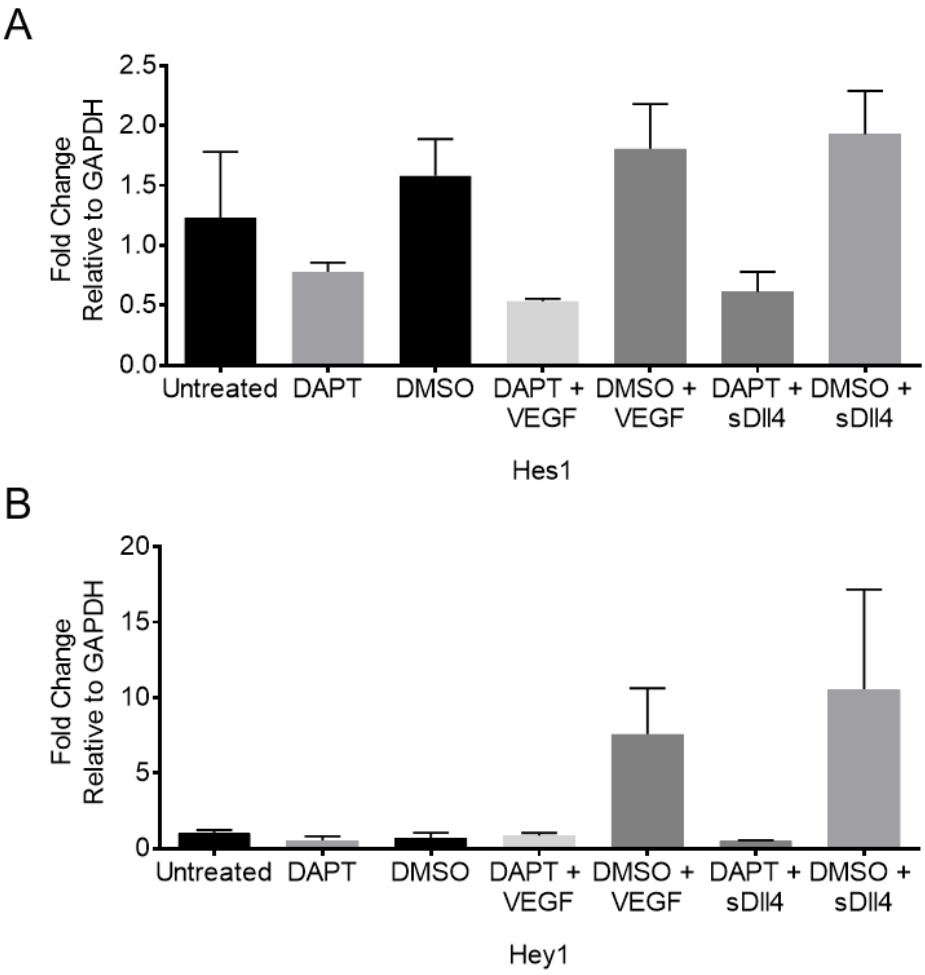


Figure 3.3 The induction of Notch signalling by sDll4 can be prevented with addition of DAPT. *Expression levels of Hes1 (A) and Hey1(B) were measured by qPCR following 4 hours of incubation with sDll4 (1µg/ml) or VEGF(40ng/ml) recombinant proteins with or without DAPT (2µM) or 1% DMSO (n=3). DAPT decreased Hes1 and Hey1 expression levels from untreated levels. DAPT treatment in combination with either VEGF or sDll4 resulted in decreased Hes1 and Hey1 expression and expression levels that were similar to those seen previously when cells were treated with VEGF or sDll4 alone confirming sDll4 was signalling through Notch.*

As expected, treatment with Dll4 increased the expression of both Hes1 (1.9 ± 0.47, Figure 3.2G) and Hey1 (7.9 ±2.93, Figure 3.2H) above that of untreated levels (1.01 ±0.17, 1.8 ±0.15). Treatment with sDll4 also increased expression of both Hes1 (1.8 ±0.38) and Hey1 (12.5 ±7.12). Interestingly, sDll4 treatment resulted in a fold change similar to that of Dll4 for Hes1 but there was a marked (albeit not significant) difference for Hey1, where there was a 4-fold increased expression.

To ensure that the increase in expression of Hes1 and Hey1 was occurring through the Notch signalling pathway HDBECs were again treated for 4 hours with sDll4 (1µg/ml) with or without the γ-secretase inhibitor Dimethyl sulfoxide (DAPT, 2µM). As expected, when HDBECs were subject to the DAPT treatment expression of both Hes1 (0.78 ±0.078) and Hey1 (0.52 ±0.27) was reduced compared to untreated cells (Hes1 1.33 ±0.36, Hey1 1.04 ±0.19). This was also the case when DAPT was given in combination with sDll4 (Hes1 0.61 ±0.17, Hey1 0.54 ±0.029) clearly indicating it induces Hes1 and Hey1 through the same pathway. As DAPT was dissolved in a solution containing 1% DMSO, which can be toxic to cells (Sperling and Larsen, 1979; Bentley *et al.*, 2014; Galvao *et al.*, 2014), a DMSO (2µM) with or without sDll4 group was included as an additional control. Treatment with DMSO alone resulted in slightly elevated Hes1 expression (1.6 ±0.31) and very similar Hey1 expression levels (0.71 ±0.36) compared to untreated cells.

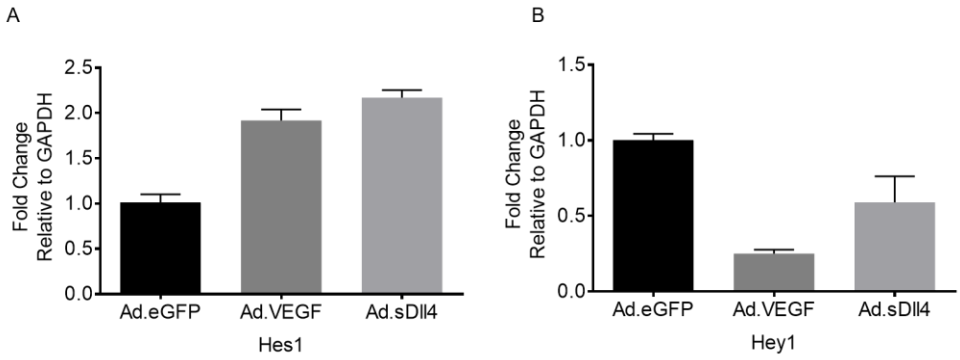


Figure 3.4 Ad.sDll4 induces Hes1 but not Hey1. *Confluent HDBECs were treated with virus conditioned media for either Ad.eGFP, Ad.sDll4 or Ad.VEGF for 4 hours before expression of Hes1 and Hey1 were measured by qPCR (n=3). Ad.sDll4 treatment resulted in a 2.17 (±0.084) fold increase expression (A) however, Hey1 expression was unexpectedly decreased by both Ad.sDll4 (0.59 ±0.172) and Ad.VEGF (0.25 ±0.026, B).*

When treated in combination with sDll4 expression levels of both Hes1 (1.9 ±.0.36) and Hey1 (10.5 ±6.6) were increased to similar levels as when treated with sDll4 only suggesting that any effect that the DMSO had on cells was negligible. It was also necessary to assess the effect that the sDll4 adenovirus (Ad.sDll4) had on Notch signalling. Again, HDBECs were treated for 4 hours with adenovirus conditioned media (See Chapter 2). While Ad.sDll4 resulted in a 2.17 (±0.084SEM) fold change (Figure 3.4) in Hes1 expression interestingly both Ad.sDll4 and Ad.VEGF resulted in a decrease in Hey1 expression (0.59 ±0.172SEM and 0.25 ±0.026SEM respectively) compared to Ad.eGFP.

3.3.3 The Effect of Ad.sDll4 on Endothelial Cell Tube Formation

As Dll4/Notch signalling has been extensively reported to be involved in angiogenesis and especially new vessel sprout formation (Hellstrom *et al.*, 2007; Lobov *et al.*, 2007) with inhibition of this pathway resulting

in hyper-sprouting and non-functional vessels, I next wanted to investigate how Notch induction would affect angiogenesis and the formation of a vascular plexus. I hypothesised that if sDll4 was sufficient to induce Notch signalling, using Ad.sDll4 conditioned media in the *in vitro* angiogenesis assay (described in chapter 2) would result in tubules which would be less angiogenic (fewer sprouts and longer tubules) than those induced by Ad.VEGF or Ad.eGFP.

Cells were treated with virus conditioned media for either Ad.eGFP, Ad.VEGF, Ad.sDll4 or Ad.VEGF and Ad.sDll4 together. Staining was quantified using ImageJ (see Chapter 2.8.3).

In images where cells had been treated with Ad.eGFP, singular tubes that were generally not connected to one another were produced. Whereas the tubes in the other treatment conditions were generally more interconnected. Ad.VEGF images tended to have tubes that were clustered towards one area as opposed to both Ad.sDll4 and Ad.sDll4 + Ad.VEGF which appeared to cover the field of view more evenly (Figure 3.5A).

As expected, cells treated with Ad.VEGF resulted in a significantly higher density of tubes than the control Ad.eGFP ($p<0.001$, Figure 3.5B). Treatment with Ad.sDll4 also resulted in a significantly higher density of tubes than Ad.eGFP, however this was still less than Ad.VEGF. Interestingly, when Ad.sDll4 and Ad.VEGF were given in combination the density of tubes was very similar to that of Ad.sDll4 alone ($p<0.05$). Conversely, where the tube density for all treatments increased above that of Ad.eGFP, the mean tube segment length for all

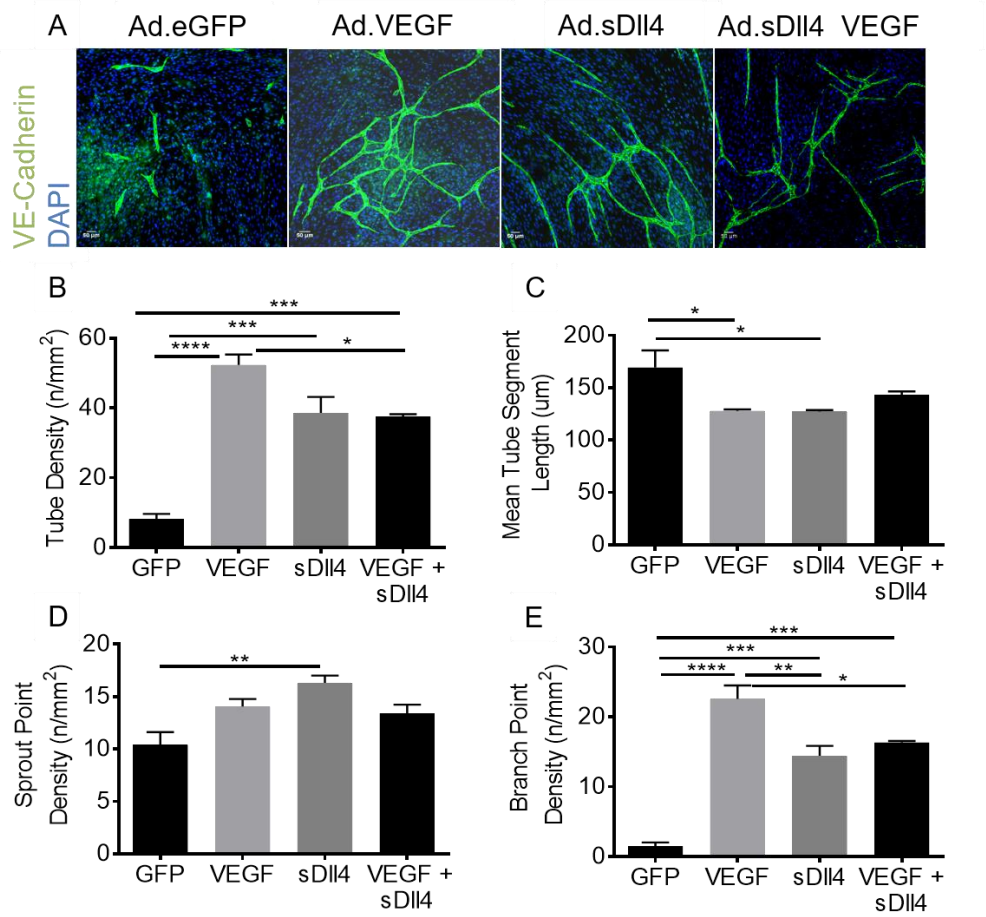


Figure 3.5 Ad.sDll4 induced tubes with less branches but more sprouts than Ad.VEGF. *HDBECs co-cultured with fibroblasts were given virus conditioned media for either Ad.eGFP, Ad.VEGF, Ad.sDll4 or Ad.VEGF + Ad.sDll4 every other day for 2 weeks (n=3). Cells were stained for VE-Cadherin (green) and DAPI (blue, A). Both Ad.sDll4 and Ad.sDll4 + Ad.VEGF resulted in a significantly higher tube density (Ad.sDll4 p=0.0004, Ad.sDll4 + Ad.VEGF p=0.0005), than the control, Ad.eGFP (B) yet shorter mean tube lengths (C). Ad.sDll4 resulted in tubes with the most sprouts (16.33 ±0.677 p=0.0091), however Ad.VEGF alone and in combination with Ad.sDll4 also increased this (D). All three treatments increased branch density with Ad.VEGF inducing the most. The data was analysed by one-way ANOVA with a Bonferroni post-test and was considered significant if p<0.05.*

3 conditions decreased (Figure 3.5C). When given alone, Ad.VEGF and Ad.sDll4's mean tube segment length both significantly decreased to 127.9μm±1.56 and 127.5μm±1.31 respectively ($p>0.05$, when compared to control Ad.eGFP). When given in combination, tube segment length was slightly longer.

The sprout density was increased above Ad.eGFP levels when treated with Ad.VEGF although surprisingly, Ad.sDll4 alone resulted in the highest sprout density: 16.3 ±0.68 ($p=0.0091$, when compared to control, Figure 3.5D). When cells were treated with Ad.sDll4 and Ad.VEGF were given together the increase in sprout density seen by Ad.sDll4 alone was reduced to 13.4/mm^2, similar to the levels of Ad.VEGF alone.

The density of branch points was increased significantly above Ad.eGFP for all conditions. Ad.VEGF resulted in the highest density of branches (22.6 ±1.93, $p>0.0001$). Interestingly, when Ad.sDll4 was given alone, although branch point density significantly increased to 14.5/mm^2 ($p=0.0004$, compared to Ad.eGFP), it was slightly lower than when given in combination with Ad.VEGF suggesting that while Ad.sDll4 stimulates tube formation when given in combination with Ad.VEGF there is a switch from growth by sprouting to growth by branching.

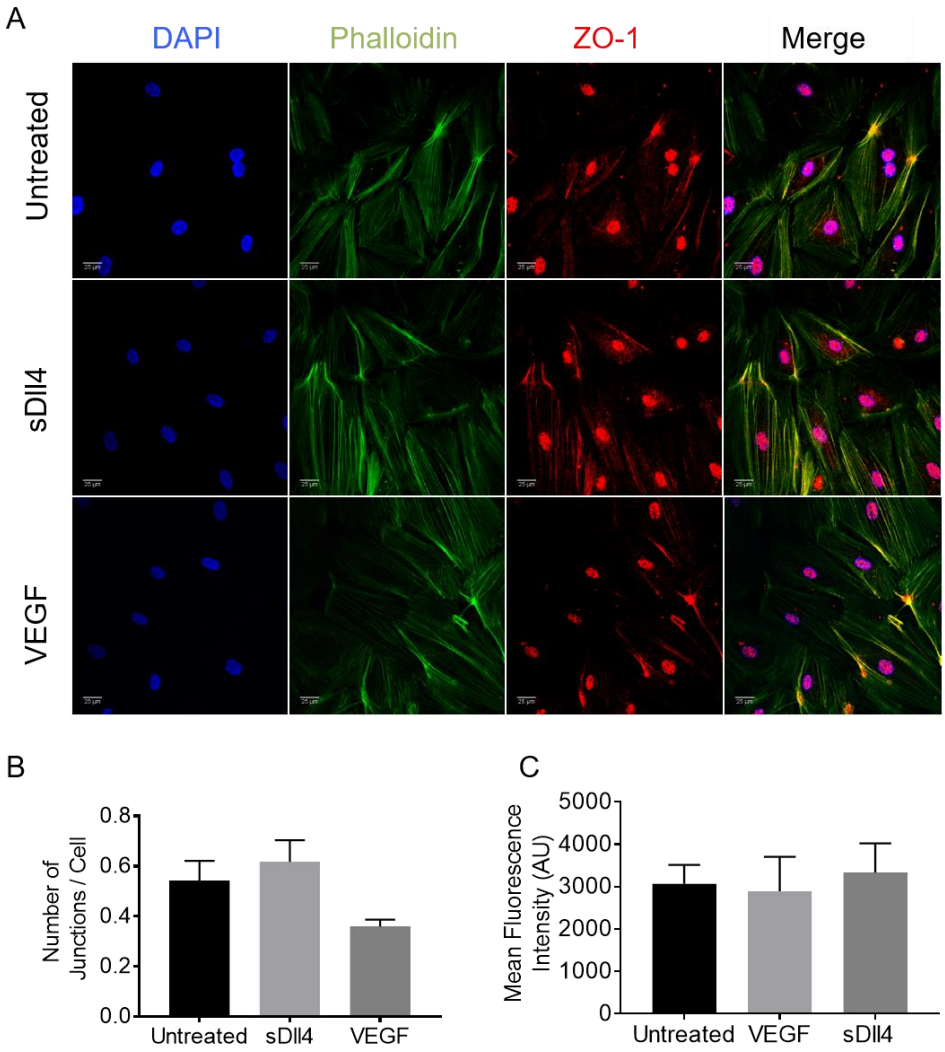


Figure 3.6 sDll4 has no effect on ZO-1 tight junctions. *Confluent HDBECs were treated for 4 hours with either sDll4 (1µg/m) or VEGF (40ng/ml) recombinant proteins before cells were fixed and stained for ZO-1 (red), phalloidin (green) and DAPI (blue, A, n=3). Treatment with sDll4 had no effect on the number of ZO-1 junctions per cell formed (B) although there was a slight decrease resulting from VEGF treatment. Junctional fluorescence was also investigated and resulted in a minor increase in fluorescence by sDll4(C).*

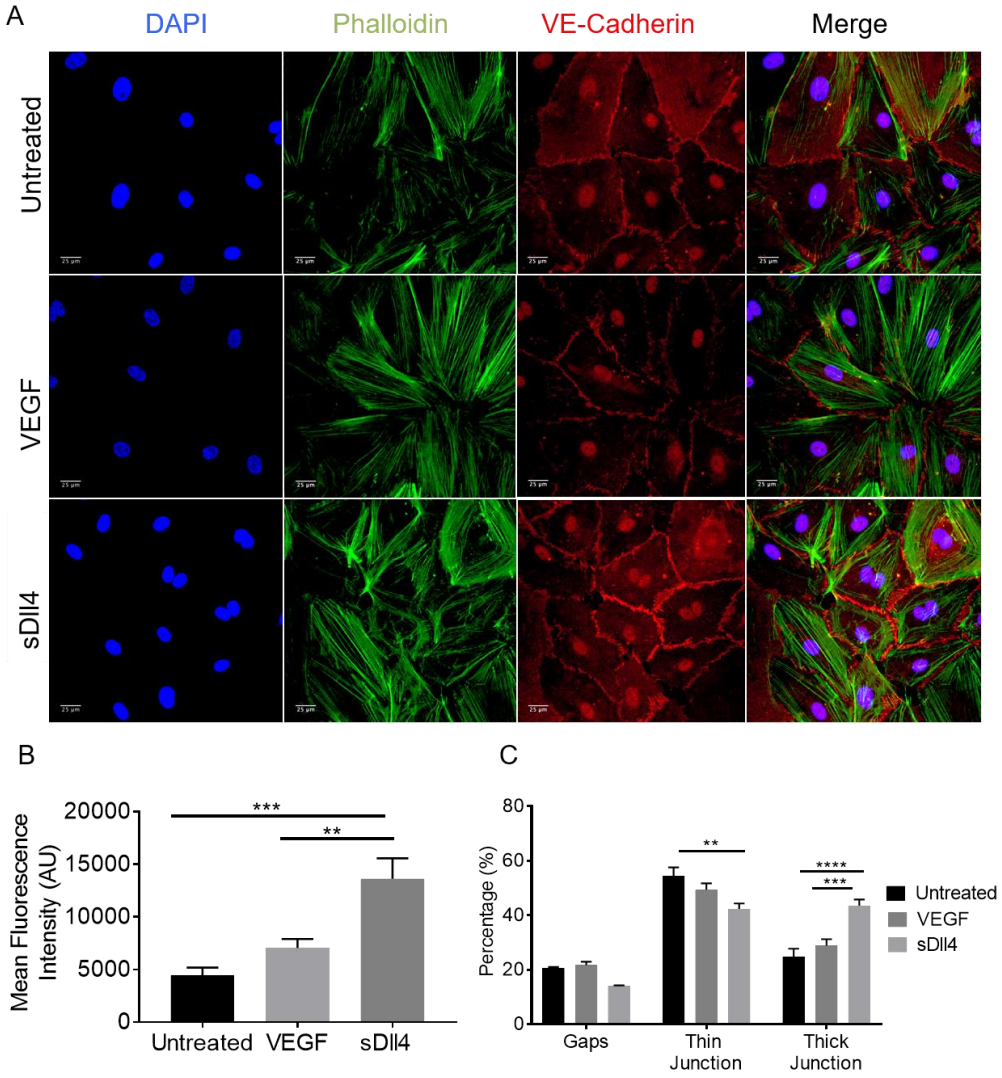


Figure 3.7 sDll4 increased VE-Cadherin thick junctions and fluorescence intensity. *HDBECs were grown to confluency and then treated for 4 hours with sDll4 (1µg/ml) or VEGF (40ng/ml) recombinant protein. Cells were stained for VE-Cadherin (red), Phalloidin (green), and DAPI (blue, A). sDll4 treated cells produced significantly more intense staining than either untreated (p=0.001) or VEGF samples (p=0.048, One-way ANOVA with a Bonferroni post-test. n=3, C). sDll4 treatment was found to have a significantly higher percentage of thicker junctions than both untreated (p<0.001) and VEGF conditions (p=0.003, Two-way ANOVA, with a Bonferroni post-test, n=3, B). sDll4 treated cells also resulted in the lowest percentage of gaps with 14% (±0.213).*

The Effect of sDll4 on Endothelial Cell Barrier Function

Next, I wanted to investigate how the induction of Notch signalling by sDll4 affects endothelial barrier function. Firstly, monolayers of HDBECs were treated with either sDll4 (1µg/ml) or VEGF (40ng/ml) and then either adherens or tight junctions were stained for (see Chapter 2).

Tight junctions were stained using a ZO-1 antibody. Interestingly, images for all treatments show strong staining in the nucleus as well as some junctional staining with no clear differences (Figure 3.6A). Quantification of the number of junctions per cell illustrated that there were no significant differences between any condition. Untreated cells resulted in 0.62 junctions/cell (0.086) however, treatment with VEGF lead to the fewest junctions per cell (0.36 junctions/cell ±0.027). On the other hand, sDll4 did result in a small rise from 0.543 junctions/cell (±0.0785) although there was only a difference of less than 0.3 junctions/cell between all 3 conditions (Figure 3.6B).

The fluorescence intensity of the junctions was also assessed to investigate if the reason why there had been no change in the number or junctions per cell was that the junctions were just now more concentrated with ZO-1 rather than increasing the numbers of junctions. However, this seems not to be the case as there was no significant differences between groups (Figure 3.6C)

Adherens junctions were stained up using a VE-Cadherin antibody and Phalloidin and DAPI were used to help distinguish cells. Confocal images visibly show a more intense and clearer junctional stain in those samples treated with sDll4 than in those treated with VEGF or those left

untreated (Figure 3.7A). The junctional fluorescence intensity for each group were then analysed to investigate the difference in intensity that I was seeing in the images. VEGF treated samples saw a small, but not significant increase in fluorescence intensity compared to untreated samples (Figure 3.7B). Those cells treated with sDll4 resulted in a large and significant increase over both VEGF ($p=0.0048$) and untreated samples ($p=0.0001$, One-way ANOVA with a Bonferroni post-test, $n=9$) affirming what I could see from the images.

Images were also quantified to evaluate the make-up of the intercellular junctions: the number and length of junctions per cell, the percentage of these that were thick or thin junctions and the percentage of the junction that was occupied by junctional gaps (Figure 3.7C). As expected, VEGF treated samples gave rise to the highest percentage of junctional gaps (21.7% ±1.22) while samples treated with sDll4 lead to the least number of junctional gaps (14.1% ±0.213).

Those samples treated with VEGF also resulted in slightly less thin junctions (49.3% ±2.36) than the untreated samples (54.5% ±3.07. Figure 3.7b) whereas those treated with sDll4 were made up of significantly fewer thin junctions (42.3% ±2.01, $p=0.002$) compared to untreated samples. This meant that sDll4 treatment gave rise to a significantly higher percentage of thick junctions (43.6% ±2.21, $p<0.0001$) than both VEGF (28.9% ±2.33) and untreated (2.89% ±2.86) samples therefore suggesting a tighter barrier.

3.4 Discussion

3.4.1 sDll4 Increases NICD Levels In Vitro

The Notch signalling pathway that occurs upon the binding of one of its ligands has been well described (Andersson, Sandberg and Lendahl, 2011; Guruharsha, Kankel and Artavanis-Tsakonas, 2012). Upon Ligand interaction with Notch a series of proteolytic cleavages occurs leading to the eventual release of NICD. When NICD is cleaved it then translocates to the nucleus, therefore if Notch signalling is induced then an increase in NICD would be expected with it being more highly expressed in the nucleus (Guruharsha, Kankel and Artavanis-Tsakonas, 2012). This is what was observed when HDBECs were treated with sDll4 (Figure 3.1). Surprisingly, while VEGF treated cells resulted in a higher proportion of cells with NICD staining than in untreated conditions the staining itself was found mainly in the cytoplasm and was of a granular appearance. The NICD staining in sDll4 treated cells on the other hand, was found to be present in the majority of cells and also had a very granular appearance but there also seemed to be more staining located in the nucleus than the other groups. It is possible that the differences seen between VEGF and sDll4 are because some or most of the NICD has already reached the nucleus, activated Hes1 and Hey1 expression and has been or is being degraded. The differences in levels of Hes1 and Hey1 expression that was seen after the same incubation length (Figure 3.2) further supports

the idea that the activation of Notch signalling by VEGF and sDll4 occurs at differing time points.

Confluent endothelial monolayers confer a basal level of Dll4/Notch signalling therefore a basal level of NICD staining was expected and explains the staining seen in untreated cells. Interestingly, the staining in untreated cells (see arrows in Figure 3.1A) and a few VEGF treated cells also seemed to suggest that NICD localised near to the nuclear envelop albeit still in the cytoplasm. This could possibly be indicative of the NICD translocating into the nucleus, again suggesting that VEGF and Dll4 mediated nuclear localisation of NICD occurs with different kinetics.

3.4.2 sDll4 Increases Hes1 and Hey1 Expression Through Induction of Notch Signalling

The signalling cascade of Notch leads to the upregulation of genes such as transcription factors of the Hes/Hey superfamily for instance Hes1 and Hey1. Studies have capitalised on this signalling cascade to understand the Dll4/Notch signalling and the role it plays in development and angiogenesis. A recombinant Dll4 fused to the fragment crystallisation (FC) portion of IgG, which blocks Dll4 activation of Notch, resulted in a marked increase in poorly perfused vessels with increased sprouting and branching in tumour angiogenesis (Noguera-Troise *et al.*, 2006; Scehnet *et al.*, 2007). In addition to this, researchers such as Trindade *et al*. (2008), reported that Dll4 signalling induction/overexpression resulted in arterialisation as well as halting vessel formation supporting previous data despite opposing

methodologies. In the present study, both full length and soluble recombinant Dll4 protein has been used to induce Notch signalling. While there are several ways to approach the study of this pathway, few choose to use full length Dll4. This could be due to it being a larger protein than its soluble counterpart and so there is the possibility that it is too large to reach and bind Notch when it is not anchored to the membrane. However, the data presented above in Figure 3.2A and B clearly show that both Dll4 and sDll4 upregulate the Notch target genes Hes1 and Hey1 and therefore indicate that, at least *in vitro*, this is not the case. While this could potentially be due to both proteins having the same sequence (see 3.2.1) it is also feasible that *in vitro* endothelial cell monolayers, which tend to be made up of cells with a more evenly distributed volume than their *in vivo* counterparts which are usually thicker around the nuclear region of the cell and thinner towards the periphery (Nagy *et al.*, 2008), are able to present Notch in a way that is more easily accessible to the full length Dll4 recombinant protein than during *in vivo* studies. Furthermore, unlike other studies that have used Dll4 and sDll4 fusion proteins to inhibit endogenous Dll4 (Lobov *et al.*, 2007; Scehnet *et al.*, 2007; Larrivée *et al.*, 2012) the data here showed that the sDll4 used in the present experiments was in fact inducing Notch signalling. This difference is possibly down to using the recombinant soluble protein as opposed to the sDll4 combined with the FC region of IgG as more commonly seen in the literature. This type of sDll4 may allow it to bind to Notch but not induce the signalling pathway and thereby block signalling.

Interestingly despite upregulation of both Hes1 and Hey1 genes, Hey1 expression increased about 10-fold whereas Hes1 only increased 2-fold. While this is still a notable increase, neither were statistically significant as there were some large deviations from mean (see Figure 3.2) which meant that the coefficient of variation of the data was also high. This could possibly be due to slight variations in confluency or Glyceraldehyde 3-phosphate dehydrogenase (GAPDH) levels between experiments or even pipetting errors, however even with the variability the trend of increased Hes1 and Hey1 expression was seen for each experiment.

The differences seen between Hes1 and Hey1 expression levels on the other hand, may simply be due to favouring of Hey1 over Hes1 under these conditions. Alternatively, the reduced expression levels of Hes1 compared to Hey1 after 4 hours of treatment supports the oscillatory pattern of expression of Hes1 described by Hirata (2002). They reported that when endothelial cells were serum treated, both mRNA and protein expression of Hes1 oscillated with a 2-hour periodicity.

The γ-secretase inhibitor DAPT is a potent inhibitor of Notch signalling (Geling *et al.*, 2002; Diez *et al.*, 2007). Upon ligand binding of Notch, the enzyme γ-secretase is vital in the subsequent cleavage of the NICD, which can then move to the nucleus. It is at this cleavage point in the Notch cascade that DAPT works by inhibiting the γ-secretase enzyme ensuring that any downstream effects are negated. It has also been used to disrupt Notch signalling and elucidate the roles of Dll4/Notch in angiogenesis with Hellstrom et al (2007) determining that

Dll4 negatively regulates sprouting angiogenesis in addition to playing a role in post-angiogenic remodelling (Lobov *et al.*, 2011). I wanted to know whether the effect seen by sDll4 could be prevented by the γ-secretase inhibitor DAPT, since this would confirm that sDll4 was acting through Notch and not another mechanism. The decrease in expression of Hes1 and Hey1 when treated with DAPT alone in comparison to untreated samples indicates that there is a baseline of endogenous Notch signalling occurring in the monolayer of cells as seen previously (Shutter *et al.*, 2000). Given that γ-secretase acts after the ligand has bound to Notch a complete inhibition of any sDll4 effect, such as that seen in Figure 3.3A and B, would be expected unless the signalling occurred through a concurrent parallel mechanism.

3.4.3 Ad.sDll4 Induces Hes1 Expression but Not Hey1.

The custom-made adenovirus encoding mouse sDll4 was produced primarily for my *in vivo* studies (see section 3.2.1 for sequence). Prior to the *in vivo* studies, it was also necessary to assess how the virus interacts with Notch. Using HDBECs treated with virus conditioned media Hes1 and Hey1 expression was assessed by qPCR as described in Chapter 2. While the resulting Hes1 expression showed a two-fold increase (Figure 3.4a), similar to what was seen with sDll4 protein Hey1 expression unexpectedly decreased for both Ad.sDll4 and Ad.VEGF (Figure 3.4b). The decrease seen by Ad.sDll4 may well be because the virus encodes the mouse sDll4 gene and these were human cells. Despite Dll4 being a highly-conserved gene there are still several amino acid differences between the human and mouse Dll4 in both the MNNL

and DSL regions (see section 3.2.1) which are integral for Dll4's ability to bind to Notch (Rebay *et al.*, 1991). These differences may mean the mouse Ad.sDll4 is unable to fully activate the signals needed to induce Hey1 expression. In contrast this cannot be the case for the Ad.VEGF virus as it encodes human $VEGF_{165}$a. This suggests that there is an alternative explanation such as the adenovirus itself or the conditioned media did not contain equal amounts of protein, that other solutes found in conditioned media not including the virus caused the reduction in expression of Hey1, or that Ad.sDLL4 induces different kinetics of Hey1 from sDLL4. To investigate if this is the case, conditioned media that had not been infected with adenovirus could be tested or the adenoviruses could potentially be added straight onto the endothelial cells instead therefore controlling concentration more effectively.

Interestingly embryonic cells that were made to overexpress mouse Dll4 were shown to result in a 3 fold increase in Hey1 expression (Trindade *et al.*, 2008) supporting the data presented in section 3.3.2 but not the data presented here. However, in a study using human umbilical vein endothelial cells (HUVECs) transduced with Dll4 qPCR analysis showed a decrease in Hey1 expression although there was still an increase in expression of another Notch target gene, Hey2 (Williams *et al.*, 2006). The differences in expression in Hey1 that is seen with the use of the different ligand constructs and varying experimental approaches to Notch activation suggest that the upregulation of the Notch target genes may indeed be subject to both these conditions

which would go some way to explaining the complexity of Notch signalling.

3.4.4 Ad.sDll4 Induces Tube Formation

Endothelial differentiation assays which are used to measure the ability of endothelial cells to form three dimensional structures such as tubes are commonly used to study all aspects of angiogenesis from VEGF and it's receptors (Koolwijk *et al.*, 2001) to tumour angiogenesis (Matsuo *et al.*, 2009) and micro-RNAs (Fang *et al.*, 2011). Studies investigating Dll4/Notch signalling most commonly using blockade of Dll4 in co-culture systems have resulted in the increased production of vessels that were also shown to be immature (Scehnet *et al.*, 2007; Dill *et al.*, 2012) as well as increased sprout formation (Ridgway *et al.*, 2006).

The data presented here are a result of stimulation of Notch signalling as opposed to inhibition, however the significant increase in tube density does not support previously published data (Scehnet *et al.*, 2007; Dill *et al.*, 2012). When these results were taken in conjunction with the unexpected decrease in Hey1 expression seen earlier I became suspicious to whether the adenovirus conditioned media was stimulating growth and if the sDll4 was not working as expected, if at all. To investigate this, I set out to repeat the experiment using recombinant sDll4 and VEGF however the amount of recombinant protein needed to complete the experiment once was too large and costly and so this route was not pursued.

Furthermore, the increase in sprouting and decrease in mean tubule length seen in Figure 3.5 also does not complement the published data although this is most likely down to the large variance in methodology used for these assays. While the data presented here is the outcome of a 2 week experiment of endothelial cells cultured on top of fibroblasts, other studies conclusions, for example, are drawn after less than 24 hours of experimentation and with the use of Matrigel (Scehnet *et al.*, 2007; Dill *et al.*, 2012) suggesting results may be time dependent as well as subject to the co-culture methodology used.

3.4.5 sDll4 Increases Adherens but Not Tight Junctions

Endothelial cell-cell junctions are critical in forming and maintaining the vessel barrier. It is becoming clearer that VE-Cadherin junctions play a key role in the maintenance of vascular integrity. For example, VE-Cadherin interactions have been shown to inhibit angiogenic growth *in vitro*. Abraham et al (2009) reported that partially blocking VE-Cadherin in established capillary-like 3D HUVEC tubules enhanced sprouting. In addition, partial knockdown of VE-Cadherin in zebrafish embryos compromised vascular integrity and tubulogenesis which also led to ectopic sprouting (Montero-Balaguer *et al.*, 2009) demonstrating how vital VE-Cadherin is especially during development.

Moreover, in cultured endothelial cells VE-Cadherin limits proliferation by contact inhibition (Lampugnani *et al.*, 2003, 2006). They also reported that this led to the suppression of VEGFR2 induced pro-mitogenic signals. Here, I presented data where Notch induction by sDll4 resulted in the formation of VE-Cadherin-containing junctions that

were thicker but with fewer gaps than untreated control samples (Figure 3.7) indicative of stronger junctions and increased integrity. This, in association with the reported downregulation of VEGFR2 by Dll4/Notch signalling in angiogenesis (Suchting *et al.*, 2007) adds further strength to the importance of VE-Cadherin in barrier function.

Additionally, the data presented here suggests Notch signalling is key in maintaining vascular integrity during angiogenesis as suggested by a study which reported that blocking Notch with DAPT in either embryoid bodies or mouse retinas resulted in a VE-Cadherin profile that was typical of actively sprouting endothelial cells concluding that VE-Cadherin and so endothelial junctions are regulated by Notch during sprouting angiogenesis (Bentley *et al.*, 2014). Conversely, Gavard and Gutkind (2006) proposed that VEGF destabilises intercellular junctions by promoting VE-Cadherin endocytosis after only 30 minutes. However, they also reported that once the VEGF stimulus was removed the VE-Cadherin re-localised to the cell membrane and re-formed cell-cell contacts as well as being able to block the internalisation with a VEGFR2 inhibitor. This suggests that VE-Cadherin internalisation is both stimulus and time dependent and so once VEGF induces Notch signalling the subsequent downregulation of VEGFR2 would prevent any further destabilisation.

sDll4 did not have a significant effect on ZO-1 junction formation despite Tornavaca et al (2015) reporting that ZO-1 depletion by siRNA in cultured endothelial cells resulted in tight junction disruption, redistribution of active myosin II from junctions to stress fibres and a

reduction in tension on VE-Cadherin suggesting that ZO-1 is essential for barrier formation, regulating cadherin-mediated cell-cell tension and cytoskeletal organisation. However, it is possible that these effects could be due to the control that adherens junctions have over tight junctions. Tornavaca *et al* (2015) also went on to report that VE-Cadherin acts upstream of ZO-1 as siRNA depletion of VE-Cadherin in endothelial cells resulted in disrupted tight junctions and decreased ZO-1 expression. In addition, it has been reported that VE-Cadherin is involved in upregulating a key tight junction protein, claudin-5 (Taddei *et al.*, 2008) through the phosphorylation forkhead box factor FoxO1 via Akt activation and by stopping the translocation of β-catenin to the nucleus. This upstream regulation of ZO-1 and tight junctions in general would suggest that they would form after adherens junctions and so it could be possible that the ZO-1 junction formation seen here may have developed further if given more time.

3.5 Concluding Remarks

The soluble portion of Dll4 was found to be sufficient to stimulate NICD translocation to the nucleus and an increase in expression of the Notch target genes Hes1 and Hey1. Surprisingly Ad.sDll4 conditioned media was able to stimulate tubule formation and sprouting *in vitro* as well as increasing Hes1 expression but decreasing Hey1 expression. Furthermore, sDll4 also influenced barrier function by increasing the percentage of thick adherens junction while decreasing the junctional gaps but had no effect on tight junction formation after 4 hours. These results show that sDLL4 recombinant protein stimulates Notch-1 signalling and VE-Cadherin dependent adherens junctions in endothelial cells. They also indicate that Ad.sDLL4 is capable of inducing Notch-1 signalling in endothelial cells.

Chapter 4: Dll4/Notch Signalling Regulates Vascular Permeability Through cAMP/PKA Dependent Pathway

4.1 Introduction

The permeability of vessels, or their ability to regulate the movement of fluid and solutes between the blood and tissue, is essential to ensure that the hydrostatic pressure gradient (and oncotic pressure gradient for protein permeability) remain balanced. Integral to this is the endothelial barrier which acts as the primary point where the exchange of water and solutes are regulated. Loss of control in the barrier function can lead to a dangerous drop in blood pressure because of a reduced vascular volume. If left uncorrected, it can result in critical harm to vital organs such as the brain, heart and kidneys as well as the development of oedema which is often associated with pathologies such as age-related macular degeneration and most cancers e.g. glioblastomas (Stummer, 2007; Lin, 2013).

There are a few different assays that have been developed to aid the understanding of vascular permeability regulation. The *in vitro* trans endothelial electrical resistance (TEER) assay (Shuler and Hickman, 2015) measures the resistance across a monolayer of cultured endothelial cells using direct current and is inversely proportional to the permeability. Another widely used *in vitro* permeability assay is the use

of transwells (Siflinger-Birnboim *et al.*, 1987), whereby confluent endothelial cells sit atop a permeable membrane and endothelial permeability is measured by the amount of fluorescent dye-bound albumin that is able to pass through into the lower chamber of the transwell (Cooper *et al.*, 1987; Behzadian *et al.*, 2003). While both these assays will give a good indication of how the permeability is affected, they lack other variables, such as shear stress, that are found *in vivo*. It is also worth noting that while increases in permeability by agents such as VEGF have been shown to act within 1 minute *in vivo* (Bates and Curry, 1996), this increase can take hours *in vitro* (Nagy *et al.*, 2008).

While *in vivo* permeability assays allow for a more relevant understanding of permeability regulation, popular Evans' blue dye based assays still have drawbacks. These assays originally developed by Miles and Miles (1952) use dyes such as Evans' blue that are non-covalently bound to albumin and injected into an animal. The accumulation of the dye is then measured after a period (often at least 30 minutes) and the permeability is defined as the amount of albumin-dye complex that is present in the tissue of interest. This can be quantified by extracting the dye and measuring the intensity spectrophotometrically (Nagy *et al.*, 2006). However, this does not always distinguish between the dye that has extravasated the vessel and that which is still within it. In addition, it cannot be known for certain how much of the dye is bound to the albumin and how much is free dye

and the assay itself can be argued that it uses indirect measurements that measure diffusive gradients rather than true permeability.

Conversely, the cannulation and artificial perfusion of frog and rat mesenteric microvessels in vivo can allow for the measurement of permeability when undertaken using carefully controlled experimental conditions. The variations of this technique to account for measurements of Lp, or Ps have been well defined (Michel *et al.*, 1974; Michel, 1980; Kendall and Michel, 1995; Michel and Curry, 1999; Adamson *et al.*, 2004) and it is their ability to be able to control for both hydrostatic and oncotic pressures which has helped elicit the effects of many molecules, such as vascular endothelial growth factor (VEGF, Bates and Curry, 1996), Angiopoeitin1 (Ang1, Salmon et al., 2009) and cyclic adenosine monophosphate (cAMP, He et al., 2000) on vascular permeability.

It has been well documented that during angiogenesis VEGF is upregulated (Leung *et al.*, 1989; Zhang *et al.*, 2000; Shibuya, 2013; Jin, Kaluza and Jakobsson, 2014) and is a potent inducer of increased vessel permeability (Bates and Curry, 1996, 1997; Pocock *et al.*, 2000). This occurs mainly through VEGF binding to VEGF receptor 2 (VEGFR2) on the surface membrane of endothelial cells (Eichmann and Simons, 2012; Shibuya, 2013). This ligand-receptor interplay is also able to upregulate the Notch ligand, Dll4 (Lobov *et al.*, 2007). Dll4 can then bind to Notch on an adjacent endothelial cell causing both cells to polarise and take on either the Dll4 highly expressing tip cell phenotype or the Notch highly expressing stalk cell phenotype, enabling the

formation of a new sprout (Hellstrom *et al.*, 2007; Cristofaro *et al.*, 2013). Interestingly this signalling also acts as a negative feedback loop (Lobov *et al.*, 2007), down regulating VEGFR2 and so actively managing how many new sprouts are allowed to form.

Although Dll4 has been intensely studied in its role in sprouting angiogenesis, it is becoming more apparent that it may also be important in other pathways. For example, Dll4 has been reported to be a marker for arterialisation during development (Lawson *et al.*, 2001) as well as being basally expressed in arterial calibre vessels but not veins (Shutter *et al.*, 2000; Cristofaro *et al.*, 2013). The expression of Dll4 in mature quiescent arterial vessels suggests that it has a further role outside of angiogenesis which may also be arterial specific.

Dll4 inhibition studies report that lack of Dll4/notch signalling results in non-productive angiogenesis (Noguera-Troise *et al.*, 2006) often with hyper-sprouting and any vessels that do form often have poor perfusion (Scehnet *et al.*, 2007). This has led to the view that this signalling pathway is anti-angiogenic or a marker of quiescence. More recently, this view has been supported by the discovery that NICD, which is cleaved off upon binding with Dll4 enhances cell adhesion to extracellular matrix proteins through increased integrin activity (Hodkinson *et al.*, 2007). For example, activated human myeloid cells transfected with NICD showed increased adhesion to fibronectin. Furthermore, Dou *et al* (2008) demonstrated that loss of the recombination signal-binding protein Jκ (RBP-jκ, a suppressor of Hairless/LAG-1 (CSL) family DNA-binding protein and which interacts

with NICD in the nucleus) in adult endothelial cells reinitiated angiogenesis indicating that notch signalling plays a role in maintaining endothelial cell quiescence.

The increasing amounts of data linking Notch induction to quiescence and cell-cell adhesion described above, suggests that the Dll4/Notch pathway is involved in the regulation of cell-cell junctions and thus permeability. In the previous chapter I established a link between Dll4/Notch signalling and increased VE-Cadherin expression at the endothelial junction. VE-Cadherin is a well-known component of adherens junctions and has been shown to be linked to endothelial permeability. It would therefore be reasonable to hypothesise that increased VE-Cadherin expression due to Dll4/Notch signalling would lead to a reduction in vascular permeability and so I set out to investigate how the induction of Notch by sDll4 would affect vascular permeability *in vivo*.

4.2 Methods

All techniques used in this chapter are described in detail in Chapter 2 and are briefly summarized here.

For hydraulic conductivity (Lp) experiments, Male Han Wistar rats were anaesthetized and then had their gut exposed. The mesentery was draped over a quartz pillar and bathed in warmed Ringer's solution. A refillable glass micropipette was then used to cannulate a post-capillary venule and the vessel was perfused, continuously, with BSA-Ringer's solution (1%). A bent pipette used to occlude the vessel was then placed in position downstream on the cannulation site (but not occluding the vessel). The pipette was next refilled with the control solution; BSA-Ringer's solution (1%) with washed red blood cells (RBC) and the vessel was occluded at 15-20 second intervals. After approximately 8min the pipette was refilled again with either the control solution, Dll4 (1µg/ml), sDll4 (1µg/ml), or the PKA inhibitor H89 dihydrochloride (H89, 1µM) and repeated occlusion of the vessel was continued.

Concentrations for sDll4 and VEGF were chosen as previously described in Chapter 3. The concentration for H89 was chosen based on previous data using the hydraulic conductivity method (He, Zeng and Curry, 2000). Time periods were also chosen based on the literature (Noguera-Troise *et al.*, 2006)

Microvessel Lp was measured using a video recording of each vessel. The velocity of a single RBC during each vessel occlusion, its distance

from the occlusion site and the vessel's radius were used to calculate the transcapillary water flow per unit area (J_v/S). Lp was then calculated as the slope of the relation between J_v/S and pressure. Mann-Whitney tests was performed using the fold change compared to baseline maximal responses for BSA versus Dll4 and BSA versus sDll4. Kruskal-Wallis test (with Dunn's multiple comparison test) was performed for comparison of maximal responses for sDll4 versus H89 and H89 + sDll4. Confidence levels were set at 95% and all data is presented as mean ±SEM unless otherwise stated.

To determine Hes1 and Hey1 expression changes, HDBECs were cultured until confluent prior to treatment with recombinant sDll4 or VEGF with or without the PKA inhibitor H89-dihydrochloride (H89) for 4 hours. Hes1 and Hey1 expression levels were then measured by qPCR. A one-way ANOVA with a Bonferroni post-test was used to compare between groups. Confidence intervals of 95% were used to determine statistical significance and all data is presented as mean ±SEM unless otherwise stated.

4.3 Results

4.3.1 Part 1: Developing a Working Lp Rig and Rat Tray

4.3.1.1 Building the Rig

Prior to commencing the Lp experiments, I needed to first design and build the equipment (rig) to do the Lp experiments on. It was essential that the rig allowed for the imaging of the mesentery by intravital video microscopy whilst keeping the tissue warm, moist and the animal under gaseous anaesthetic. This was achieved using a two-tiered air table where the microscope (on a movable stage) would sit on the lower tier, the rat could be placed over the objective lenses on the upper tier and the air table would help remove any vibrations (Figure 4.1). The mesentery would then be kept warm and moist by dripping Ringer's solution onto it after it had passed through a heated coil attached to a water bath set to 37°C (Figure 4.2C, D and E).

To control for the pressure within the cannulated vessel I built a manometer that fed into the back of the cannulating pipette (Figure 4.2A and B). The pipette was also attached to a refilling system controlled by a syringe pump. This enabled the pipette to be refilled with different perfusates without the need to recannulate. Originally, a manual micromanipulator held the pipette however, to improve handling of the pipette and the smoothness of cannulation it was decided to move to a motorised micromanipulator (Figure 4.2F). Two other manual micromanipulators were also used, one each for the restraining pipette (Figure 4.2G) and one for the occluder (Figure 4.2H).

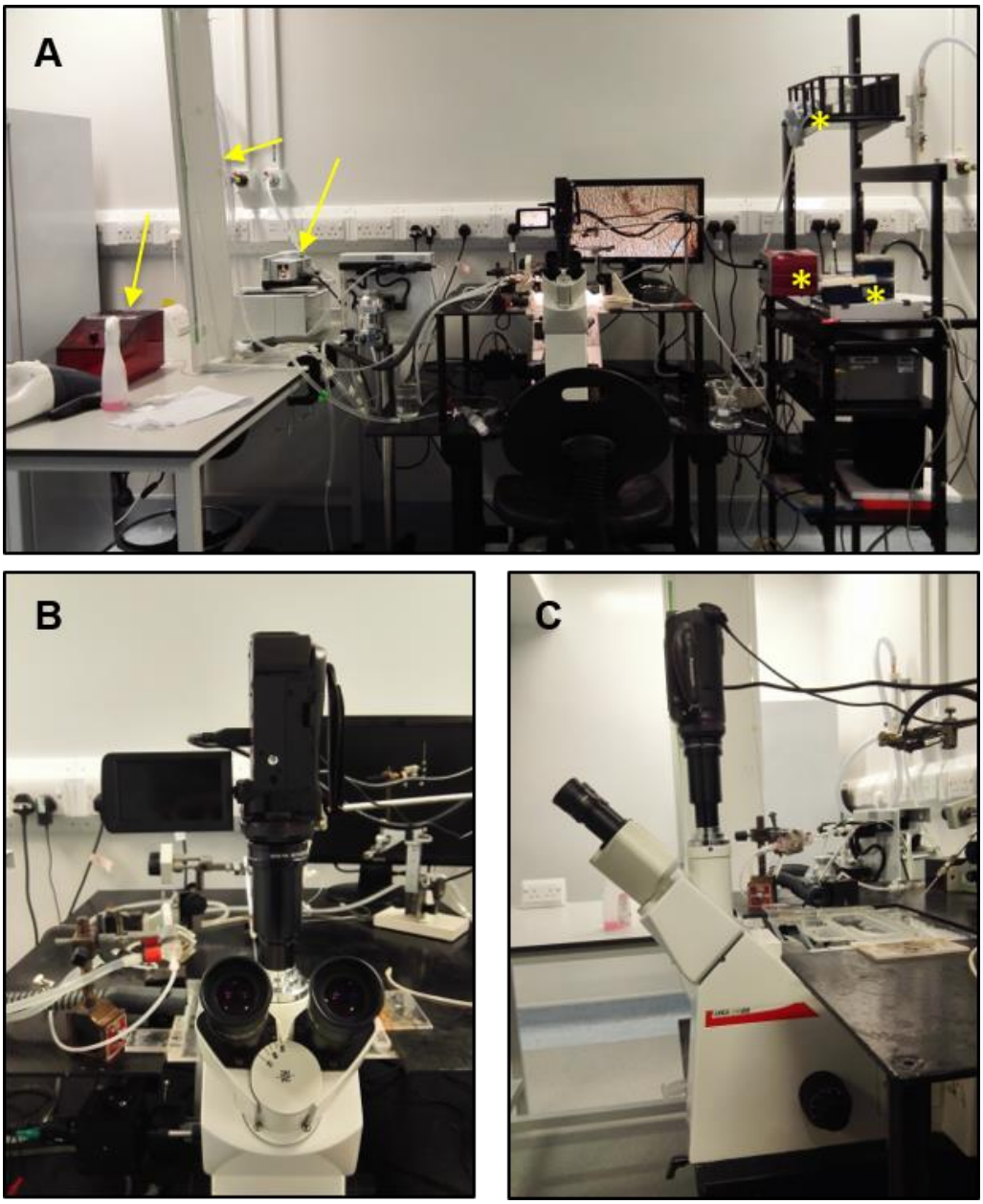


Figure 4.1 Fully operational Lp Rig. *A) image of the entire Lp rig set-up including animal preparation area and anesthetic induction box on the left of the image along with the manometer and water bath (arrows). The air table where the microscope sits and where the experiment took place can be found in the center of the image and to the right a shelving unit which holds the dripper bottle, light source and extra micropipettes, restrainers and occluders (asterixis). B) Researcher's view of the rig showing the microscope eyepiece and connected video camera as well as the various micromanipulators used during experimental procedures in the background. C) side-on view of the rig clearly showing how the video camera connects to the microscope. The microscope sits on the lower shelf of the air table which allowed for the tray to be suspended over the objectives where it rested on the top shelf. The top shelf is also where the micromanipulators which hold the micropipettes were positioned.*

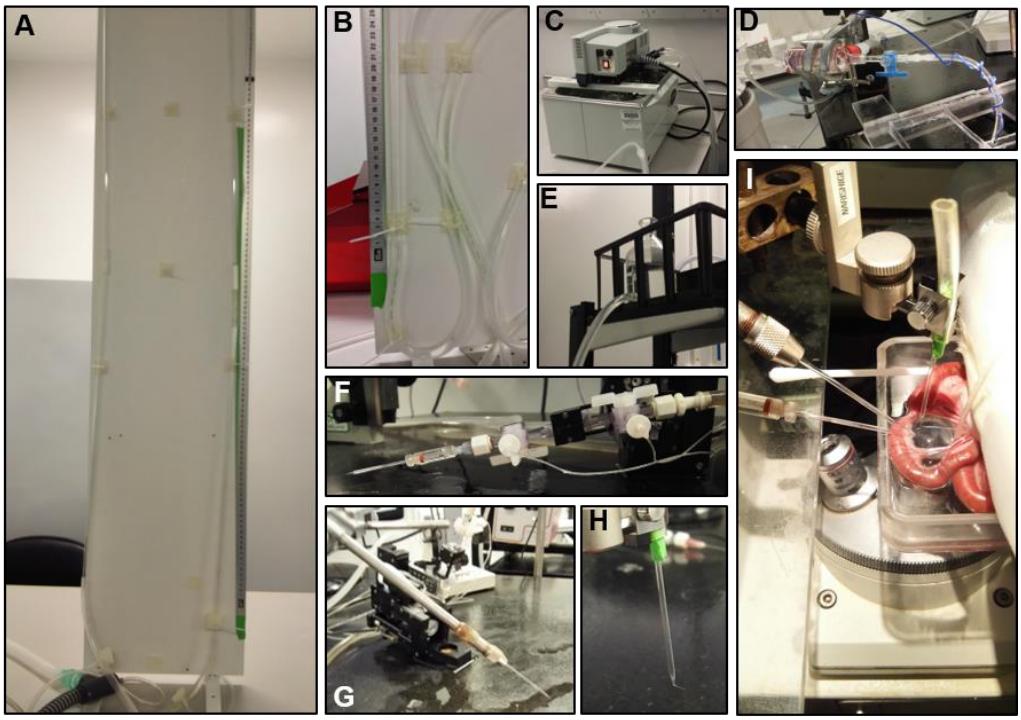


Figure 4.2 The working parts of the Lp rig. *A) Image of the manometer used to control the hydrostatic pressure. B) close-up of manometer showing cm scale. C) Water bath with pump used to heat the mammalian Ringer's solution. D) Image of the dripper connected to a heated coil. The heated coil is connected to the water bath and the Ringer's solution is warmed as it flows through this and into the dripper which superfuses Ringer's solution into the mesentery. E) Image of the Dripper bottle which contains a fresh stock of Ringer's solution and is elevated to maintain flow from the bottle through the dripper to the mesentery. F) Cannulation pipette connected to both the refilling system and the manometer, all of which is held by a hydraulic micromanipulator. G) Restraining pipette held by a micromanipulator. H) Occluding pipette held by a micromanipulator. I) Image showing anaesthetized rat on the rat tray suspended over the microscope objectives. The gut is draped over the quartz pillar and the arrangement of the cannulation pipette, restrainer and occluder is clearly shown.*

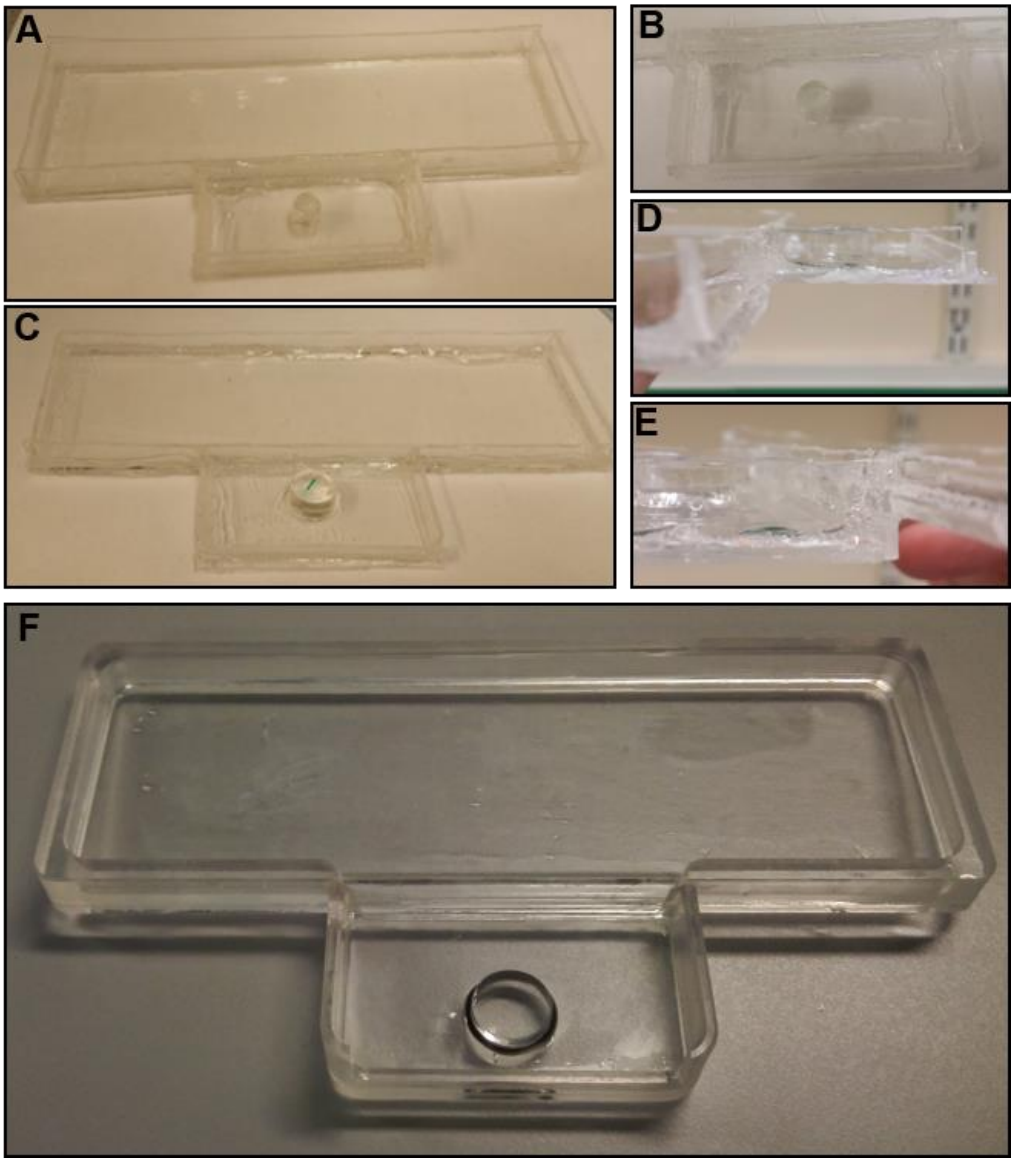


Figure 4.3 Development of the rat tray. *A) the 1st prototype made from Perspex and contained a Perspex pillar (B) to allow the mesentery to rest on. However, the visibility through the Perspex pillar rendered it unusable. C) The 2nd prototype which used glass pillars instead. The tray was placed level to the holding compartment (D) however this was out of the range of the objective focus so a 3rd prototype was constructed and the experimental compartment was dropped 0.5cm (E). The glass pillar was also replaced with a quartz pillar as this would scratch less and incorporated into the final design (F).*

4.3.1.2 Developing a working Rat Tray

As well as the rig, it was also necessary to create a tray that would allow the exposed mesenteric vasculature to be imaged. The tray also needed to include a compartment where the exposed gut can be contained, kept warm and moist as well as where the experiment is undertaken.

Using Perspex, the first prototype tray was created to fit over the objectives on the microscope (Figure 4.3A). In the experimental compartment, it contained a Perspex pillar that would allow the mesentery to lie on it above the level of the gut enabling easier cannulation. The pillar was created by dissolving Perspex in chloroform to form a viscous solution. A section of a glass tube was then filled with this solution and left until the chloroform evaporates (Figure 4.3B). Unfortunately, the pillar was left with many air bubbles and so visibility through the pillar was poor. The second prototype dealt with this issue by replacing the Perspex pillar with a glass one (Figure 4.3C and D). However, the glass scratched easily, which would have hindered experiments. It also became evident that the focal range of the 10x objective (the objective that would be used in experiments) did not reach the top of the pillar where the tissue would be resting. To eliminate these issues, prototype 3 used a quartz pillar and the experimental compartment was lowered 0.5cm (Figure 4.3E). A final version was then made up based on prototype 3 but with an added side hole to allow the waste fluid to be siphoned off (Figure 4.3F) and with

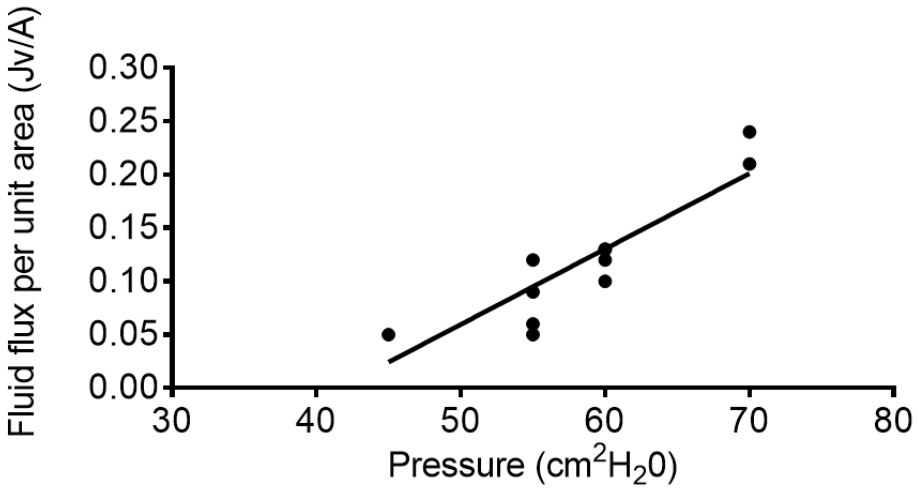


Figure 4.4 fluid flux per unit area was measured at different pressures within the same vessel*. An example graph of the experiment performed 5 times. As expected as the pressure increases so too does the amount of fluid that can leave the vessel. This indicated that the experiment set-up was working and that I could move on to testing the effects of notch signalling on permeability.*

dimensions of 25cm x 8cm x 1.5cm for the main part of the tray and 5cm x 3cm x 1.5cm for the experimental compartment.

4.3.1.3 Calibration of the Rig

I then set out to determine whether the rig could be successfully used to measure permeability by identifying whether fluid flux could be measured across the vessel wall proportionally to pressure. This experiment was first conducted by Michel *et al* (1974) when they were developing this technique. They reported that as the pressure was increased the fluid flux per unit area of capillary wall also increased linearly. We aimed to replicate this data to confirm that the rig was calibrated properly and performing the way we expected. Figure 4.4 shows that I could increase the fluid flux per unit area of capillary wall each time I increased the pressure and I proceeded to validate the experimental design.

4.3.2 Part 2: How Does Dll4/NOTCH Signaling Effect Microvascular Permeability?

4.3.2.1 Effect of refilling the pipette on microvascular permeability

Prior to testing changes in micro vessel permeability upon perfusion with a test substance it was important to establish if the act of refilling the pipette via the syringe pump mechanism altered the pressure in any way. This was achieved by refilling the pipette with the control solution, 1% BSA-Ringer's.

As expected, upon reperfusion with the BSA-Ringer's solution there was no initial significant change in Lp (Figure 4.5A) with it changing only from baseline levels of 13.43±3.04 x 10^{-7} $cm.s^{-1}.cmH_2O^{-1}$ to 14.53±2.79 x 110^{-7} $cm.s^{-1}.cmH_2O^{-1}$. Despite slight variation above and below the average baseline measurements, there was still no significant change in Lp even after 12 minutes of reperfusion (Figure 4.5B). This is more easily seen in Figure 4.5C which shows the mean fold change in Lp relative to baseline levels where the highest change is only 1.53 (±0.16) at 45 seconds' post reperfusion.

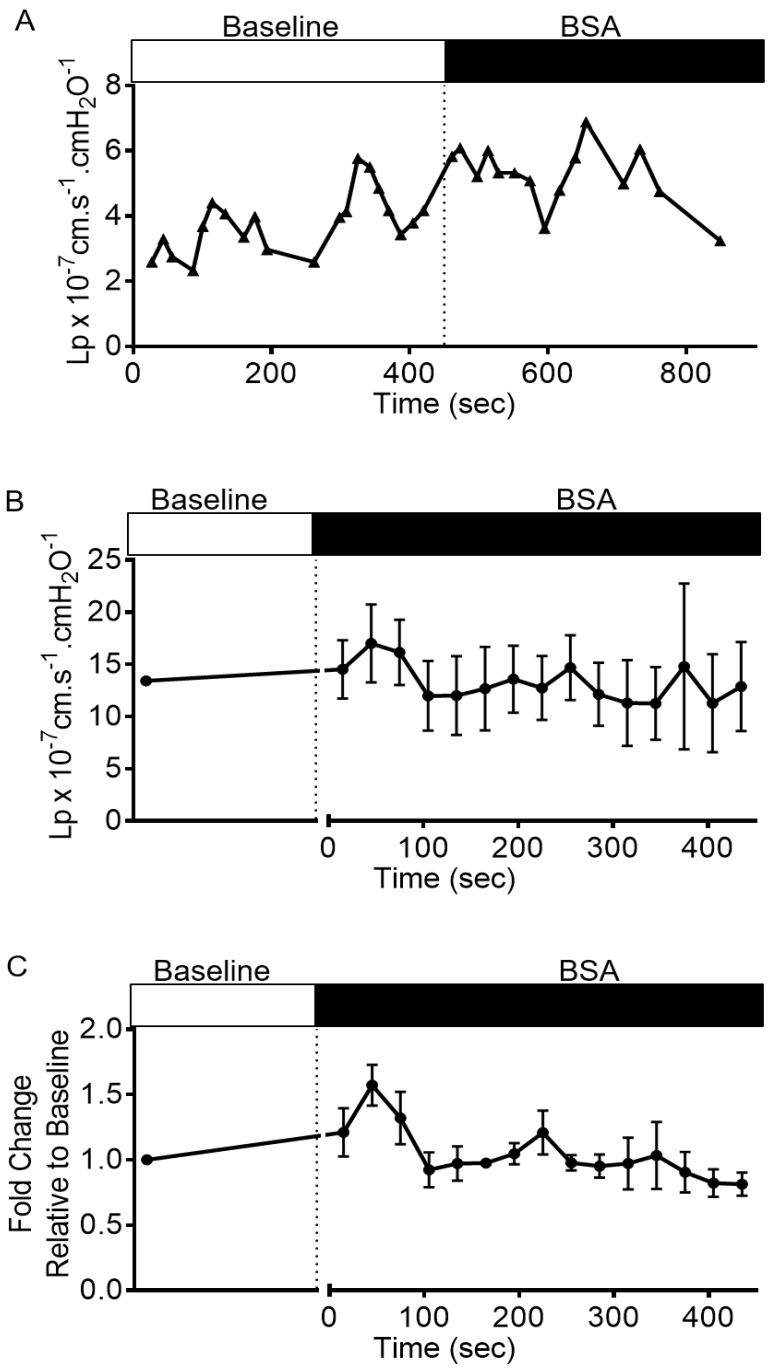


Figure 4.5 Reperfusion with BSA does not alter vascular *permeability. Post-capillary venules were perfused with BSA-Ringer's solution containing washed red blood cells before being reperfused with the same solution. Downstream of the cannulation site the vessel was occluded at regular intervals and the Lp was calculated from video recordings. Reperfusion of the BSA solution resulted in no significant change in Lp as can be seen in A) example of a single experiment and B) the mean Lp measurements of all five vessels. This was even more apparent when the fold change in Lp relative to each vessels baseline was calculated (C) where although there is an initial fold increase of 1.53 (± 0.16) it then drops back down to around baseline levels for the remainder of the experiment.*

4.3.2.2 Effect of recombinant Dll4 on microvascular permeability

In chapter 3 it was established that recombinant full length Dll4 could induce Notch signalling just as well as its soluble counterpart. For this reason, I decided to take the recombinant Dll4 forward into my Lp experiments.

Perfusing with recombinant Dll4 resulted in no significant change in microvascular permeability (Figure 4.6). Nevertheless, there were slight fluctuations from the baseline seen over the time course (Figure 4.6A and B) with the highest permeability measured seen at 585 seconds ($5.16\pm0.49 \times 10^{-7}$ $cm.s^{-1}.cmH_2O^{-1}$) and the lowest seen at 765 seconds ($2.89 \pm0.69 \times 10^{-7}$ $cm.s^{-1}.cmH_2O^{-1}$). When the fold change in LP was is compared relatively to the baseline the lack of change in permeability was clearly seen especially when compared to control BSA reperfusion, (Figure 4.6C). The largest change from baseline levels was seen at 585 seconds and was only a fold change of 1.31 (±0.28) whereas there was only a difference of 0.03 (±0.011) between BSA and Dll4 maximal responses (Figure 4.6D).

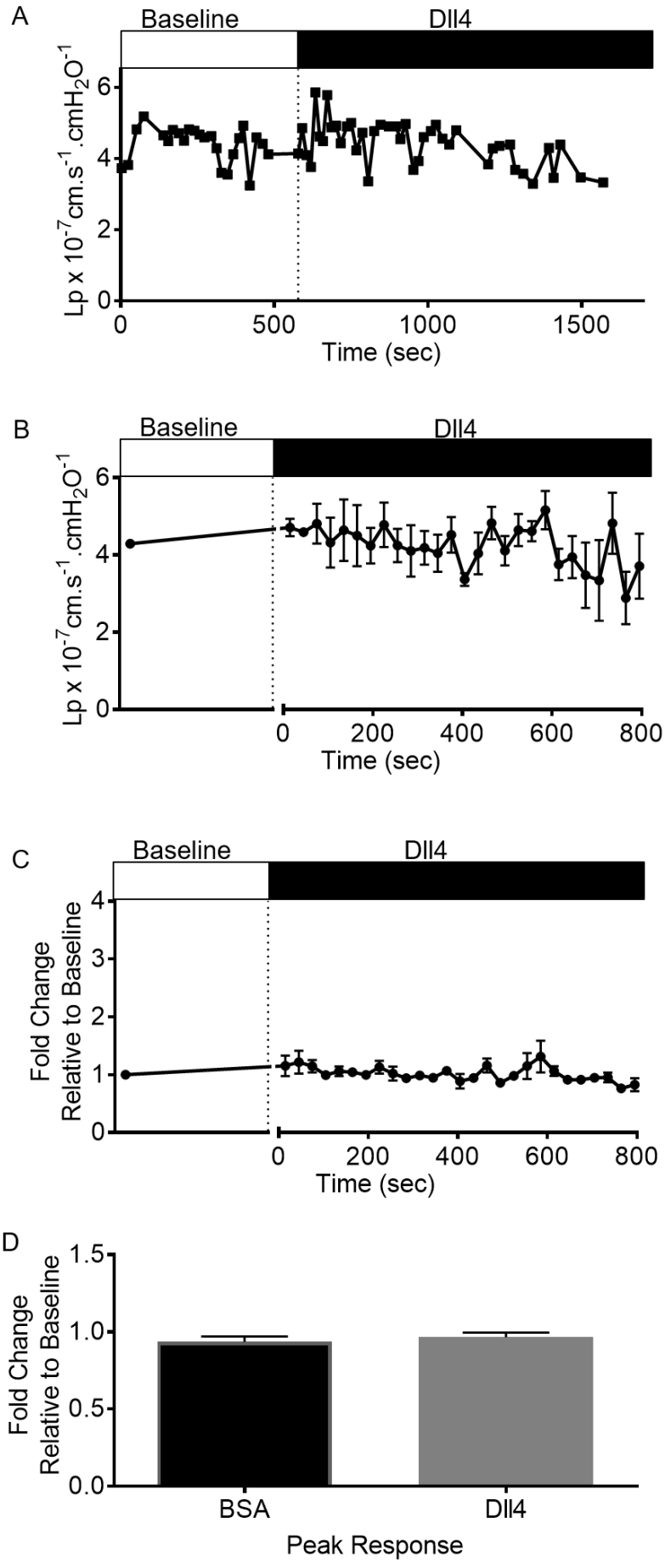
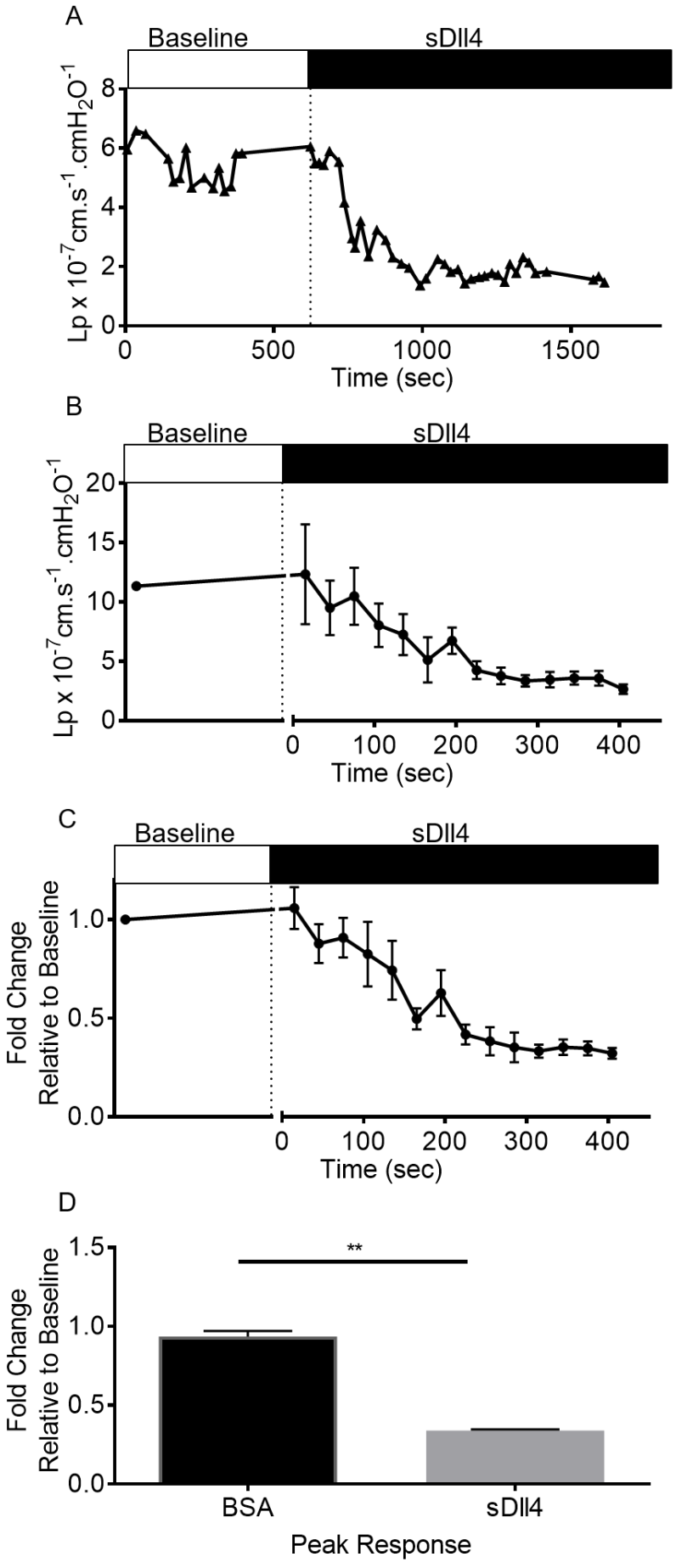

A
Baseline
Dll4
Lp x 10-7cm.s-1.cmH2O-1
0
2
4
6
0
500
1000
1500
Time (sec)
B
Baseline
Dll4
Lp x 10-7cm.s-1.cmH2O-1
0
2
4
6
0
200
400
600
800
Time (sec)
C
Baseline
Dll4
Fold Change
Relative to Baseline
0
1
2
3
4
0
200
400
600
800
Time (sec)
D
Fold Change
Relative to Baseline
0.0
0.5
1.0
1.5
BSA
Dll4
Peak Response

Figure 4.6 Perfusion with full length Dll4 has no effect on permeability. *A) Example of a single experiment indicating that Dll4 perfusion showed no significant change from baseline levels. B) Mean Lp measurements for all vessels (n=5) again showing that Dll4 perfusion does not affect permeability. C) Furthermore, the fold change relative to baseline measurements for each vessel clearly show no change in permeability and this was further evident when the maximal response (maximum change from baseline) relative to baseline for both BSA and Dll4 were plotted (D)*

4.3.2.3 sDll4 decreases microvascular permeability

As there was no effect seen by Dll4, I then proceeded to investigate if perfusing with sDll4 would influence Lp. Within minutes of perfusing with sDll4 Lp consistently began to fall below baseline from 12.3 x±4.2 10^{-7} $cm.s^{-1}.cmH_2O^{-1}$ to 7.25±1.74 x 10^{-7} $cm.s^{-1}.cmH_2O^{-1}$ at 135 seconds (Figure 4.7A and B). Lp then continued to decrease until it plateaued at 3.45±0.65 x 10^{-7} $cm.s^{-1}.cmH_2O^{-1}$ at around 300 seconds where it remained until the end of the experiment. To determine if the effect of sDll4 persisted two of the experiments were extended to approximately 1000 seconds (one of which can be seen in Figure 4.7A) and the fold change in Lp compared to baseline measurements was plotted (Figure 4.7C). This enabled the effects to be seen more clearly and allowed then analysis of the maximal responses to each treatment. As the initial data suggested, the maximal response of sDll4 was extremely significant compared to reperfusion with BSA alone (BSA 0.94 ±0.078, sDll4 0.34 ±0.014, p=0.0079, Figure 4.7D) indicating that sDll4 had reduced microvessel permeability to 34% of control values


A
Baseline
sDll4
Lp x 10-7cm.s-1.cmH2O-1
0
2
4
6
8
0
500
1000
1500
Time (sec)
B
Baseline
sDll4
Lp x 10-7cm.s-1.cmH2O-1
0
5
10
15
20
0
100
200
300
400
Time (sec)
C
Baseline
sDll4
Fold Change Relative to Baseline
0.0
0.5
1.0
0
100
200
300
400
Time (sec)
D
**
Fold Change Relative to Baseline
0.0
0.5
1.0
1.5
BSA
sDll4
Peak Response

.

Figure 4.7 Perfusion with sDll4 results in a decrease in permeability in rat mesenteric microvessels. *Perfusion with sDll4 showed a clear decrease in permeability compared to BSA within 120 sec until it plateaued at 300sec (12.34 ±4.2 to 7.250 ±1.74 x 10^{-7}cm.s-1.cmH2O-1 n=5. A and B). This difference is more easily seen when the change in permeability is compared relative to each vessel's baseline (C). Recordings taken during the maximal response (maximum change from baseline) showed a 0.35 (±0.01, n=5) fold change relative to baseline. And was significantly different from perfusing with BSA alone, (p=0.0079, D).*

4.3.2.4 Effect of H89-dihydrochloride on Notch signalling

I then investigated the mechanism by which sDll4 was acting to decrease the permeability. As an agent well known to decrease permeability I first wanted to investigate if cyclic adenosine monophosphate (cAMP) was involved in the mechanism. Using the same model as Chapter 3, HDBECs were treated as before (sDll4, VEGF or sDll4 + VEGF) but this time with the addition of the PKA inhibitor H89-dihydrochloride (H89) and the change in expression of Hes1 and Hey1 were measured by qPCR.

Cells treated with H89 alone resulted in very minor changes in expression with a fold decrease of 0.97 (±0.14) seen in Hes1 (Figure 4.8A) expression and a fold increase of 1.42 (±0.41) in Hey1 expression (Figure 4.8B). Interestingly, those cells treated with a combination of H89 and sDll4 lead to a fold change of 0.82 (+±0.027) in expression of Hes1 which is much less than the 1.84 (±0.38) fold change when sDll4 was given on its own. This trend was repeated in cells treated with H89 + VEGF where there was a fold change of 1.8 (±0.21) down from 2.7

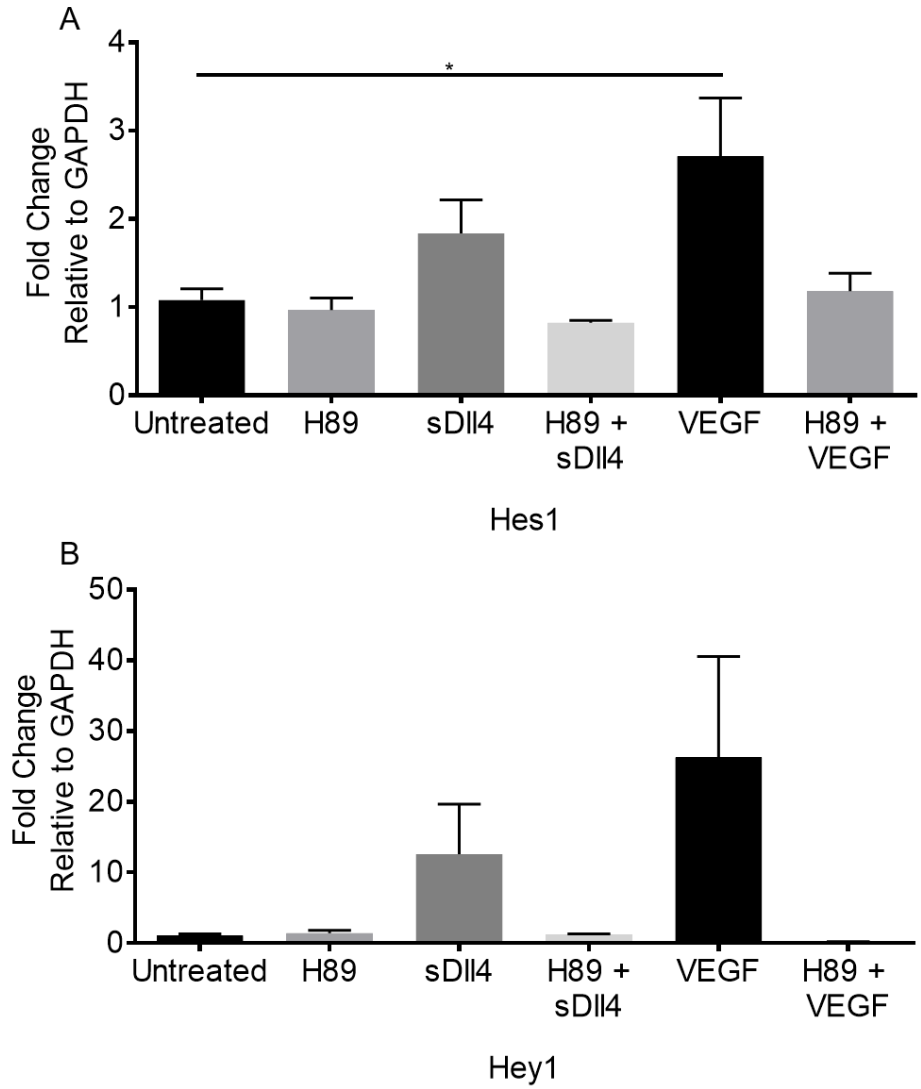


Figure 4.8 The PKA inhibitor H89 dihydrochoride (H89) prevents the induction of Notch target genes Hes1 and Hey1 by sDLL4 and VEGF. *HDBECs were treated with H89 (1μM) with or without sDll4 (1μg/ml) or $VEGF_{165}$a (40ng/ml) for 4 hours (n=3). The expression of either Hes1 or Hey1 in relation to GAPDH was measured by qPCR. sDll4 showed a clear increase in expression of both Hes1 (A) and Hey1 (B). When given with H89 this effect was blocked. VEGF also increased expression of Hes1(p=0.0459, one-way ANOVA with Bonferroni post-test) and Hey1 when given alone but this was also blocked with H89.*

(±0.66) when VEGF was given alone indicating that cAMP was involved in the VEGF-DLL4 pathway. In addition to this, Hey1 expression also showed a similar inclination with those cells treated with H89 + sDll4 resulting in a fold change of 1.97 (±0.13) far less than those treated with

only sDll4 which resulted in a fold change of 12.5 (±7.12). moreover, a fold change of 1.19 (±0.13) produced by H89 + VEGF treatment was also a large decrease compared to treatment with only VEGF (26.3 ±14.2). Interestingly, following statistical analysis by one-way ANOVA only Hes1 expression saw a significant change (p=0.0351).

4.3.2.5 H89-dihydrochloride prevents sDll4 from decreasing hydraulic conductivity

Given that H89 prevented the increase in Hes1 and Hey1 in endothelial cells seen by sDll4 I then wanted to investigate if it could also alleviate the decrease in Lp described earlier. Using the same approach as for sDll4, vessels were first perfused with BSA and a baseline for each vessel was established. Next, to dampen down any endogenous Dll4/Notch signaling that may have been occurring H89 was perfused on its own for approximately 5 minutes (Figure 4.9A). During this period, the Lp was seen to increase from 6.44±1.69 $x10^{-7}$ $cm.s^{-1}.cmH_2O^{-1}$ to 8.41±1.75 $x10^{-7}$ $cm.s^{-1}.cmH_2O^{-1}$ before decreasing back to 6.38±1.78 $x10^{-7}$ $cm.s^{-1}.cmH_2O^{-1}$ (Figure 4.9B). However, there was no overall significant change from baseline as demonstrated in Figure 4.9E.

After approximately 5 minutes the perfusate was changed so that a combination of H89 + sDll4 was being perfused through the vessel. However, unlike perfusion of sDll4, the combination of H89 + sDll4 resulted in no overall change in permeability. Despite fluctuations in Lp

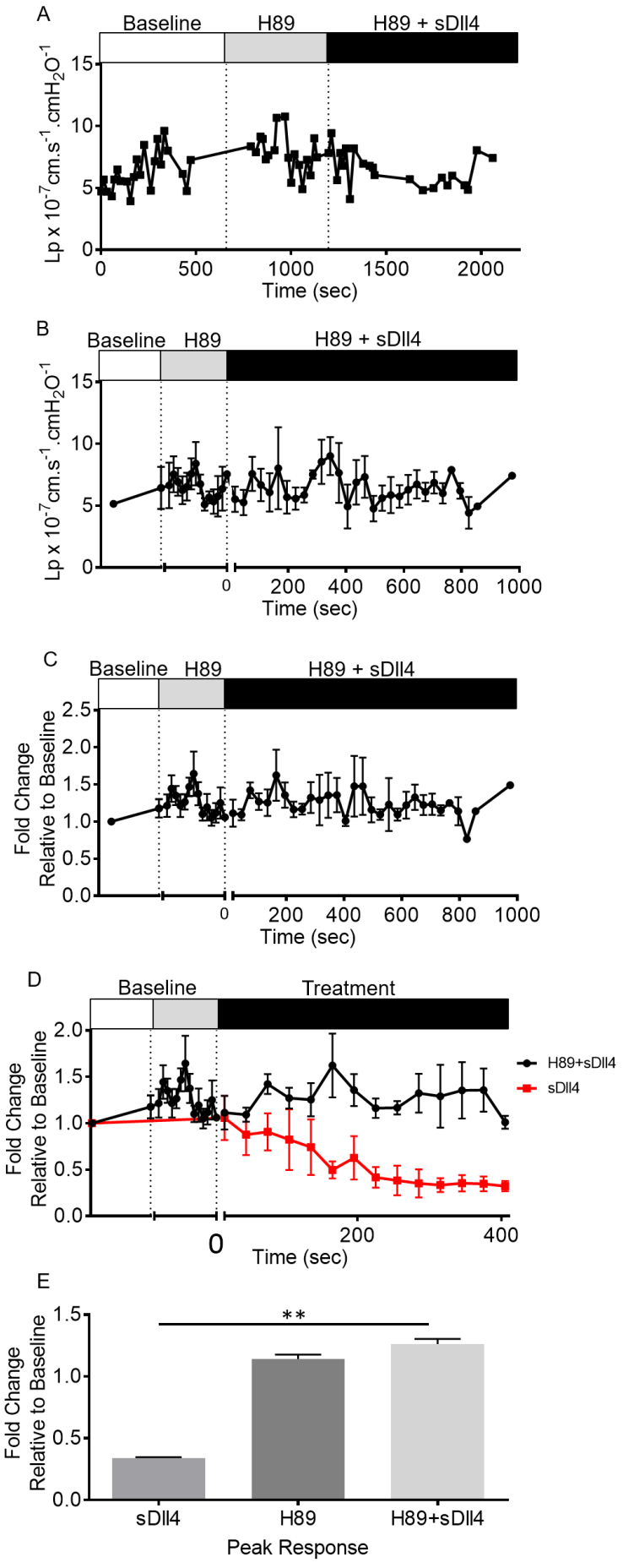

A
Baseline
H89
H89 + sDll4
Lp x 10-7cm.s-1.cmH2O-1
Time (sec)
B
Baseline
H89
H89 + sDll4
Lp x 10-7cm.s-1.cmH2O-1
Time (sec)
C
Baseline
H89
H89 + sDll4
Fold Change Relative to Baseline
Time (sec)
D
Baseline
Treatment
H89+sDll4
sDll4
Fold Change Relative to Baseline
Time (sec)
E
**
Fold Change Relative to Baseline
sDll4
H89
H89+sDll4
Peak Response

Figure 4.9 sDll4 reduces microvessel permeability through a PKA dependent pathway. *Post-capillary venules were perfused with BSA-Ringer's solution containing washed red blood (RBC) cells. The same vessel was then perfused with H89 for approximately 5 minutes before the addition of H89 + sDll4 (A). Perfusion with the combination of H89 +sDll4 did not result in a change in Lp despite constant fluctuations around baseline (B and C, n=4) and compared to the decrease seen by sDll4 (D). Comparisons of maximal responses for both H89(1.14 ±0.035) and H89 + sDll4 (1.26 ± 0.41) showed that sDll4 maximal response (0.34 ±0.0063) was significantly different from both (P=0.0033).*

from 9.02±1.54 x10^{-7} cm.s^{-1}.cmH_2O^{-1} to 4.4±1.28 x10^{-7} cm.s^{-1}.cmH_2O^{-1} this only equated to a fold change range of 1.36 (±0.31) to 0.77 (±0.035) relative to baseline (Figure 4.9C). Additionally, there was only a maximal response of 1.26 (±0.041) compared to 0.34 (±0.006) seen by sDll4 alone although this was significantly different from the maximal response seen by sDLl4 alone (p=0.0033, Figure 4.9D and E).

These data in combination with the Hes1 and Hey1 expression data indicate that PKA/cAMP has a clear role in the pathway that allows Dll4 to regulate permeability.

4.4 Discussion

4.4.1 Dll4/Notch Signaling Regulates Microvascular Permeability

While it is known that Dll4/Notch signalling regulates tip and stalk cell formation and organisation in sprouting angiogenesis, the pathway has also been implicated in the maintenance of vascular quiescence (Hellstrom *et al.*, 2007; Jakobsson *et al.*, 2010; Lobov *et al.*, 2007; Suchting *et al.*, 2007). Studies using zebra fish embryos demonstrated that artificial over activation of Notch lead to endothelial quiescence during development (Leslie *et al.*, 2007). In addition, Ehling *et al* (2013) reported that Notch was vital for the regulation of retinal blood vessel maturation and quiescence in adolescent mice and this was further supported by Dou *et al* (2008) who saw vascular growth reinitiated in multiple tissues upon the loss of RBP-Jκ in Cre-LoxP-mediated conditional gene deletion mutant mice.

Quiescence occurs when the endothelium forms a contact-inhibited monolayer that has tight intracellular junctions and can mediate homeostasis. One such property that the endothelium must regulate is what it allows to enter and leave the vessel, or its permeability. Quiescent vessels, in general, have a good ability to regulate their permeability (Mehta and Malik, 2006; Goddard, Luisa Iruela-Arispe and Iruela-Arispe, 2013). Here I presented data that shows that the induction of Notch signalling reduces vascular permeability (Figure 4.7). If permeability is reduced, then one would expect there to be increased

barrier function possibly because of tighter intracellular junctions and/or a thickening of the glycocalyx therefore meaning a more quiescent vessel.

Interestingly, arterial calibre vessels have been shown to have a more restrictive endothelium with isolated perfused lung preparations under basal conditions showing a gradation in permeability of approximately 19% in arterial regions, 42% in microvascular regions and 37% in venous regions (Parker *et al.*, 2006). In addition, pulmonary endothelial cells formed a monolayer that was approximately 4 times less permeable to albumin than monolayers formed from venous or arterial endothelial cells and TEER was found to be lower in cells from larger arteries than microvascular endothelial cells (Mehta and Malik, 2006; Aird, 2007). Furthermore, the arterial segment of the vasculature has up to 18 times more of the tight junction protein, occludin, than in venular areas (Mehta and Malik, 2006) which is also most abundantly expressed in brain endothelial cells where regulation over barrier function is essential to maintain the blood-brain barrier (Bolton, Anthony and Perry, 1998; Van Itallie *et al.*, 2010; Mavrakis *et al.*, 2012). This indicates that the arterial system has tighter control over barrier function which is also where basal levels of Dll4/Notch signalling have been reported (Benedito *et al.*, 2008; Cristofaro *et al.*, 2013; Liu *et al.*, 2003) further supporting the claim that Dll4/Notch regulate vascular permeability.

In the previous chapter I showed that both Dll4 and sDll4 could induce Notch signalling *in vitro*. However, this does not seem to be the case *in*

vivo, at least for this methodology. Both Dll4 and sDll4 are recombinant proteins and as solutes in the perfusate are subject to certain conditions that determine whether they will be able to reach their target, Notch. One of the key conditions is the osmotic reflection coefficient (see chapter 1 for an explanation) which varies depending on the membrane (in this case the vessel wall), pore size and the molecule size (Schultz, Valentine and Choi, 1979). While in the present study I have not measured the exact pore sizes of each vessel, the size of the vessels that were chosen were all a similar size (25-50μm) and of a naive, post-capillary venule origin. Therefore, it could be reasonable to assume that the pore size would be similar from vessel to vessel. There is however, a difference between the size of the two proteins. While sDll4 has a molecular weight of approximately 50 kilodaltons (kDA), Dll4 is a larger protein of 74 kDA. Although this is only a difference of approximately 24kDA it is possible that this is a large enough difference to increase the osmotic reflection coefficient (σ) sufficiently to prevent Dll4 from reaching Notch resulting in a difference of effects between the full length and soluble proteins. For instance, σ could be increased from 0.9 by sDll4 to 0.98 by Dll4 and thereby result in a reduction in the partition coefficient from 0.1 to 0.02 reducing the concentration of Dll4 to 20% which could be significant enough to prevent it exerting its effects on permeability

Interestingly, the *in vitro* data presented in chapter 3 showed that Notch was being induced after 4 hours. Despite this, the data presented here in Figure 4.7 clearly shows that the effect that sDll4 has on permeability

occurs far quicker than this. Both sDll4 and Dll4 experiments were only perfused for a maximum of 1500 seconds (see Figure 4.6 and Figure 4.7) and while Dll4 showed no signs of influencing the permeability during this period it is possible that the effects could take longer to occur. However, it is important to note that keeping an animal under gaseous anaesthesia for up to 4 hours would not only be costly but would be more complex and difficult in terms of keeping the animal alive for the entire experiment as well as maintaining constant perfusion of the proteins, especially when the *in vivo* data collected so far suggest that there would be no added benefit.

The short period that it takes to see a decrease in permeability by sDll4 suggests that this may not be a transcriptional effect. On the other hand, the continued and pro-longed response that was seen in a pilot Lp experiment where the vessel was re-perfused with BSA for up to 15 minutes after perfusion with sDll4 (see Figure 4.10) indicates that we cannot rule out a subsequent transcriptional response that maintains the decrease in permeability even after the stimulus is removed. Studies looking into the effects of VEGF on vascular permeability reported that despite the response to VEGF being immediate yet short-lived vessels required at least 15 minutes' absence of VEGF before the vessel could be stimulated again (Bates and Curry, 1997). It may also be the case that a longer period of recovery is needed here as well.

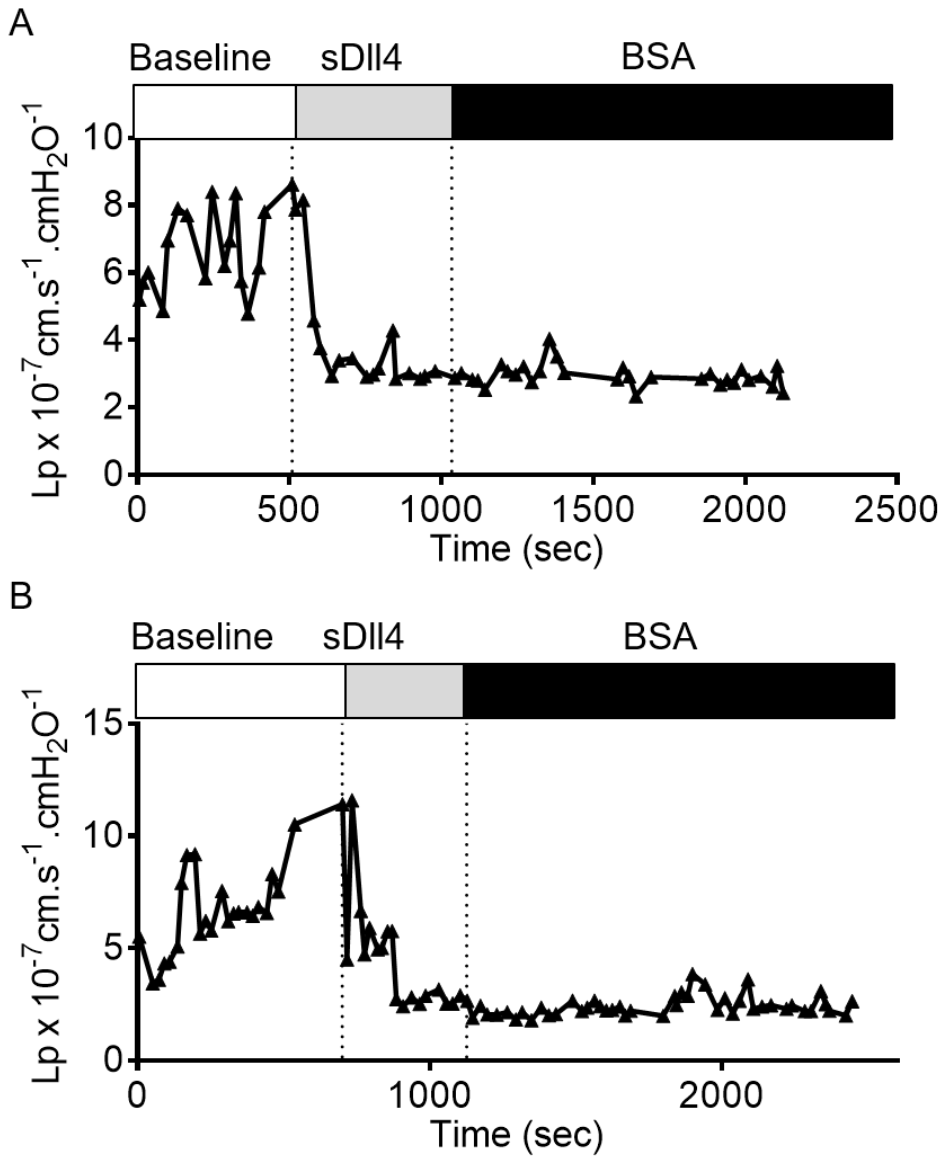


Figure 4.10 Two individual experiments (A and B) from pilot data indicating the lasting effect of sDll4 perfusion*. After establishment of a baseline with BSA perfusion, post-capillary venules were perfused with sDll4 as previously described for at least 10 minutes. The perfusate was then switched back to BSA and Lp was recorded for at least 15 minutes. As before, Lp decreased upon perfusion until it hit a plateau, however this effect was not alleviated when sDll4 was no longer present.*

4.4.2 Dll4 Regulates Permeability in a PKA Dependent Manner

While I had hypothesised that the induction of Notch would decrease permeability, the rapid decrease that was seen was not expected. I then set out to uncover the mechanism by which sDll4 was working. There are few substances that are known to decrease vascular permeability one of which is cAMP. Using the same Lp methodology as above He *et al* (2000) saw Lp increase after inhibition of cAMP-dependent protein kinase (PKA) demonstrating the significant role that cAMP plays in regulating vascular permeability. More recently a link between Notch and cAMP during vascular development and endothelial cell differentiation has been suggested. When cAMP was induced in cultured endothelial cells, VEGF-induced differentiation was not only increased but resulted in endothelial cells of arterial calibre; the fate of which Dll4 expressing cells are also known to favour (Shutter *et al.*, 2000; Liu *et al.*, 2003; Diez *et al.*, 2007). They proposed that this occurred by cAMP activating PI3K which leads to an arterial fate for vascular progenitors through the simultaneous activation of Notch and β-catenin signalling (Yurugi-Kobayashi *et al.*, 2006). From this mounting evidence, I hypothesised that Dll4/Notch may be regulating vascular permeability through cAMP.

In the present study, after the addition of the PKA inhibitor H89, the effect that sDll4 had on the microvascular permeability was prevented (Figure 4.8) demonstrating that Dll4/Notch is acting through a cAMP/PKA dependent pathway. Interestingly, while Adamson *et al*

(1998) also demonstrated that the induction of cAMP by rolipram or forskolin decreases microvascular permeability, transmission electron microscope sections of the perfused tissue indicated that this was through an increase in tight junctions. The data presented here and in chapter 3 on the other hand, suggests the decrease in permeability may be due to increased VE-Cadherin adherens junctions. However, as no perfused tissue sections were taken for either immunofluorescence or electron microscopy staining I did not determine whether adherens or tight junctions were affected *in vivo*.

More recently a study of inhibition of PKA by endothelial cell-specific expression of dominant negative PKA in mice resulted in embryonic vascular defects, haemorrhage and lethality midgestation (Nedvetsky *et al.*, 2016). Inhibition of PKA during perinatal retinal angiogenesis of the heterozygote mice led to hypersprouting, excessive tip cell formation and increased migration, all typical effects also seen during Notch inhibition (Hellstrom *et al.*, 2007; Suchting *et al.*, 2007). Despite the similarities to Notch inhibition when HUVECs were treated with a cAMP analog there was no significant change in luminescence by a transfected luciferase Notch reporter either in the presence or absence of Dll4 stimulation (Nedvetsky *et al.*, 2016). In addition, Dll4 stimulation did not affect the activity of a luciferase PKA reporter either indicating that Notch was not acting upstream or downstream of PKA. This contrasts with the data presented here, suggesting that PKA and Dll4/Notch may work simultaneously along separate paths during developmental angiogenesis but a part of the same pathway that

maintains vascular integrity in mature vessels or alternatively Dll4 could be using a pathway that does not involve Notch.

Endothelial barrier stabilisation through a PKA dependent pathway has been well studied. Activation of PKA has been shown to regulate barrier function through the inhibition of the Rho GTPase, Rac-1. Using the sordelli lethal toxin (LT) a bacterial toxin with glucosyltransferase function, Waschke *et al* (2004), reported that in post capillary venules cAMP reduced the LT induced permeability increase previously seen (Waschke, Baumgartner, *et al.*, 2004; Waschke, Drenckhahn, Adamson and Curry, 2004) through a PKA mechanism that inhibits the GTPase Rac-1. In addition, Rac-1 inhibition resulted in increased myosin contraction and reduction in VE-Cadherin mediated adhesion using a laser tweezer technique with VE-Cadherin coated microbeads (Waschke, Drenckhahn, Adamson, Barth, *et al.*, 2004). Furthermore, PKA has been shown to act by inhibiting RhoGTPase -mediated cytoskeletal contractility, vasodilator-stimulated phosphoprotein-mediated cytoskeletal changes and reduction of myosin light chain phosphorylation which are all essential elements to maintaining endothelial barrier function (Wysolmerski and Lagunoff, 1991; Comerford *et al.*, 2002).

cAMP has also been shown to regulate endothelial permeability through a PKA-independent pathway via directly activating exchange proteins (EPAC) or cAMP regulated guanine exchange factor (cAMP-GEF, Bos et al., 1998). EPAC activates the Rap1 and Rap2 GTPases and is mainly involved in cell-cell adhesion maintenance. The activation of

Rap1 by the cAMP analogue 8-pCPT-2'-O-methyl-cAMP which binds EPAC but ineffectively binds PKA resulted in upregulation of VE-Cadherin showing that it can be regulated independently of PKA (Christensen *et al.*, 2003; Holz *et al.*, 2006). This conflicts with the data presented here, which indicates a PKA dependent regulation of VE-Cadherin. On the other hand, it is possible that Notch may be able to activate both pathways and this could explain why only a marginal increase in permeability was seen when H89 was given compared to the significant increase seen by He *et al* (2000) previously. Moreover, it was shown that the activation of EPAC and PKA by cAMP lead to the stimulation of two parallel but independent signalling pathways which both regulate endothelial integrity and cell migration lending further support to this idea.

During angiogenesis, VEGF, has been shown to destabilise endothelial cell junctions through the activation of Rac leading to increased permeability (Gavard and Gutkind, 2006). Eliceiri *et al* (1999) reported that this could prevented by blocking VEGF-induced Src-dependent Rac activation in chick embryos. Through this same activation of Src stimulating the GEF, Vav2, its target RAC1 and the p21-activated kinase (PAK) through the dimerization of VEGFR2. It was also reported that VEGF binding in HUVECs led to the internalisation of VE-Cadherin and so the destabilisation of cell-cell junctions (Gavard and Gutkind, 2006). Moreover, as the Dll4/Notch signalling during angiogenesis subsequently downregulates VEGFR2 expression (Williams *et al.*, 2015) it would therefore be reasonable to speculate that this

downregulation of VEGFR2 would then prevent the VEGF-induced signalling that leads to VE-Cadherin internalisation and thereby control vascular permeability.

Furthermore, it is well known that the highly expressing Dll4 tip cells protrude and extend filopodia and migrate along a VEGF gradient during angiogenesis (Hellstrom *et al.*, 2007; Lobov *et al.*, 2007; De Smet *et al.*, 2009). The GTPase Rac1 has also been implemented in the stimulation of lamellipodia, often found at the leading edge of migrating endothelial cells (Ridley *et al.*, 1992; Guo *et al.*, 2006). Additionally, a further GTPase, CDC42, which can also be activated through the cAMP/PKA pathway has been shown to be involved in the production of filopodia (Nobes and Hall, 1995) suggesting possible ways in which Dll4/Notch signalling through PKA imposes its regulation on vascular permeability at least during the angiogenic process.

4.5 Concluding Remarks

The data presented here demonstrates that Dll4/Notch signalling helps regulate vascular permeability and that this is done through a cAMP/PKA dependent pathway. While there is growing evidence supporting this, it is not yet clear which of the downstream effectors of cAMP/PKA signalling discussed above are involved and to what extent or indeed if other unknown pathways are involved.

Chapter 5: Dll4 and Arteriolargenesis

5.1 Introduction

In the previous two chapters I have shown that the induction of Notch signalling by Dll4 increases the number of adherens junctions *in vitro* and regulates vessel permeability in a cAMP/PKA dependent manner in naïve vessels *in vivo*. Both these findings were achieved using non-angiogenic phenotypes and so in this chapter I aim to investigate how Dll4/Notch signalling affects physiological angiogenesis and if this pathway is also involved in arteriolargenesis (the formation of arterioles) using the rat mesenteric angiogenesis assay.

First developed by Wang *et al* (2004) to study the angiogenic effect of VEGF, the 2-dimensional vessel network of the mesentery allows for easy measurement of vessel structural parameters such as vessel density and average vessel length. While the mesentery has also been used to study the response to the injection of tumour cells (Heuser, Taylor and Folkman, 1984) and to a variety of angiogenic and non-angiogenic molecules when injected into the peritoneum (Norrby, Jakobsson and Sörbo, 1986; Mukhopadhyay *et al.*, 1998; Norrby *et al.*, 2008) these studies only dealt with how the vasculature responded to exogenous factors. Wang *et al* (2004) on the other hand, developed the rat mesenteric angiogenesis assay to be able to study the effect of overexpressing endogenous angiogenic factors using an adenovirus-mediated gene transfer in the infected fat cells which surround the

mesentery. The model has helped decipher the roles of several angiogenic factors including VEGF, Angiopoietin 1 (ANG1), endothelial nitric oxide synthase (eNOS), VEGFR2 (Wang *et al.*, 2004; Benest *et al.*, 2006, 2008; Stone *et al.*, 2016) and now Dll4/Notch signalling as well.

The role of Dll4/Notch in angiogenesis is well known and includes its regulation of tip and stalk cells (Hellstrom *et al.*, 2007; Suchting *et al.*, 2007; Jakobsson *et al.*, 2010) formation during sprouting angiogenesis and mediating endothelial cell VEGF response levels through regulation of VEGF receptor expression (Williams *et al.*, 2006; Lobov *et al.*, 2007). However, there is evidence that this pathway also plays a part in the remodelling and maturation phase of vessels into the vascular hierarchy commonly seen in the mature vasculature. For instance, Dll4 has been shown to be expressed in the arterial endothelium (Shutter *et al.*, 2000) and has been reported to be a marker for endothelial arterial differentiation during development (Liu *et al.*, 2003; Cristofaro *et al.*, 2013). In addition, Lobov *et al* (2011) showed that Dll4 is in involved in post-angiogenic vessel remodelling through the regulation of blood flow and vasoconstriction.

Ang1 also plays a role in the growth of new vessels and like VEGF and Dll4 also results in embryonic lethality when the gene is deleted (Suri *et al.*, 1996). Similarly, Ang1 has also been reported to induce sprout formation in endothelial cells *in vitro* (Koblizek *et al.*, 1998) whereas there is still debate as to the effect it has on proliferation. Witzenbichler *et al* (1998) reported that after 48 hours of stimulation with Ang1,

endothelial cells showed no increase in proliferation as opposed to Kanda *et al* (2005) who saw a dose dependent increase in proliferation of endothelial cells *in vitro*. Additionally, Ang1 has been implicated in the vessel remodelling process and maturation process through the enlargement of vessels (Thurston *et al.*, 2005) and the recruitment of mural cells (Stone *et al.*, 2016).

It has also been reported that the effects of Ang1 are dependent upon endothelial nitric oxide (Babaei *et al.*, 2003) which is produced after the catalysis of l-arginine by the calcium dependent enzyme, endothelial nitric oxide synthase (eNOS, Zhao *et al.*, 2015). The increase in blood flow caused by endothelial nitric oxide has been shown to be a driving factor in the recruitment of mural cells (Price, Owens and Skalak, 1994) with Hansen-Smith *et al* (2001) reporting an increase in arteriolar development as indicated by increased VSMCs present on smaller order vessels.

Studies in the rat mesentery by Benest *et al* (2006, 2008) and more recently Stone *et al* (2016) reported that capillary arterialisation (formation of arterioles or arteriolar genesis) was more pronounced producing a higher density of vessels which included a greater proportion of larger vessels (vessels with a diameter 16-35μm) with more branches and less sprouts when an Ang1 + eNOS adenovirus combination was administered compared to when each was given separately. It was also noted that the addition of VEGF to the Ang1 + eNOS combination likewise aided the maturation process resulting in increased functional vessels which had vascular smooth muscle cell

coverage and were in general larger and with fewer branches than the Ang1 + eNOS combination albeit with increased sprout formation.

Dll4 acts downstream of VEGF during angiogenesis. This, in addition to the evidence that it is involved in vessel maturation and remodelling discussed above suggests it is possible that the Dll4/Notch pathway is involved in this process. I therefore aimed to investigate the hypothesis that the induction of Notch signalling resulting from the injection of Ad.sDll4 would result in a less angiogenic vasculature compared to VEGF and that it would result in longer, larger and less branched vessels resembling a more endogenous phenotype when given in combination with Ad.Ang1, Ad.eNOS and/or Ad.VEGF.

5.2 Methods

Male Wistar rats were anaesthetised (2% isoflurane) and a small incision was made in the abdomen. The gut was teased out and the adenoviruses were injected into the fat pad of a panel at 5 x 10^8 PFU/mL as in previous studies (Wang *et al.*, 2004; Benest *et al.*, 2008; Stone *et al.*, 2016). The two panels either side of the injected panel were then tattooed with Monastral blue so it could be found later and the rat was recovered. On day 7 the rat was anaesthetised, the panel located, fixed with 4% PFA and the rat culled. The panel was then taken for immunofluorescence staining. Panels were stained with antibodies for Isolectin B4 (IB4) a marker for blood vessels, Ki67 a marker for proliferating endothelial cells and DAPI to stain nuclei. Panels were imaged by confocal microscopy and analysed using ImageJ. All data are presented as ±SEM and considered statistically significant if $p<0.05$ unless otherwise stated.

Adenovirus groups used were as follows;

- Ad.eGFP (n=8)
- Ad.VEGF (n=8)
- Ad.sDll4 (n=8)
- Ad.VEGF + Ad.sDll4 (n=8)
- Ad.Ang1 + Ad.eNOS (n=5)
- Ad.Ang1 + AdeNOS + Ad.VEGF (n=5)
- Ad.Ang1 + Ad.eNOS + Ad.sDll4 (n=5)
- Ad.Ang1 + AdeNOS + Ad.VEGF + Ad.sDll4 (n=5)

All methods are described in detail in Chapter 2

5.3 Results

5.3.1 Overexpression of sDll4 Leads to a More Quiescent Vasculature.

Adenoviruses encoding either eGFP, VEGF, sDll4 or a combination of both sDll4 and VEGF were injected into the fat pad of the mesentery in rats. A week later the tissue was removed and stained to detect vessels (IB4) and proliferating endothelial cells (Ki67). The tissue was then imaged by confocal microscopy and representative images from each group can be seen in Figure 5.1. The Images were then quantified using ImageJ (see Chapter 2) and the results can be seen in Figure 5.2.

As indicated in the images, quantification revealed that those panels injected with Ad.eGFP contained vessels at the lowest density of all groups, as expected (Figure 5.2A), but still contained proliferating endothelial cells at a density of 299.5/mm^2 (±37.5, figure 5.2B). The vessels had a mean vessel segment length of 65.26μm (±2.86, Figure 5.2C) and a mean diameter of 10.04μm (±0.26, Figure 5.2D). Ad.eGFP injected panels also contained a small number of sprout points (15.91 ±1.68μm, Figure 5.2E) and a branch point density of 173.8 ±25.13/mm2, Figure 5.2F).

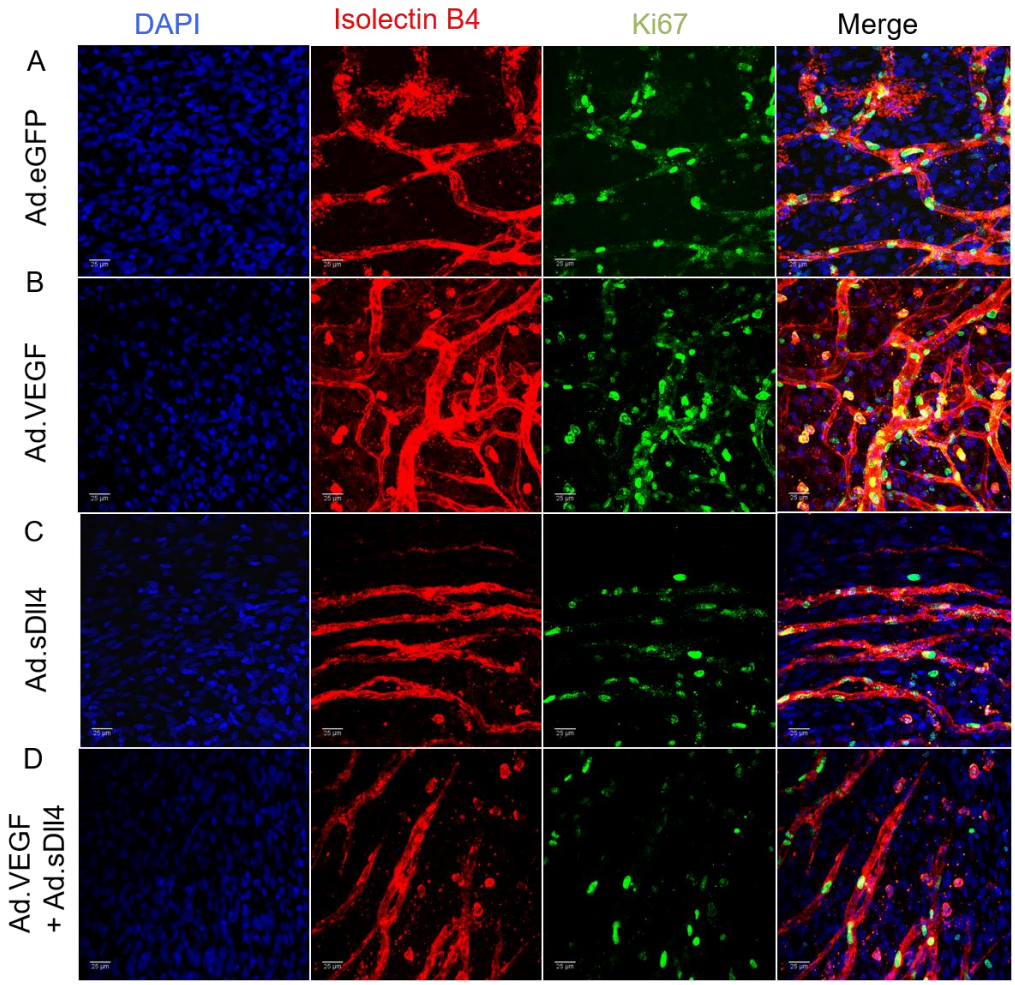


Figure 5.1 Representative images of mesentery panels taken for staining on day 7. *Panels were stained with DAPI for nuclei (blue), IB4 for blood vessels (red) and Ki67 for proliferating cells (green, n=3). Panels injected with Ad.eGFP (A) resulted in vessels with some proliferating nuclei. Ad.VEGF panels (B) panels appeared to show an increase in both the number of vessels and proliferating nuclei with vessels often intertwining with each other. Panels injected with Ad.sDll4 (C) or Ad.VEGF + Ad.sDll4 (D) showed fewer vessels and proliferating nuclei with vessels looking longer and less chaotic than Ad.VEGF alone.*

Images of those panels injected with Ad.VEGF (Figure 5.1B) showed vessels that appeared much shorter than their Ad.eGFP counterparts and these vessels also consistently presented increased Ki67 staining compared to Ad.eGFP suggesting a larger number of proliferating endothelial cells were present. Additionally, the images also suggested

that there was a greater number of sprout points than seen in Ad.eGFP panels.

Image analysis confirmed that Ad.VEGF produced the highest density of vessels (498.2 ±18.72/mm^2 Figure 5.2A) and proliferating endothelial cells (417.4 ±37.57/mm2, Figure 5.2B) but the shortest vessels (51.2 ±3.29μm). Despite this the diameter of the vessels were still very similar to the Ad.eGFP group with a mean of 9.95μm (±0.33). Panels injected with Ad.VEGF resulted in a significantly higher density of sprout points (31.56 ±2.46/mm^2, $p<0.0001$) yet a lower density of branches compared to Ad.eGFP (152.3 ±9.04/mm^2).

Interestingly, in images of mesenteric panels where Ad.sDll4 had been injected (Figure 5.1C) the number of vessels seemed to be similar to those seen in Ad.VEGF-injected panels; however, these vessels appeared to be longer and less chaotic. Ad.sDll4 injection also resulted in fewer endothelial cells stained for the proliferation marker, Ki67 than in Ad.VEGF samples and the number of sprout points likewise seemed to be reduced

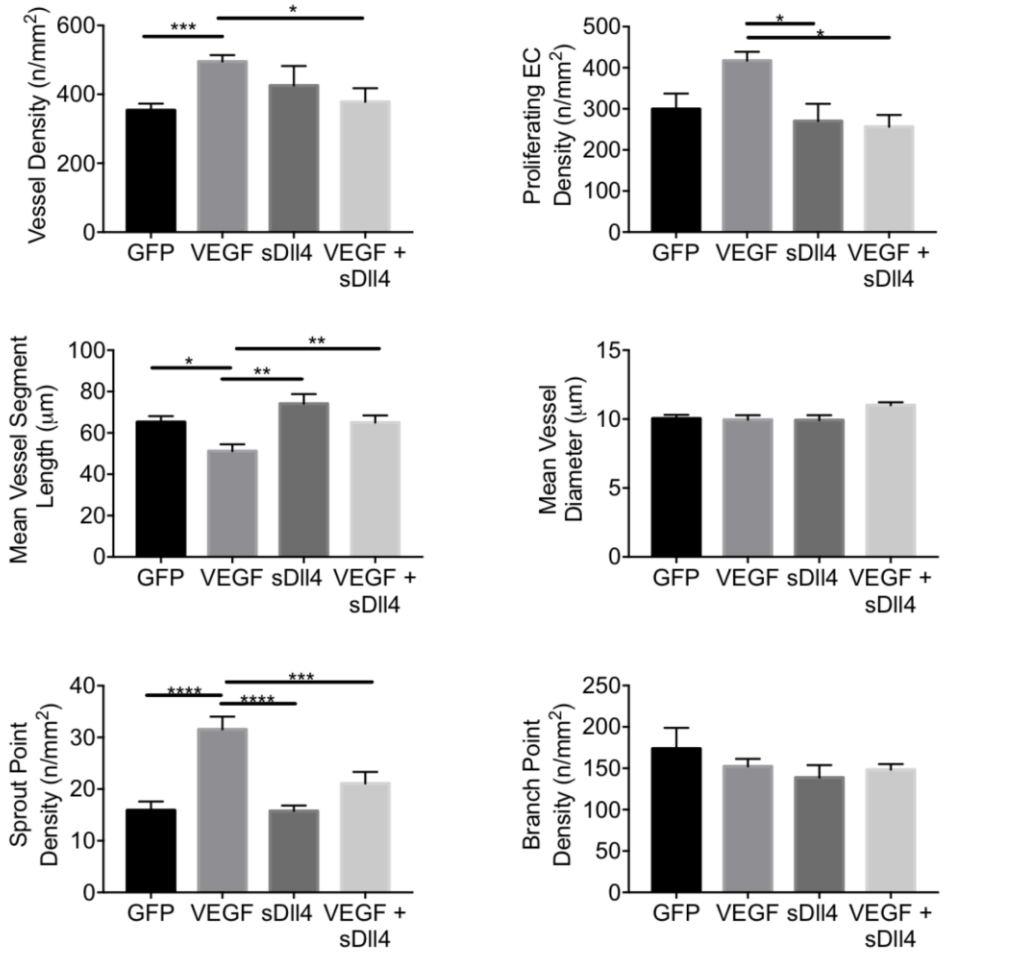


Figure 5.2 Induction of Notch signalling through Ad.sDll4 results in a less angiogenic vasculature*. Rat mesenteric fat pads were injected with either Ad.eGFP, Ad.VEGF, Ad.sDll4 or Ad.VEGF + Ad.sDll4 and 1 week later the same panels were taken for staining (n=8). A) Vessel Density. B) Proliferating Endothelial cell density (Ki67+ve, IB4+ve vessels). C) Vessel length, D) Vessel diameter, E. Sprout point density. F. Branch point density. All Analysis One way ANOVA. *=p<0.05, **=p<0.01, ***=p<0.001. Post-hoc analysis, Benjamini, Kreuker and Yekutieli* (1995; 2001)

As can be seen in Figure 5.2 Ad.sDll4 panels led to a small increase in the number of vessels (425.4 ±56.92/mm^2), which was not significantly different from Ad.eGFP or Ad.VEGF, and a decrease in proliferating endothelial cells compared with Ad.VEGF ($p<0.05$). These vessels were also significantly longer (74.17 ±4.61μm) than the Ad.VEGF group ($p<0.001$).

Interestingly, the mean vessel diameter (9.93 ±0.35μm) for these vessels was almost identical to those injected with Ad.VEGF and very similar to Ad.eGFP. Additionally, the density of sprout points (15.78 ±1.02/mm^2) was also almost identical to Ad.eGFP and Ad.sDll4 injected panels led to the least density of branches (138.8 ±14.96/mm^2).

Those panels that were injected with both Ad.VEGF and Ad.sDll4 (Figure 5.1D) resulted in images which appeared similar to those seen in Ad.eGFP. There were fewer vessels in these images than either Ad.VEGF or Ad.sDll4 groups and proliferating endothelial cells also appeared to be similar to that seen on Ad.eGFP panels.

Quantification of the Ad.VEGF + Ad.sDll4 images revealed that this group resulted in the smallest density of proliferating endothelial cells (256.3 ±28.77/mm^2). The density and length of the vessels produced were also shown to be similar to when Ad.eGFP was injected whereas the diameter was the largest of all groups (11.01 ±0.21μm). interestingly, this group also showed a small increase in sprout points compared to both Ad.eGFP and Ad.sDll4 groups although not to the same extent as Ad.VEGF and the density of branches (148.3 ±6.68/ mm^2) was only slightly lower than when Ad.VEGF was given alone.

5.3.2 Ad.sDll4 in Combination with Ad.Ang1 + Ad.eNOS ± Ad.VEGF Leads to a More Organised, Quiescent Vasculature

I next wanted to investigate if Dll4/Notch signalling had an influence on arteriolargenesis. As previously Ang1 and eNOS had been shown to be key players in arteriolargenesis (Benest *et al.*, 2008; Stone *et al.*, 2016) I set out to investigate how the addition or absence of Ad.sDll4 and Ad.VEGF to Ad.Ang1 + Ad.eNOS affected arteriogenesis.

The images in Figure 5.3 clearly show that while panels injected with Ad.Ang1 + Ad.eNOS produced less Ki67 staining than when Ad.VEGF was also injected, the vessels appeared to be arranged in a somewhat chaotic way for both. This is compared to when Ad.sDll4 was given along with Ad.Ang1 +Ad.eNOS where the vessels appear in a more ordered fashion with less intertwining. This was also the case when all four viruses were given together and both this groups showed a marked decrease in Ki67 staining indicating less proliferating endothelial cells and suggesting less overall growth.

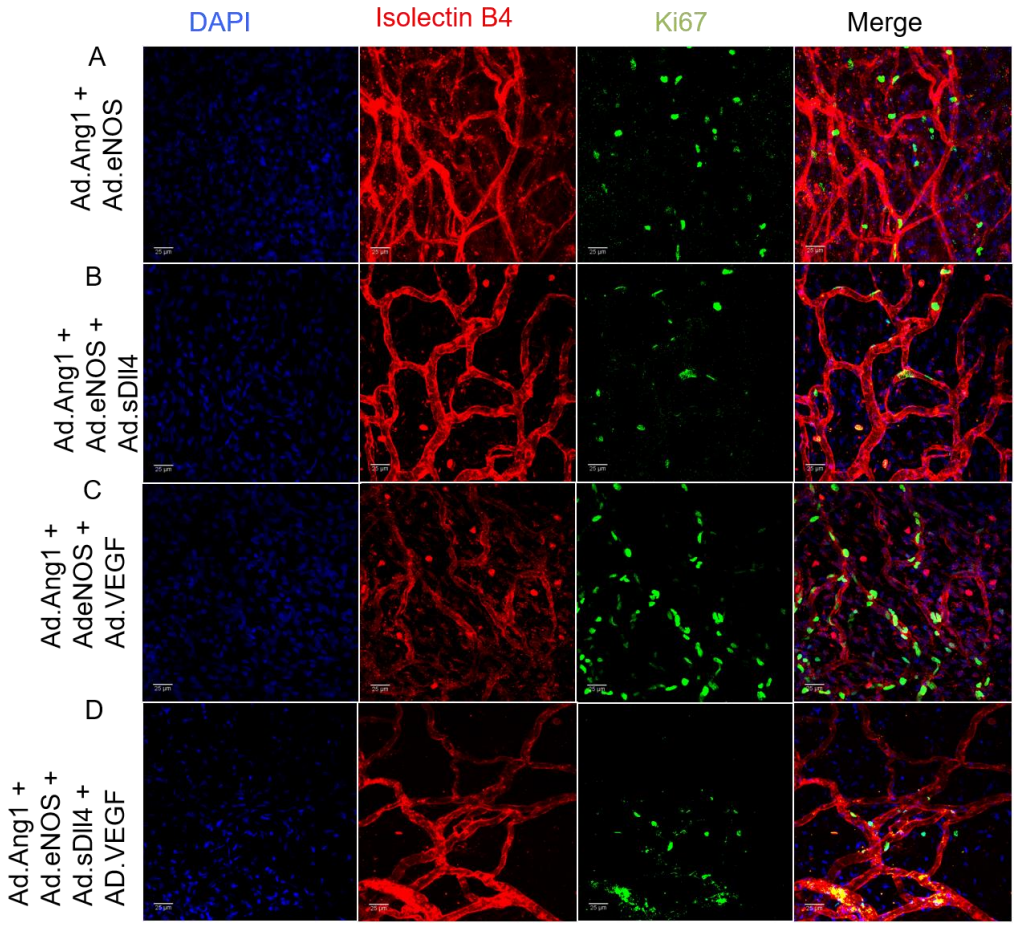


Figure 5.3 Addition of Ad.sDll4 leads to a more organised quiescent vasculature. *Representative images of mesenteric panels injected with Ad.Ang1 + Ad.eNOS or Ad.Ang1 + Ad.eNOS + Ad.VEGF with or without Ad.sDll4 (n=8). Panels were stained with the nuclei marker DAPI (blue), the blood vessel marker IB4 (red) and the proliferation marker Ki67 (green). Ad.Ang1 + Ad.eNOS (A) and Ad.Ang1 + Ad.eNOS + Ad.VEGF (C) panels appeared more chaotic than when Ad.sDll4 was also injected with these combinations (B and D) where vessels appeared to be more organised. Ad.sDll4 panels also appeared to show more Ki67 staining indicating higher proliferation.*

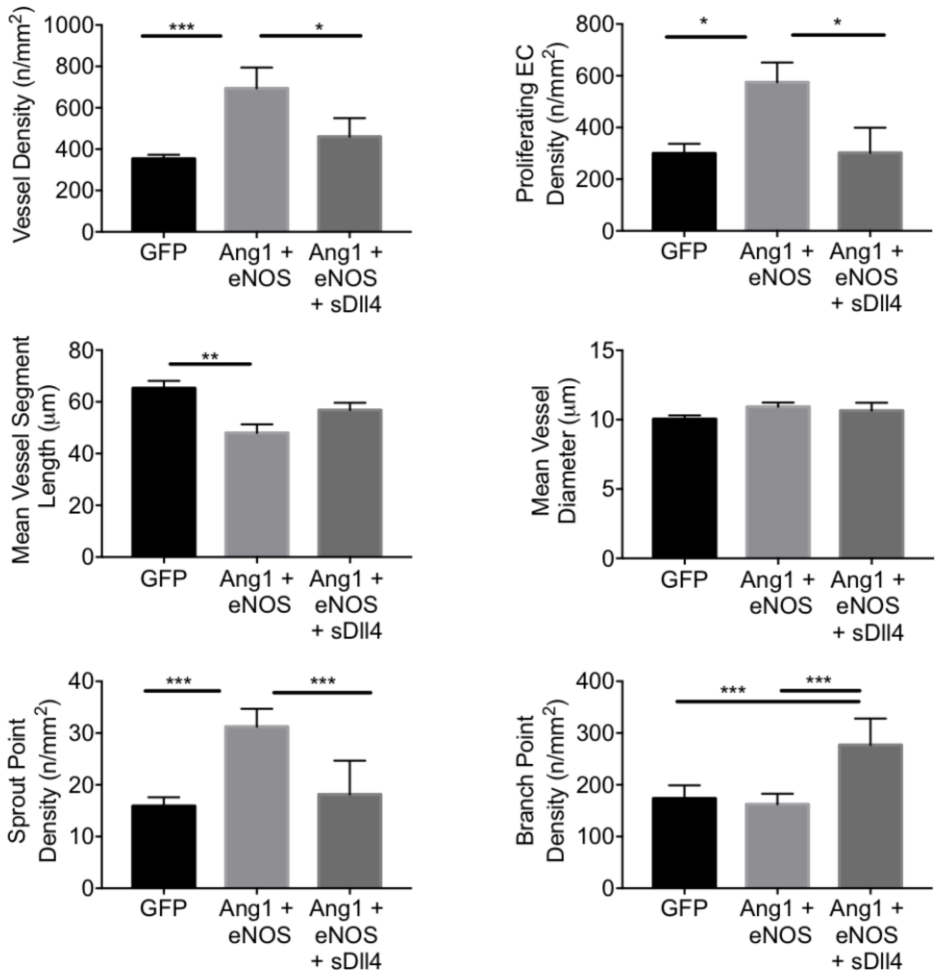


Figure 5.4 Ad.sDll4 results in a less active vasculature*. As previously described rat mesenteric panels were taken for staining 1 week after being injected with Ad.eGFP, Ad.Ang1 + Ad.eNOS with or without Ad.sDll4 (n=5). A) Vessel Density. B) Proliferating Endothelial cell density (Ki67+ve vessels). C) Vessel length, D) Vessel diameter, E. Sprout point density. F. Branch point density. All Analysis One way ANOVA. *=p<0.05, **=p<0.01, ***=p<0.001. Post-hoc analysis, Benjamini, Kreuker and Yekutieli* (1995; 2001)

Upon quantification of the images it was revealed that panels which were injected with both Ad.Ang1 + Ad.eNOS (693.9 ±100.5/mm^2, p=0.0002) and Ad.Ang1 + Ad.eNOS + Ad.sDll4 (530.6 ±95.2/mm^2, p=0.0387) resulted in a significant increase in vessels compared to Ad.eGFP although the addition of Ad.sDll4 resulted in significantly fewer vessels than Ad.Ang1 +Ad.eNOS only. Ad.Ang1 and Ad.eNOS resulted in a significant increase in proliferating endothelial cells (574.8 ±76.54/mm^2, p=0.0089) compared to Ad.eGFP (Figure 5.4). However, when Ad.sDll4 was injected along with Ad.Ang1 + Ad.eNOS the density of proliferating endothelial cells was reduced to that of Ad.eGFP panels.

Ad.Ang1 +Ad.eNOS resulted in shorter vessels than Ad.eGFP (48 ±3.33μm, p=0.002) but this was not a significant decrease (56.79 ±2.85μm) with the addition of Ad.sDll4 there was no change in the average diameter of the vessels.

Ad.Ang1 + Ad.eNOS panels gave rise to a significant increase in sprouts (31.25 ±3.45/mm^2, p=0.0002) compared to Ad.eGFP which was also similar to that seen earlier by Ad.VEGF (see Figure 5.5) In contrast, when Ad.sDll4 was also added, the density of sprouts remained at a comparable level to Ad.eGFP. Conversely, it was the Ad.Ang1 + Ad.eNOS + Ad.sDll4 group that resulted in a significant increase in branches (336.3 ±41.2/mm^2, p=0.0015) with Ad.Ang1 + Ad.eNOS remaining at Ad.eGFP levels.

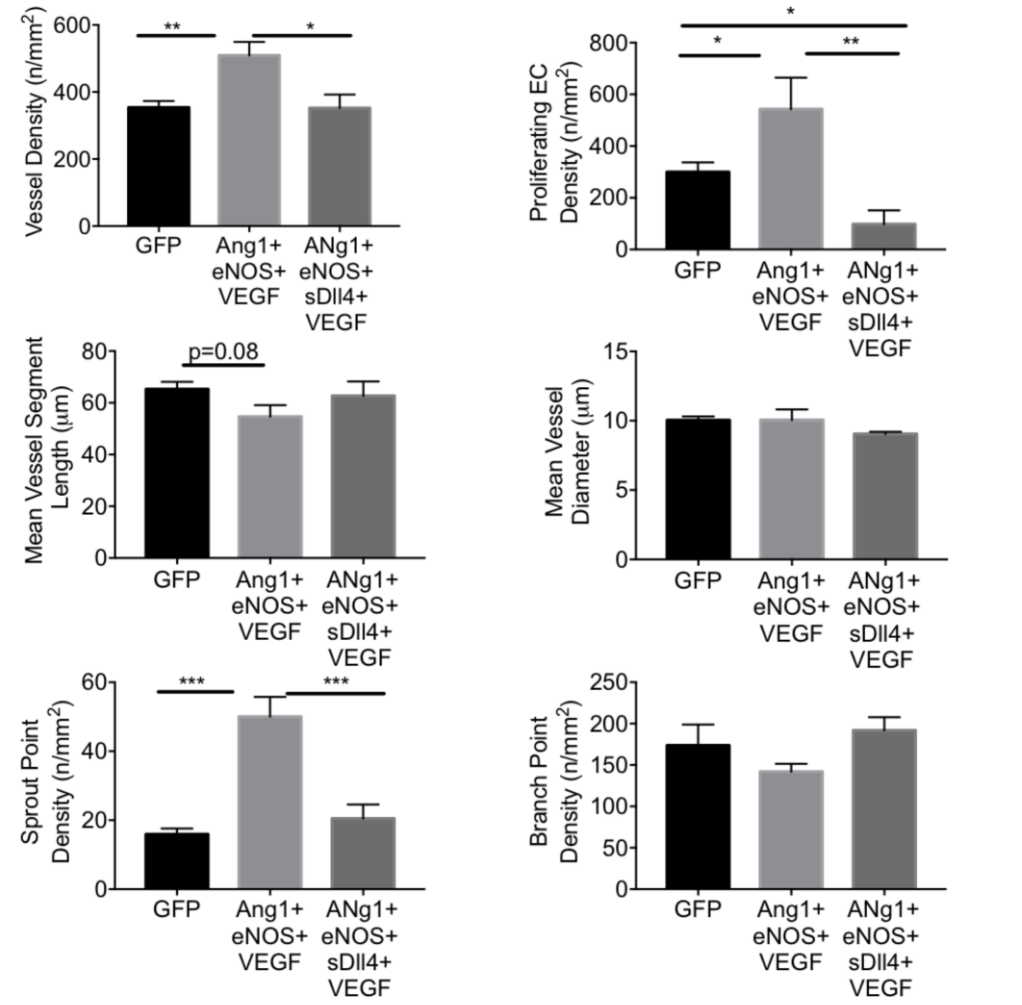


Figure 5.5 Ang1 + eNOS + VEGF + sDll4 results in vessels that are similar to but more branched than Ad.eGFP*. One week after adenovirus injections mesentery panels were taken for staining Panels were imaged by confocal microscopy and then analysed using ImageJ image analysis software (n=5). A. Vessel Density. B) Proliferating Endothelial cell density (Ki67+ve vessels). C) Vessel length, D) Vessel diameter, E. Sprout point density. F. Branch point density. All Analysis One way ANOVA. *=p<0.05, **=p<0.01, ***=p<0.001. Post-hoc analysis, Benjamini, Kreuker and Yekutieli* (1995; 2001)

As Benest *et al* (2006) and Stone *et al* (2016) had already shown that VEGF also plays a role in the maturing of the vasculature when in combination with Ang1 and eNOS I next looked at how the addition of sDll4 would affect the vessels formed.

When Ad.VEGF was combined with Ad.Ang1 + Ad.eNOS and Ad.Ang1 there was an increase in vessels compared to Ad.eGFP whereas the addition of Ad.sDll4 led to fewer vessels than when it was not given. When Ad.VEGF was combined with Ad.Ang1 + Ad.eNOS (Figure 5.5) there was a significant increase in proliferating endothelial cells (538.8 ±124.6/mm^2, p=0.0433). However, as before, when Ad.sDll4 was also added this dropped below the density seen by Ad.eGFP to 179.5 ±91.15/mm^2.

Both groups also led to a small decrease in vessel length compared to Ad.eGFP although the group with Ad.sDll4 (58.99 ±5.66μm) produced slightly longer vessels than the group without (54.63 ±4.48μm) and surprisingly there was no difference in the diameter of vessels between any of the groups.

The Ad.Ang1 + Ad.eNOS + Ad.VEGF group led to a significant increase in sprouts (50 ±5.77/mm^2, p<0.0001) compared to Ad.eGFP however when Ad.sDll4 was present the density of sprouts was only slightly higher than Ad.eGFP. On the other hand, branch point density only increased more than Ad.eGFP when Ad.sDll4 was present whereas there were slightly fewer branches when it was not present.

5.4 Discussion

5.4.1 Induction of Notch Signalling by Ad.sDll4 Dampens the Angiogenic Response

Inhibition of Dll4/Notch signalling has been shown to result in vessels taking up an angiogenic phenotype in several different models. For instance, Hellström *et al* (2007) reported that the inhibition of Notch signalling by either γ- secretase inhibitors, genetic inactivation of one allele or endothelial specific gene deletion resulted in increased tip cell formation in the developing retina. In addition, heterozygous deletion of Dll4 or inhibition of Notch through γ-secretase inhibitors was also shown to lead to increased tip cell marker genes, increased filopodia production and hyper branching in the retina (Suchting *et al.*, 2007). Furthermore, using endothelial cell spheroids and murine Matrigel plugs Scehnet *et al* (2007) showed that inhibiting Notch signalling using a sDll4 fusion protein (sDll4-Fc) induced sprouting and increased vascular structures although these structures were without lumens and lacked perfusion. In contrast, when Notch signalling was induced in HUVECs which were retrovirally transfected to overexpress Dll4, Williams *et al* (Williams *et al.*, 2006) observed less proliferation and migration in response to VEGF compared to vehicle transfected cells. They also reported a downregulation of VEGFR2 and neuropillin1 in those cells overexpressing Dll4.

Here, I present data where Notch signalling has been induced through the injection of an adenovirus encoding sDll4 using the rat mesenteric

angiogenesis assay first described by Wang *et al* (2004). While this model has been previously used to study other associated angiogenic factors including VEGF (Wang *et al.*, 2004), Ang1 (Benest *et al.*, 2006) and eNOS (Benest *et al.*, 2008) until now the model had not been used to study Dll4/Notch signalling. Despite this, the data presented here clearly shows that induction of Notch signalling resulted in a less angiogenic vasculature supporting previously published work in other models discussed above demonstrating that the rat mesenteric angiogenesis assay is a reliable model for studying the effects of Dll4/Notch signalling.

In previous studies using this model Ad.eGFP injected panels resulted in fewer sprouts and proliferating endothelial cells and although there was similarity in the density of vessels the present data was much more variable. It was also interesting to note that while the average length of vessels was similar to that seen in Benest *et al* (2006), Wang *et al* (2004) saw much longer vessels for this group. Despite these variations, the relative changes in the vasculature seen when Ad.VEGF is given is comparable between studies for all parameters except sprouting. There was a quantitative (but not qualitative) difference between Benest *et al* (2006) and the present study in terms of sprout points where Benest *et al* reported a greater increase than was seen here. This difference is unlikely to be a strain difference (the same strain of rats was used), a vector difference (the same vector was used), or a methodological difference (the same methodologies were very similar). The most likely explanation is that it was due to

differences in location, as the Benest et al study was undertaken in a non-specified pathogen free laboratory, whereas this study was undertaken in a clean facility. This difference appears to be relatively minor, as the other parameters are similar, for instance, panels injected with Ad.VEGF still resulted in more, shorter vessels with increased proliferating endothelial cells and sprout points which was also seen previously indicating that the assay was working as expected.

In chapter 3 I established that Ad.sDll4 induced Notch signalling. In vitro, this resulted in an increase in sprout points and tube density compared to Ad.eGFP. However, when injected into the mesenteric fat pad Ad.sDll4 produced vessels that were longer, had less proliferating endothelial cells and sprout points suggesting the more quiescent phenotype that would be expected if Notch was being induced (see Figure 5.2). Interestingly, the density of vessels increased slightly (but not significantly) compared to Ad.eGFP panels and taking into account that the endothelial cell proliferation remained the same and sprouting decreased compared to Ad.eGFP it is possible that the growth in the number of vessels is due to intussusceptive angiogenic processes rather than sprouting.

Interestingly, when Ad.VEGF and Ad.sDll4 were given together the resulting vasculature was similar to that produced by Ad.eGFP suggesting that the pro-angiogenic properties of VEGF and the anti-angiogenic properties of sDll4 cancelled each other out. This is not surprising as VEGF has been shown to be an upstream regulator of Dll4 expression (Liu *et al.*, 2003) and Dll4/Notch signalling has been

reported to negatively regulate VEGF through the downregulation of VEGFR2 (Lobov *et al.*, 2007). Therefore, it would be reasonable to expect that the addition of both sides of this intertwined pathway at equal quantities would balance each other out.

5.4.2 Addition of Ad.sDll4 Leads to a More Endogenous-like Vasculature

While the role of Dll4/Notch signalling in angiogenesis has been well reported it is emerging that the pathway may also play a role in the remodelling and maturation of the vasculature. For instance, in an oxygen-induced retinopathy model during normal development, inhibition of the Dll4/Notch pathway resulted in reduced vessel occlusion subsequently maintaining blood flow and preventing capillary regression (Lobov *et al.*, 2011). In addition, the vasodilator adrenomedullin was found to be upregulated while the vasoconstrictor angiotensin was suppressed. Furthermore, deletion of the Notch regulated Ankyrin repeat protein, which negatively regulates Notch, resulted in the opposite effects leading Lobov *et al* (2011) to conclude that Dll4/Notch controls remodelling and regression through regulation of vasoconstriction and blood flow.

Endothelial nitric oxide which is also involved in the regulation of blood flow (Rees, Palmer and Moncada, 1989) has been implicated in vessel remodelling and maturation as well. Yu *et al* (Yu *et al.*, 2005) reported that after ischemic injury in eNOS knockout mice there were defects in arteriogenesis, functional blood flow and pericyte recruitment. Additionally, increased blood flow, or shear stress, has been shown to

result in thickened vessels walls (Unthank *et al.*, 1996; Tuttle *et al.*, 2001), and induced remodelling (Rissanen *et al.*, 2005) while lack of blood flow can lead to pruning and regression of the vessel (Morawietz *et al.*, 2000; Lobov *et al.*, 2011).

Previously Benest *et al* (2008) demonstrated that injection of Ad.Ang1 + Ad.eNOS + Ad.VEGF in the rat mesenteric fat pad stimulated arteriolar genesis and recruitment of VSMC. VSMC are also known to express Notch2, Notch3 and the ligand Jag1 although during vascular injury Notch1 has been shown to interact with VSMC (Oyama *et al.*, 2010; Wang *et al.*, 2012). For example Notch3 knockout mice resulted in defects in the maturation of smooth muscle and arterial specification and in double deletion studies where Notch2 and Notch3 were deleted severe cardiovascular abnormalities were seen as there was no smooth muscle differentiation (Domenga *et al.*, 2004; Wang *et al.*, 2012). Notch signalling has also been reported to interact with other signalling pathways that are involved in VSMC recruitment and differentiation such as PDGF-B where Notch can directly induce the transcription of PDGFR-β and thereby enhance PDGF-B signalling effects (Jin *et al.*, 2008). Additionally Notch also works with TGFβ to regulate VSMC differentiation and the transcription of smooth muscle cell contractile genes through the interaction of NICD and a transcription factor with the TGFβ pathway known as SMAD2/3 (Tang *et al.*, 2010).

In the present study, Ad.Ang1 + Ad.eNOS + Ad.VEGF resulted in similar vascular and sprout point densities (see Figure 5.5) as seen by

Benest et al (2008). The proliferating endothelial cell density, on the other hand, was much higher in the present study but this was also the case earlier for Ad.eGFP and Ad.VEGF (see Figure 5.2) and the relative increase compared to Ad.eGFP seen in the two studies was still similar signifying results are still comparable.

Interestingly, in a more recent study Ad.Ang1 +Ad.eNOS were injected into the rat mesenteric fat pad together and resulted in a decrease in the density of sprouts in addition to significantly increasing VSMC recruitment compared to when each virus is given separately indicating the stimulation of arteriolargenesis can also be achieved with just these two factors (Stone *et al.*, 2016).

Curiously, when Ad.sDll4 was injected along with Ad.Ang1 + Ad.eNOS fewer vessels were produced. they were also longer with fewer proliferating endothelial cells and sprout points than when only Ad.Ang1 + Ad.eNOS was given suggesting that this adenovirus combination results in a less angiogenic vasculature (see Figure 5.4). While Ad.eNOS allows for flow induced angiogenic responses and remodelling (Benest *et al.*, 2008) Ang1 has been shown to be involved in the stabilisation of vessels rather than promoting angiogenesis. Thurston *et al* (2005) reported that Ang1 was able to promote vessel enlargement without sprouting in mouse pups although this may be due to the connection with endothelial nitric oxide seen by Babaei *et al* (2003) who reported that Ang1 angiogenic responses in both cultured endothelial cells and *in vivo* were dependent on endothelium-derived nitric oxide. In addition, Ang1 has been shown to produce vessels that

are resistant to inflammatory agent-induced leakiness *in vivo* (Thurston *et al.*, 1999, 2000) and inhibit VEGF-induced Ca^{2+} influx through the transient receptor canonical-1 preserving barrier function (Jho *et al.*, 2005) and leading to a more mature, stabilised vessel. Moreover, Ang1 has also been shown to restore the hierarchal order of larger vessels, rescue oedema and haemorrhaging in growing retinal vasculature in mouse neonates in the absence of mural cells (Uemura *et al.*, 2002).

The induction of Notch signalling has been shown to regulate sprouting angiogenesis (Hellstrom *et al.*, 2007; Scehnet *et al.*, 2007; Suchting *et al.*, 2007; Liu *et al.*, 2012) and has been recognised as a marker of quiescence (Ehling *et al.*, 2013). It would therefore be reasonable to expect that the addition of all 3 viruses would result in a flow induced angiogenic response from Ad.eNOS that would then be counteracted by the Notch signalling induced by Ad.sDll4 allowing the remodelling actions of Ad.Ang1 to occur as seen in the present study.

Furthermore, Ang1 has been shown to stimulate the transcriptional activity of β-catenin through PI3K/AKT-mediated phosphorylation of glycogen synthase kinase 3β (GSK3β). This leads to the upregulation of Dll4 and NICD expression whereas deletion of β-catenin by siRNA blocked Ang1-induced Dll4 expression. The same study then went onto show that Ang1 or NICD could upregulate Dll4 through the RBP-Jκ binding site within intron 3 of the Dll4 gene and that β-catenin formed a complex with NICD/RBP-Jκ to enhance Dll4 expression(Zhang *et al.*, 2011) lending support to the idea of cooperation between Ang1 and Dll4/Notch signalling throughout the post-angiogenic process.

Intriguingly, when all four adenoviruses were injected together the resulting vasculature appeared the least angiogenic (see Figure 5.5). While the combination of all four viruses still led to an increase in the number of vessels compared to Ad.eGFP, they were longer, had more branches but fewer proliferating endothelial cells and sprouts than any of the other groups containing Ad.Ang1 + Ad.eNOS. On top of this when Ad.Ang1 + Ad.eNOS + Ad.VEGF +Ad.sDll4 were compared to Ad.eGFP panels they were alike in all parameters except for the density of vessels and branches where Ad.Ang1 + Ad.eNOS + Ad.VEGF +Ad.sDll4 resulted in an increase. It is possible that this is because this combination of angiogenic factors closely resemble endogenous situations thereby allowing for a well-regulated, organised vasculature to form. Furthermore, the addition of Ad.sDll4 into the Ad.Ang1 + Ad.eNOS + Ad.VEGF group led to a switch in sprout and branch point densities. It is possible that this switch is due to the Ad.sDll4 preventing the vessels from continuing to grow and remodel using sprouting and instead switched in favour of non-sprouting angiogenesis which would explain the relative change seen in sprout and branch point densities yet the similarity in vessel length, diameter and density seen between the two groups. It is therefore reasonable to conclude that both the Ad.Ang1 + Ad.eNOS + Ad.sDll4 and Ad.Ang1 + Ad.eNOS + Ad.VEGF+ Ad.sDll4 groups resulted in a less angiogenic vasculature.

As the recruitment of mural cells is a large part of arteriolargenesis Benest *et al* (2006, 2008) and Stone *et al* (2016) also investigated how varying combinations of Ad.Ang1, Ad.eNOS and Ad.VEGF affected this.

They measured the coverage of both pericytes and smooth muscle cells and reported that Ad.Ang1 was able to produce the highest percentage of pericyte ensheathment with Ad.Ang1 + Ad.eNOS the second most. However, only Ad.Ang1 + Ad.eNOS and Ad.Ang1 + Ad.eNOS + Ad.VEGF were able to stimulate VSMC recruitment. While it was the intention of this study to also investigate mural cell recruitment unlike IB4 and Ki67, the antibodies for staining pericytes (NG2) and VSMC (α-smooth muscle actin) proved difficult to optimise in this tissue. After several months, antibodies and methodologies I finally succeeded in staining some mesenteries, but due to time and funding constraints, I could not repeat the experiment to gain the tissue needed for the staining. As the data presented here shows similar trends to that previously reported by Benest *et al* (2006, 2008) and Stone *et al* (2016) on arteriolargenesis in this model, and the data shown in the next chapter supports the concept that Dll4 also stimulates arteriolargenesis, further studies using these adenovirus combinations are needed to uncover how mural cell recruitment is affected.

5.5 Concluding Remarks

In this chapter I have demonstrated that the induction of Notch signalling by Ad.sDll4 reduced the angiogenic response in the rat mesentery. The data clearly supports previous studies undertaken using other models indicating that the rat mesenteric angiogenesis assay is a competent model for the study of Dll4/Notch activity *in vivo*. I also established that the Dll4/Notch pathway plays a role in the post-angiogenic remodelling and maturation of vessels taming the pro-angiogenic responses initiated by Ad.eNOS and Ad.VEGF. However, as the recruitment of pericytes and VSMC is a vital part of this process further work into how Dll4/Notch signalling affects this is needed for a better understanding of the role Dll4/Notch plays.

Chapter 6: Dll4 and Peripheral Ischaemia

6.1 Introduction

Peripheral arterial disease (PAD) is a debilitating condition that results in insufficient blood supply to the extremities of the body (Gornik, 2005). This is usually due to a blockage in the arteries by a cholesterol plaque caused by atherosclerosis (Kullo and Leeper, 2015). It is a disease that is common in Western industrialised nations and the incidence increases with age although smoking, diabetes, dyslipidaemia and hypertension can all increase the risk of developing PAD (Kullo and Leeper, 2015).

A blockage in the vessel can lead to intermittent or chronic tissue ischaemia due to decreased blood flow to areas downstream of the blockage. In healthy subjects, functional reperfusion of the ischaemic tissue can occur through rerouting blood flow around the blockage using a collateral vessel network (Ziegler *et al.*, 2010). The shift in blood flow into the collateral network results in the growth of new, and the remodelling of existing vessels, in order to cope with the increased volume as well as to resupply the areas of tissue from where the flow has been diverted. The possibility of stimulating patients' own vasculature to grow, remodel and reperfuse the ischemic tissue as a less invasive option to angioplasty attracted researchers to investigate this process and the mouse hindlimb ischemia model was developed to aid this (Niiyama *et al.*, 2009).

In the previous chapter I demonstrated that inducing Notch signalling with an adenovirus encoding sDll4 results in a less angiogenic, but more organised vasculature and when this was combined with Ang1 + eNOS ± VEGF there was a switch from growth by sprouting to branching. This increase in branches is suggestive of a switch to intussusceptive angiogenesis which is thought to mainly occur post-sprouting during the remodelling and maturation phase of vascular growth, a process important in recovery from ischemic injury. I therefore wanted to investigate how Dll4/Notch signalling affects the formation of a collateral network and blood flow recovery after ischemic injury.

Using the hindlimb ischemia model eNOS has been shown to be key in ischemic reperfusion. Homozygous eNOS knockout mice have been shown to have defects in arteriogenesis, functional blood flow after muscle stimulation and pericyte recruitment, and this, was rescued with a local intramuscular delivery of adenovirus encoding eNOS (Yu *et al.*, 2005). Additionally, when eNOS was injected into the adductor muscle in a rat hindlimb ischemia model, enhanced angiogenesis was also reported (Robert S. Smith *et al.*, 2002).

Ang1 has also been shown to promote an angiogenic response after ischemic injury (Shyu *et al.*, 1998) and to increase vessel size, especially when given in combination with VEGF (Chae *et al.*, 2000) while VEGF alone is known to increase blood flow and angiogenesis. This is in addition to data presented by Benest *et al* (2006, 2008) and Stone *et al* (2016) which demonstrated that Ang1, eNOS and VEGF all play a role in arteriolar genesis in the mesenteric model.

Interestingly, a study by Al Haj Zen *et al* (2010) reported that inhibition of Dll4/Notch signalling after ischemic injury resulted in a disorganised, low perfused capillary network with increased sprouts, delayed blood flow and muscle hypoxia generation. However, this increased the response to VEGF stimulation with animals showing a quicker recovery of blood flow that reached up 80% of normal levels after 4 weeks when VEGF was combined with Dll4 inhibition as opposed to when given separately (Cao *et al.*, 2009). Dll4 has also been linked to the recruitment of pericytes with the loss of Dll4 function leading to a reduction in pericytes in tumour vasculature (Scehnet *et al.*, 2007). On the other hand, this was also the case for over stimulation of Dll4 (Scehnet *et al.*, 2007) suggesting it may be dose dependent. Furthermore, Dll4 has been linked to regulating post-angiogenic vessel remodelling and regression by controlling vasoconstriction and dilatation (Lobov *et al.*, 2011).

Taking the above information in combination with the findings from the other chapters I set out to test the hypothesis that inducing Notch signalling after ischemic injury in the hindlimb would not enhance blood flow as there will be little angiogenic growth stimulated and no change in vessel diameter was seen previously (see chapter 5). I also predicted that when given in combination with Ang1 + eNOS there would be a switch towards arteriolar development and VSMC recruitment enabling a more functional collateral network to form.

6.2 Methods

6.2.1 Adenoviruses

Adenovirus combinations used for this study were as follows;

- Ad.sDll4 (n=14)
- Ad.Ang1 + Ad.eNOS + Ad.sDll4 (n=12)
- Ad.Ang1 + Ad.eNOS + Ad.VEGF + Ad.sDll4 (n=12)
- Ad.eGFP (n=12)

Colleagues in the laboratory undertaking similar projects kindly provided me results for mice injected with

- Ad.Ang1 + Ad.eNOS (n=12)
- Ad.Ang1 + Ad.eNOS + Ad.VEGF (n=12)

to aid understanding of the data collected for the groups listed above and to prevent unnecessary overuse of animals.

6.2.2 Experimental Protocol

Surgeries were carried out predominantly by Dr. Machado with my assistance, and I did some surgeries under her supervision. I undertook all the imaging after initial training for experiments involving GFP or Ad.DLL4. The Ad.Ang1/Ad.eNOS/Ad.VEGF experiments were undertaken by Dr Machado.

Male C57Bl6 mice were first anaesthetised (2% isoflurane) before their hind limbs were imaged using a colour laser speckle imaging apparatus and software (FLIP2 Moor instruments) ensuring that there was blood flow to both limbs. Following imaging the mice were transferred to the

surgical area where after a small incision was made in the hindlimb and the femoral nerve was separated from the femoral artery. The latter was coagulated above the epigastric bifurcation. Appropriate combinations of adenoviruses encoding for either eGFP, sDll4, Ang1, eNOS or VEGF were then injected into the adductor muscle before the limb was sutured back up. Prior to recovering the animal, it was first re-imaged to ensure that the surgery was successful in inducing ischemia. The mice where then imaged on day 3, 7, 14 and 21 before they were culled and the muscle from both hind limbs were dissected out, frozen in liquid nitrogen and then stored at -80℃.

Multiple 5μm thick sections of tissue were then cut using a cryostat and sections at different points throughout the muscle were taken forward for staining. The tissue was stained for capillaries (IB4), arterioles (α-smooth muscle actin-cy3) and nuclei (DAPI) and then imaged by confocal microscopy. Using ImageJ image analysis software capillary and arteriolar densities were calculated.

All data are presented as ±SEM and was considered statistically significant if $p<0.05$ unless otherwise stated. All methods are described in detail in Chapter 2.

6.3 Results

6.3.1 Ad.sDll4 is Deleterious to the Recovery of Blood Flow

The speckle images were analysed using the FLIP2 software (Moor Instruments) and the ischemic to contralateral blood flow ratio was calculated for each time point. The images seen in Figure 6.1 are representative images from each group showing the blood flow seen before surgery, immediately after and at days 3, 7, 14 and 21. Blue represents a low supply of blood whereas yellow and red represent a high supply of blood to the hindlimb. As expected all animals showed a marked reduction in blood flow in the ischemic hindlimb immediately after surgery by a dark blue colour compared to before the surgery indicating procedure success. Mice that were injected with Ad.eGFP showed an increase in blood flow recovery over time with the ischemic hindlimb appearing to have greater light blue coverage. Interestingly, when the images were analysed the recovery from ischemic injury of Ad.eGFP appears to plateau after day 14 at approximately 60% of levels prior to ischemia induction (Figure 6.2A).

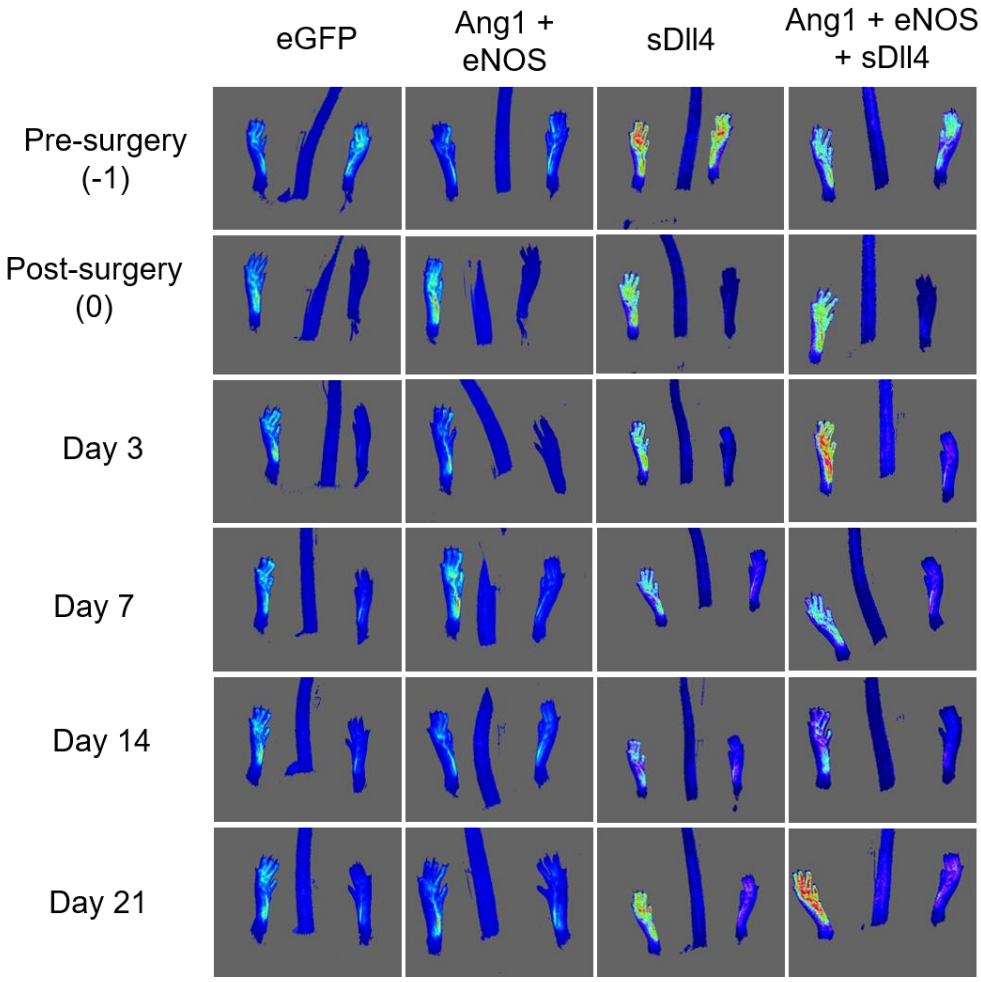


Figure 6.1 Representative blood flow images from each group taken before and after surgery and on days 3, 7, 14 and 21. *Dark blue represents low blood flow whereas red represents high blood flow. The contralateral limb is the left paw. The ischemic limb (right paw) showed a marked shift towards dark blue immediately after surgery indicating ischemia had been induced and as blood flow was recovered a shift back towards red and yellow colours seen prior to surgery was seen. The ischemic limb of Ad.Ang1 + Ad.eNOS (n=12) appears to recover blood to the greatest extent when compared to the contralateral whereas Ad.sDll4 (n=14) and Ad.Ang1 + Ad.eNOS + Ad.sDll4 groups (n=12) still appear to have a large difference in blood flow between ischemic and contralateral limbs at day 21.*

The difference in colour between the ischemic and contralateral hind limbs appeared to narrow sooner in Ad.Ang1 + Ad.eNOS injected animals than in Ad.eGFP animals. Analysis of the images demonstrated that those mice injected with Ad.Ang1 + Ad.eNOS resulted in a significantly greater recovery of blood flow ($p=0.0048$, Figure 6.2A). Even after only 3 days the ischemic to contralateral blood flow ratio had increased from 0.213 ±0.16 immediately after surgery to 0.432 ±0.043 whereas Ad.eGFP was only 0.268 ±0.028. This trend of greater recovery of blood flow continued by Ad.Ang1 + Ad.eNOS continued for the duration of the experiment although, like Ad.eGFP, after day 14 there also appeared to be a plateau in recovery.

Unlike Ad.Ang1 + Ad.eNOS mice, Ad.sDll4 mice images showed slower recovery with some dark blue tones that are associated with images following ischaemic induction still visible up to a week later. Even by day 21 there was still a noticeable difference between ischemic and contralateral blood flow where in Ad.Ang1 + Ad.eNOS mice this had become less so. Upon analysis of the images it was shown that the Ad.sDll4 mice recovered blood flow in the ischemic hindlimb at a similar rate to Ad.eGFP until day 7 (Figure 6.2B). Between days 7 and 14 Ad.sDll4 ischemic to contralateral ratio reduced from 0.508 ±.031 to 0.473 ±0.017 whereas Ad.eGFP continued to recover. By day 21, Ad.sDll4 had increased blood flow to back to similar levels as Ad.eGFP.

When Ad.sDll4 mice were compared to Ad.Ang1 + Ad.eNOS mice (Figure 6.2C), Ad.sDll4 blood flow was clearly lower and recovery overall was worse than Ad.Ang1 + Ad.eNOS ($p=0.0003$). This was

especially evident at day 14 (p=0.0001) where Ad.Ang1 + Ad.eNOS mice continued to recover blood flow to the hindlimb whereas Ad.sDll4 decreased slightly. Ad.sDll4 did go on to increase blood flow recovery and after 21 days was not significantly different from Ad.Ang1 + Ad.eNOS.

I then looked at how combining Ad.Ang1, Ad.eNOS and Ad.sDll4 would affect the recovery of blood flow. The images show by day 3 that the dark blue tones have disappeared although there is still a large difference between the light blue ischemic hindlimb and the red and yellow contralateral. The images show that the ischemic hindlimb continues to recover although at day 14 both hind paws appeared to have reduced blood flow compared to day 3 and 7 and then on day 21 the contralateral returned to a red colour indicating the variation that can be seen even within the same mouse.

Interestingly, when the images were analysed the addition of Ad.sDll4 to Ad.Ang1 + Ad.eNOS resulted in an almost identical rate of blood flow recovery as Ad.eGFP (Figure 6.2D) Figure 6.2When compared to Ad.Ang1 + Ad.eNOS there was a significant difference in overall blood flow recovery ($p<0.0001$, Figure 6.2E) in addition to days 7 and 14 where the ischemic to contralateral blood flow ratio was also significantly different between the two groups (day 7 $p=0.033$, Day 14 $p=0.0052$). Ad.Ang1 + Ad.eNOS + Ad.sDll4 did not recovered blood flow to the same amount as Ad.Ang1 + Ad.eNOS mice, although flow did not reach significant difference on day 21.

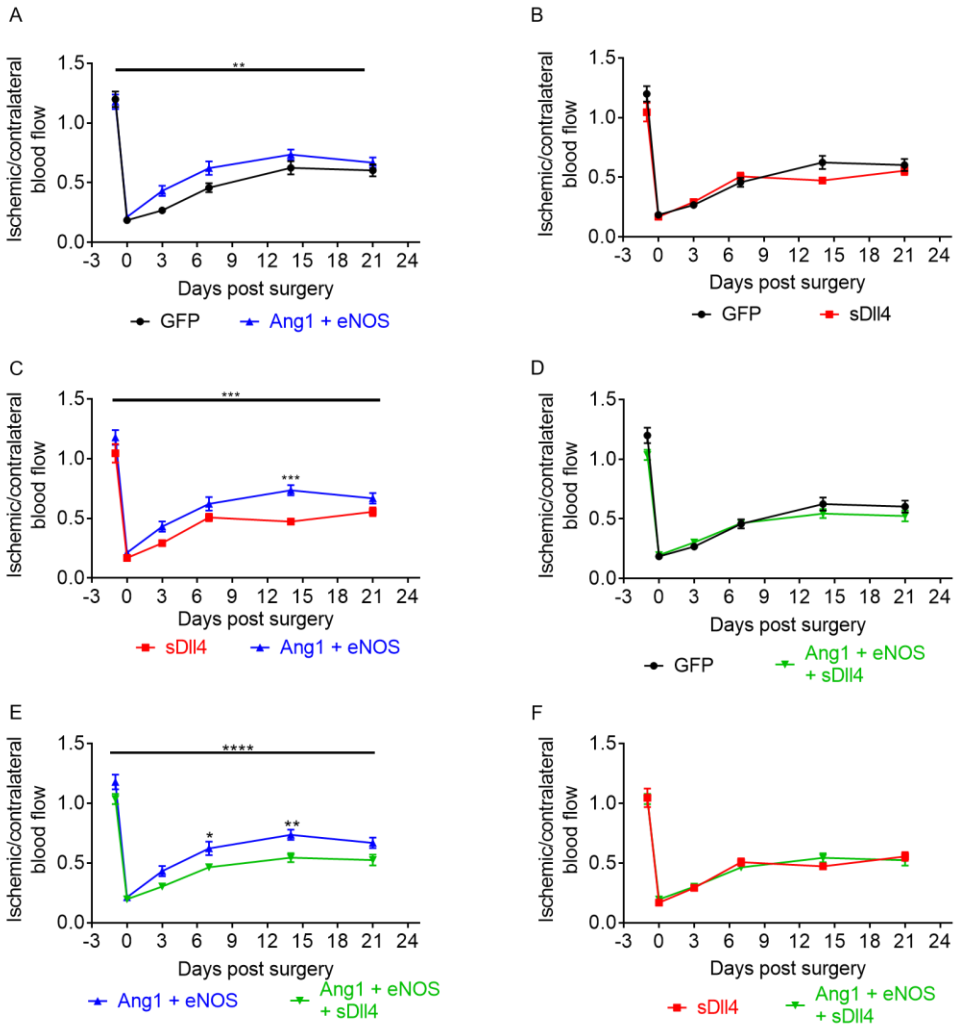


Figure 6.2 Ad.sDll4 is deleterious to blood flow recovery. *Speckle images were analysed and the ischemic to contralateral hindlimb blood flow ratio was calculated and analysed using a Two-Way ANOVA with a Sidak post-test. Ad.Ang1 + Ad.eNOS (n=12) resulted in an enhanced recovery of blood flow compared to Ad.eGFP (A, p=0.0048, n=12), Ad.sDll4 (n=14) led to a similar recovery as Ad.eGFP (B). There was a significant difference in blood flow recovery between Ad.Ang1 + Ad.eNOS and Ad.sDll4 (C, p=0.0003), notably at day 14 (p=0.0001). When Ad.Ang1, Ad.eNOS and Ad.sDll4 were given together (n=12) recovery of blood flow was similar to Ad.eGFP until day 7 where it then began to slow and plateau at day 14 (D). Ad.Ang1 + Ad.eNOS, Ad.Ang1 + Ad.eNOS + Ad.sDll4 had significantly different blood flow recovery overall (E, p<0.0001) and at days 7 (p=0.033) and 14 (p=0.0052) whereas this group was also very similar to Ad.sDll4 alone (F). *=p<0.05 compared with control.*

In addition, when compared to Ad.sDll4 mice (Figure 6.2F), there was only a slight, non-significant difference in ischemic to contralateral blood flow ratio on day 14. While at this time point Ad.sDll4 saw a small decrease the addition of Ad.Ang1 + Ad.eNOS to Ad.sDll4 appeared to prevent this and led to a small increase from 0.464 ±0.022 at day 7 to 0.544 ±0.038 at day 14 although this was still less than Ad.eGFP. This also demonstrated that addition of sDLL4 blocked the effect of Ad.Ang1 + AdeNOS on recovery from ischemia.

As VEGF in combination with Ang1 and eNOS has also been shown to be influential in arteriolar genesis (Benest *et al.*, 2006) I next investigated how adding in sDll4 to this combination would affect blood flow recovery after ischemic injury. Ad.Ang1 + Ad.eNOS + Ad.VEGF produced images which appear to show only a small difference between ischemic and contralateral at day 3 and 7 (Figure 6.3). By day 14 the ischemic hind paw appears to have recovered further although there appears to be only a small further increase in light blue colour by day 21. Analysis of the images revealed that Ad.Ang1 + Ad.eNOS + Ad.VEGF resulted in a quicker and better recovery of blood flow than Ad.eGFP until day 14 (Figure 6.4A). By day 21 however, the ischemic to contralateral blood flow ratio for Ad.Ang1 + Ad.eNOS + Ad.VEGF was only marginally higher than Ad.eGFP.

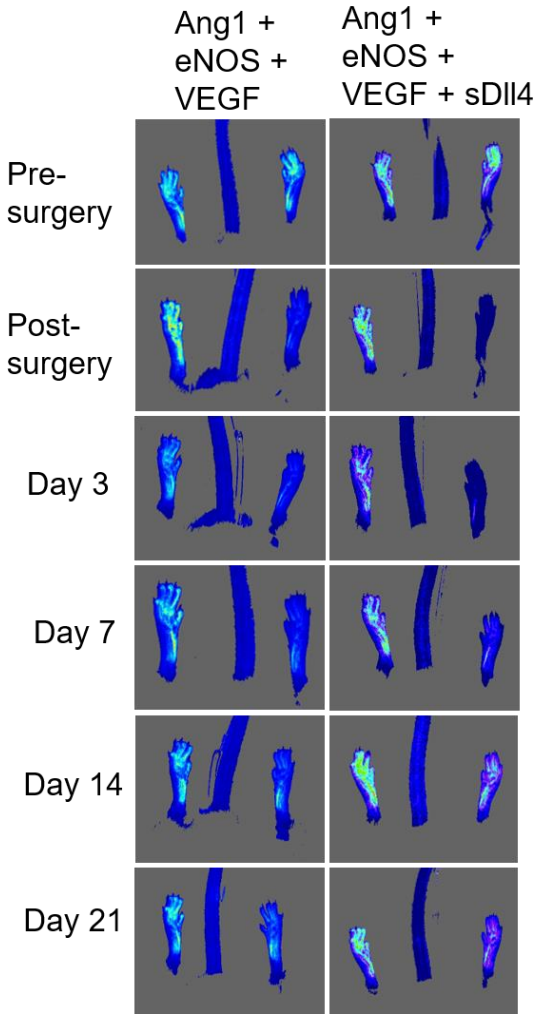


Figure 6.3 Representative Speckle images taken before and after surgery and at days 3, 7, 14 and 21. *Immediately after surgery there is a shift towards a blue coloured ischemic limb (left paw) indicating ischemia has been induced. The Ad.Ang1 + Ad.eNOS + Ad.VEGF + Ad.sDll4 (n=12) appears to recover slower than when Ad.sDll4 (n=14) is emitted and even appears to regress slightly between day 14 and 21.*

When Ad.sDll4 was added into the Ad.Ang1 + Ad.eNOS + Ad.VEGF the combination of virus images show the ischemic hind paw remaining dark blue for longer than without Ad.sDll4. At day 21 there still appears to be a larger difference in colour between the ischemic and contralateral hind paws when Ad.sDll4 is included than when it is left out. After analysis of the images it was found that there was a greater recovery of blood flow at day 3 compared to Ad.eGFP (Figure 6.4B). By day 7 Ad.eGFP had increased to the same levels as Ad.Ang1 + Ad.eNOS + Ad.VEGF + Ad.sDll4 and while Ad.eGFP mice continued to increase their ischemic to contralateral blood flow ratio, Ad.Ang1 + Ad.eNOS + Ad.VEGF + Ad.sDll4 mice only increased marginally to 0.55 ±0.031 at day 14 from 0.491 ±0.028 at day 7. Interestingly, Ad.Ang1 + Ad.eNOS + Ad.VEGF + Ad.sDll4 blood flow then decreased to 0.475 ±0.046 at day 21 as opposed to Ad.eGFP which had plateaued. In addition, when compared to Ad.Ang1 + Ad.eNOS + Ad.VEGF, Ad.Ang1 + Ad.eNOS + Ad.VEGF + Ad.sDll4 (Figure 6.4C) resulted in the same recovery of blood flow at day 3 however, by day 7 the addition of Ad.sDll4 was slowing down the recovery and this continued to day 14. Interestingly, both groups showed a decrease in blood flow between day 14 and 21 by a similar amount indicating that the addition of Ad.sDll4 hinders recovery.

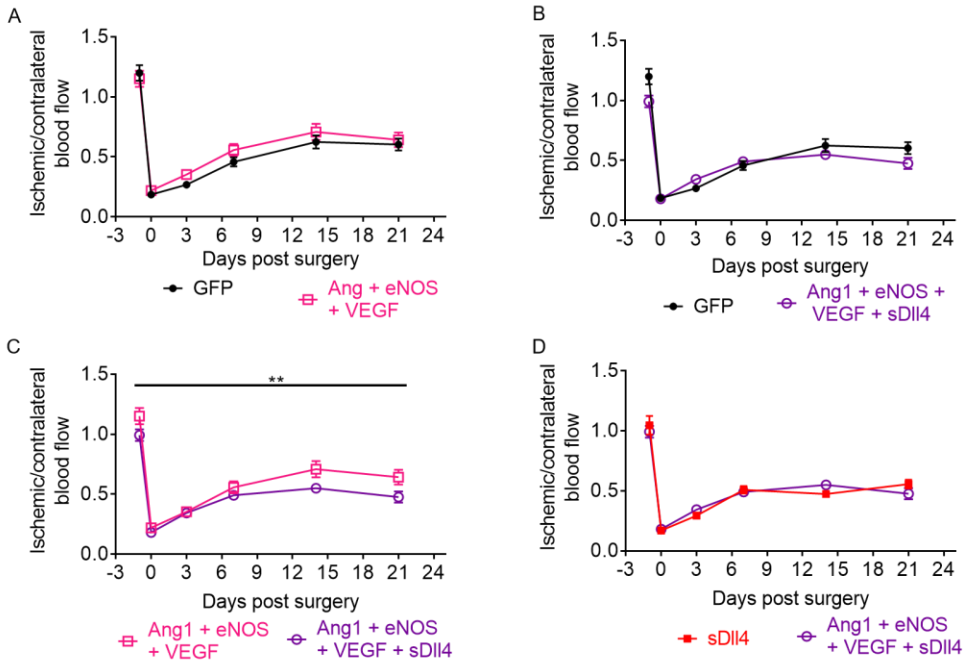


Figure 6.4 Ad.VEGF and Ad.sDll4 have an additive negative effect on blood flow recovery after ischemic injury. *Ad.Ang1 + Ad.eNOS + Ad.VEGF (n=12) led to an enhanced blood flow recovery compared to Ad.eGFP (A, n=12). When Ad.sDll4 (n=14) was added to this combination by day 14 blood flow recovery slowed and then regressed by day 21 (B). Ad.Ang1 + Ad.eNOS + Ad.VEGF ± Ad.sDll4 groups (n=12) resulted in similar blood flow at day 3 as Ad.Ang1 + Ad.eNOS + Ad.VEGF. by day 14 an overall significant difference in blood flow recovery had developed (C, p=0.0035, two-way ANOVA with a sidak post-test). Ad.sDll4 only versus Ad.Ang1 + Ad.eNOS + Ad.VEGF + Ad.sDll4 showed a very similar recovery in blood flow until day 7 (D).*

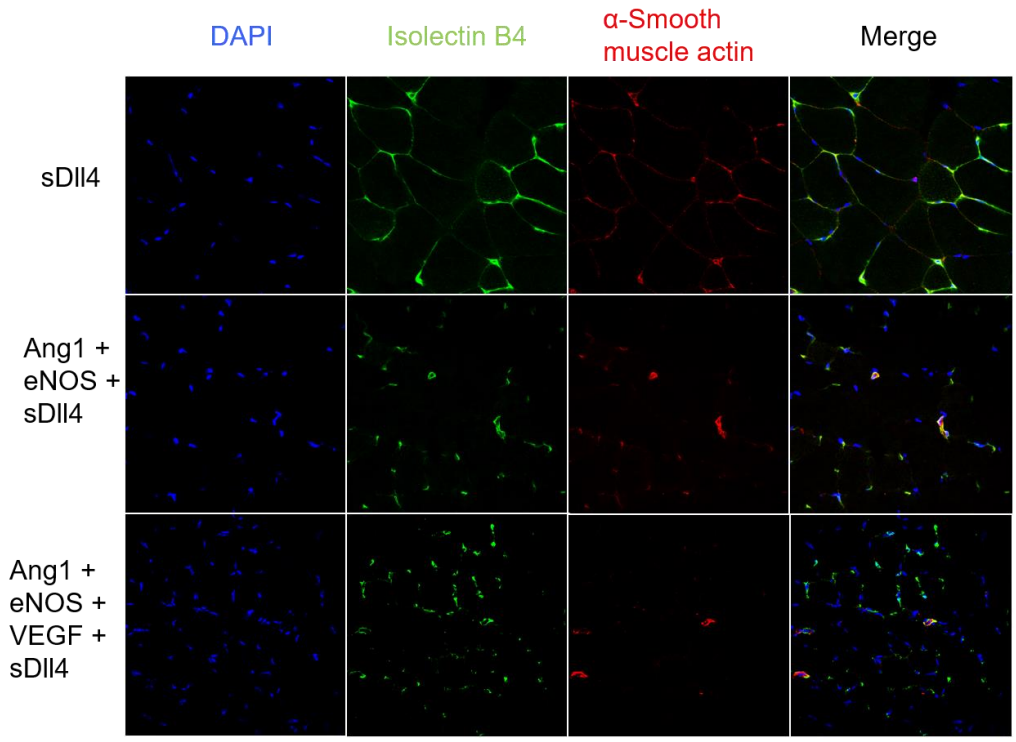


Figure 6.5 Representative images of ischemic adductor muscle tissue sections stained for capillaries and arterioles. *Tissue was frozen before being cut into 5μm sections and stained with DAPI for nuclei, IB4 for capillaries and α-smooth muscle actin for arterioles (n=3). Ad.sDll4 capillaries appear to be arranged in a hexagonal format whereas both Ad.Ang1 + Ad.eNOS + Ad.sDll4 and Ad.Ang1 + Ad.eNOS + Ad.VEGF + Ad.sDll4 appear less organised with the latter seemingly having the most capillaries. Ad.sDll4 has the most arterioles although they appear smaller than either Ad.Ang1 + Ad.eNOS + Ad.sDll4 or Ad.Ang1 + Ad.eNOS + Ad.VEGF + Ad.sDll4.*

6.3.2 Capillary Density

After imaging on day 21 mice were culled and the muscles from both hind limbs were frozen and stored at -80℃. The tissue was sectioned into 5μm thick sections and slices from different points throughout the muscle were chosen for staining. Capillaries, arterioles and nuclei were stained and the tissue images by confocal microscopy. While Ad.sDll4 capillaries appear to be arranged in a hexagonal format (Figure 6.5) both Ad.Ang1 + Ad.eNOS + Ad.sDll4 and Ad.Ang1 + Ad.eNOS + Ad.VEGF + Ad.sDll4 appear less organised with the latter seemingly

having the most capillaries. Ad.sDll4 has the most arterioles although they appear smaller than either Ad.Ang1 + Ad.eNOS + Ad.sDll4 or Ad.Ang1 + Ad.eNOS + Ad.VEGF + Ad.sDll4.

Those mice that were given Ad.eGFP were still able to produce 129.4 ±7.51 capillaries per mm^2 indicating the proficiency for an endogenous ischemic response (Figure 6.6A). Ad.sDll4 mice resulted in the formation of significantly more capillaries (210.6 ±8.28/mm^2, $p<0.0001$) than Ad.eGFP as well as those given Ad.Ang1 + Ad.eNOS which produced similar numbers of capillaries to Ad.eGFP. interestingly when Ad.Ang1, Ad.eNOS and Ad.sDll4 were combined the number of capillaries produced was the highest of all four groups at 234 ±7.92/mm^2.

When I looked at arteriolar densities in these four groups (Figure 6.6B), Ad.eGFP only produced 12.08 ±1.14/mm^2 whereas Ad.sDll4 injection led to the highest number of arterioles with 90.28 ±11.68/mm^2 ($p<0.0001$). as with the capillary densities, Ad.Ang1 + Ad.eNOS mice produced a similar number of arterioles as Ad.eGFP however Ad.Ang1 + Ad.eNOS + Ad.sDll4 did not lead to the most arterioles. While this group did lead to an increase over Ad.eGFP is still only produced approximately half the number that Ad.sDll4 did.

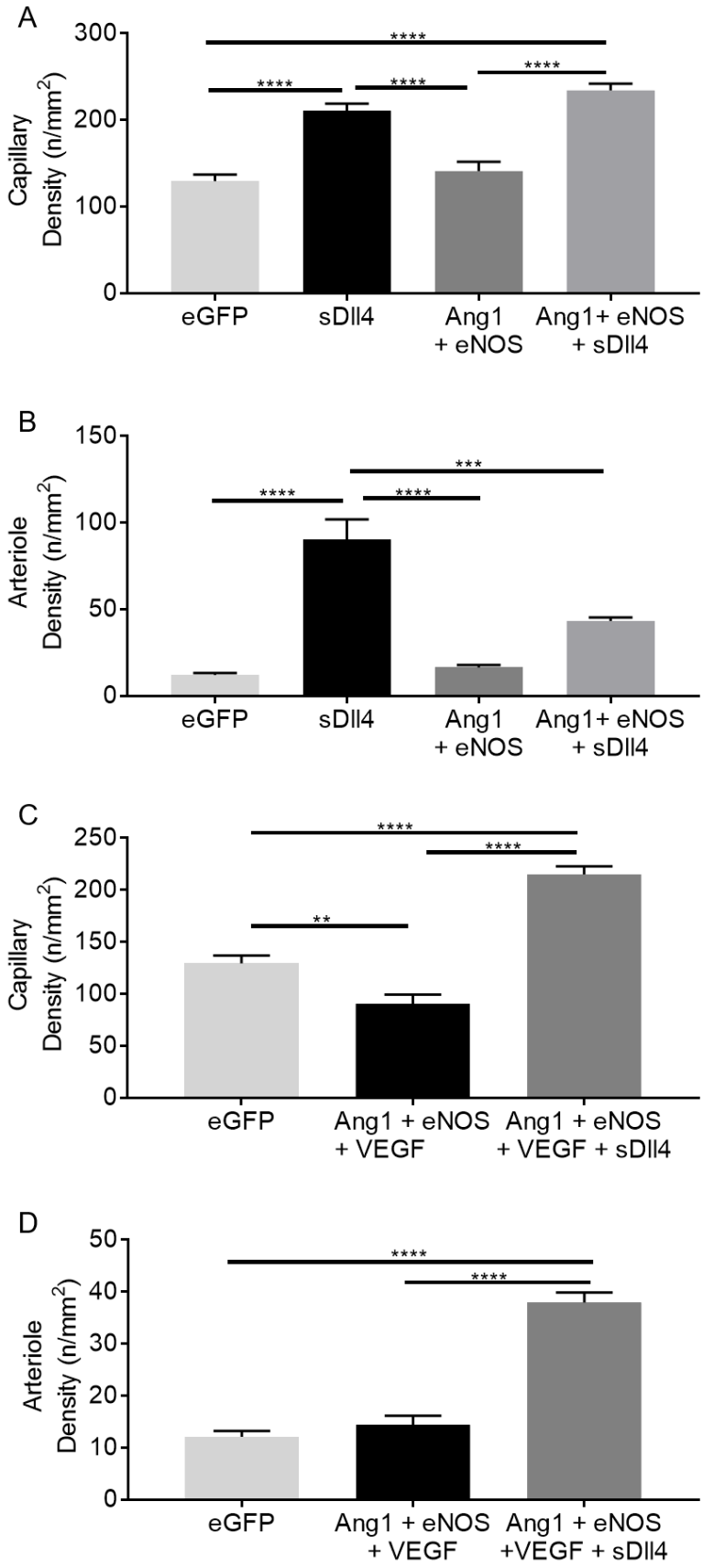

A
Capillary Density (n/mm2)
300
200
100
0
****
****
****
****
eGFP
sDll4
Ang1 + eNOS
Ang1+ eNOS + sDll4
B
Arteriole Density (n/mm2)
150
100
50
0
***
****
****
eGFP
sDll4
Ang1 + eNOS
Ang1+ eNOS + sDll4
C
Capillary Density (n/mm2)
250
200
150
100
50
0
****
****
**
eGFP
Ang1 + eNOS + VEGF
Ang1 + eNOS + VEGF + sDll4
D
Arteriole Density (n/mm2)
50
40
30
20
10
0
****
****
eGFP
Ang1 + eNOS + VEGF
Ang1 + eNOS +VEGF + sDll4

Figure 6.6 Addition of Ad.sDll4 increases both capillary and arteriolar density. *Ad.sDll4 (n=3) resulted in a significant increase in capillaries over Ad.eGFP (A, p<0.0001, n=6)) whereas Ad.Ang1 + Ad.eNOS produced a similar number (n=3). Ad.Ang1 + Ad.eNOS + Ad. sDll4 resulted in a capillary density similar to Ad.sDll4 alone. Similarly, Ad.sDll4 led to a significant rise in arterioles (B, p<0.0001) compared to Ad.eGFP. Ad.Ang1 + Ad.eNOS resulted in similar numbers of arterioles to Ad.eGFP. When Ad.sDll4 was added to this combination there was an increase but only to 43.26 ±1.99/mm^2. Ad.Ang1 + Ad.eNOS + Ad.VEGF resulted in a decrease in capillaries compared to Ad.eGFP (p=0.0035) although when Ad.sDll4 was included there was again a significant increase (C, p<0.0001). Likewise, Ad.Ang1 + Ad.eNOS + Ad.VEGF produced a similar density of arterioles to Ad.eGFP but this too increased significantly when Ad.sDll4 was included (D, p<0.0001).*

I then went on to analyse how the addition of Ad.sDll4 into the Ad.Ang1 + Ad.eNOS + Ad.VEGF combination affects the production of capillaries and arterioles (Figure 6.6C). While Ad.Ang1 + Ad.eNOS + Ad.VEGF resulted in a decrease in capillary formation compared to Ad.eGFP, addition of Ad.sDll4 resulted in a significant increase in the number of capillaries (215.1 ±7.79/mm^2, p<0.0001) compared to both groups. Similarly, Ad.Ang1 + Ad.eNOS + Ad.VEGF resulted in a similar number of arterioles as Ad.eGFP as well as Ad. Ang1 + Ad.eNOS (Figure 6.6D). when Ad.sDll4 was added in there was a significant increase in arterioles over the other two groups (37.92 ±1.95/mm^2, p<0.0001).

6.4 Discussion

6.4.1 Ad.sDll4 Does Not Enhance Blood Flow Recovery Following Ischaemic Injury

It has been previously shown that inhibiting Dll4 leads to an increase in capillaries but that they are poorly perfused (Noguera-Troise *et al.*, 2006). However, here I show that when Notch signalling is induced by Ad.sDll4 there is little difference (if slightly worse) in the recovery of blood flow after ischemic injury from Ad.eGFP. Interestingly, a similar study which used a sDll4 adenovirus that inhibited Notch signalling and injected the virus into the adductor and gracilis and digitalis flexor as opposed to the present study where only the adductor was injected reported impaired blood flow recovery (Al Haj Zen *et al.*, 2010).

The sDll4 adenovirus used by Al Haj Zen *et al* (2010) was derived from the human form of Dll4 whereas in the present study the mouse form was used. In chapter 3 I showed that there was a difference in the induction of Hey1 by the human recombinant sDll4 protein and the mouse Ad.sDll4 and I also illustrated that there are differences between the mouse and human amino acid sequence. It is therefore possible that the difference in Hey1 induction through Notch signalling could be due to a difference in amino acid sequence and thus the binding affinity of sDll4 to Notch. This may also be true of the difference between Al Haj Zen *et al* 's study and the data presented here. In addition, while both Ad.sDll4s are of a similar length they do not begin and end at the exact same amino acid which again could result in differences in

binding affinity. However, they both do contain the DSL region which is critical for Notch binding therefore suggesting that it is the differences in amino acid sequence that are likely to be more important. Furthermore, as shown in chapter 3 the Ad.sDll4 used in this study induced Hes1 expression but not Hey1 at the time point studied. It could be suggested that Ad.sDll4 only partially induces Notch signalling and this is why there is poor perfusion but increased vessel density and why the data here appears to conflict with previous data.

Al Haj Zen *et al* (2010) also used CD1 mice whereas the present study used C57Bl6 mice. It therefore may be possible that using different strains of mice could explain the lack of opposite results for inducing and inhibiting Notch signalling in this model. In addition, a study by Helisch *et al* (2006) reported that three different strains of mice led to three different blood flow recovery rates after ischemic injury further supporting this.

In addition, the extra virus injections in the gracilis and digitalis flexor used by Al Haj Zen *et al* (2010) may give a greater overall effect on Dll4/Notch signalling than just injecting into the adductor which could explain why in the present study Ad.sDll4 is similar to Ad.eGFP.

On the other hand, when Ad.sDll4 is added to Ad.Ang1 + Ad.eNOS it significantly reduces blood flow recovery compared to Ad.Ang1 + Ad.eNOS as well as being similar to Ad.sDll4 alone (Figure 6.2). This suggests that while on its own Ad.sDll4 has little effect on blood flow recovery any effects on the vasculature it has overrides the effects of Ad.Ang1 + Ad.eNOS.

Nitric oxide produced through the catalysis of L-arginine by eNOS is known to induce vasodilation through the relaxation of smooth muscle (Ignarro *et al.*, 1987; Palmer, Ashton and Moncada, 1988; Robert S. Smith *et al.*, 2002; Umbrello *et al.*, 2013) and has been shown to play a role in recovery after ischemic injury. Using eNOS knockout mice Yu *et al* (2005) reported that following ischemic injury mice showed defects in arteriogenesis, functional blood flow reserve after muscle stimulation and pericyte recruitment although this could be rescued by intramuscular injection of an eNOS adenovirus. Similar results were also seen in a rat hindlimb ischemia model where injection with an eNOS adenovirus resulted in increased blood perfusion to the hindlimb along with increased angiogenesis (Robert S. Smith *et al.*, 2002). In addition, Ang1 has also been shown to be beneficial to recovery post ischemia. Using a rabbit hindlimb ischemia model Shyu *et al* (1998) showed that gene transfer of plasmid DNA encoding Ang1 enhanced collateral vessel formation following ischemic injury. Ang1 is also known to be to recruit mural cells (Maisonpierre *et al.*, 1997; Iivanainen *et al.*, 2003; Kobayashi *et al.*, 2006) as well as having a vital role in arteriolar genesis (Benest *et al.*, 2006, 2008; Stone *et al.*, 2016). Moreover, it is thought that the growth and remodelling of arterioles is as important as the growth and sprouting of capillaries during revascularisation post-ischemia (Bailey *et al.*, 2008; Ziegler *et al.*, 2010; Silvestre, Smadja and Levy, 2013).therefore a positive impact on blood flow recovery would be expected by an Ad.Ang1 + Ad.eNOS combination as is seen here.

Interestingly, both Ang1 and eNOS have been associated with Dll4/Notch signalling. Patenaude *et al* (2014) reported that inhibition of Notch signalling was shown to result in decreased endothelial nitric oxide production whereas Zhang *et al* (2011) demonstrated that Ang1/Tie2 signalling increases basal Notch signalling by upregulating Dll4 through AKT mediated activation of β-catenin thereby increases quiescence.

Additionally, monocyte infiltration has been shown to be important in arteriogenesis through the breakdown of the extracellular matrix and the proliferation of vascular smooth muscle and endothelial cells (Ito *et al.*, 1997; Arras *et al.*, 1998; Heil *et al.*, 2002; Schaper, 2009; Silvestre, Smadja and Levy, 2013). However, the ability to create space for cells to proliferate and migrate into and to remodel and form new vessels may be compromised in the groups where Ad.sDll4 is given due to the increase in adherens junctions and decrease in permeability seen in previous chapters (3 and 4).

Despite previous studies using both rabbit and rat hindlimb ischemia models demonstrating that VEGF can increase blood flow recovery and capillary density the data presented here in Figure 6.2, Figure *6.4* and Figure *6.6* suggests that it is deleterious to the effect of Ad.Ang1 + Ad.eNOS. however, Ad.Ang1 + Ad.eNOS + Ad.VEGF does still result in an increased recovery of blood flow over Ad.eGFP (Figure 6.4) suggesting that Ad.VEGF only partially affects the effect seen by Ad.Ang1 + Ad.eNOS. moreover, Chae *et al* (2000) reported that the combination of Ang1 + eNOS resulted in enhanced blood flow,

increased capillary density and larger vessels than when given separately, further supporting this.

Curiously, at day 3 Ad.Ang1 + Ad.eNOS + Ad.VEGF + Ad.sDll4 had recovered blood flow to a similar capacity as that of Ad.Ang1 + Ad.eNOS + Ad.VEGF but by day 7 the recovery of blood flow has slowed and the difference between the two groups only widens. By day 14, Ad.Ang1 + Ad.eNOS + Ad.VEGF + Ad.sDll4 blood flow ratio has dropped below Ad.eGFP and by day 21 has decreased further to below the Ad.sDll4 only group. This suggests that while the addition of Ad.VEGF and Ad.sDll4 to Ad.Ang1 + Ad.eNOS appears to have a positive influence on hindlimb blood flow recovery initially this benefit soon becomes a hindrance to recovery. This could possibly be because the induction of Notch by Ad.sDll4 leads to the reduction in VEGFR2 and therefore a reduction in VEGF signalling. This would mean that downstream effects such as increases in shear stress and vasodilation and thus any remodelling of the vessel would also be inhibited. Furthermore when Cao *et al* (2009) gave VEGF and the γ-secretase inhibitor DAPT post ischemic injury they found that together they lead to a faster recovery in blood flow than on their own supporting the above data which suggests that the induction of Notch impedes recovery of blood flow post ischemia.

It is also possible that the addition of all the growth factors at the same time point is disrupting the endogenous recovery process and the addition of the different viruses at varying points in the recovery process would result in enhanced blood flow recovery. For example, Ad.sDll4 is

the only group where the blood flow ratio at day 21 is the highest suggesting that if the study were extended the recovery may continue whereas those groups containing Ad.Ang1 + Ad.eNOS all peak at day 14. It may therefore be more effective to introduce Ad.sDll4 at a later timepoint.

Moreover, the studies undertaken here injected all the adenoviruses at the same concentration despite evidence that Ang1, VEGF and Dll4 can all exert their effects dose dependently (S Takeshita *et al.*, 1994; Koblizek *et al.*, 1998; Papapetropoulos *et al.*, 1999; Duarte *et al.*, 2004). While equal concentrations may be useful to gain an understanding of how the different growth factors interact, it may be more beneficial going forward to understand the relative endogenous concentrations of each at varying points throughout angiogenesis and arteriolargenesis enabling the creation of a more endogenous-like post-ischemic blood flow recovery plan.

6.4.2 Ad.sDll4 Increases Capillary and Arteriolar Density in the Ischaemic Adductor Muscle

Unexpectedly it was found that despite hindering blood flow recovery Ad.sDll4 increased both capillary and arteriolar density and this was also the case when it was added into both the Ad.Ang1 + Ad.eNOS and Ad.Ang1 + Ad.eNOS + Ad.VEGF groups. In addition, Ad.Ang1 + Ad.eNOS which had the best blood flow recovery of all the groups resulted in capillary and arteriolar densities similar to Ad.eGFP. This suggests that it may not be the number of vessels that is important but the functionality of these vessels. Likewise, a study using $Dll4^{+/-}$ mice

found that despite an increase in collateral vessel formation after ischemic injury there was not an increase in blood flow leading them to also conclude that it is the quality of the vessel not the quantity that matters (Cristofaro *et al.*, 2013).

The induction of Notch signalling has been shown to lead to quiescence in the vessel (Ehling *et al.*, 2013; Zhang *et al.*, 2014) although it is upregulated in the proliferating stalk cell during sprouting angiogenesis indicating its regulation over this process (Jin *et al.*, 2010; Ribatti and Crivellato, 2012; Zhang *et al.*, 2014). In chapter 3 I demonstrated that Notch signalling increases VE-Cadherin expression at the junctions and so may interfere with proliferation and migration during any vessel growth or remodelling. Similarly, it may be possible that the tissue is trying to recover the supply of blood to the now ischemic area but due to the tighter junctions the existing vessels cannot enlarge to compensate for the extra blood flow that is being redirected there. Instead the vasculature could possibly be forced to form a network of smaller vessels, explaining the increase in capillaries and arterioles seen. Conversely, Ad.Ang1 + Ad.eNOS mice would have the ability to enlarge and remodel as seen by Stone *et al* (2016) to allow the vessels to cope with an increase in flow.

6.5 Concluding Remarks

Despite producing a significant increase in both capillary and arteriolar density, injection with Ad.sDll4 following ischemic injury did not aid blood flow recovery. In contrast, mice given Ad.Ang1 + Ad.eNOS did have improved blood flow recovery yet with similar numbers of capillaries and arterioles to Ad.eGFP indicating that it is the functionality of these vessels that it important and not the quantity. Thus, sDLL4 appears to be able to induce arteriolargenesis and angiogenesis in hindlimb ischemia, but is not sufficient to improve functional blood flow to the hind paw.

Chapter 7: Discussion

This study aimed to determine the role that Dll4 plays in the regulation of physiological neovascularisation with emphasis on its control of endothelial barrier integrity. This was investigated using a combination of recombinant protein and adenovirus versions of the extracellular portion of Dll4 (sDll4) in both *in vitro* and *in vivo* experiments the results of which are described and discussed in detail in chapters 3-7. Here, I will briefly discuss the data and its limitations, future research directions and the implications of this work to the field.

7.1 Summary of Findings and Future Work

7.1.1 Dll4 Induces VE-Cadherin Expression

The endothelial junctional proteins which form tight, adherens and gap junctions are essential in maintaining the endothelial barrier integrity while also allowing intercellular signalling and therefore it is important to understand the processes and molecules involved in their regulation. In this thesis, I demonstrated a direct link between the induction of Notch signalling by Dll4 and increased VE-Cadherin expression at the endothelial cell-cell contacts. While this link has been previously alluded to through reports that have shown that VE-Cadherin is expressed on the anterior plasma membrane and filopodia (Almagro *et al.*, 2010) in tip cells in addition to the suggestion that the continual flux in Notch levels in endothelial cells competing to be the leading tip cell in the sprout results in differential VE-Cadherin turnover (Jakobsson *et al.*, 2010;

Bentley *et al.*, 2014), until now this has not been investigated directly. In addition, data showing increased sprouting in established capillary-like 3D tubules following partial blocking of VE-Cadherin (Abraham *et al.*, 2009) and compromised vascular integrity and tubulogenesis on top of increased sprouting in zebrafish embryos which had a partial VE-Cadherin knockdown (Montero-Balaguer *et al.*, 2009) further support the data presented here. Although I have shown clear evidence that Dll4 plays a role in adherens junctions regulation and thus the regulation of endothelial barrier integrity, it is important to take into consideration that this is *in vitro* data only and further studies using *in vivo* models are needed to ensure that this signalling pathway also occurs in a more physiologically relevant setting as well.

7.1.2 Dll4/Notch Signalling Regulates Vascular Permeability

One of the major functions of the vascular wall is the regulation of fluid and solute exchange between the blood and tissues. As one of the main transport routes across the vascular wall is regulated by intercellular junctions and I had already established that Dll4 plays a role in the regulation of adherens junctions I wanted to investigate if Dll4 also played a role in regulating permeability. Using the Landis-Michel technique I demonstrated the ability of Dll4 signalling through Notch to control the permeability of intact naive microvessels. I then went on to show that this was through a cAMP/PKA dependent pathway.

While there is limited published data linking Dll4 to permeability control these findings do confer support to the view that Dll4/Notch signalling is

a marker of quiescence (Scehnet *et al.*, 2007; Dou *et al.*, 2008; Ehling *et al.*, 2013). In Addition, the induction of cAMP results in arterial calibre endothelial cells which is a known fate of Dll4 expressing cells and was thought to occur through PI3K activation by cAMP and subsequent simultaneous activation of β-catenin and Notch (Shutter *et al.*, 2000; Liu *et al.*, 2003; Yurugi-Kobayashi *et al.*, 2006; Diez *et al.*, 2007). β-catenin itself is involved in the formation of adherens junctions and has been linked to Dll4 signalling via Wnt/β-catenin signalling (Corada *et al.*, 2010). Moreover, PKA was shown to regulate barrier function through Rac1 whereas inhibition of Rac1 resulted in reduced VE-Cadherin expression (Waschke, Drenckhahn, Adamson and Curry, 2004; Waschke, Drenckhahn, Adamson, Barth, *et al.*, 2004) overall consistent with the findings presented here.

However, it is important to take into consideration that the VE-Cadherin expression was only tested *in vitro* and so it cannot be known for certain that Dll4's effects on permeability are a result of increased adherens junctions especially when Adamson *et al* (1998) reported that cAMP resulted in increased tight junctions. In addition, the permeability experiments were undertaken on post-capillary venules. It is therefore possible that the results may vary between continuous and fenestrated vessels as it did for Ang1 (Salmon *et al.*, 2009) as well as in the larger arteries and venules and between tissues. Furthermore, in this study I only tested the permeability to water which only covers part of the barriers function. The effects of Dll4 on the permeability to solutes such

as albumin is yet to be determined and is necessary to obtain a more complete view of the control of vascular integrity.

In order to address these new questions several directions of further study are required. This would include electron microscopy visualisation of vessels following permeability experiments to determine ultrastructural changes such as increased or decreased junctions and investigating the effect of Dll4 on permeability in fenestrated endothelial. Modifications to the Landis-Michel technique such as larger micropipettes, double cannulation or ex vivo experiments may enable the measurement of permeability in larger vessels and the use of fluorescently labelled albumin has been used previously for determination of permeability to solutes (Betteridge *et al.*, 2015) .

7.1.3 Addition of Ad.sDll4 During Arteriolargenesis Leads to a More Endogenous-like Vasculature

The consequences of disrupting Dll4/Notch signalling during angiogenesis have been well documented in a variety of models including genetic or chemical inhibition in the retina (Hellstrom *et al.*, 2007; Suchting *et al.*, 2007), murine Matrigel plugs and endothelial cell spheroids (Scehnet *et al.*, 2007) and monolayers (Williams *et al.*, 2006). In this thesis, I used the rat mesenteric angiogenesis assay and an adenovirus encoding the extracellular domain of Dll4 to induce Notch signalling. This resulted in a reduced angiogenic response in line with previously published data confirming that this was a relevant model to investigate Dll4/Notch signalling.

The formation of a functional vascular network which includes the full hierarchy of vessels from arteries and veins to capillaries and arterioles is vital for homeostasis. Increasing evidence for a role in vascular stabilisation and maturation for Dll4 (Shutter *et al.*, 2000; Liu *et al.*, 2003; Lobov *et al.*, 2011; Cristofaro *et al.*, 2013) in addition to a recent report that Dll4 interacts with Notch3 on pericytes (Schulz *et al.*, 2015) led me to investigate the hypothesis that Dll4/Notch signalling is involved in arteriolargenesis. Previously Benest *et al* (2006, 2008) and Stone *et al* (2008) have shown that Ang1, eNOS and VEGF are all involved in the formation of arterioles with Ang1s stabilisation and mural cell recruitment capabilities, the increase in flow and enlargement of the vessel due to eNOS and which are all enhanced when VEGF was also included. The addition of Ad.sDll4 into Ang1 + eNOS or Ang1 + eNOS + VEGF adenovirus combinations reduced the pro-angiogenic response previously seen by eNOS and VEGF (Benest *et al.*, 2006, 2008; Stone *et al.*, 2016) and led to a more endogenous-like vasculature when all four adenoviruses were given together. This is consistent with the literature which indicates that Dll4/Notch signalling favours quiescence (Hodkinson *et al.*, 2007; Scehnet *et al.*, 2007; Dou *et al.*, 2008) in addition to the logic that two pro-angiogenic signals and two anti-angiogenic signals would balance each other out.

However, it is important to note that while Benest *et al* (2006, 2008) and Stone *et al* (2016) demonstrated the value of Ang1 and eNOS to VSMC recruitment in this study I was unable to measure this (see chapter 5). Thus, the involvement of Dll4 in arteriolargenesis may only be indirectly

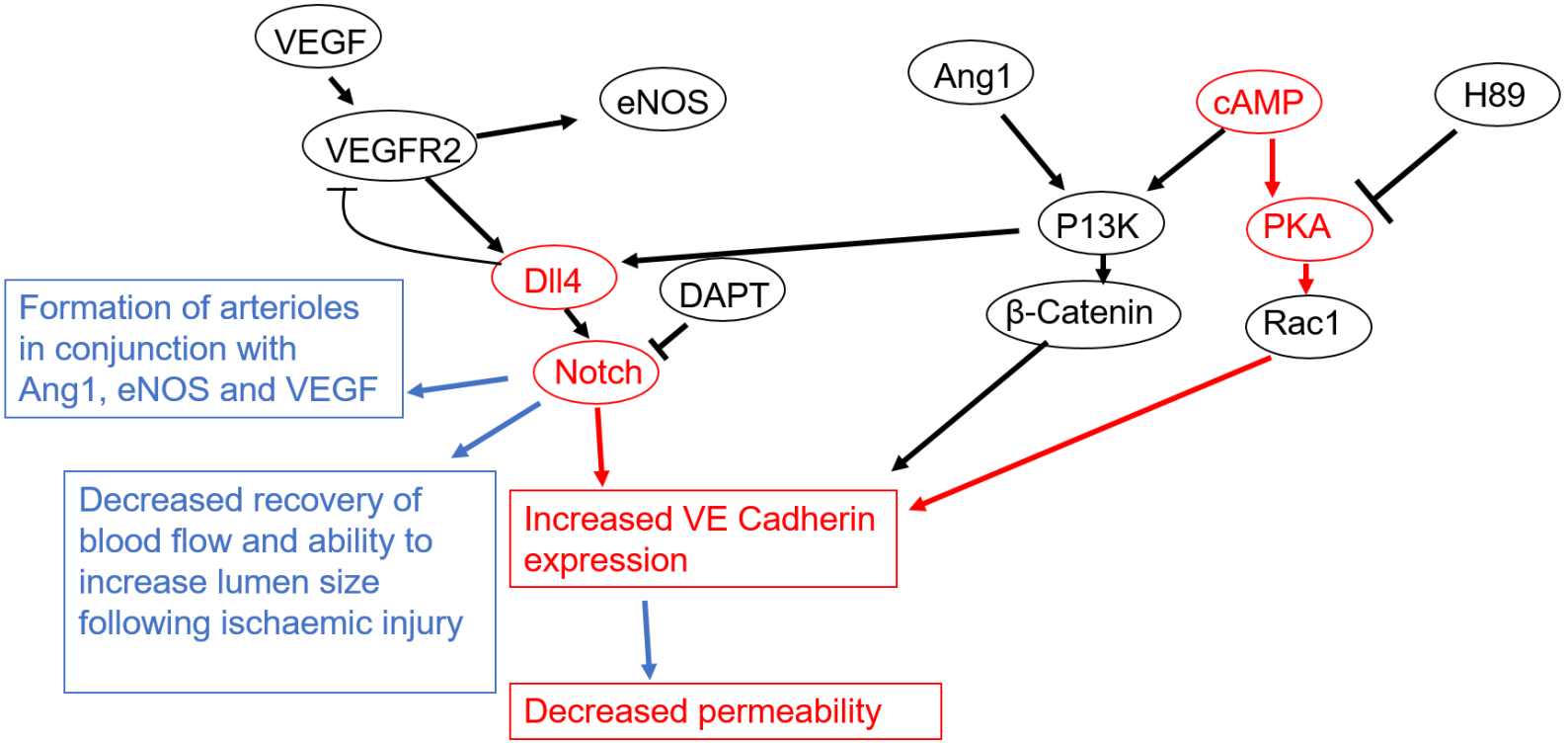


Figure 7.1 Summary Diagram of how the work done in this thesis adds to our knowledge. *Areas highlighted in red indicated mechanisms and results that were explored in this thesis. Parts highlighted in blue are areas that were explored but need significant further research.*

inferred and it is therefore vital that any future studies begin by investigating the effect of Dll4 on mural cell recruitment. Additionally, it would be of interest to combine this model with the Landis-Michel technique to enable the measurement of permeability coefficients in induced vessels using various combinations of adenoviruses along with recording their responses to permeability changing agents such as VEGF and Dll4. This would allow a greater insight into vessel physiology with potential future therapeutic outcomes.

7.1.4 Following Ischaemic Injury Dll4/Notch Signalling Enables Collateral Vessel Growth but Hinders Blood Flow Recovery

Peripheral arterial disease (PAD) is one of the major contributors to cardiovascular disease, the biggest killer worldwide (Bhatnagar *et al.*, 2015). In some instances, the blockage of the vessel occurs slowly, over time and so the blood can be successfully rerouted using a collateral network. Subsequently, there has been much research using the mouse hindlimb ischaemia model with the aim of developing a treatment plan whereby a patient's own vasculature is stimulated to grow thereby alleviating the need for surgery.

The apparent switch observed in chapter 5 from growth by sprouting to growth by intussusception, which is thought to be indicative of remodelling, suggested that Dll4 may play a part in the growth and remodelling of a collateral vascular network post-ischaemic injury.

However when Ad.sDll4 was given either alone or together with Ad.Ang1 + Ad.eNOS ± Ad.VEGF it was shown to hinder blood flow recovery in the hind paw. On the other hand, examination of the adductor tissue following the 21 day time course revealed that despite impairing blood flow recovery the addition of Ad.sDll4 led to a dramatic increase in both capillary and arteriolar density.

While inhibition of Dll4 resulting in poorly perfused vessels (Noguera-Troise *et al.*, 2006) would appear to contradict the data presented here, other reports using the same model as this study demonstrated that inhibition of Dll4/Notch signalling resulted in better blood flow recovery (Cao *et al.*, 2009). In addition Cristofaro *et al* (2013) put forward the theory that it is not necessarily the density of vessels that is important but the functionality of the vessels which is probably the case here. Moreover, the permeability and intracellular junction findings provide further support for this as the increase in VE-Cadherin and decrease in permeability may likely inhibit the enlargement of the vessels and so more, smaller vessels are formed to compensate for this.

However, it is important to take into consideration that the blood flow was measured in the hind paw whereas the vessels were analysed in the adductor muscle where the adenoviruses were injected. While changes in and around this muscle will invariably have an effect of the downstream flow of blood to the paw the distance between the two could possibly mean there is a lag between the vascular changes in the muscle and an increase in blood flow in the hind paw. Measuring the blood flow of the muscle, changing where the adenoviruses are injected

or extending the length of the experiment could possibly account for this. Furthermore, all the adenoviruses were given at the same time and concentration despite reports that Ang1, VEGF and Dll4 work in dose dependant manners (Satoshi Takeshita *et al.*, 1994; Koblizek *et al.*, 1998; Papapetropoulos *et al.*, 1999; Duarte *et al.*, 2004). While this gives an understanding of how they all interact future studies may gain greater insight by first understanding the relative concentrations of each growth factor throughout the angiogenic and arteriolargenic processes.

7.2 Implications

This thesis was the first study to directly demonstrate the link between Dll4 and VE-Cadherin expression and subsequently the role that Dll4 plays in the regulation of vascular permeability along with providing an insight into the mechanism by which it exerts this control. The data from this study has enabled a greater understanding of the vascular barrier but has also highlighted the vast amount of information that still needs to be uncovered and understood. Thus, the findings presented here will undoubtedly open several new research directions which may possibly include delving further into the signalling pathway between Dll4/Notch and the decrease in permeability as well as its control over solute permeability, interactions with other permeability mediating agents such as VEGF, Ang1 and the glycocalyx and eventually even its use as a therapeutic where pathologically high permeability is an issue.

In addition, this thesis has helped add to the understanding of arteriolargenesis during both physiological and pathological vessel

growth. While further research into areas such as the effect of Dll4 on mural cell recruitment and the effects of differing concentrations of growth factors and time courses are clear directions to take, there are also possible future therapeutic implications as well. For example, the data presented here suggests that there is a real possibility that a treatment strategy that would stimulate revascularisation using a patient's own vasculature can be developed and so would alleviate the need for invasive surgery. Furthermore, by taking stock of the permeability and arteriolargenesis data and using similar methodology, future researchers may be able to identify the underlying dysfunctions in various similar vessel pathologies, such as those seen in cancer, CVD and age related macular degeneration, thereby enabling the development of a more targeted therapeutic regimen.

7.3 Concluding Remarks

The formation of an intact, functional vasculature that can respond to various stimuli appropriately is critical for maintaining homeostasis. One of the main functions of the vessel is to provide a barrier and regulate the exchange of fluid and solutes between the blood and tissues and disruption to this can lead to oedema, proteinuria and dangerous drop in blood pressure. All common symptoms in a variety of pathologies including CVD and cancer.

The Dll4/Notch signalling pathway was once primarily known for its role in tip and stalk cell selection during sprouting angiogenesis however it is becoming clearer that it has much larger and diverse roles

encompassing many aspects of blood vessel physiology, some of which I have explored in this thesis. I demonstrated that Dll4 can regulate vascular permeability through a pathway which involved cAMP/PKA and VE-Cadherin expression bringing a better understanding of the effecters of Dll4/Notch signalling and vascular integrity as a whole. I also showed that Dll4/Notch signalling is involved in the formation of arterioles in both a physiological setting and post-ischaemic injury. While further studies are needed to elucidate Dll4s complete role during this process we are another step closer towards the development of therapeutic revascularisation strategies.

References

Abraham, S. *et al.* (2009) *VE-Cadherin-Mediated Cell-Cell Interaction Suppresses Sprouting via Signaling to MLC2 Phosphorylation*. doi: 10.1016/j.cub.2009.02.057.

Adamson, R. H. (1990) 'Permeability of frog mesenteric capillaries after partial pronase digestion of the endothelial glycocalyx.', *The Journal of Physiology*, 428(1), pp. 1–13. doi: 10.1113/jphysiol.1990.sp018197.

Adamson, R. H. *et al.* (1998) 'Microvascular permeability and number of tight junctions are modulated by cAMP', *American Journal of Physiology-Heart and Circulatory Physiology*, 274(6), pp. H1885–H1894.

Adamson, R. H. *et al.* (2004) 'Oncotic pressures opposing filtration across non-fenestrated rat microvessels', *The Journal of physiology*, 557(3), pp. 889–907.

Adamson, R. H. *et al.* (2013) 'Microvascular permeability to water is independent of shear stress, but dependent on flow direction.', *American journal of physiology. Heart and circulatory physiology*, 304(8), pp. H1077-84. doi: 10.1152/ajpheart.00956.2012.

Adamson, R. H., Lenz, J. F. and Curry, F. E. (1994) 'Quantitative laser scanning confocal microscopy on single capillaries: permeability measurement.', *Microcirculation (New York, N.Y. : 1994)*, 1(4), pp. 251–65. doi: 10.3109/10739689409146752.

Adamson, R. H. and Michel, C. C. (1993) ‘Pathways through the intercellular clefts of frog mesenteric capillaries’, *J Physiol*, 466(1), pp. 303–327. doi: 10.1113/jphysiol.1993.sp019722.

Aird, W. C. (2007) ‘Phenotypic Heterogeneity of the Endothelium’, *Circulation Research*, 100(2), pp. 158–173. doi: 10.1161/01.RES.0000255691.76142.4a.

Alheid, U., Frölich, J. C. and Förstermann, U. (1987) ‘Endothelium-derived relaxing factor from cultured human endothelial cells inhibits aggregation of human platelets.’, *Thrombosis research*, 47(5), pp. 561–71. doi: 10.1016/0049-3848(87)90361-6.

Almagro, S. *et al.* (2010) ‘The motor protein myosin-X transports VE-cadherin along filopodia to allow the formation of early endothelial cell-cell contacts.’, *Molecular and cellular biology*. American Society for Microbiology, 30(7), pp. 1703–1717. doi: 10.1128/MCB.01226-09.

Alphonsus, C. S. and Rodseth, R. N. (2014) ‘The endothelial glycocalyx: A review of the vascular barrier’, *Anaesthesia*, 69(7), pp. 777–784. doi: 10.1111/anae.12661.

Andersson, E. R., Sandberg, R. and Lendahl, U. (2011) ‘Notch signaling: simplicity in design, versatility in function’, *Development*, 138(17). Available at: http://dev.biologists.org/content/138/17/3593.short (Accessed: 25 April 2017).

Antonetti, D. A. *et al.* (1998) ‘Vascular Permeability in Experimental Diabetes Is Associated With Reduced Endothelial Occludin Content’,

Diabetes, 47(14), pp. 1953–1960.

Antonetti, D. A. *et al.* (1999) ‘Vascular Endothelial Growth Factor Induces Rapid Phosphorylation of Tight Junction Proteins Occludin and Zonula Occluden 1: A POTENTIAL MECHANISM FOR VASCULAR PERMEABILITY IN DIABETIC RETINOPATHY AND TUMORS’, *Journal of Biological Chemistry*. American Society for Biochemistry and Molecular Biology, 274(33), pp. 23463–23467. doi: 10.1074/jbc.274.33.23463.

Arras, M. *et al.* (1998) ‘Monocyte activation in angiogenesis and collateral growth in the rabbit hindlimb’, *Journal of Clinical Investigation*. American Society for Clinical Investigation, 101(1), pp. 40–50. doi: 10.1172/JCI119877.

Ashton, N. (1966) ‘Oxygen and the Growth and Development of Retinal Vessels’, *American Journal of Ophthalmology*, 62(3), pp. 412–435. doi: 10.1016/0002-9394(66)91322-5.

Aslam, M. *et al.* (2014) ‘cAMP controls the restoration of endothelial barrier function after thrombin-induced hyperpermeability via Rac1 activation.’, *Physiological reports*, 2(10), p. e12175. doi: 10.14814/phy2.12175.

Avery, R. L. *et al.* (2006) ‘Intravitreal bevacizumab (Avastin) for neovascular age-related macular degeneration’, *Ophthalmology*, 113(3), p. 363–372.e5. doi: 10.1016/j.ophtha.2005.11.019.

Azzi, S., Hebda, J. K. and Gavard, J. (2013) ‘Vascular permeability and drug delivery in cancers.’, *Frontiers in oncology*, 3, p. 211. doi:

10.3389/fonc.2013.00211.

Babaei, S. *et al.* (2003) ‘Angiogenic actions of angiopoietin-1 require endothelium-derived nitric oxide’, *The American journal of pathology*, 162(6), pp. 1927–1936. doi: 10.1016/S0002-9440(10)64326-X.

Baeten, J. T. and Lilly, B. (2017) ‘Notch Signaling in Vascular Smooth Muscle Cells’, *Vascular Pharmacology*, 78, pp. 351–382. doi: 10.1016/bs.apha.2016.07.002.

Bailey, A. M. *et al.* (2008) ‘Arteriolar remodeling following ischemic injury extends from capillary to large arteriole in the microcirculation.’, *Microcirculation (New York, N.Y. : 1994)*, 15(5), pp. 389–404. doi: 10.1080/10739680701708436.

Balda, M. S. and Matter, K. (2016) ‘Tight junctions as regulators of tissue remodelling’, *Current Opinion in Cell Biology*, 42, pp. 94–101. doi: 10.1016/j.ceb.2016.05.006.

Baldi, A. *et al.* (2004) ‘Characterization of tissue specific expression of Notch-1 in human tissues.’, *Biology of the cell / under the auspices of the European Cell Biology Organization*. Blackwell Publishing Ltd, 96(4), pp. 303–11. doi: 10.1016/j.biolcel.2004.01.005.

Bates, D. O. and Curry, F. E. (1996) ‘Vascular endothelial growth factor increases hydraulic conductivity of isolated perfused microvessels’, *American Journal of Physiology-Heart and Circulatory Physiology*, 271(6), pp. H2520–H2528.

Bates, D. O. and Curry, F. E. (1997) ‘Vascular endothelial growth factor increases microvascular permeability via a Ca (2+)-dependent

pathway', *American Journal of Physiology-Heart and Circulatory Physiology*, 273(2), pp. H687–H694.

Becam, I. *et al.* (2010) 'A Role of Receptor Notch in Ligand cis-Inhibition in Drosophila', *Current Biology*, 20(6), pp. 554–560. doi: 10.1016/j.cub.2010.01.058.

Becker, B. F., Chappell, D. and Jacob, M. (2010) 'Endothelial glycocalyx and coronary vascular permeability: The fringe benefit', *Basic Research in Cardiology*. Springer-Verlag, 105(6), pp. 687–701. doi: 10.1007/s00395-010-0118-z.

Beckers, J. *et al.* (1999) 'Expression of the mouse Delta1 gene during organogenesis and fetal development', *Mechanisms of Development*, 84(1–2), pp. 165–168. doi: 10.1016/S0925-4773(99)00065-9.

Behzadian, M. A. *et al.* (2003) 'VEGF-induced paracellular permeability in cultured endothelial cells involves urokinase and its receptor.', *The FASEB journal : official publication of the Federation of American Societies for Experimental Biology*. Federation of American Societies for Experimental Biology, 17(6), pp. 752–754. doi: 10.1096/fj.02-0484fje.

Belch, J. *et al.* (2011) 'Effect of fibroblast growth factor NV1FGF on amputation and death: A randomised placebo-controlled trial of gene therapy in critical limb ischaemia', *The Lancet*, 377(9781), pp. 1929–1937. doi: 10.1016/S0140-6736(11)60394-2.

Bell, R. D. *et al.* (2010) 'Pericytes Control Key Neurovascular Functions and Neuronal Phenotype in the Adult Brain and during Brain Aging',

Neuron. Elsevier, 68(3), pp. 409–427. doi: 10.1016/j.neuron.2010.09.043.

Benedito, R. *et al.* (2008) 'Loss of Notch signalling induced by Dll4 causes arterial calibre reduction by increasing endothelial cell response to angiogenic stimuli', *BMC developmental biology*, 8(1), p. 117.

Benedito, R. *et al.* (2009) 'The Notch Ligands Dll4 and Jagged1 Have Opposing Effects on Angiogenesis', *Cell*, 137(6), pp. 1124–1135. doi: 10.1016/j.cell.2009.03.025.

Benedito, R. *et al.* (2012) 'Notch-dependent VEGFR3 upregulation allows angiogenesis without VEGF–VEGFR2 signalling', *Nature*. Nature Research, 484(7392), pp. 110–114. doi: 10.1038/nature10908.

Benest, A. V *et al.* (2006) 'VEGF and angiopoietin-1 stimulate different angiogenic phenotypes that combine to enhance functional neovascularization in adult tissue', *Microcirculation*, 13(6), pp. 423–437. doi: 10.1080/10739680600775940.

Benest, A. V *et al.* (2008) 'Arteriolar genesis and angiogenesis induced by endothelial nitric oxide synthase overexpression results in a mature vasculature', *Arterioscler Thromb Vasc Biol*, 28(8), pp. 1462–1468. doi: 10.1161/ATVBAHA.108.169375.

Benjamin, L. E., Hemo, I. and Keshet, E. (1998) 'A plasticity window for blood vessel remodelling is defined by pericyte coverage of the preformed endothelial network and is regulated by PDGF-B and VEGF.', *Development (Cambridge, England)*, 125(9), pp. 1591–1598.

Benjamini, Y. and Hochberg, Y. (1995) 'Controlling the False Discovery

Rate: A Practical and Powerful Approach to Multiple Controlling the False Discovery Rate: a Practical and Powerful Approach to Multiple Testing', *Journal of the Royal Statistical Society*, 57(1), pp. 289–300. doi: 10.2307/2346101.

Benjamini, Y. and Yekutieli, D. (2001) 'The control of the false discovery rate in multiple testing under dependency', *Annals of Statistics*, 29(4), pp. 1165–1188. doi: 10.1214/aos/1013699998.

Bentley, K. *et al.* (2014) 'The role of differential VE-cadherin dynamics in cell rearrangement during angiogenesis', *Nature cell biology*, 16(4), pp. 309–321. doi: 10.1038/ncb2926.

Bernier-Latmani, J. *et al.* (2015) 'DLL4 promotes continuous adult intestinal lacteal regeneration and dietary fat transport', *Journal of Clinical Investigation*. American Society for Clinical Investigation, 125(12), pp. 4572–4586. doi: 10.1172/JCI82045.

Betteridge, K. *et al.* (2015) 'Simultaneous Determination of Microvascular Endothelial Glycocalyx Structure and Albumin Flux in vivo', *FASEB Journal*, 29(1 supplement), p. LB552.

Bhatnagar, P. *et al.* (2015) 'The epidemiology of cardiovascular disease in the UK 2014.', *Heart (British Cardiac Society)*, p. heartjnl-2015-307516-. doi: 10.1136/heartjnl-2015-307516.

Bolton, S. J., Anthony, D. C. and Perry, V. H. (1998) 'Loss of the tight junction proteins occludin and zonula occludens-1 from cerebral vascular endothelium during neutrophil-induced blood-brain barrier breakdown in vivo', *Neuroscience*, 86(4), pp. 1245–1257. doi:

10.1016/S0306-4522(98)00058-X.

Bouloumié, A. (1999) ‘Vascular endothelial growth factor up-regulates nitric oxide synthase expression in endothelial cells’, *Cardiovascular Research*. Oxford University Press, 41(3), pp. 773–780. doi: 10.1016/s0008-6363(98)00228-4.

Braet, F. and Wisse, E. (2002) ‘Structural and functional aspects of liver sinusoidal endothelial cell fenestrae: a review’, *Comparative hepatology*. BioMed Central, 1(1), p. 1. doi: 10.1186/1476-5926-1-1.

Brzozowa, M. *et al.* (2013) ‘The Notch ligand Delta-like 4 (DLL4) as a target in angiogenesis-based cancer therapy?’, *Contemporary Oncology/Wspolczesna Onkologia*, 17(3).

Busse, R., Lackhoff, A. and Bassenge, E. (1987) ‘Endothelium-derived relaxant factor inhibits platelet activation’, *Naunyn-Schmiedeberg’s Archives of Pharmacology*. Springer-Verlag, 336(5), pp. 566–571. doi: 10.1007/BF00169315.

Cao, L. *et al.* (2009) ‘Promoting angiogenesis via manipulation of VEGF responsiveness with notch signaling’, *Biomaterials*, 30(25), pp. 4085–4093. doi: 10.1016/j.biomaterials.2009.04.051.

Cao, Y. *et al.* (2007) ‘Systemic overexpression of angiopoietin-2 promotes tumor microvessel regression and inhibits angiogenesis and tumor growth’, *Cancer Research*, 67(8), pp. 3835–3844. doi: 10.1158/0008-5472.CAN-06-4056.

Carmeliet, P. *et al.* (1996) ‘Abnormal blood vessel development and lethality in embryos lacking a single VEGF allele’, *Nature*, 380(6573),

pp. 435–439. doi: 10.1038/380435a0.

Carmeliet, P. (2003) ‘Angiogenesis in health and disease’, *Nat Med*, 9(6), pp. 653–660. doi: 10.1038/nm0603-653.

Carmeliet, P. *et al.* (2009) ‘Branching morphogenesis and antiangiogenesis candidates: tip cells lead the way.’, *Nature reviews. Clinical oncology*, 6(6), pp. 315–26. doi: 10.1038/nrclinonc.2009.64.

Carmeliet, P. and Jain, R. . (2011) ‘Molecular mechanisms and clinical applications of angiogenesis.’, *Nature*, 473(7347), pp. 298–307. doi: 10.1038/nature10144.

Celis, J. F. de and Bray, S. J. (2000) ‘The Abruptex domain of Notch regulates negative interactions between Notch, its ligands and Fringe.’, *d*, 127(6), pp. 1291–302.

Chae, J. K. *et al.* (2000) ‘Coadministration of angiopoietin-1 and vascular endothelial growth factor enhances collateral vascularization.’, *Arteriosclerosis, thrombosis, and vascular biology*, 20(12), pp. 2573–2578. doi: 10.1161/01.ATV.20.12.2573.

Chambers, R. and Zweifach, B. W. (1947) ‘Intercellular cement and capillary permeability’, *Physiol Rev*, 27(3), pp. 436–463. Available at: http://physrev.physiology.org/content/27/3/436.short (Accessed: 2 March 2017).

Chappell, J. C. *et al.* (2009) ‘Local Guidance of Emerging Vessel Sprouts Requires Soluble Flt-1’, *Developmental Cell*, 17(3), pp. 377–386. doi: 10.1016/j.devcel.2009.07.011.

Christensen, A. E. *et al.* (2003) ‘cAMP analog mapping of Epac1 and

cAMP kinase: Discriminating analogs demonstrate that Epac and cAMP kinase act synergistically to promote PC-12 cell neurite extension', *Journal of Biological Chemistry*. American Society for Biochemistry and Molecular Biology, 278(37), pp. 35394–35402. doi: 10.1074/jbc.M302179200.

Claxton, S. and Fruttiger, M. (2004) 'Periodic Delta-like 4 expression in developing retinal arteries', *Gene Expression Patterns*, 5(1), pp. 123–127. doi: 10.1016/j.modgep.2004.05.004.

Clough, G. and Michel, C. C. (1979) 'The effect of albumin on the labelling of endothelial cell vesicles with ferritin in the frog [proceedings].', *The Journal of physiology*, 289, p. 72P–73P. Available at: http://www.ncbi.nlm.nih.gov/pubmed/458712 (Accessed: 2 March 2017).

Comerford, K. M. *et al.* (2002) 'Role of vasodilator-stimulated phosphoprotein in PKA-induced changes in endothelial junctional permeability.', *The FASEB journal : official publication of the Federation of American Societies for Experimental Biology*. Federation of American Societies for Experimental Biology, 16(6), pp. 583–585. doi: 10.1096/fj.01-0739fje.

Cooper, J. A. *et al.* (1987) 'Measurement of albumin permeability across endothelial monolayers in vitro.', *Journal of applied physiology (Bethesda, Md. : 1985)*, 62(3), pp. 1076–1083.

Corada, M. *et al.* (2010) 'The Wnt/β-catenin pathway modulates vascular remodeling and specification by upregulating Dll4/notch

signaling', *Developmental Cell*, 18(6), pp. 938–949. doi: 10.1016/j.devcel.2010.05.006.

Cordle, J., Johnson, S., *et al.* (2008) 'A conserved face of the Jagged/Serrate DSL domain is involved in Notch trans-activation and cis-inhibition.', *Nature structural & molecular biology*. Nature Publishing Group, 15(8), pp. 849–57. doi: 10.1038/nsmb.1457.

Cordle, J., Redfield, C., *et al.* (2008) 'Localization of the delta-like-1-binding site in human Notch-1 and its modulation by calcium affinity', *Journal of Biological Chemistry*. American Society for Biochemistry and Molecular Biology, 283(17), pp. 11785–11793. doi: 10.1074/jbc.M708424200.

Cristofaro, B. *et al.* (2013) 'Dll4-Notch signaling determines the formation of native arterial collateral networks and arterial function in mouse ischemia models', *Development*, 140(8), pp. 1720–1729. doi: 10.1242/dev.092304.

Curry, F. E. (1974) 'A Hydrodynamic Description Application Transcapillary of the Osmotic Reflection to the Pore Theory of Exchange', *Microvascular Research*, 252, pp. 236–252.

Curry, F. E. (1984) 'Mechanics and thermodynamics of transcapillary exchange', *Handbook of Physiology. The Cardiovascular System. Microcirculation*, 4(pt 1), pp. 309–374.

Curry, F. E., Huxley, V. H. and Adamson, R. H. (1983) 'Permeability of single capillaries to intermediate-sized colored solutes.', *The American journal of physiology*. American Physiological Society, 245(3), pp.

H495-505. Available at: http://www.ncbi.nlm.nih.gov/pubmed/6604463 (Accessed: 3 March 2017).

Curry, F. E. and Michel, C. C. (1980) ‘A fiber matrix model of capillary permeability’, *Microvascular research*. Academic Press Inc., 20(1), pp. 96–99. doi: 10.1016/0026-2862(80)90024-2.

D’Souza, B., Meloty-Kapella, L. and Weinmaster, G. (2010) *Canonical and non-canonical notch ligands*, *Current Topics in Developmental Biology*. doi: 10.1016/S0070-2153(10)92003-6.

Daneman, R. *et al.* (2010) ‘Pericytes are required for blood-brain barrier integrity during embryogenesis’, *Nature*. Nature Research, 468(7323), pp. 562–566. doi: 10.1038/nature09513.

Danesh-Meyer, H. V. *et al.* (2012) ‘Connexin43 mimetic peptide reduces vascular leak and retinal ganglion cell death following retinal ischaemia’, *Brain*, 135(2), pp. 506–520. doi: 10.1093/brain/awr338.

Davis, M. E. *et al.* (2001) ‘Shear stress regulates endothelial nitric oxide synthase expression through c-Src by divergent signaling pathways’, *Circ Res*, 89(11), pp. 1073–1080. Available at: http://www.ncbi.nlm.nih.gov/pubmed/11717166 (Accessed: 22 February 2017).

Davis, S. *et al.* (1996) ‘Isolation of angiopoietin-1, a ligand for the TIE2 receptor, by secretion-trap expression cloning’, *Cell*, 87(7), pp. 1161–1169. doi: 10.1016/S0092-8674(00)81812-7.

Dejana, E. and Vestweber, D. (2013) ‘The role of VE-cadherin in vascular morphogenesis and permeability control’, *Progress in*

Molecular Biology and Translational Science, 116, pp. 119–144. doi: 10.1016/B978-0-12-394311-8.00006-6.

Diez, H. *et al.* (2007) ‘Hypoxia-mediated activation of Dll4-Notch-Hey2 signaling in endothelial progenitor cells and adoption of arterial cell fate’, *Experimental Cell Research*, 313(1), pp. 1–9. doi: 10.1016/j.yexcr.2006.09.009.

Van Dijk, C. G. M. *et al.* (2015) ‘The complex mural cell: Pericyte function in health and disease’, *International Journal of Cardiology*, 190(1), pp. 75–89. doi: 10.1016/j.ijcard.2015.03.258.

Dill, M. T. *et al.* (2012) ‘Disruption of Notch1 induces vascular remodeling, intussusceptive angiogenesis, and angiosarcomas in livers of mice’, *Gastroenterology*, 142(4), p. 967–977.e2. doi: 10.1053/j.gastro.2011.12.052.

Dimmeler, S. *et al.* (1999) ‘Activation of nitric oxide synthase in endothelial cells by Akt-dependent phosphorylation.’, *Nature*. Nature Publishing Group, 399(June), pp. 601–605. doi: 10.1038/21224.

Djokovic, D. *et al.* (2010) ‘Combination of Dll4/Notch and Ephrin-B2/EphB4 targeted therapy is highly effective in disrupting tumor angiogenesis.’, *BMC cancer*, 10(1), p. 641. doi: 10.1186/1471-2407-10-641.

Domenga, V. *et al.* (2004) ‘Notch3 is required for arterial identity and maturation of vascular smooth muscle cells’, *Genes and Development*. Cold Spring Harbor Laboratory Press, 18(22), pp. 2730–2735. doi: 10.1101/gad.308904.

Dou, G.-R. *et al.* (2008) ‘RBP-J, the transcription factor downstream of Notch receptors, is essential for the maintenance of vascular homeostasis in adult mice.’, *The FASEB journal : official publication of the Federation of American Societies for Experimental Biology*, 22(5), pp. 1606–1617. doi: 10.1096/fj.07-9998com.

Duarte, A. *et al.* (2004) ‘Dosage-sensitive requirement for mouse Dll4 in artery development’, *Genes & development*, 18(20), pp. 2474–2478.

Ehling, M. *et al.* (2013) ‘Notch controls retinal blood vessel maturation and quiescence.’, *Development (Cambridge, England)*, 140(14), pp. 3051–61. doi: 10.1242/dev.093351.

Eichmann, A. and Simons, M. (2012) ‘VEGF signaling inside vascular endothelial cells and beyond’, *Current Opinion in Cell Biology*. NIH Public Access, 24(2), pp. 188–193. doi: 10.1016/j.ceb.2012.02.002.

Eilken, H. M. and Adams, R. H. (2010) ‘Dynamics of endothelial cell behavior in sprouting angiogenesis’, *Current Opinion in Cell Biology*, pp. 617–625. doi: 10.1016/j.ceb.2010.08.010.

Eliceiri, B. P. *et al.* (1999) ‘Selective requirement for Src kinases during VEGF-induced angiogenesis and vascular permeability’, *Molecular cell*, 4(6), pp. 915–924. doi: 10.1016/S1097-2765(00)80221-X.

Erickson, K. K., Sundstrom, J. M. and Antonetti, D. A. (2007) ‘Vascular permeability in ocular disease and the role of tight junctions’, *Angiogenesis*. Kluwer Academic Publishers, 10(2), pp. 103–117. doi: 10.1007/s10456-007-9067-z.

Esser, S. *et al.* (1998) ‘Vascular endothelial growth factor induces VE-

cadherin tyrosine phosphorylation in endothelial cells', *J.Cell Sci.*, 111 (Pt 1(0021–9533 (Print)), pp. 1853–1865. Available at: http://jcs.biologists.org/content/111/13/1853.short (Accessed: 6 April 2017).

Estrach, S. *et al.* (2011) 'Laminin-binding integrins induce Dll4 expression and notch signaling in endothelial cells', *Circulation Research*. American Heart Association, Inc., 109(2), pp. 172–182. doi: 10.1161/CIRCRESAHA.111.240622.

Fagiani, E. and Christofori, G. (2013) 'Angiopoietins in angiogenesis', *Cancer Letters*, pp. 18–26. doi: 10.1016/j.canlet.2012.08.018.

Fang, L. *et al.* (2011) 'MicroRNA miR-93 promotes tumor growth and angiogenesis by targeting integrin-β8.', *Oncogene*. Nature Publishing Group, 30(7), pp. 806–821. doi: 10.1038/onc.2010.465.

Feng, D. *et al.* (1996) 'Vesiculo-vacuolar organelles and the regulation of venule permeability to macromolecules by vascular permeability factor, histamine, and serotonin.', *Journal of Experimental Medicine*. The Rockefeller University Press, 183(5), pp. 1981–6. doi: 10.1084/jem.183.5.1981.

Ferrara, N. and Henzel, W. J. (1989) 'Pituitary follicular cells secrete a novel heparin-binding growth factor specific for vascular endothelial cells', *Biochemical and Biophysical Research Communications*, 161(2), pp. 851–858. doi: 10.1016/0006-291X(89)92678-8.

Fiuza, U. M. *et al.* (2010) 'Mechanisms of ligand-mediated inhibition in notch signaling activity in Drosophila', *Developmental Dynamics*. Wiley-

Liss, Inc., 239(3), pp. 798–805. doi: 10.1002/dvdy.22207.

Florian, J. A. *et al.* (2003) ‘Heparan sulfate proteoglycan is a mechanosensor on endothelial cells’, *Circulation Research*, 93(10), pp. e136–e142. doi: 10.1161/01.RES.0000101744.47866.D5.

Fu, B. M. *et al.* (1994) ‘A junction-orifice-fiber entrance layer model for capillary permeability: application to frog mesenteric capillaries’, *J Biomech Eng*. American Society of Mechanical Engineers, 116(4), pp. 502–513. doi: 10.1115/1.2895802.

Fujimoto, K. (1995) ‘Pericyte-endothelial gap junctions in developing rat cerebral capillaries: A fine structural study’, *The Anatomical Record*. Wiley Subscription Services, Inc., A Wiley Company, 242(4), pp. 562–565. doi: 10.1002/ar.1092420412.

Funahashi, Y. *et al.* (2010) ‘Notch regulates the angiogenic response via induction of VEGFR-1.’, *Journal of angiogenesis research*. BioMed Central, 2(1), p. 3. doi: 10.1186/2040-2384-2-3.

Gale, N. W. *et al.* (2004) ‘Haploinsufficiency of delta-like 4 ligand results in embryonic lethality due to major defects in arterial and vascular development’, *Proceedings of the National Academy of Sciences of the United States of America*. National Academy of Sciences, 101(45), pp. 15949–15954. doi: 10.1073/pnas.0407290101.

Galvao, J. *et al.* (2014) ‘Unexpected low-dose toxicity of the universal solvent DMSO’, *FASEB Journal*. Federation of American Societies for Experimental Biology, 28(3), pp. 1317–1330. doi: 10.1096/fj.13-235440.

Gavard, J. and Gutkind, J. S. (2006) ‘VEGF controls endothelial-cell

permeability by promoting the beta-arrestin-dependent endocytosis of VE-cadherin.', *Nature Cell Biology*, 8(11), pp. 1223–1234. doi: 10.1038/ncb1486.

Geling, A. *et al.* (2002) 'A γ-secretase inhibitor blocks Notch signaling in vivo and causes a severe neurogenic phenotype in zebrafish', *EMBO Reports*. European Molecular Biology Organization, 3(7), pp. 688–694. doi: 10.1093/embo-reports/kvf124.

Gerhardt, H. *et al.* (2003) 'VEGF guides angiogenic sprouting utilizing endothelial tip cell filopodia', *The Journal of cell biology*. Rockefeller University Press, 161(6), pp. 1163–1177. doi: 10.1083/jcb.200302047.

Gerthoffer, W. T. (2016) 'Mechanisms of Vascular Smooth Muscle Cell Migration', *Circulation Research*, 100(5). doi: 10.1161/01.RES.0000258492.96097.47.

Giannotta, M., Trani, M. and Dejana, E. (2013) 'VE-cadherin and endothelial adherens junctions: active guardians of vascular integrity', *Developmental Cell*, 26(5), pp. 441–454. doi: 10.1016/j.devcel.2013.08.020.

Glass, C. A. and Bates, D. O. (2004) 'The role of endothelial cell Ca2+ store release in the regulation of microvascular permeability in vivo.', *Experimental Physiology*. Blackwell Science Ltd, 89(4), pp. 343–351. doi: 10.1113/expphysiol.2003.026948.

Goddard, L. M., Luisa Iruela-Arispe, M. and Iruela-Arispe, M. L. (2013) 'Cellular and molecular regulation of vascular permeability', *Thromb Haemost*. Schattauer Publishers, 109(3), pp. 407–415. doi:

10.1160/TH12-09-0678.

Gornik, H. L. (2005) ‘Peripheral Arterial Disease’, *Circulation*, 111(13), pp. e169–e172. doi: 10.1161/01.CIR.0000160581.58633.8B.

Gouverneur, M. *et al.* (2006) ‘Fluid shear stress stimulates incorporation of hyaluronan into endothelial cell glycocalyx.’, *American journal of physiology. Heart and circulatory physiology*, 290(1), pp. H458–H452. doi: 10.1152/ajpheart.00592.2005.

Grotte, G. (1956) ‘Passage of dextran molecules across the blood-lymph barrier’, *Acta Chir Scand Suppl*, 211, pp. 1–84. Available at: http://www.ncbi.nlm.nih.gov/pubmed/13326154 (Accessed: 1 March 2017).

Guo, F. *et al.* (2006) ‘Genetic deletion of Rac1 GTPase reveals its critical role in actin stress fiber formation and focal adhesion complex assembly’, *Journal of Biological Chemistry*. American Society for Biochemistry and Molecular Biology, 281(27), pp. 18652–18659. doi: 10.1074/jbc.M603508200.

Guruharsha, K. G., Kankel, M. W. and Artavanis-Tsakonas, S. (2012) ‘The Notch signalling system: recent insights into the complexity of a conserved pathway.’, *Nature reviews. Genetics*. Nature Publishing Group, 13(9), pp. 654–66. doi: 10.1038/nrg3272.

Al Haj Zen, A. *et al.* (2010) ‘Inhibition of delta-like-4-mediated signaling impairs reparative angiogenesis after ischemia’, *Circulation Research*, 107(2), pp. 283–293. doi: 10.1161/CIRCRESAHA.110.221663.

Hale, A. T. *et al.* (2014) ‘Endothelial krüppel-like factor 4 regulates

angiogenesis and the notch signaling pathway', *Journal of Biological Chemistry*. American Society for Biochemistry and Molecular Biology, 289(17), pp. 12016–12028. doi: 10.1074/jbc.M113.530956.

Hansen-Smith, F. *et al.* (2001) 'Growth of arterioles precedes that of capillaries in stretch-induced angiogenesis in skeletal muscle.', *Microvascular research*, 62(1), pp. 1–14. doi: 10.1006/mvre.2001.2308.

Hargrave, R. W., Huxley, V. H. and Thipakorn, B. (1995) 'Seasonal variations of capillary hydraulic conductivity and volume status.', *The American journal of physiology*, 268(2 Pt 2), pp. R468-74. Available at: http://ajpregu.physiology.org/content/268/2/R468.short (Accessed: 6 September 2017).

He, P. and Curry, F. E. (1993) 'Differential actions of cAMP on endothelial [Ca2+]i and permeability in microvessels exposed to ATP.', *The American journal of physiology*, 265(3 Pt 2), pp. H1019-23. Available at: http://www.ncbi.nlm.nih.gov/pubmed/8214108 (Accessed: 28 September 2016).

He, P., Zeng, M. and Curry, F. E. (2000) 'Dominant role of cAMP in regulation of microvessel permeability', *Am.J.Physiol Heart Circ.Physiol*, 278(4), pp. H1124–H1133. Available at: http://ajpheart.physiology.org/content/ajpheart/278/4/H1124.full.pdf (Accessed: 28 September 2016).

Heil, M. *et al.* (2002) 'Blood monocyte concentration is critical for enhancement of collateral artery growth.', *American journal of physiology. Heart and circulatory physiology*, 283(6), pp. H2411-9. doi:

10.1152/ajpheart.01098.2001.

Helisch, A. *et al.* (2006) ‘Impact of mouse strain differences in innate hindlimb collateral vasculature’, *Arteriosclerosis, Thrombosis, and Vascular Biology*, 26(3), pp. 520–526. doi: 10.1161/01.ATV.0000202677.55012.a0.

Hellstrom, M. *et al.* (2007) ‘Dll4 signalling through Notch1 regulates formation of tip cells during angiogenesis’, *Nature*, 445(7129), pp. 776–780. doi: 10.1038/nature05571.

Henry, C. B. and Duling, B. R. (2000) ‘TNF-alpha increases entry of macromolecules into luminal endothelial cell glycocalyx.’, *American journal of physiology. Heart and circulatory physiology*, 279, pp. H2815–H2823.

Heupel, W.-M. *et al.* (2009) ‘Endothelial barrier stabilization by a cyclic tandem peptide targeting VE-cadherin transinteraction in vitro and in vivo’, *Journal of Cell Science*, 122, pp. 1616–1625. doi: 10.1242/jcs.040212.

Heuser, L. S., Taylor, S. H. and Folkman, J. (1984) ‘Prevention of carcinomatosis and bloody malignant ascites in the rat by an inhibitor of angiogenesis’, *Journal of Surgical Research*. Academic Press, 36(3), pp. 244–250. doi: 10.1016/0022-4804(84)90094-5.

Hirase, T. *et al.* (1997) ‘Occludin as a possible determinant of tight junction permeability in endothelial cells.’, *Journal of cell science*, 110 (Pt 1(14), pp. 1603–1613.

Hirata, H. *et al.* (2002) ‘Oscillatory expression of the bHLH factor Hes1

regulated by a negative feedback loop.', *Science (New York, N.Y.)*. American Association for the Advancement of Science, 298(5594), pp. 840–843. doi: 10.1126/science.1074560.

Hodkinson, P. S. *et al.* (2007) 'Mammalian NOTCH-1 activates β1 integrins via the small GTPase R-Ras', *Journal of Biological Chemistry*. American Society for Biochemistry and Molecular Biology, 282(39), pp. 28991–29001. doi: 10.1074/jbc.M703601200.

Hofman, P. *et al.* (2000) 'VEGF-A induced hyperpermeability of blood-retinal barrier endothelium in vivo is predominantly associated with pinocytotic vesicular transport and not with formation of fenestrations. Vascular endothelial growth factor-A.', *Current eye research*, 21(2), pp. 637–45. doi: 10.1076/0271-3683(200008)2121-VFT637.

Holmes, D. I. R. and Zachary, I. (2005) 'The vascular endothelial growth factor (VEGF) family: angiogenic factors in health and disease.', *Genome biology*. BioMed Central, 6(2), p. 209. doi: 10.1186/gb-2005-6-2-209.

Holz, G. G. *et al.* (2006) 'Cell physiology of cAMP sensor Epac.', *The Journal of physiology*. Blackwell Publishing Ltd, 577(Pt 1), pp. 5–15. doi: 10.1113/jphysiol.2006.119644.

Hood, J. D. *et al.* (1998) 'VEGF upregulates ecNOS message, protein, and NO production in human endothelial cells.', *The American journal of physiology*, 274(3 Pt 2), pp. H1054-8. doi: 10.1016/0003-2697(87)90021-2.

Hu, X. *et al.* (2000) 'Starling forces that oppose filtration after tissue

oncotic pressure is increased', *American Journal of Physiology-Heart and Circulatory Physiology*, 279(4), pp. H1724–H1736.

Ignarro, L. J. *et al.* (1987) 'Endothelium-derived relaxing factor produced and released from artery and vein is nitric oxide (endothelium-dependent relaxation/vascular smooth muscle/cyclic GMP)', *Medical Sciences*, 84, pp. 9265–9269. doi: 10.1073/pnas.84.24.9265.

Iivanainen, E. *et al.* (2003) 'Angiopoietin-regulated recruitment of vascular smooth muscle cells by endothelial-derived heparin binding EGF-like growth factor.', *FASEB journal : official publication of the Federation of American Societies for Experimental Biology*. Federation of American Societies for Experimental Biology, 17(12), pp. 1609–21. doi: 10.1096/fj.02-0939com.

Iruela-Arispe, M. L. and Davis, G. E. (2009) 'Cellular and Molecular Mechanisms of Vascular Lumen Formation', *Developmental Cell*, pp. 222–231. doi: 10.1016/j.devcel.2009.01.013.

Van Itallie, C. M. *et al.* (2010) 'Occludin is required for cytokine-induced regulation of tight junction barriers.', *Journal of cell science*, 123(Pt 16), pp. 2844–2852. doi: 10.1242/jcs.065581.

Ito, W. D. *et al.* (1997) 'Monocyte chemotactic protein-1 increases collateral and peripheral', *Circ Res*, 80(6), pp. 829–837.

Jacob, M. and Chappell, D. (2013) 'Reappraising Starling', *Current Opinion in Critical Care*, 19(4), pp. 282–289. doi: 10.1097/MCC.0b013e3283632d5e.

Jakobsson, L. *et al.* (2010) 'Endothelial cells dynamically compete for

the tip cell position during angiogenic sprouting', *Nature cell biology*, 12(10), pp. 943–953.

Jayson, G. C. *et al.* (2002) 'Molecular imaging and biological evaluation of HuMV833 anti-VEGF antibody: implications for trial design of antiangiogenic antibodies', *Journal of the National Cancer Institute*. Oxford University Press, 94(19), pp. 1484–1493. doi: 10.1093/jnci/94.19.1484.

Jho, D. *et al.* (2005) 'Angiopoietin-1 opposes VEGF-induced increase in endothelial permeability by inhibiting TRPC1-dependent Ca 2+ influx', *Circulation Research*, 96(12), pp. 1282–1290. doi: 10.1161/01.RES.0000171894.03801.03.

Jin, H. *et al.* (2010) 'A PKA-Csk-pp60Src signaling pathway regulates the switch between endothelial cell invasion and cell-cell adhesion during vascular sprouting', *Blood*, 116(25), pp. 5773–5783. doi: 10.1182/blood-2010-07-296210.

Jin, S. *et al.* (2008) 'Notch signaling regulates platelet-derived growth factor receptor-beta expression in vascular smooth muscle cells.', *Circulation research*, 102(12), pp. 1483–91. doi: 10.1161/CIRCRESAHA.107.167965.

Jin, Y., Kaluza, D. and Jakobsson, L. (2014) 'VEGF, Notch and TGFβ/BMPs in regulation of sprouting angiogenesis and vascular patterning.', *Biochemical Society transactions*, 42(6), pp. 1576–1583. doi: 10.1042/BST20140231.

Kalén, M. *et al.* (2011) 'Gamma-secretase inhibitor treatment promotes

VEGF-A-driven blood vessel growth and vascular leakage but disrupts neovascular perfusion', *PLoS ONE*. Edited by C. Samakovlis. Public Library of Science, 6(4), p. e18709. doi: 10.1371/journal.pone.0018709.

Kanda, S. *et al.* (2005) 'Angiopoietin 1 is mitogenic for cultured endothelial cells', *Cancer Research*, 65(15), pp. 6820–6827. doi: 10.1158/0008-5472.CAN-05-0522.

Keck, P. J. *et al.* (1989) 'Vascular permeability factor, an endothelial cell mitogen related to PDGF', *Science*, 246(4935), pp. 1309–1312. doi: 10.1126/science.2479987.

Kendall, S. and Michel, C. C. (1995) 'The measurement of permeability in single rat venules using the red cell microperfusion technique.', *Experimental physiology*, 80(3), pp. 359–72. doi: 10.1113/expphysiol.1995.sp003853.

Kim, I. *et al.* (1999) 'Molecular cloning, expression, and characterization of angiopoietin-related protein. angiopoietin-related protein induces endothelial cell sprouting.', *The Journal of biological chemistry*. American Society for Biochemistry and Molecular Biology, 274(37), pp. 26523–8. doi: 10.1074/jbc.274.37.26523.

Kim, M.-H., Harris, N. and Tarbell, J. (2005) 'Regulation of hydraulic conductivity in response to sustained changes in pressure', *American Journal of Physiology-Heart and Circulatory Physiology*, 289(6), pp. H2551--H2558. doi: 10.1152/ajpheart.00602.2005.

Kobayashi, H. *et al.* (2006) 'Hepatocyte growth factor mediates angiopoietin-induced smooth muscle cell recruitment', *Blood*, 108(4),

pp. 1260–1266. doi: 10.1182/blood-2005-09-012807.

Koblizek, T. I. *et al.* (1998) ‘Angiopoietin-1 induces sprouting angiogenesis in vitro.’, *Current biology : CB*, 8(9), pp. 529–32. doi: 10.1016/S0960-9822(98)70205-2.

Komarova, Y. and Malik, A. B. (2010) *Regulation of endothelial permeability via paracellular and transcellular transport pathways.*, *Annual review of physiology*. Annual Reviews. doi: 10.1146/annurev-physiol-021909-135833.

Koolwijk, P. *et al.* (2001) ‘Involvement of VEGFR-2 (kdr / ¯ k-1) but not VEGFR-1 (¯ t-1) in VEGF-A and VEGF-C-induced tube formation by human microvascular endothelial cells in ® brin matrices in vitro’, *Angiogenesis*. Kluwer Academic Publishers, 2(1), pp. 53–60. doi: 10.1023/A:1016637700638.

Kopan, R. and Ilagan, M. X. G. (2009) ‘The Canonical Notch Signaling Pathway: Unfolding the Activation Mechanism’, *Cell*, 137(2), pp. 216–233. doi: 10.1016/j.cell.2009.03.045.

Korn, C. and Augustin, H. G. (2015) ‘Mechanisms of Vessel Pruning and Regression’, *Developmental Cell*, pp. 5–17. doi: 10.1016/j.devcel.2015.06.004.

Krebs, L. T. *et al.* (2000) ‘Notch signaling is essential for vascular morphogenesis in mice’, *Genes & development*. Cold Spring Harbor Laboratory Press, 14(11), pp. 1343–1352. doi: 10.1101/gad.14.11.1343.

Kroll, J. and Waltenberger, J. (1998) ‘VEGF-A induces expression of eNOS and iNOS in endothelial cells via VEGF receptor-2 (KDR).’,

Biochemical and biophysical research communications, 252(3), pp. 743–746. doi: 10.1006/bbrc.1998.9719.

Krueger, J. *et al.* (2011) 'Flt1 acts as a negative regulator of tip cell formation and branching morphogenesis in the zebrafish embryo.', *Development (Cambridge, England)*, 138(10), pp. 2111–20. doi: 10.1242/dev.063933.

Kullo, I. J. and Leeper, N. J. (2015) 'The Genetic Basis of Peripheral Arterial Disease', *Circulation Research*, 116(9).

Kurz, H. *et al.* (1996) 'First blood vessels in the avian neural tube are formed by a combination of dorsal angioblast immigration and ventral sprouting of endothelial cells', *Developmental Biology*, 173(1), pp. 133–147. doi: 10.1006/dbio.1996.0012.

Ladi, E. *et al.* (2005) 'The divergent DSL ligand Dll3 does not activate Notch signaling but cell autonomously attenuates signaling induced by other DSL ligands', *Journal of Cell Biology*, 170(6), pp. 983–992. doi: 10.1083/jcb.200503113.

Lampugnani, M. G. *et al.* (2002) 'VE-Cadherin Regulates Endothelial Actin Activating Rac and Increasing Membrane Association of Tiam', *Molecular biology of the cell*. American Society for Cell Biology, 13(April), pp. 1175–1189. doi: 10.1091/mbc.01–07–0368.

Lampugnani, M. G. *et al.* (2003) 'Contact inhibition of VEGF-induced proliferation requires vascular endothelial cadherin, beta-catenin, and the phosphatase DEP-1/CD148', *Journal of Cell Biology*. Rockefeller University Press, 161(4), pp. 793–804. doi: 10.1083/jcb.200209019.

Lampugnani, M. G. *et al.* (2006) ‘Vascular endothelial cadherin controls VEGFR-2 internalization and signaling from intracellular compartments’, *Journal of Cell Biology*. Rockefeller University Press, 174(4), pp. 593–604. doi: 10.1083/jcb.200602080.

Lampugnani, M. G. *et al.* (2010) ‘CCM1 regulates vascular-lumen organization by inducing endothelial polarity.’, *J Cell Sci*, 123(Pt 7), pp. 1073–80. doi: 10.1242/jcs.059329.

Landis, E. (1927) ‘Micro-Injection Studies of capillary Permeability’, *JOURNAL OF PHYSIOLOGY*, 82(2).

Larrivée, B. *et al.* (2012) ‘ALK1 Signaling Inhibits Angiogenesis by Cooperating with the Notch Pathway’, *Developmental Cell*, 22(3), pp. 489–500. doi: 10.1016/j.devcel.2012.02.005.

Lawson, N. D. *et al.* (2001) ‘Notch signaling is required for arterial-venous differentiation during embryonic vascular development.’, *Development (Cambridge, England)*, 128(19), pp. 3675–3683. Available at: http://www.ncbi.nlm.nih.gov/pubmed/11585794%5Cnhttp://dev.biologists.org/content/128/19/3675.long (Accessed: 7 October 2016).

Lederman, R. J. *et al.* (2002) ‘Therapeutic angiogenesis with recombinant fibroblast growth factor-2 for intermittent claudication (the TRAFFIC study): A randomised trial’, *Lancet*, 359(9323), pp. 2053–2058. doi: 10.1016/S0140-6736(02)08937-7.

Lee, C. Y. and Bautch, V. L. (2011) ‘Ups and downs of guided vessel sprouting: the role of polarity’, *Physiology*, 26(5), pp. 326–333. doi:

10.1152/physiol.00018.2011.

Lee, H. J. *et al.* (2004) ‘Biological characterization of angiopoietin-3 and angiopoietin-4’, *The FASEB Journal*. Federation of American Societies for Experimental Biology, 18(11), pp. 1200–8. doi: 10.1096/fj.03-1466com.

Leslie, J. D. *et al.* (2007) ‘Endothelial signalling by the Notch ligand Delta-like 4 restricts angiogenesis.’, *Development (Cambridge, England)*, 134(5), pp. 839–844. doi: 10.1242/dev.003244.

Leung, D. W. *et al.* (1989) ‘Vascular endothelial growth factor is a secreted angiogenic mitogen.’, *Science (New York, N.Y.)*, 246(4935), pp. 1306–1309. doi: 10.1126/science.2479986.

Levick, J. R. and Michel, C. C. (2010) ‘Microvascular fluid exchange and the revised Starling principle’, *Cardiovascular Research*, 87(2), p. cvq062. doi: 10.1093/cvr/cvq062.

Li, J., Zhang, Y. P. and Kirsner, R. S. (2003) ‘Angiogenesis in wound repair: Angiogenic growth factors and the extracellular matrix’, *Microscopy Research and Technique*. Wiley Subscription Services, Inc., A Wiley Company, 60(1), pp. 107–114. doi: 10.1002/jemt.10249.

Lichtenbeld, H. C. *et al.* (1999) ‘Effect of local anti-VEGF antibody treatment on tumor microvessel permeability.’, *Microvascular research*, 57(3), pp. 357–62. doi: 10.1006/mvre.1998.2140.

Lin, Z.-X. (2013) ‘Glioma-related edema: new insight into molecular mechanisms and their clinical implications’, *Chinese Journal of Cancer*. BioMed Central, 32(1), pp. 49–52. doi: 10.5732/cjc.012.10242.

Liu, H., Kennard, S. and Lilly, B. (2009) ‘NOTCH3 expression is induced in mural cells through an autoregulatory loop that requires Endothelial-expressed JAGGED1’, *Circulation Research*, 104(4), pp. 466–475. doi: 10.1161/CIRCRESAHA.108.184846.

Liu, R. *et al.* (2012) ‘Inhibition of Notch signaling by Dll4-Fc promotes reperfusion of acutely ischemic tissues’, *Biochemical and Biophysical Research Communications*, 418(1), pp. 173–179. doi: 10.1016/j.bbrc.2012.01.002.

Liu, Z. J. *et al.* (2003) ‘Regulation of Notch1 and Dll4 by Vascular Endothelial Growth Factor in Arterial Endothelial Cells: Implications for Modulating Arteriogenesis and Angiogenesis’, *Molecular and Cellular Biology*, 23(1), pp. 14–25. doi: 10.1128/mcb.23.1.14-25.2003.

Lobov, I. B. *et al.* (2007) ‘Delta-like ligand 4 (Dll4) is induced by VEGF as a negative regulator of angiogenic sprouting’, *Proceedings of the National Academy of Sciences*. National Academy of Sciences, 104(9), pp. 3219–3224. doi: 10.1073/pnas.0611206104.

Lobov, I. B. *et al.* (2011) ‘The Dll4/Notch pathway controls postangiogenic blood vessel remodeling and regression by modulating vasoconstriction and blood flow’, *Blood*, 117(24), pp. 6728–6737. doi: 10.1182/blood-2010-08-302067.

Loudon, M. F., Michel, C. C. and White, I. F. (1979) ‘The labelling of vesicles in frog endothelial cells with ferritin.’, *The Journal of physiology*. Wiley-Blackwell, 296, pp. 97–112. Available at: http://www.ncbi.nlm.nih.gov/pubmed/316823 (Accessed: 2 March

2017).

Louvi, A., Arboleda-Velasquez, J. F. and Artavanis-Tsakonas, S. (2006) ‘CADASIL: A critical look at a notch disease’, *Developmental Neuroscience*. Karger Publishers, pp. 5–12. doi: 10.1159/000090748.

Lu, X. *et al.* (2004) ‘The netrin receptor UNC5B mediates guidance events controlling morphogenesis of the vascular system’, *Nature*. Nature Publishing Group, 432(7014), pp. 179–186. doi: 10.1038/nature03080.

Luft, J. H. (1966) ‘Fine structures of capillary and endocapillary layer as revealed by ruthenium red.’, in *Federation proceedings*, p. 1773. Available at: http://www.ncbi.nlm.nih.gov/pubmed/5927412 (Accessed: 2 March 2017).

Maisonpierre, P. C. *et al.* (1997) ‘Angiopoietin-2, a Natural Antagonist for Tie2 That Disrupts in vivo Angiogenesis’, *Science*, 277(5322), pp. 55–60. doi: 10.1126/science.277.5322.55.

Makino, H. *et al.* (2012) ‘Long-term follow-up evaluation of results from clinical trial using hepatocyte growth factor gene to treat severe peripheral arterial disease’, *Arterioscler Thromb Vasc Biol*, 32(10), pp. 2503–2509. doi: 10.1161/atvbaha.111.244632.

Mason, J. C. *et al.* (1979) ‘The ultrastructure of frog mesenteric capillaries of known filtration coefficient’, *Q.J.Exp.Physiol Cogn Med.Sci.*, 64(3), pp. 217–224. doi: 10.1113/expphysiol.1979.sp002474.

Matsuo, Y. *et al.* (2009) ‘CXCL8/IL-8 and CXCL12/SDF-lα co-operatively promote invasiveness and angiogenesis in pancreatic

cancer', *International Journal of Cancer*. Wiley Subscription Services, Inc., A Wiley Company, 124(4), pp. 853–861. doi: 10.1002/ijc.24040.

Mavrakis, A. G. *et al.* (2012) 'Occludin dislocation in brain capillary endothelium of rats with bile duct ligation induced cholestasis', *Neuroscience Letters*, 528(2), pp. 180–184. doi: 10.1016/j.neulet.2012.08.066.

Mayerson, H. S. *et al.* (1960) 'Regional differences in capillary permeabilitv', *American Journal of Physiology*, 198(1), pp. 155–160.

Mehta, D. and Malik, A. B. (2006) 'Signaling mechanisms regulating endothelial permeability.', *Physiological reviews*, 86(1), pp. 279–367. doi: 10.1152/physrev.00012.2005.

Mentzer, S. J. and Konerding, M. A. (2014) 'Intussusceptive angiogenesis: Expansion and remodeling of microvascular networks', in *Angiogenesis*, pp. 499–509. doi: 10.1007/s10456-014-9428-3.

Michel, C. C. *et al.* (1974) 'A development of the Landis technique for measuring the filtration coefficient of individual capillaries in the frog mesentery', *Experimental physiology*, 59(4), pp. 283–309.

Michel, C. C. (1979) 'The investigation of capillary permeability in single vessels', *Acta Physiologica Scandinavica. Supplementum*, 463, pp. 67–74. Available at: http://www.ncbi.nlm.nih.gov/pubmed/382745 (Accessed: 2 March 2017).

Michel, C. C. (1980) 'Filtration coefficients and osmotic reflexion coefficients of the walls of single frog mesenteric capillaries.', *The Journal of physiology*. Wiley-Blackwell, 309, pp. 341–55. doi:

10.1113/jphysiol.1980.sp013512.

Michel, C. C. and Curry, F. E. (1999) ‘Microvascular permeability.’, *Physiological reviews*, 79(3), pp. 703–61. Available at: http://physrev.physiology.org/content/79/3/703.abstract (Accessed: 23 February 2017).

Michel, C. C. and Phillips, M. E. (1987) ‘Steady-state fluid filtration at different capillary pressures in perfused frog mesenteric capillaries.’, *The Journal of physiology*, 388, pp. 421–35. doi: 10.1113/jphysiol.1987.sp016622.

Miles, A. A. and Miles, E. M. (1952) ‘Vascular reactions to histamine, histamine-liberator and leukotaxine in the skin of guinea-pigs.’, *The Journal of physiology*, 118(2), pp. 228–57. doi: 10.1113/jphysiol.1952.sp004789.

Minnear, F. L., Zhu, L. and He, P. (2005) ‘Sphingosine 1-phosphate prevents platelet-activating factor-induced increase in hydraulic conductivity in rat mesenteric venules: pertussis toxin sensitive’, *American Journal of Physiology-Heart and Circulatory Physiology*, 289(2), pp. H840–H844.

Montero-Balaguer, M. *et al.* (2009) ‘Stable vascular connections and remodeling require full expression of VE-cadherin in zebrafish embryos’, *PLoS ONE*. Edited by P. Callaerts. Public Library of Science, 4(6), p. e5772. doi: 10.1371/journal.pone.0005772.

Morawietz, H. *et al.* (2000) ‘Regulation of the endothelin system by shear stress in human endothelial cells’, *The Journal of Physiology*.

Blackwell Science Ltd, 525(3), pp. 761–770. doi: 10.1111/j.1469-7793.2000.00761.x.

Morishita, R. *et al.* (2011) ‘Phase I/IIa clinical trial of therapeutic angiogenesis using hepatocyte growth factor gene transfer to treat critical limb ischemia’, *Arteriosclerosis, Thrombosis, and Vascular Biology*, 31(3), pp. 713–720. doi: 10.1161/ATVBAHA.110.219550.

Mukhopadhyay, D. *et al.* (1998) ‘Vascular permeability factor/vascular endothelial growth factor -mediated signaling in mouse mesentery vascular endothelium’, *Cancer Research*, 58(6), p. 1278.

Mulivor, A. W. and Lipowsky, H. H. (2009) ‘Inhibition of Glycan Shedding and Leukocyte-Endothelial Adhesion in Postcapillary Venules by Suppression of Matrixmetalloprotease Activity with Doxycycline’, *Microcirculation*, 16(8), pp. 657–666. doi: 10.3109/10739680903133714.

Murakami, T., Felinski, E. A. and Antonetti, D. A. (2009) ‘Occludin phosphorylation and ubiquitination regulate tight junction trafficking and vascular endothelial growth factor-induced permeability’, *Journal of Biological Chemistry*. American Society for Biochemistry and Molecular Biology, 284(31), pp. 21036–21046. doi: 10.1074/jbc.M109.016766.

Murohara, T. *et al.* (1998) ‘Nitric oxide synthase modulates angiogenesis in response to tissue ischemia’, *Journal of Clinical Investigation*. American Society for Clinical Investigation, 101(11), pp. 2567–2578. doi: 10.1172/JCI1560.

Nagasawa, K. *et al.* (2006) ‘Possible involvement of gap junctions in the

barrier function of tight junctions of brain and lung endothelial cells', *Journal of Cellular Physiology*. Wiley Subscription Services, Inc., A Wiley Company, 208(1), pp. 123–132. doi: 10.1002/jcp.20647.

Naghavi, M. *et al.* (2015) 'Global, regional, and national age-sex specific all-cause and cause-specific mortality for 240 causes of death, 1990-2013: A systematic analysis for the Global Burden of Disease Study 2013', *The Lancet*, 385(9963), pp. 117–171. doi: 10.1016/S0140-6736(14)61682-2.

Nagy, J. A. *et al.* (2006) 'Permeability properties of tumor surrogate blood vessels induced by VEGF-A.', *Laboratory investigation; a journal of technical methods and pathology*. Nature Publishing Group, 86(8), pp. 767–780. doi: 10.1038/labinvest.3700436.

Nagy, J. A. *et al.* (2008) 'Vascular permeability, vascular hyperpermeability and angiogenesis', *Angiogenesis*, pp. 109–119. doi: 10.1007/s10456-008-9099-z.

Nedvetsky, P. I. *et al.* (2016) 'cAMP-dependent protein kinase A (PKA) regulates angiogenesis by modulating tip cell behavior in a Notch-independent manner', *Development*, 143(19). doi: 10.1242/dev.134767.

Nielsen, M. S. *et al.* (2012) 'Gap junctions', *Comprehensive Physiology*. Hoboken, NJ, USA: John Wiley & Sons, Inc., 2(3), pp. 1981–2035. doi: 10.1002/cphy.c110051.

Nieuwdorp, M. *et al.* (2006) 'Endothelial glycocalyx damage coincides with microalbuminuria in type 1 diabetes', *Diabetes*, 55(4), pp. 1127–1132. doi: 10.2337/diabetes.55.04.06.db05-1619.

Niiyama, H. *et al.* (2009) ‘Murine model of hindlimb ischemia.’, *Journal of visualized experiments : JoVE*. MyJoVE Corporation, (23), pp. 12–14. doi: 10.3791/1035.

Nishishita, T. and Lin, P. C. (2004) ‘Angiopoietin 1, PDGF-B, and TGF-β gene regulation in endothelial cell and smooth muscle cell interaction’, *Journal of Cellular Biochemistry*. Wiley Subscription Services, Inc., A Wiley Company, 91(3), pp. 584–593. doi: 10.1002/jcb.10718.

Nitta, T. *et al.* (2003) ‘Size-selective loosening of the blood-brain barrier in claudin-5-deficient mice.’, *The Journal of cell biology*, 161(3), pp. 653–60. doi: 10.1083/jcb.200302070.

Nobes, C. D. and Hall, A. (1995) ‘Rho, rac and cdc42 GTPases: regulators of actin structures, cell adhesion and motility’, *Biochemical Society Transactions*, 23(3), pp. 456–459. Available at: http://www.ncbi.nlm.nih.gov/entrez/query.fcgi?cmd=Retrieve&db=PubMed&dopt=Citation&list_uids=8566347 (Accessed: 6 October 2016).

Noguera-Troise, I. *et al.* (2006) ‘Blockade of Dll4 inhibits tumour growth by promoting non-productive angiogenesis.’, *Nature*. Nature Publishing Group, 444(7122), pp. 1032–1037. doi: 10.1038/nature05355.

Norrby, K. (2002) ‘Mast cells and angiogenesis. Review article’, *APMIS*. Munksgaard International Publishers, 110(5), pp. 355–371. doi: 10.1034/j.1600-0463.2002.100501.x.

Norrby, K. *et al.* (2008) ‘Relaxin, a Potent Microcirculatory Effector, Is Not Angiogenic’, *International Journal of Microcirculation*. Karger Publishers, 16(5), pp. 227–231. doi: 10.1159/000179178.

Norrby, K., Jakobsson, A. and Sörbo, J. (1986) ‘Mast-cell-mediated angiogenesis: a novel experimental model using the rat mesentery.’, *Virchows Archiv. B, Cell pathology including molecular pathology*. Springer-Verlag, 52(3), pp. 195–206. doi: 10.1007/BF02889963.

Noseda, M. *et al.* (2006) ‘Smooth Muscle alpha-actin is a direct target of Notch/CSL’, *Circulation Research*, 98(12), pp. 1468–1470. doi: 10.1161/01.RES.0000229683.81357.26.

Oyama, N. *et al.* (2010) ‘Smooth Muscle Notch1 Mediates Neointimal Formation Following Vascular Injury’, *Circulation*, 119(20), pp. 2686–2692. doi: 10.1161/CIRCULATIONAHA.108.790485.Smooth.

Palmer, R. M., Ashton, D. S. and Moncada, S. (1988) ‘Vascular endothelial cells synthesize nitric oxide from L-arginine.’, *Nature*. Nature Publishing Group, pp. 664–666. doi: 10.1038/333664a0.

Papapetropoulos, A. *et al.* (1999) ‘Direct actions of angiopoietin-1 on human endothelium: evidence for network stabilization, cell survival, and interaction with other angiogenic growth factors’, *Laboratory Investigation*, 79(2), pp. 213–223. Available at: http://www.ncbi.nlm.nih.gov/pubmed/10068209 (Accessed: 18 November 2016).

Pappenheimer, JR; Renkin, EM; Borrero, L. (1951) ‘Filtration, diffusion and molecular sieving through peripheral capillary membranes; a contribution to the pore theory of capillary permeability.’, *Am J Physiol*, 167(1), pp. 13–46. doi: 10.1016/0371-1951(51)80019-5.

Pappenheimer, J. and Soto-Rivera, A. (1948) ‘Effective osmotic

pressure of the plasma proteins and other quantities associated with the capillary circulation in the hindlimbs of cats and dogs.', *Am J Physiol*, 152(3), pp. 471–491. Available at: http://www.ncbi.nlm.nih.gov/pubmed/18863145 (Accessed: 28 February 2017).

Parker, J. C. *et al.* (2006) 'Hydraulic conductance of pulmonary microvascular and macrovascular endothelial cell monolayers', *American journal of physiology. Lung cellular and molecular physiology*, 36688(1), pp. 30–37. doi: 10.1152/ajplung.00317.2005.

Patenaude, A. *et al.* (2014) 'Endothelial-specific notch blockade inhibits vascular function and tumor growth through an enos-dependent mechanism', *Cancer Research*, 74(9), pp. 2402–2411. doi: 10.1158/0008-5472.CAN-12-4038.

Phng, L. K. *et al.* (2009) 'Nrarp Coordinates Endothelial Notch and Wnt Signaling to Control Vessel Density in Angiogenesis', *Developmental Cell*. Elsevier, 16(1), pp. 70–82. doi: 10.1016/j.devcel.2008.12.009.

Pocock, T. M. *et al.* (2000) 'VEGF and ATP act by different mechanisms to increase microvascular permeability and endothelial [Ca(2+)]', *American Journal of Physiology-Heart and Circulatory Physiology*, 279(4), pp. H1625–H1634. Available at: http://ajpheart.physiology.org/content/ajpheart/279/4/H1625.full.pdf (Accessed: 3 March 2017).

Potente, M., Gerhardt, H. and Carmeliet, P. (2011) 'Basic and therapeutic aspects of angiogenesis', *Cell*, pp. 873–887. doi:

10.1016/j.cell.2011.08.039.

Price, R. J., Owens, G. K. and Skalak, T. C. (1994) ‘Immunohistochemical identification of arteriolar development using markers of smooth muscle differentiation. Evidence that capillary arterialization proceeds from terminal arterioles’, *Circulation research*, 75(3), pp. 520–527.

Pries, A. R., Reglin, B. and Secomb, T. W. (2005) ‘Remodeling of Blood Vessels’, *Hypertension*, pp. 725–731. Available at: http://hyper.ahajournals.org/content/46/4/725.abstract (Accessed: 15 February 2017).

Radomski, M. W., Palmer, R. M. J. and Moncada, S. (1987) ‘The anti-aggregating properties of vascular endothelium: interactions between prostacyclin and nitric oxide’, *British Journal of Pharmacology*. Blackwell Publishing Ltd, 92(3), pp. 639–646. doi: 10.1111/j.1476-5381.1987.tb11367.x.

Rasmussen, H. S., Rasmussen, C. S. and Macko, J. (2002) ‘VEGF gene therapy for coronary artery disease and peripheral vascular disease’, *Cardiovascular Radiation Medicine*, 3(2), pp. 114–117. doi: 10.1016/S1522-1865(02)00158-0.

Raya, A. *et al.* (2004) ‘Notch activity acts as a sensor for extracellular calcium during vertebrate left-right determination.’, *Nature*. Nature Publishing Group, 427(6970), pp. 121–128. doi: 10.1038/nature02190.

Rebay, I. *et al.* (1991) ‘Specific EGF repeats of Notch mediate interactions with Delta and Serrate: implications for Notch as a

multifunctional receptor.', *Cell*. Elsevier, 67(4), pp. 687–99. doi: 10.1016/0092-8674(91)90064-6.

Rees, D. D., Palmer, R. M. and Moncada, S. (1989) 'Role of endothelium-derived nitric oxide in the regulation of blood pressure.', *Proceedings of the National Academy of Sciences of the United States of America*, 86(9), pp. 3375–8. doi: 10.1073/pnas.86.9.3375.

Reitsma, S. *et al.* (2007) 'The endothelial glycocalyx: composition, functions, and visualization', *Pflügers Archiv - European Journal of Physiology*. Springer-Verlag, 454(3), pp. 345–359. doi: 10.1007/s00424-007-0212-8.

Renkin, E. M. *et al.* (1977) 'Transport pathways for fluid and large molecules in microvascular endothelium of the dog's paw', *Microvascular Research*, 14(2), pp. 205–214. doi: 10.1016/0026-2862(77)90019-X.

Ribatti, D. (2014) 'History of research on angiogenesis', *Chemical Immunology and Allergy*. Karger Publishers, pp. 1–14. doi: 10.1159/000353311.

Ribatti, D. and Crivellato, E. (2012) '"Sprouting angiogenesis", a reappraisal', *Developmental Biology*, pp. 157–165. doi: 10.1016/j.ydbio.2012.09.018.

Ribatti, D., Nico, B. and Crivellato, E. (2011) 'The role of pericytes in angiogenesis', *The International journal of developmental biology*. UPV/EHU Press, 55(3), pp. 261–8. doi: 10.1387/ijdb.103167dr.

Ridgway, J. *et al.* (2006) 'Inhibition of Dll4 signalling inhibits tumour

growth by deregulating angiogenesis', *Nature*, 444(7122), pp. 1083–1087. doi: 10.1038/nature05313.

Ridley, A. J. *et al.* (1992) 'The small GTP-binding protein rac regulates growth factor-induced membrane ruffling', *Cell*. Cell Press, 70(3), pp. 401–410. doi: 10.1016/0092-8674(92)90164-8.

Rissanen, T. T. *et al.* (2005) 'Blood flow remodels growing vasculature during vascular endothelial growth factor gene therapy and determines between capillary arterialization and sprouting angiogenesis', *Circulation*, 112(25), pp. 3937–3946. doi: 10.1161/CIRCULATIONAHA.105.543124.

Robert S. Smith, J. *et al.* (2002) 'Human Endothelial Nitric Oxide Synthase Gene Delivery Promotes Angiogenesis in a Rat Model of Hindlimb Ischemia', *Arteriosclerosis, Thrombosis, and Vascular Biology*, 22(8), pp. 1279–1285. doi: 10.1161/01.ATV.0000026613.18742.67.

Roberts, W. G. G. and Palade, G. E. G. E. (1995) 'Increased microvascular permeability and endothelial fenestration induced by vascular endothelial growth factor.', *Journal of cell science*, 108 (Pt 6(6), pp. 2369–79. Available at: http://jcs.biologists.org/content/108/6/2369.short (Accessed: 6 April 2017).

de Rooij, J. *et al.* (1998) 'Epac is a Rap1 guanine-nucleotide-exchange factor directly activated by cyclic AMP.', *Nature*. Nature Publishing Group, 396(6710), pp. 474–477. doi: 10.1038/24884.

Ruhrberg, C. *et al.* (2002) 'Spatially restricted patterning cues provided

by heparin-binding VEGF-A control blood vessel branching morphogenesis', *Genes and Development*. Cold Spring Harbor Laboratory Press, 16(20), pp. 2684–2698. doi: 10.1101/gad.242002.

Saaristo, A., Suominen, E. and Yla-Herttuala, S. (2005) 'Gene transfer as a tool to induce therapeutic vascular growth in plastic surgery', *Handchirurgie Mikrochirurgie Plastische Chirurgie*. Nature Publishing Group, 37(6), pp. 375–382. doi: 10.1055/s-2005-872984.

Sainson, R. C. A. and Harris, A. L. (2008) 'Regulation of angiogenesis by homotypic and heterotypic notch signalling in endothelial cells and pericytes: From basic research to potential therapies', *Angiogenesis*. Springer Netherlands, pp. 41–51. doi: 10.1007/s10456-008-9098-0.

Salmon, A. H. J. *et al.* (2009) 'Angiopoietin-1 alters microvascular permeability coefficients in vivo via modification of endothelial glycocalyx', *Cardiovascular research*. Oxford University Press, 83(1), pp. 24–33. doi: 10.1093/cvr/cvp093.

Salmon, A. H. J. and Satchell, S. C. (2012) 'Endothelial glycocalyx dysfunction in disease: Albuminuria and increased microvascular permeability', *Journal of Pathology*. John Wiley & Sons, Ltd., pp. 562–574. doi: 10.1002/path.3964.

Sanchez-Irizarry, C. *et al.* (2004) 'Notch subunit heterodimerization and prevention of ligand-independent proteolytic activation depend, respectively, on a novel domain and the LNR repeats.', *Molecular and cellular biology*. American Society for Microbiology, pp. 9265–9273. doi: 10.1128/MCB.24.21.9265-9273.2004.

Sandoo, A. *et al.* (2010) ‘The endothelium and its role in regulating vascular tone.’, *The open cardiovascular medicine journal*, 4(1), pp. 302–12. doi: 10.2174/1874192401004010302.

Scehnet, J. S. *et al.* (2007) ‘Inhibition of Dll4-mediated signaling induces proliferation of immature vessels and results in poor tissue perfusion’, *Blood*, 109(11), pp. 4753–4760.

Schaper, W. (2009) ‘Collateral circulation. Past and present’, *Basic Research in Cardiology*, pp. 5–21. doi: 10.1007/s00395-008-0760-x.

Scheppke, L. *et al.* (2012) ‘Notch promotes vascular maturation by inducing integrin-mediated smooth muscle cell adhesion to the endothelial basement membrane’, *Blood*, 119(9), pp. 2149–2158. doi: 10.1182/blood-2011-04-348706.

Schultz, J. S., Valentine, R. and Choi, C. Y. (1979) ‘Reflection coefficients of homopore membranes: effect of molecular size and configuration.’, *The Journal of general physiology*, 73(1), pp. 49–60. Available at: http://www.pubmedcentral.nih.gov/articlerender.fcgi?artid=2215232&tool=pmcentrez&rendertype=abstract (Accessed: 23 September 2016).

Schulz, G. B. *et al.* (2015) ‘Cerebral Cavernous Malformation-1 Protein Controls DLL4-Notch3 Signaling between the Endothelium and Pericytes’, *Stroke*, 46(5), pp. 1337–1343. doi: 10.1161/STROKEAHA.114.007512.

Senger, D. *et al.* (1983) ‘Tumor cells secrete a vascular permeability factor that promotes accumulation of ascites fluid’, *Science*, 219(4587).

doi: 10.1126/science.6823562.

Shen, B. Q., Lee, D. Y. and Zioncheck, T. F. (1999) ‘Vascular endothelial growth factor governs endothelial nitric-oxide synthase expression via a KDR/Flk-1 receptor and a protein kinase C signaling pathway.’, *The Journal of biological chemistry*. American Society for Biochemistry and Molecular Biology, 274(46), pp. 33057–33063. doi: 10.1074/jbc.274.46.33057.

Shibuya, M. (2013) ‘Vascular endothelial growth factor and its receptor system: Physiological functions in angiogenesis and pathological roles in various diseases’, *Journal of Biochemistry*. Oxford University Press, pp. 13–19. doi: 10.1093/jb/mvs136.

Shirahama, T. and Cohen, A. S. (1972) ‘The role of mucopolysaccharides in vesicle architecture and endothelial transport. An electron microscope study of myocardial blood vessels.’, *Journal of Cell Biology*, 52(1), pp. 198–206.

Shuler, L. and Hickman, J. J. (2015) ‘TEER measurement techniques for in vitro barrier model systems’, *J Lab Autom*. NIH Public Access, 20(2), pp. 107–126. doi: 10.1177/2211068214561025.TEER.

Shutter, J. R. *et al.* (2000) ‘Dll4, a novel Notch ligand expressed in arterial endothelium’, *Genes & development*, 14(11), pp. 1313–1318.

Shyu, K. G. *et al.* (1998) ‘Direct intramuscular injection of plasmid DNA encoding angiopoietin-1 but not angiopoietin-2 augments revascularization in the rabbit ischemic hindlimb.’, *Circulation*, 98(19), pp. 2081–7. doi: 10.1161/01.CIR.98.19.2081.

Siekmann, A. F., Affolter, M. and Belting, H.-G. (2013) ‘The tip cell concept 10 years after: New players tune in for a common theme’, *Experimental Cell Research*, 319, pp. 1255–1263. doi: 10.1016/j.yexcr.2013.01.019.

Siekmann, A. F. and Lawson, N. D. (2007) ‘Notch signalling limits angiogenic cell behaviour in developing zebrafish arteries.’, *Nature*. Nature Publishing Group, 445(7129), pp. 781–784. doi: 10.1038/nature05577.

Siflinger-Birnboim, A. *et al.* (1987) ‘Molecular sieving characteristics of the cultured endothelial monolayer’, *Journal of Cellular Physiology*. Wiley Subscription Services, Inc., A Wiley Company, 132(1), pp. 111–117. doi: 10.1002/jcp.1041320115.

Silvestre, J. S., Smadja, D. M. and Levy, B. I. (2013) ‘POSTISCHEMIC REVASCULARIZATION: FROM CELLULAR AND MOLECULAR MECHANISMS TO CLINICAL APPLICATIONS’, *Physiological Reviews*, 93(4), pp. 1743–1802. doi: 10.1152/physrev.00006.2013.

Skalak, T. C. and Price, R. J. (1996) ‘The role of mechanical stresses in microvascular remodeling.’, *Microcirculation (New York, N.Y. : 1994)*, 3(2), pp. 143–65. doi: 10.3109/10739689609148284.

De Smet, F. *et al.* (2009) ‘Mechanisms of Vessel Branching’, *Arteriosclerosis, Thrombosis, and Vascular Biology*, 29(5). doi: 10.1161/ATVBAHA.109.185165.

Sörensen, I., Adams, R. H. and Gossler, A. (2009) ‘DLL1-mediated Notch activation regulates endothelial identity in mouse fetal arteries’,

Blood, 113(22), pp. 5680–5688. doi: 10.1182/blood-2008-08-174508.

Sperling, S. and Larsen, I. G. (1979) ‘Toxicity of dimethylsulfoxide (DMSO) to human corneal endothelium in vitro.’, *Acta ophthalmologica*, 57(5), pp. 891–8. Available at: http://www.ncbi.nlm.nih.gov/pubmed/525310 (Accessed: 17 October 2016).

De Spiegelaere, W. *et al.* (2012) ‘Intussusceptive angiogenesis: A biologically relevant form of angiogenesis’, *Journal of Vascular Research*, pp. 390–404. doi: 10.1159/000338278.

Starling, E. H. (1896) ‘On the Absorption of Fluids from the Connective Tissue Spaces.’, *The Journal of physiology*, 19(4), pp. 312–326. doi: 10.1086/327033.

Stewart, K. S. *et al.* (2012) ‘Delta-like ligand 4 – Notch signaling regulates bone marrow – derived pericyte / vascular smooth muscle cell formation’, *Blood*, 117(2), pp. 719–726. doi: 10.1182/blood-2010-05-284869.The.

Stone, J. *et al.* (1995) ‘Development of retinal vasculature is mediated by hypoxia-induced vascular endothelial growth factor (VEGF) expression by neuroglia.’, *The Journal of neuroscience : the official journal of the Society for Neuroscience*, 15(7 Pt 1), pp. 4738–4747.

Stone, O. A. *et al.* (2016) ‘Differential regulation of blood flow induced neovascularisation and mural cell recruitment by VEGF and angiopoietin signalling.’, *The Journal of physiology*. doi: 10.1113/JP273430.

Strilić, B. *et al.* (2009) ‘The Molecular Basis of Vascular Lumen Formation in the Developing Mouse Aorta’, *Developmental Cell*. Elsevier, 17(4), pp. 505–515. doi: 10.1016/j.devcel.2009.08.011.

Stummer, W. (2007) ‘Mechanisms of tumor-related brain edema.’, *Neurosurgical focus*. American Association of Neurological Surgeons, 22(5), p. E8. doi: 10.3171/foc.2007.22.5.9.

Suchting, S. *et al.* (2007) ‘The Notch ligand Delta-like 4 negatively regulates endothelial tip cell formation and vessel branching.’, *Proceedings of the National Academy of Sciences of the United States of America*. National Academy of Sciences, 104(9), pp. 3225–30. doi: 10.1073/pnas.0611177104.

Sundberg C *et al.* (2002) ‘Stable expression of angiopoietin-1 and other markers by cultured pericytes: phenotypic similarities to a subpopulation of cells in maturing vessels during later stages of angiogenesis in vivo.’, *Lab Invest*, 82(4), pp. 387–401. doi: 10.1038/labinvest.3780433.

Suri, C. *et al.* (1996) ‘Requisite role of angiopoietin-1, a ligand for the TIE2 receptor, during embryonic angiogenesis’, *Cell*, 87(7), pp. 1171–1180. doi: 10.1016/S0092-8674(00)81813-9.

Taddei, A. *et al.* (2008) ‘Endothelial adherens junctions control tight junctions by VE-cadherin-mediated upregulation of claudin-5.’, *Nature cell biology*. Nature Publishing Group, 10(8), pp. 923–934. doi: 10.1038/ncb1752.

Takeshita, S. *et al.* (1994) ‘Intramuscular administration of vascular endothelial growth factor induces dose-dependent collateral artery

augmentation in a rabbit model of chronic limb ischemia', *Circulation*, 90(5 Pt 2), p. II228-34. Available at: http://www.ncbi.nlm.nih.gov/pubmed/7525111 (Accessed: 18 January 2017).

Takeshita, S. *et al.* (1994) 'Therapeutic angiogenesis: A single intraarterial bolus of vascular endothelial growth factor augments revascularization in a rabbit ischemic hind limb model', *Journal of Clinical Investigation*. American Society for Clinical Investigation, 93(2), pp. 662–670. doi: 10.1172/JCI117018.

Tang, Y. *et al.* (2010) 'Notch and Transforming Growth Factor-β (TGFβ) Signaling Pathways Cooperatively Regulate Vascular Smooth Muscle Cell Differentiation', *Journal of Biological Chemistry*. American Society for Biochemistry and Molecular Biology, 285(23), pp. 17556–17563. doi: 10.1074/jbc.M109.076414.

von Tell, D., Armulik, A. and Betsholtz, C. (2006) 'Pericytes and vascular stability', *Experimental Cell Research*, 312(5), pp. 623–629. doi: 10.1016/j.yexcr.2005.10.019.

Thurston, G. *et al.* (1999) 'Leakage-resistant blood vessels in mice transgenically overexpressing angiopoietin-1.', *Science (New York, N.Y.)*, 286(5449), pp. 2511–4. doi: 10.1126/science.286.5449.2511.

Thurston, G. *et al.* (2000) 'Angiopoietin-1 protects the adult vasculature against plasma leakage', *Nature medicine*. Nature Publishing Group, 6(4), pp. 4–7. doi: 10.1038/74725.

Thurston, G. *et al.* (2005) 'Angiopoietin 1 causes vessel enlargement,

without angiogenic sprouting, during a critical developmental period', *Development*, 132(14), pp. 3317–3326. doi: 10.1242/dev.01888.

Thurston, G. and Kitajewski, J. (2008) 'VEGF and Delta-Notch: interacting signalling pathways in tumour angiogenesis.', *British journal of cancer*. Nature Publishing Group, 99(8), pp. 1204–1209. doi: 10.1038/sj.bjc.6604484.

Tornavaca, O. *et al.* (2015) 'ZO-1 controls endothelial adherens junctions, cell-cell tension, angiogenesis, and barrier formation', *Journal of Cell Biology*. Rockefeller University Press, 208(6), pp. 821–838. doi: 10.1083/jcb.201404140.

Trindade, A. *et al.* (2008) 'Overexpression of delta-like 4 induces arterialization and attenuates vessel formation in developing mouse embryos', *Blood*, 112(5), pp. 1720–1729. doi: 10.1182/blood-2007-09-112748.

Turnpenny, P. D. *et al.* (2003) 'Novel mutations in, a somitogenesis gene encoding a ligand for the Notch signalling pathway, cause a DLL3 consistent pattern of abnormal vertebral segmentation in spondylocostal dysostosis', *Journal of medical genetics*. BMJ Publishing Group Ltd, 40(5), pp. 333–339. doi: 10.1136/JMG.40.5.333.

Tuttle, J. L. *et al.* (2001) 'Shear level influences resistance artery remodeling: wall dimensions, cell density, and eNOS expression.', *American journal of physiology. Heart and circulatory physiology*, 281(3), pp. H1380–H1389.

Uemura, A. *et al.* (2002) 'Recombinant angiopoietin-1 restores higher-

order architecture of growing blood vessels in mice in the absence of mural cells', *Journal of Clinical Investigation*. American Society for Clinical Investigation, 110(11), pp. 1619–1628. doi: 10.1172/JCI200215621.

Umbrello, M. *et al.* (2013) 'The key role of nitric oxide in hypoxia: hypoxic vasodilation and energy supply-demand matching', *Antioxid Redox Signal.* Mary Ann Liebert, Inc. 140 Huguenot Street, 3rd Floor New Rochelle, NY 10801 USA, 19(14), pp. 1690–1710. doi: 10.1089/ars.2012.4979.

Unthank, J. L. *et al.* (1996) 'Wall Remodeling During Luminal Expansion of Mesenteric Arterial Collaterals in the Rat', *Circulation Research*, 79(5), pp. 1015–1023. doi: 10.1161/01.RES.79.5.1015.

Valenzuela, D. M. *et al.* (1999) 'Angiopoietins 3 and 4: diverging gene counterparts in mice and humans.', *Proceedings of the National Academy of Sciences of the United States of America*. National Academy of Sciences, 96(5), pp. 1904–9. doi: 10.1073/pnas.96.5.1904.

Victorino, G. P., Newton, C. R. and Curran, B. (2004) 'Modulation of microvascular hydraulic permeability by platelet-activating factor.', *The Journal of trauma*, 56(2), pp. 379–84. doi: 10.1097/01.TA.0000042156.89779.6C.

Villa, N. *et al.* (2001) 'Vascular expression of Notch pathway receptors and ligands is restricted to arterial vessels', *Mechanisms of Development*, 108(1–2), pp. 161–164. doi: 10.1016/S0925-4773(01)00469-5.

Vink, H., Constantinescu, A. A. and Spaan, J. A. E. (2000) ‘Oxidized Lipoproteins Degrade the Endothelial Surface Layer’, *Circulation*, 101(13), pp. 1500–1502. doi: 10.1161/01.CIR.0000015465.73933.3B.

Wachtel, M. *et al.* (1999) ‘Occludin proteolysis and increased permeability in endothelial cells through tyrosine phosphatase inhibition.’, *Journal of cell science*, 112 (Pt 2(23), pp. 4347–56. Available at: http://www.ncbi.nlm.nih.gov/pubmed/10564652 (Accessed: 24 February 2017).

Wallez, Y. *et al.* (2007) ‘Src kinase phosphorylates vascular endothelial-cadherin in response to vascular endothelial growth factor: identification of tyrosine 685 as the unique target site.’, *Oncogene*. Nature Publishing Group, 26(August 2006), pp. 1067–1077. doi: 10.1038/sj.onc.1209855.

Wallez, Y. and Huber, P. (2008) ‘Endothelial adherens and tight junctions in vascular homeostasis, inflammation and angiogenesis.’, *Biochimica et biophysica acta*, 1778(3), pp. 794–809. doi: 10.1016/j.bbamem.2007.09.003.

Wang, G. *et al.* (2015) ‘Origin and differentiation of vascular smooth muscle cells’, *The Journal of Physiology*, 593(14), pp. 3013–3030. doi: 10.1113/JP270033.

Wang, Q. *et al.* (2012) ‘Notch2 and notch3 function together to regulate vascular smooth muscle development’, *PLoS ONE*. Edited by Q. Xiao. Public Library of Science, 7(5), p. e37365. doi: 10.1371/journal.pone.0037365.

Wang, W.-Y. *et al.* (2004) ‘An Adenovirus-Mediated Gene-Transfer

Model of Angiogenesis in Rat Mesentery', *Microcirculation*. Blackwell Publishing Ltd, 11(4), pp. 361–375. doi: 10.1080/10739680490437568.

Waschke, J., Drenckhahn, D., Adamson, R. H., Barth, H., *et al.* (2004) 'cAMP protects endothelial barrier functions by preventing Rac-1 inhibition', *Am.J.Physiol Heart Circ.Physiol*, 287(6), pp. H2427–H2433. doi: 10.1152/ajpheart.00556.2004.

Waschke, J., Baumgartner, W., *et al.* (2004) 'Requirement of Rac activity for maintenance of capillary endothelial barrier properties', *American Journal of Physiology*, 286(0363–6135 (Print)), pp. H394–H401. doi: 10.1152/ajpheart.00221.2003.

Waschke, J., Drenckhahn, D., Adamson, R. H. and Curry, F. E. (2004) 'Role of adhesion and contraction in Rac 1-regulated endothelial barrier function in vivo and in vitro', *Am.J.Physiol Heart Circ.Physiol*, 287(0363–6135 (Print)), pp. H704–H711. doi: 10.1152/ajpheart.01076.2003.

Weinbaum, S., Tarbell, J. M. and Damiano, E. R. (2007) 'The Structure and Function of the Endothelial Glycocalyx Layer', *Annual Review of Biomedical Engineering*. Annual Reviews, 9(1), pp. 121–167. doi: 10.1146/annurev.bioeng.9.060906.151959.

Weis, S. *et al.* (2004) 'Endothelial barrier disruption by VEGF-mediated Src activity potentiates tumor cell extravasation and metastasis', *Journal of Cell Biology*, 167(2), pp. 223–229. doi: 10.1083/jcb.200408130.

WHO (2015) *WHO _ Cardiovascular diseases (CVDs)*, *Cardiovascular*

diseases (CVDs). World Health Organization. doi: Fact sheet N°317.

Williams, C. K. *et al.* (2006) 'Up-regulation of the Notch ligand Delta-like 4 inhibits VEGF-induced endothelial cell function', *Blood*, 107(3), pp. 931–939. doi: 10.1182/blood-2005-03-1000.

Williams, C. K. *et al.* (2015) 'Up- - regulation of the Notch ligand Delta- - like 4 inhibits VEGF- - induced endothelial cell function', 107(3), pp. 931–939. doi: 10.1182/blood-.

Winkler, E. A., Bell, R. D. and Zlokovic, B. V (2011) 'Central nervous system pericytes in health and disease.', *Nature neuroscience*. Nature Research, 14(11), pp. 1398–1405. doi: 10.1038/nn.2946.

Witzenbichler, B. *et al.* (1998) 'Chemotactic properties of angiopoietin-1 and -2, ligands for the endothelial-specific receptor tyrosine kinase Tie2', *Journal of Biological Chemistry*. American Society for Biochemistry and Molecular Biology, 273(29), pp. 18514–18521. doi: 10.1074/jbc.273.29.18514.

Wolf, M. B. (1996) 'Determination of the magnitude of the water-exclusive pathway in cat skeletal muscle microvasculature', *Microcirculation*, 3(1), pp. 59–73. doi: 10.3109/10739689609146783.

WOLF, M. B. (2002) 'A Three-Pathway Pore Model Describes Extensive Transport Data from Mammalian Microvascular Beds and Frog Microvessels', *Microcirculation*, 9(6), pp. 497–511. doi: 10.1080/mic.9.6.497.511.

Wolf, M. B. and Watson, P. D. (1989) 'Measurement of osmotic reflection coefficient for small molecules in cat hindlimbs', *Am J Physiol*,

256(1).

Wong, N. D. (2014) ‘Epidemiological studies of CHD and the evolution of preventive cardiology.’, *Nature reviews. Cardiology*. Nature Research, 11(5), pp. 276–89. doi: 10.1038/nrcardio.2014.26.

Wu, J. *et al.* (2005) ‘Molecular determinants of NOTCH4 transcription in vascular endothelium’, *Mol Cell Biol*. American Society for Microbiology, 25(4), pp. 1458–1474. doi: 10.1128/MCB.25.4.1458-1474.2005.

Wysolmerski, R. B. and Lagunoff, D. (1991) ‘Regulation of permeabilized endothelial cell retraction by myosin phosphorylation’, *American Journal of Physiology*, 261(1 Pt 1), pp. C32-40. Available at: http://www.ncbi.nlm.nih.gov/entrez/query.fcgi?cmd=Retrieve&db=PubMed&dopt=Citation&list_uids=1858858 (Accessed: 4 October 2016).

Yemisci, M. *et al.* (2009) ‘Pericyte contraction induced by oxidative-nitrative stress impairs capillary reflow despite successful opening of an occluded cerebral artery.’, *Nature medicine*. Nature Publishing Group, 15(9), pp. 1031–1037. doi: 10.1038/nm.2022.

Yoo, S. Y. and Kwon, S. M. (2013) ‘Angiogenesis and its therapeutic opportunities’, *Mediators of Inflammation*. Hindawi, p. 127170. doi: 10.1155/2013/127170.

Yu, J. *et al.* (2005) ‘Endothelial nitric oxide synthase is critical for ischemic remodeling, mural cell recruitment, and blood flow reserve.’, *Proceedings of the National Academy of Sciences of the United States of America*. National Academy of Sciences, 102(31), pp. 10999–1004. doi: 10.1073/pnas.0501444102.

Yurchenco, P. D. (2011) ‘Basement membranes: Cell scaffoldings and signaling platforms’, *Cold Spring Harbor Perspectives in Biology*, 3(2), pp. 1–27. doi: 10.1101/cshperspect.a004911.

Yurugi-Kobayashi, T. *et al.* (2006) ‘Adrenomedullin/cyclic AMP pathway induces notch activation and differentiation of arterial endothelial cells from vascular progenitors’, *Arteriosclerosis, Thrombosis, and Vascular Biology*, 26(9), pp. 1977–1984. doi: 10.1161/01.ATV.0000234978.10658.41.

Zhang, F. *et al.* (2009) ‘Compositional analysis of heparin/heparan sulfate interacting with fibroblast growth factor.fibroblast growth factor receptor complexes.’, *Biochemistry*. American Chemical Society, 48(35), pp. 8379–8386. doi: 10.1021/bi9006379.

Zhang, J. *et al.* (2011) ‘Angiopoietin-1/Tie2 signal augments basal notch signal controlling vascular quiescence by inducing delta-like 4 expression through AKT-mediated activation of β-catenin’, *Journal of Biological Chemistry*. American Society for Biochemistry and Molecular Biology, 286(10), pp. 8055–8066. doi: 10.1074/jbc.M110.192641.

Zhang, L. *et al.* (2003) ‘Tumor-derived Vascular Endothelial Growth Factor Up-Regulates Angiopoietin-2 in Host Endothelium and Destabilizes Host Vasculature , Supporting Angiogenesis in Ovarian Cancer Tumor-derived Vascular Endothelial Growth Factor Up-Regulates Angiopoietin-2 in’, *Cancer Research*, 63(12).

Zhang, P. *et al.* (2014) ‘Notch signaling in blood vessels: From morphogenesis to homeostasis’, *Science China Life Sciences*, pp. 774–

780. doi: 10.1007/s11427-014-4716-0.

Zhang, Z. G. *et al.* (2000) ‘VEGF enhances angiogenesis and promotes blood-brain barrier leakage in the ischemic brain’, *Journal of Clinical Investigation*. American Society for Clinical Investigation, 106(7), pp. 829–838. doi: 10.1172/JCI9369.

Zhao, Y., Vanhoutte, P. M. and Leung, S. W. S. (2015) ‘Vascular nitric oxide: Beyond eNOS’, *Journal of Pharmacological Sciences*, pp. 83–94. doi: 10.1016/j.jphs.2015.09.002.

Ziegler, M. A. *et al.* (2010) ‘Marvels, mysteries, and misconceptions of vascular compensation to peripheral artery occlusion.’, *Microcirculation (New York, N.Y. : 1994)*. Blackwell Publishing Ltd, pp. 3–20. doi: 10.1111/j.1549-8719.2010.00008.x.